

Dissertation for Doctor of Philosophy

**Distributed Formation Control of Multi-agent Systems:  
Bearing-Based Approaches and Applications**

Minh Hoang Trinh

School of Mechanical Engineering

Gwangju Institute of Science and Technology

2018

Distributed Formation Control of Multi-agent Systems:  
Bearing-Based Approaches and Applications

Advisor: Hyo-Sung Ahn

by

Minh Hoang Trinh

School of Mechanical Engineering

Gwangju Institute of Science and Technology

A thesis submitted to the faculty of the Gwangju Institute of Science and  
Technology in partial fulfillment of the requirements for the degree of Doctor  
of Philosophy in the School of Mechanical Engineering

Gwangju, Republic of Korea

May 21, 2018

Approved by

Professor Hyo-Sung Ahn

Thesis Advisor

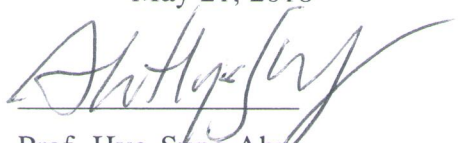
Distributed Formation Control of Multi-agent Systems:  
Bearing-Based Approaches and Applications

Minh Hoang Trinh

Accepted in partial fulfillment of the requirements for the  
degree of Doctor of Philosophy

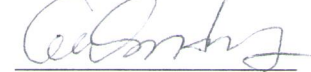
May 21, 2018

Thesis Advisor



Prof. Hyo-Sung Ahn

Committee Member



Prof. Euiseok Hwang

Committee Member



Prof. Hyunsuk Kang

Committee Member



Prof. Jeong-Ok Choi

Committee Member



Dr. Kwang-Kyo Oh

*Dedicated to my family.*

PhD/ME      Minh Hoang Trinh. Distributed Formation Control of Multi-agent Systems: 20152062 Bearing-Based Approaches and Applications. School of Mechanical Engineering. 2018. 200p. Advisor: Prof. Hyo-Sung Ahn.

## Abstract

This thesis studies three distributed control problems in multi-agent systems, namely formation control, pointing consensus, and matrix-weighted consensus. It turns out that these problems, of which formulations and applications are quite different, can be all approached from different bearing-based perspectives. Here, the bearing is the unit vector containing the directional information from an agent to its neighboring agent.

The first problem studies formations with the leader-first follower (LFF) and the directed cycle structures. For LFF formations, the bearing-based Henneberg construction to generate LFF graphs is introduced and different bearing-only control laws to achieve the desired formation are proposed. Further strategies to stabilize formation without a common reference frame, to rescale and to rotate the target formation are then investigated. Moreover, experiment in quadrotor systems is reported to support the analysis. For formations on directed cycles, a feasibility condition for the set of desired bearing vectors and a local stability analysis in the two-dimensional space are provided.

The second problem is pointing consensus, in which the agents in the system are required to consent their headings to a common point in the space. This problem finds applications in camera networks, satellite formations, and antenna arrays. For instance, pointing consensus is important in coordinating multiple collectors and combiner spacecrafts in synthetic aperture radars for space missions such as earth observation and studying evolution of black holes or other planets. We present a pointing consensus strategy by solving three small problems, namely, bearing-only network localization, target decision and heading coordination. Based on this strategy, two bearing-only decentralized solutions to the Fermat-Weber location problem are also proposed.

The third problem studies a consensus algorithm in which the interconnection between agents is characterized by a nonnegative definite matrix weighted graph. Using matrix

weights instead of scalar weights opens up the possibility of modeling a larger class of multi-layer networked systems, for examples, the traffic network and the social network. When the matrix-weighted graph is undirected, necessary and sufficient conditions for achieving average consensus or cluster consensus are given. Moreover, sufficient conditions for reaching a consensus are provided when the graph is directed. Matrix-weighted consensus with switching topologies and time delays is also examined.

©2018

Minh Hoang Trinh

ALL RIGHTS RESERVED

# Contents

<b>Abstract</b>	<b>i</b>
<b>List of Contents</b>	<b>iii</b>
<b>List of Tables</b>	<b>vii</b>
<b>List of Figures</b>	<b>viii</b>
<b>Notations</b>	<b>xii</b>
<b>I Introduction and Preliminaries</b>	<b>xiv</b>
<b>1 Introduction</b>	<b>1</b>
1.1 Motivation . . . . .	1
1.2 Literature review and contributions . . . . .	2
1.2.1 Bearing-based formation control . . . . .	2
1.2.2 Pointing consensus . . . . .	9
1.2.3 Matrix-weighted consensus . . . . .	11
1.3 Outline of the thesis . . . . .	13
<b>2 Preliminaries</b>	<b>14</b>
2.1 Algebraic graph theory . . . . .	14
2.2 Bearing rigidity theory . . . . .	16
2.3 Almost global input-to-state stability . . . . .	18
2.4 Finite-time stability theory . . . . .	20
2.5 Some useful lemmas . . . . .	20
<b>II Bearing-Based Formation Control</b>	<b>22</b>
<b>3 Bearing-Based Control of Leader-First Follower Formations</b>	<b>23</b>
3.1 Bearing-based Henneberg construction . . . . .	23
3.1.1 Bearing assignment for formation control . . . . .	23

3.1.2	Bearing-based Henneberg construction . . . . .	25
3.1.3	Properties of LFF formations . . . . .	28
3.2	Bearing-only control of LFF formations . . . . .	31
3.2.1	Problem formulation . . . . .	31
3.2.2	Almost global stabilization of LFF formations . . . . .	32
3.2.3	Global stabilization of LFF formations . . . . .	43
3.2.4	Finite-time bearing-only formation control . . . . .	46
3.3	Bearing-based control of LFF formations via orientation alignment . . . . .	49
3.3.1	Problem formulation . . . . .	49
3.3.2	Proposed control strategy . . . . .	50
3.3.3	Stability analysis . . . . .	53
3.4	Bearing-based control of LFF formations via global orientation estimation . . . . .	57
3.4.1	Problem formulation . . . . .	57
3.4.2	Global orientation estimation . . . . .	58
3.4.3	Distributed bearing-based formation control . . . . .	61
3.5	Regulating the target formation . . . . .	63
3.5.1	Controlling the formation's orientation . . . . .	63
3.5.2	Rescaling the formation . . . . .	64
3.6	Simulation results . . . . .	65
3.6.1	Simulation 1: Achieving the desired formation . . . . .	65
3.6.2	Simulation 2: Rotating formation by switching leader's orientation . . . . .	66
3.6.3	Simulation 3: Rescaling the formation . . . . .	66
3.7	Implementation on quadrotor systems . . . . .	67
<b>4</b>	<b>Formations on Directed Cycles with Bearing-Only Measurements</b>	<b>70</b>
4.1	Problem formulation and the proposed control law . . . . .	70
4.1.1	Problem formulation . . . . .	70
4.1.2	The bearing-only control law . . . . .	77
4.2	The directed cycle formation in the plane . . . . .	77
4.2.1	The three agent formations . . . . .	78
4.2.2	The $n$ -agent formations . . . . .	86
4.3	The triangular formation in the three dimensional space . . . . .	91

4.3.1	Preliminary results . . . . .	92
4.3.2	The dynamical model . . . . .	93
4.3.3	Stability analysis . . . . .	96
4.3.4	The $n$ -agent case . . . . .	101
4.4	Simulations . . . . .	101
4.4.1	Simulation 1: A three-agent formation in the plane . . . . .	101
4.4.2	Simulation 2: A six-agent formation in the plane . . . . .	102
4.4.3	Simulation 3: A three-agent formation in the three-dimensional space	103
<b>III</b>	<b>The Pointing Consensus Problem</b>	<b>105</b>
<b>5</b>	<b>Pointing Consensus and Bearing-Based Solutions to the Fermat-Weber Location Problem</b>	<b>106</b>
5.1	Problem formulation . . . . .	106
5.2	The pointing consensus strategy . . . . .	109
5.2.1	Bearing rigidity and the pointing consensus problem . . . . .	110
5.2.2	The proposed strategy . . . . .	112
5.2.3	Stability analysis . . . . .	114
5.2.4	Discussion on the desired target point . . . . .	120
5.3	A decentralized bearing-based solution to the Fermat-Weber location problem	123
5.3.1	The Fermat-Weber location problem . . . . .	124
5.3.2	A decentralized formulation of the FWLP . . . . .	125
5.3.3	The proposed solutions . . . . .	126
5.3.4	Stability analysis . . . . .	128
5.4	Simulation results . . . . .	131
5.4.1	Simulation 1: Pointing toward the centroid . . . . .	131
5.4.2	Simulation 2: Pointing toward the Fermat-Weber point . . . . .	132
<b>IV</b>	<b>Matrix-Weighted Consensus</b>	<b>135</b>
<b>6</b>	<b>Matrix-Weighted Consensus and Its Applications</b>	<b>136</b>
6.1	Preliminaries and problem formulation . . . . .	136

6.1.1	Matrix-weighted graphs . . . . .	136
6.1.2	Matrix-weighted consensus protocols . . . . .	139
6.2	Algebraic condition for reaching a consensus . . . . .	141
6.3	Algebraic graph theory of consensus and clustered consensus . . . . .	144
6.4	Applications . . . . .	155
6.4.1	Cluster consensus . . . . .	155
6.4.2	The bearing-constrained formation control problem . . . . .	159
<b>7</b>	<b>Further Results on Matrix-Weighted Consensus</b>	<b>161</b>
7.1	Consensus with leader-following graphs . . . . .	161
7.1.1	Preliminaries and problem formulation . . . . .	161
7.1.2	Analysis and discussion . . . . .	162
7.2	Consensus with fixed and balanced matrix-weighted graphs . . . . .	169
7.3	Consensus with switching matrix-weighted graphs . . . . .	172
7.4	Consensus with time-delays . . . . .	173
<b>V</b>	<b>Conclusions</b>	<b>177</b>
<b>8</b>	<b>Summary and Further Studies</b>	<b>178</b>
8.1	Bearing-based formation control . . . . .	178
8.2	Pointing consensus . . . . .	179
8.3	Matrix-weighted consensus . . . . .	180
<b>Bibliography</b>		<b>181</b>
<b>Acknowledgements</b>		<b>201</b>

## **List of Tables**

1.1	A literature review on formation control problems. . . . .	4
6.1	Comparison between the scalar-weighted consensus and the matrix-weighted consensus.	156

## List of Figures

1.1 A group of agents has to achieve a desired formation . . . . .	2
1.2 A classification of formation control problems based on controlled variables [1] . . .	3
2.1 Examples: (a) a directed graph $G_1 = (\mathcal{V}_1, \mathcal{E}_1)$ , with $\mathcal{V}_1 = \{v_1, v_2, v_3, v_4\}$ , and $\mathcal{E}_1 = \{(v_1, v_3), (v_3, v_4), (v_4, v_1), (v_4, v_2)\}$ ; (b) an undirected graph $G_2 = (\mathcal{V}_2, \mathcal{E}_2)$ with $\mathcal{V}_2 = \{v_1, v_2, v_3, v_4\}$ , and $\mathcal{E}_2 = \{(v_1, v_3), (v_3, v_1), (v_3, v_4), (v_4, v_3), (v_4, v_1),$ $(v_1, v_4), (v_4, v_2), (v_2, v_4)\}$ . . . . .	15
3.1 An example of bearing constraint assignment: agents 2 and 3 control their bearings toward agent 1; agents 1 and 4 both control the bearing between them; agent 4 controls two bearings with regard to agents 1 and 3. . . . .	24
3.2 An LFF graph of eight vertices: vertex $v_1$ (the leader) has no neighbor, vertex $v_2$ (the first follower) has one neighbor, and each vertex $v_i$ ( $i = 3, \dots, 8$ ) has two neighbors.	25
3.3 An example of Henneberg construction. In each step, the added vertex and added edges are in yellow and red, respectively. Vertex addition is used in steps 2, 4, and 5 while edge splitting is used in steps 3 and 6. . . . .	26
3.4 Since agents 1, 2, 3 are in the same plane $\mathcal{P}_1$ , the two desired bearing vectors $\mathbf{g}_{31}^*$ and $\mathbf{g}_{32}^*$ of agent 3 must be in the same plane with $\mathbf{g}_{21}^*$ . The position $\mathbf{p}_3^*$ in $\mathbb{R}^d$ can be uniquely determined from $\mathbf{p}_1^*$ , $\mathbf{p}_2^*$ and $\mathbf{g}_{31}^*, \mathbf{g}_{32}^*$ . . . . .	28
3.5 Agent 2 adopts the control law (3.7). There are two isolated equilibria $\mathbf{p}_{2a}^*$ and $\mathbf{p}_{2b}^*$ corresponding to $\mathbf{g}_{21} = \mathbf{g}_{21}^*$ and $\mathbf{g}_{21} = -\mathbf{g}_{21}^*$ , respectively. . . . .	33
3.6 Illustration when the position of agent 3, $\mathbf{p}_3$ , is collinear with $\mathbf{p}_1$ and $\mathbf{p}_{2a}^*$ . . . . .	38
3.7 Simulation 1: Achieving the desired formation with orientation alignment. . . . .	66
3.8 Regulating the target formation . . . . .	67

3.9	Experiment setup . . . . .	68
3.10	Experiment results. . . . .	69
4.1	A directed cycle graph with six nodes. . . . .	71
4.2	Both configurations (a) and (b) satisfy all desired bearing vectors $\mathbf{g}_i^*, i = 1, \dots, 4$ but are not similar. . . . .	72
4.3	Four regions separated by two lines containing two vectors $\mathbf{g}_i^*$ and $\mathbf{g}_i^{*\perp}$ . . . . .	74
4.4	The formation (a) is a desired formation where $\mathbf{g}_i = \mathbf{g}_i^*, i = 1, 2, 3$ , while the forma- tion (b) is an undesired one where $\mathbf{g}_i = -\mathbf{g}_i^*, i = 1, 2, 3$ . . . . .	79
4.5	The directed triangle formation under control law (4.11) (left); a desired formation (right). . . . .	80
4.6	Three agents are collinear and $\alpha_1 = \alpha_2 = \alpha_3 > 0$ . . . . .	85
4.7	A desired formation is given in (a). An undesired formation is given in (b), where $\mathbf{g}_1 = -\mathbf{g}_1^*, \mathbf{g}_2 = \mathbf{g}_2^*, \mathbf{g}_3 = -\mathbf{g}_3^*$ , and $\mathbf{g}_4 = \mathbf{g}_4^*$ . . . . .	86
4.8	Formation of $n$ agents under control law (4.9). . . . .	87
4.9	Four possible directions that the desired bearing vector makes an angle $\alpha$ with the line $\Delta$ . . . . .	89
4.10	The vector $\mathbf{g}_i^*$ points North East (NE). . . . .	89
4.11	Four possible configurations of agent (i+1)'s bearings. . . . .	90
4.12	The sensing model of an agent $i$ in the 3D space. . . . .	92
4.13	Illustration of vectors $\mathbf{g}_{i,1}, \mathbf{g}_{i,2}, \mathbf{g}_{i+1,1}$ , and $\mathbf{g}_{i+1,2}$ . . . . .	94
4.14	Illustration of the proof of Theorem 4.13. . . . .	98
4.15	Simulation results of a three-agent formation under the bearing-only control law (4.9). .	102
4.16	The three-agent formation under the control law (4.9) with another initial condition. .	102

4.17	Simulation results of a six-agent formation under the bearing-only control law (4.9). . .	103
4.18	Simulation results of the six-agent formation for a different set of initial conditions. . .	103
4.19	Three agents form an equilateral triangular formation under the control law (4.9). . .	104
5.1	The rotational velocity $\Omega_i$ of the agent $i$ 's heading direction can be equivalently represented as the velocity $\mathbf{u}_i = \mathbf{P}_{\mathbf{b}_i} \mathbf{u}_i$ of the head point $\mathbf{p}'_i$ . . . . .	107
5.2	Example: A six-agent system and a common target. (a) The agents consent their heading direction into a common point $\mathbf{p}^*$ . (b) The information graph $G$ . (c) The pointing graph (objective graph). (d) The union graph $\bar{G}$ . . . . .	108
5.3	Example: A six-agent system and a common target. (a) A configuration of the union framework $\bar{G}(\bar{\mathbf{p}})$ . The configuration $\bar{\mathbf{p}}$ after (b) a translation, (c) a dilation. For both cases (b) and (c), the agents' headings still point toward a common point. . . . .	111
5.4	Suppose that the vector $\hat{\mathbf{h}}_i$ is fixed, the control law (5.8) rotates $\mathbf{b}_i$ to align with $\hat{\mathbf{h}}_i$ exponentially fast. . . . .	113
5.6	Simulation 1: The heading vectors of six agents under the proposed control laws (5.6), (5.7), (5.8). All heading vectors asymptotically point toward the centroid of the formation of six agents after 20s. . . . .	133
5.7	Simulation 2a: The headings of six agents under control laws (5.6), Algorithm 1, (5.35).134	
5.8	Simulation 2b: The headings of six agents under control laws (5.6), Algorithm 2, (5.35).134	
6.1	$\mathcal{T}$ is a positive spanning tree of $G$ . The edges in $\mathcal{E}(\mathcal{T})$ are in red color. . . . .	138
6.2	Illustration of the four-agent system in Example 6.1. . . . .	148
6.3	Example 1: The states' dynamics of four agents under the consensus protocol (6.3). .	149
6.4	Illustration of the five-agent system in Example 6.2. . . . .	151

6.5 Example 2: The states' dynamics and trajectories of four agents under the consensus protocol (6.3). . . . .	151
6.6 The vertex $i$ connects to the positive tree $\mathcal{T}$ through two semi-positive connections. . .	152
6.7 Two positive trees $\mathcal{T}_1$ and $\mathcal{T}_2$ are connected through three semi-positive connections..	153
6.8 Two graphs used in simulations: graph (a) has three clusters, graph (b) has a spanning cluster. . . . .	157
6.9 Case 1: The nine-agent system in Fig. 6.8 under the consensus protocol (6.3). . . . .	158
6.10 Case 2: Trajectories after the interaction graph switched to the graph in Fig. 6.8 (ii). .	158
7.1 Leader-follower graph, with undirected follower graph. . . . .	163
7.2 Leader-follower graph, with directed acyclic follower graph. . . . .	164

## Notations

$\mathbb{R}$	the set of real numbers
$\mathbb{R}^d$	the $d$ -dimensional Euclidean vector space
$\mathbb{R}^{d \times d}$	the set of all $d \times d$ matrices
$\alpha, \beta, \gamma, \dots$	constant real numbers
$a, b, c, \dots$	scalars
$\mathbf{a}, \mathbf{b}, \mathbf{c}, \dots$	vectors
$\mathbf{A}, \mathbf{B}, \mathbf{C}, \dots$	matrices
$\mathcal{A}, \mathcal{B}, \mathcal{C}, \dots$	sets
$A, B, C, \dots$	graphs, or scalar functions
$\mathcal{N}(\mathbf{A})$	the null space (kernel) of matrix $\mathbf{A}$
$\mathcal{R}(\mathbf{A})$	the column space (range) of matrix $\mathbf{A}$
$\dim(\mathcal{A})$	the dimension of the vector space $\mathcal{A}$
$\text{diag}(\mathbf{a})$	the diagonal matrix with the elements of vector $\mathbf{a}$ in the main diagonal
$\text{blkdiag}(\mathbf{A}_k)$	the block diagonal matrix with matrices $\mathbf{A}_k$ in the main diagonal block
$r(\mathbf{A})$	the rank of a matrix $\mathbf{A}$
$\ \mathbf{A}\ _l$	the $l$ -norm of matrix $\mathbf{A}$
$\ \mathbf{A}\ $	the Euclidean norm (the second norm) of matrix $\mathbf{A}$
$ \cdot $	the absolute value of a scalar, or the number of elements of a set
$\mathbf{1}_n$	the $n \times 1$ vector with all 1s
$\mathbf{0}_n$	the $n \times 1$ zero vector or the $n \times n$ zero matrix depending on the contexts
$\mathbf{I}_n$	the $n \times n$ identity matrix
$\otimes$	the Kronecker product

$\Sigma$	the global coordinate system (the global reference frame)
${}^i\Sigma$	the local coordinate system of agent $i$ (the body frame of agent $i$ )
$\mathbf{a}_i, \mathbf{b}_i, \mathbf{c}_i, \dots$	vectors related to agent $i$ expressed in the global reference frame $\Sigma$
$\mathbf{a}_i^i, \mathbf{b}_i^i, \mathbf{c}_i^i, \dots$	vectors related to agent $i$ expressed in its local reference frame ${}^i\Sigma$
$\mathbf{a}_{ij}, \mathbf{b}_{ij}, \mathbf{c}_{ij}, \dots$	relative vector variables between agent $i$ and agent $j$ expressed in $\Sigma$
$\mathbf{a}_{ij}^i, \mathbf{b}_{ij}^i, \mathbf{c}_{ij}^i, \dots$	relative vector variables between agent $i$ and agent $j$ expressed in ${}^i\Sigma$
$\mathbf{a}^*, \mathbf{b}^*, \mathbf{c}^*, \dots$	desired vectors

## **Part I**

# **Introduction and Preliminaries**

# Chapter 1

## Introduction

### 1.1 Motivation

Multi-agent systems (MASs) have become more and more ubiquitous recently thanks to many advances in microcontroller and communication technologies. Formations of multiple unmanned vehicles [1, 2], wireless sensor networks [3, 4], energy generation and distribution systems [5, 6], and traffic control systems [7, 8] are a few examples of MASs. A multi-agent system comprises of many subsystems, called agents, which are physically and geographically separated. The agents in the system are interconnected together via communication and/or sensing networks. Moreover, they are usually designed to cooperate together to carry out a group objective which may be hard or unable to be achieved by a single agent.

The control system society is particularly interested in two important issues in MASs: system modeling and control design. A good mathematical model must capture the dynamics of each agent, the interaction between the agents, and their collective behavior as a whole system. At the same time, the model should be simple enough for simulation, analysis, and control design. Since MASs are inherently distributed by their own nature, in many situations, designing a centralized feedback controller to coordinate all individuals is not suitable. As a result, decentralized and distributed control strategies have been widely studied recently. In decentralized/distributed control, each agent obtains the information from few other agents in the system and conducts its behavior correspondingly to attain an individual objective. Their collective behaviors eventually lead to a group's objective, which may be very different and complicated in compare with the individuals' ones. Since these

strategies require no central controller but only local information exchange, the implementation cost of MASs is reduced. Another important feature of the strategies is scalability. That is, the controller of each agent is designed similarly and does not depend on the numbers of agents in the system, i.e., the system's scale. Lastly, as the group objective is shared to all agents, the performance of the system is more robust against the malfunction or replacement of few agents.

A strategy to study MASs is examining lessons from nature, especially in formation-type behaviors such as flock of birds and school of fish. Indeed, formation-type collective behaviors have inspired different research in the realm of formation control. Meanwhile, formation control and its related problems have become the central theme to expose novel ideas in MASs.

This thesis studies three distributed control problems in MASs, namely formation control, pointing consensus, and matrix-weighted consensus. It turns out that these problems, whose formulations and applications are quite different, can be all approached from different bearing-based perspectives. The detailed introduction, literature review on these problems and the contributions of this thesis will be further discussed in the following section.

## 1.2 Literature review and contributions

### 1.2.1 Bearing-based formation control

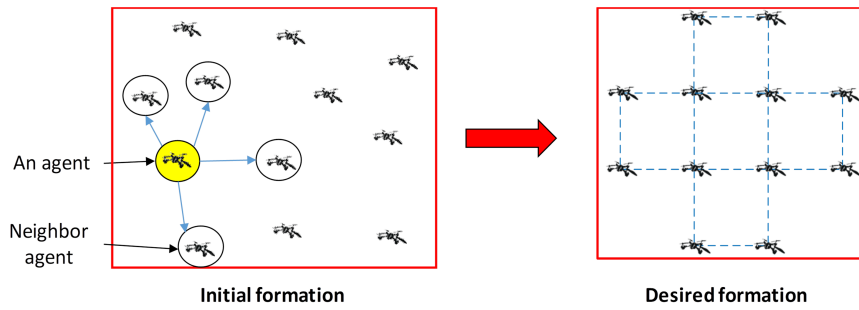


Figure 1.1. A group of agents has to achieve a desired formation

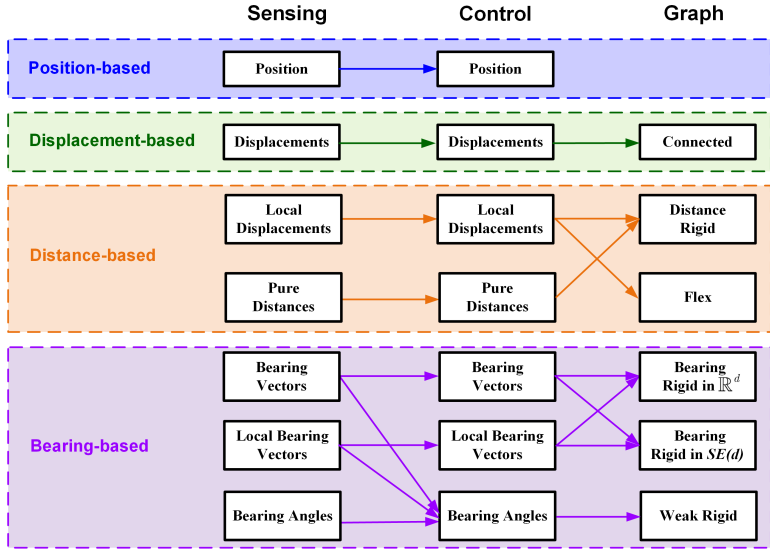


Figure 1.2. A classification of formation control problems based on controlled variables [1]

Formation control of MAss is an ongoing research topic which was motivated from formation-type collective behaviors displayed in nature [2]. In formation control problems, a group of agents, which could be unmanned aerial vehicles (UAVs), underwater unmanned vehicles (UUVs), or mobile robots, is desired to achieve a target formation shape specified by some geometric constraints (see Fig. 1.1). To achieve the group task in a distributed manner, each agent is equipped with onboard sensors to measure some formation-related variables for the control task. Depending on different scenarios, these variables can be the positions, the displacements, the distances, and the bearings (subtended angles or bearing vectors) with respect to a few other agents. Based on the controlled variables, the authors in [1] classified formation control problems into several approaches, namely position-based, displacement-based, distance-based, and bearing-based formation control as depicted in Fig. 1.2. Due to many recent advances in formation control, it is sometimes hard to categorize all existing works according to [1]. Table 1.1 gives a literature review of the recent works on formation control. In this table, a work is classified in the bearing-based setup if the control variable involves the bearings or the graph is assumed to be bearing rigid.

Table 1.1. A literature review on formation control problems.

	Sensing variables	Control variables	Graph requirements	References
Position-based	Position	Position		[18, 19]
Displacement-based	Displacement	Displacement	Connected	[20–22]
Distance-based	Local displacement, Relative orientation	Local displacement and/or Relative orientation	Connected	[23–26]
	Local displacement	Local displacement	Distance rigid	[9–11, 14, 15, 27–30]
	Local displacement	Local displacement	Flex	[31–33]
	Pure distances	Pure distances	Distance rigid	[34–36]
Bearing-based	Local bearing vectors	Angle	Simple graphs	[37–41]
	Local bearing vector	Angle	Weak rigid	[42–44]
	Bearing vector	Bearing vector	Bearing rigid in $\mathbb{R}^d$	[45–52]
	Local bearing vector, Relative orientation	Local bearing vector, Relative orientation	Bearing rigid in $SE(d)$	[53–56]
	Local bearing vector, Relative orientation	Local bearing vector and/or Relative orientation	Bearing rigid in $\mathbb{R}^d$	[49, 57, 58]
	Displacement	Displacement	Bearing rigid in $\mathbb{R}^d$	[59, 60]
Mixed bearing vector, angle & distance- based	Bearing vector, Angle, Distance	Bearing vector, Angle, Distance	Weak rigid	[43, 61–65]

In the literature, the distance-based and the bearing-based formation control are preferred since these approaches require less sensing/communication capabilities and thus, are more distributed. While distance-based formation control was extensively studied [9–15], bearing-based formation control has recently attracted much research interest due to the emergent technology of small UAVs equipped with vision sensors [16]. In bearing-based formation control problems, a group of autonomous agents has to achieve a target formation specified by some bearing information (bearing vectors and/or subtended bearing angles) [17].

A focus of bearing-based formation control is designing decentralized/distributed control laws us-

ing only bearing information. Several bearing-only navigation control laws with beacons have been studied, for example [17, 66, 67]. Consider a group of small quadcopters, the relative bearing vector, which is the unit vector obtained from a relative position vector by normalizing its length, can be acquired from the onboard cameras thanks to vision-based techniques. Since the cameras are passive sensors, in military applications where exchanging signals is prohibited, bearing-only control is preferred [68]. Further, the quadcopter system has a limited payload. To save the quadcopter’s restricted payload, the number of sensors in quadcopter systems can be reduced by employing bearing-only control laws [69].

Early works on bearing-based formation control focused on controlling the subtended bearing angle, which is invariant in each agent’s local coordinate frame [37, 40, 41, 46, 61]. For examples, the authors in [37, 39–41, 46, 61] studied planar formations consisting of three, four and  $n$  agents under control laws derived from subtended bearings. However, this approach is complicated to be extended to higher dimensional spaces. Another approach is based on bearing rigidity, in which the target formation is specified by a set of desired bearing vectors, which is sufficient to specify the formation up to scaling and translation. In two-dimensional space, the concept of bearing rigidity (or parallel rigidity) has been studied in [27, 53, 70]. Based on parallel rigidity theory, the authors in [53] defined the bearing constrained rigidity matrix for a bearing-based formation control problem. Network localization with bearing only information was also studied based on this framework [27, 71]. Recently, the authors of [49] developed a theory of bearing rigidity and infinitesimal bearing rigidity in  $\mathbb{R}^d$ . A bearing-only stabilization control law for formations with undirected graphs in  $\mathbb{R}^d$  has been proposed in [49]. Further applications of bearing rigidity theory in formation maneuvering and network localization have also been discussed [71–73, 73, 74]. However, in these works, only undirected graphs were considered. That is, bearing-only control for directed graphs has been less investigated. Thus, differently from these existing works, a part of this thesis attempts to fill a gap

in the literature on bearing-only formation control with two classes of directed graphs namely the *leader-first follower* (LFF) [75–77] and the *directed cycle* [32, 78–81]. A motivation for studying formations on these graphs comes from hardware implementability of the formation, where each agent has a limited vision-based sensing capability. Suppose we have a system of drones and each drone is equipped with a camera-based vision system. To obtain the bearing vector, each drone must detect its neighboring agents based on the image obtained from the camera. Since the detecting task may be challenging due to environmental noises and obstacles, it is desired to limit the number of neighbors in the sensing graph to keep track of. For any  $n$ -agent LFF formation, we only need to control  $2n - 3$  bearing vectors, and these vectors are distributed evenly to the followers (except for the leader and the first follower, each agent controls precisely two bearing vectors). Likewise, a directed cycle is a strongly connected graph with the least number of edges. Thus, formations on LFF and directed cycle graphs are easier to implement on hardware.

There are several initial studies in bearing-based formation control of directed graphs. For instance, in [48], by assuming the existence of three stationary beacons in the plane, it was proved that any  $n$ -agent system with an acyclic directed sensing graph is locally asymptotically stable. The reference [82] also shown local stability of LFF formations. The local stability of planar formations with directed cycle graphs plus a stationary beacon was studied in [51, 83]. However, references [51, 83] present no analysis on asymptotic stability of these formations. It is worth remarking that the analysis in the undirected case cannot be used in the directed case due to the asymmetry in the sensing graph. The lack of symmetry raises difficulties in analysis, for example, the formation’s centroid and scale are not invariant as in the undirected case [52]. The authors in [59] introduced the bearing Laplacian from a set of desired bearing vectors and defined bearing persistence based on the null space of the bearing Laplacian. However, the proposed control law in [59] requires the relative positions between neighbors, which are not available from bearing measurements. The authors in [54–56] developed

bearing-based rigidity theories in  $SE(2)$ ,  $\mathbb{R}^3 \times \mathcal{S}^1$ , and  $SE(3)$ , in which the bearing vectors are defined in the body frame of each agent. Strategies for formation control and estimation were also proposed in [54, 55], assuming that the agents can exchange their local sensing information and computations. It is also worth noting that several existing works on the leader-following and the directed cycle formation in distance-based setup can be found, for examples, [32, 84, 85].

With regard to Table 1.1, this thesis mainly studies the bearing-based formation control problems when the sensing and controlling variables are the bearing vectors and the graph is bearing rigid in  $\mathbb{R}^d$ . The contributions of this thesis to the literature of bearing-based formation control are summarized as follows:

- The leader-first follower (LFF) formation: Firstly, the bearing-based Henneberg construction and some properties of LFF formations is studied. The bearing-based Henneberg construction, unlike the bearing rigidity theory given in [49], is a basic theoretical framework for bearing-based directed graphs. The bearing-based Henneberg construction in [46] is extended to generate all LFF graphs based on two graph operations, namely vertex addition and edge splitting. In practice, LFF formations are easy to implement due to their cascade structure [86]. Moreover, an LFF formation is uniquely determined given the leader's position, the set of desired bearing vectors and the formation scale. Secondly, the stability of LFF formation under the bearing-only control law in an arbitrary dimensional space is analysed. The analysis is based on the notion of almost global input-to-state stability of cascade systems [87, 88]. Thirdly, a modified bearing-only control law is proposed to guarantee the formation to escape from any undesired equilibrium, and globally asymptotically converge to the desired one. Moreover, a finite-time control law is also introduced to improve the convergence rate of the formation. In practice, it may be unrealistic to assume the existence of a global reference frame. Even though all agents'

local body frames are initially aligned, due to drift in inertial sensing, misalignment between local frames may still happen [89]. Thus, to address this issue, as the fifth contribution, two control strategies are proposed based on orientation alignment and global orientation estimation. Under some assumptions on the initial local orientations, the formation almost globally asymptotically converges to the target formation under the proposed control strategies. Then, several extensions of the control law, including rotation and rescaling of the target formation are proposed. The ability to rotate and rescale the formation is an important feature for formation maneuvering [72, 75]. Finally, simulation results and hardware test on quadrotors systems are reported to support the analysis.

- The directed cycle formation: First of all, necessary and sufficient conditions for planar formation feasibility in terms of some algebraic constraints on the set of desired bearing vectors are derived. Then, a bearing-only control law, for agents in cyclic pursuit, is proposed to achieve some desired formation and examine the possible equilibrium formations under this law. By classifying these equilibria into the set of desired equilibria and the set of undesired ones, local properties of the equilibria in each set are investigated. Next, by transforming the dynamics of the agents from the position variables to the angular errors, it shows local asymptotic stability of the desired equilibrium and provides an estimate of the corresponding set of initial conditions. The three-agent formation is studied in detail since its sensing graph is the only one in this class satisfying the infinitesimal rigidity condition. The analysis of the  $n$ -agent case is then given as a natural extension of the three-agent scenario. Although formations of directed cycles with more than three agents in  $\mathbb{R}^2$  are not bearing rigid, studying directed cycles may aid in a better understanding of stabilizing formations with general digraphs. Finally, the analysis on directed triangular formations is extended to three dimensional space.

### 1.2.2 Pointing consensus

In recent years, the consensus algorithm [90] has been extensively studied as a decentralized solution to coordinate a group of multiple agents. Given  $n$  agents having different initial state values, by exchanging and updating the states based on the weighted sum of differences, all agents' states eventually reach the same value [90, 91]. The states of the agents could be auxiliary variables used for decision and control tasks [92, 93], or physical variables such as positions, velocities, and attitudes in the formation control or attitude synchronization problem [1, 94, 95].

Unlike the usual consensus problem, the pointing consensus (or concurrent targeting) problem requires all agents in a group to direct their heading vectors towards a common point in space. This problem found applications in camera networks, satellite formations, and antenna arrays [96]. For instance, pointing consensus is important in coordinating multiple collectors and combiner space-crafts in synthetic aperture radars (SAR) for space missions such as earth observation and studying evolution of black holes or other planets [97, 98].

There have not been many works in the literature studying the pointing consensus problem. In an early work, the authors of [99] considered a concurrent targeting problem where all agents are positioned along a straight line, and there are two agents (leaders) with their heading vectors pointed already to the target. The control law in [99] is decentralized and is able to guide all headings to match with the intersection of two leaders' heading vectors. The pointing consensus protocol in [100] relaxed the collinearity assumption on the agents' positions. However, the agents in [100] still need some pieces of a-priori information on the common target, given as a desired heading vector for one agent and several subtended angles for the other agents. Thus, even in two dimensional space, the pointing consensus problem has not been completely solved in [99, 100]. As observed in [100], a main challenge of this problem is that the agents cannot consent their heading vectors without some

knowledge on their (relative) positions in the space.

The second part of this thesis provides a solution to the pointing consensus problem in three dimensional space. It assumes that each agent in the group has additional information on some bearing vectors toward its neighbors. This assumption is acceptable, since the bearing vectors can be obtained from the cameras, passive radars, passive sonars, or sensor arrays [101]. From the bearing vector measurements, the agents can estimate their positions in the network up to a translation and a scaling if the framework defined by the bearing measurement graph and their positions is *infinitesimally bearing rigid* [49]. Next, for any given target in the space, by considering the target as a special agent, it will be shown that the target-and- $n$ -agent framework is also infinitesimally bearing rigid. Thus, without having the precise positions, if the agents can obtain the estimated positions of itself and the target up to a translation and a scaling, they can find the exact heading vectors toward the target and control their heading vectors correspondingly. Based on this argument, a solution to the pointing consensus problem is introduced. The idea is dividing the problem into three smaller problems, namely, bearing-only network localization, target decision, and heading coordination. For each sub-problem, a corresponding control law is proposed and the combination of these control laws asymptotically direct all agents' headings toward a common target from almost all initial conditions. Next, the question on how to decide the common target is discussed. It is shown that the set of constraints to determine the common target should be invariant with respect to a translation and a scaling of the whole framework. Furthermore, a decentralized version of the well-known Fermat-Weber location problem (FWLP) [102] is formulated based on the pointing consensus framework. The FWLP asks to find the point that minimizes a weighted distance sum to a set of  $n$  noncollocated points in the space. As an important problem in operational research, the FWLP was extensively studied in a centralized manner [102–104]. Differently from existing works in the literature, two decentralized solutions to the FWLP are reported based on a combination of the bearing-based localization

and finite-time consensus algorithms [105]. The proposed solutions are inspired from the Weiszfeld algorithm and the gradient descent algorithms [106, 107].

The theoretical contributions of this part are summarized as follows. The first contribution is a strategy for solving the pointing consensus consensus problem for almost all initial conditions. In solving the pointing consensus problem, an estimation control law for the bearing-based network localization problem is proposed, the connection between bearing rigidity theory and the pointing consensus problem is exploited, and the invariant property on the constraints imposing on the common target is also discussed. The second contribution is a decentralized formulation and two bearing-based solutions of the FWLP. As far as we know, decentralized solutions of the FWLP have not been studied in the literature yet.

### 1.2.3 Matrix-weighted consensus

Consensus algorithm has been extensively studied in the literature as a main tool for solving the cooperative control problems in multiagent systems [90, 108, 109]. In fact, consensus algorithm and its modifications are found in broad applications, for examples, in control of unmanned vehicle formations [1, 20, 21, 110], network synchronization [111, 112], modeling social networks [113, 114], and coordination of power distribution systems and automated traffic networks [6, 8].

Given a system of  $n$  single-integrator agents whose interconnections between agents are characterized by a weighted undirected graph  $G$ , the consensus algorithm [108] is defined as follows:

$$\dot{\mathbf{x}}_i = \sum_{j=1}^n a_{ij}(\mathbf{x}_j - \mathbf{x}_i), \forall i = 1, \dots, n, \quad (1.1)$$

where  $\mathbf{x}_i, \mathbf{x}_j \in \mathbb{R}^d$  are the state vectors of agents  $i$  and  $j$ , and  $a_{ij}$  is a positive scalar (or zero) if  $i$  and  $j$  are connected (or disconnected, respectively). It is well-known that under the consensus protocol (1.1), an average consensus is globally achieved if and only if  $G$  is connected [108].

The third part of this thesis generalizes the consensus algorithm (1.1) by using matrix weight  $A_{ij}$  instead of the scalar weight  $a_{ij}$  to describe the interconnection between two agents  $i$  and  $j$ . Here, a matrix weight could be a positive definite matrix (strong connection), a positive semidefinite matrix (weak connection), or a zero matrix (no direct connection). Thus, the matrix-weighted consensus covers a larger set of problems in multi-agent systems.

In the literature, matrix weights arise in many problems to describe the interconnections between agents. For example, the authors in [115] showed that matrix weights arises in the solution of a network localization problem. In [116], matrix weights were used to describe interconnections between coupled linear oscillators and provided conditions to synchronize these networks in some situations. The concept of deviated cyclic pursuit introduced in [117], orientation estimation in [25, 118], and formation control via complex Laplacian in [22] can be considered as consensus protocols with rotation matrix weights. Also, the bearing-based formation control setup in [59] can be formulated as a special case of the matrix-weighted consensus protocol. In the context of social networks, suppose that a group of people are discussing multiple topics, matrix weights were used to describe the logical inter-dependency of the topics [119, 120]. However, the works [119, 120] only considered a discrete-time model in which the matrix weights are the same for all edges.

In this thesis, the matrix-weighted consensus algorithm with fixed, undirected graphs is studied. Firstly, several terminologies (for e.g., positive/semipositive definite edges, positive tree, matrix-weighted Laplacian, etc), are defined and some basic algebraic properties of the matrix-weighted graph are proved. Secondly, the matrix-weighted consensus protocol is proposed and a necessary and sufficient condition for globally exponentially reaching an average consensus is provided in term of the nullspace of the matrix-weighted Laplacian. Next, due to the existence of semidefinite matrix weights, clustered consensus happens naturally even when the graph is connected. The algebraic graph theory of consensus and clustering phenomena are examined. Further, an algorithm to de-

termine all clusters in the network is provided. The algorithm initially partitions the graph into a set of clusters associated with the positive trees in the graph. If two clusters satisfy several algebraic conditions on their connections, they will be merged together at each iteration of the algorithm. The algorithm gradually reduces the number of clusters in the graph, and it ends when no two clusters can be further merged together. If there is a cluster containing all vertices in the graph, under matrix-weighted consensus protocol, a consensus is globally achieved. Otherwise, we know the exact number of clusters in the system under the matrix-weighted consensus protocol. Then, two examples are given to illustrate applications of the proposed matrix-weighted consensus algorithm. The first example demonstrates how clustered consensus can be used to gather a group of agents into several clusters. The second example is taken from the bearing-based formation control in the literature [59, 72]. Finally, further results on matrix-weighted consensus including consensus with leader-following topologies, consensus with generalized balanced graphs, and consensus with switching and time-delays are also given.

### 1.3 Outline of the thesis

This thesis contains five parts. Part I contains two chapters: introduction and preliminaries, which set the theme and background for the main chapters II–IV. Then, parts II–IV present three problems, namely, bearing-based formation control, pointing consensus, and matrix-weighted consensus; the parts are independent on each other. Each chapter contains the problem formulation, mathematically analysis, numerical simulations. Finally, part V summaries the thesis and discusses about the further research directions.

# Chapter 2

## Preliminaries

This chapter aims to provide a background for the rest of this thesis. To this end, a lot of essential definitions and results from algebraic graph theory [91, 121, 122], bearing rigidity theory [49], almost global input-to-state stability theory [87, 88], and finite-time stability theory [123] are presented. Moreover, several commonly used results about the orthogonal projection matrices are also given. It is assumed that the readers are familiar with linear algebra [124] and Lyapunov stability theory [125].

### 2.1 Algebraic graph theory

A *directed graph* (or digraph)  $G$  is an ordered pair of disjoint sets  $(\mathcal{V}(G), \mathcal{E}(G))$  such that  $\mathcal{V}(G) \neq \emptyset$  and  $\mathcal{E}(G) \subset \mathcal{V}(G) \times \mathcal{V}(G)$ . The set  $\mathcal{V}(G)$  is the set of *vertices* of  $G$  and  $\mathcal{E}(G)$  is the set of *edges*. If there is no risk of ambiguity, these are abbreviated to  $\mathcal{V}$  and  $\mathcal{E}$ , respectively. Let the vertex set be given by  $\mathcal{V} = \{v_1, \dots, v_n\}$ , then we can write  $|\mathcal{V}| = n$ . For  $i \neq j$ ,  $1 \leq i, j \leq n$ , an edge  $e_{ij} = (v_i, v_j) \in \mathcal{E}$  is said to join the vertex  $v_i$  to vertex  $v_j$ . At the same time, the vertices  $v_i, v_j$  are said to be incident to the edge  $(v_i, v_j)$ .<sup>1</sup> The vertex  $v_i$  is called the tail or initial vertex, while  $v_j$  is called the head or terminal vertex. Since the graph  $G$  is directed,  $(v_i, v_j) \in \mathcal{E}$  does not imply that  $(v_j, v_i) \in \mathcal{E}$ . For an edge  $(v_i, v_j)$ ,  $v_j$  is said to be adjacent to  $v_i$  (or  $v_j$  is a neighbor vertex of  $v_i$ ),  $v_i$  is a parent vertex of  $v_j$  and  $v_j$  is a child vertex of  $v_i$ . Also, define the set  $\mathcal{N}_i = \{j = 1, \dots, n | (v_i, v_j) \in \mathcal{E}\}$  as the neighborhood of  $v_i$  and refer to  $|\mathcal{N}_i|$  as the *degree* of vertex  $i$ . In Fig. 2.1, each vertex is depicted by a small cycle and each directed edge  $(v_i, v_j)$  is depicted by an arrow from  $v_i$  to  $v_j$ . A *walk*  $W$

---

<sup>1</sup>Note that we do not consider self-loop edge  $(v_i, v_i)$ .

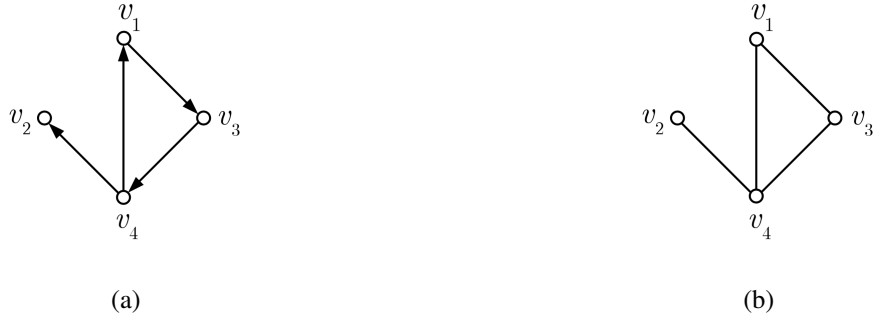


Figure 2.1. Examples: (a) a directed graph  $G_1 = (\mathcal{V}_1, \mathcal{E}_1)$ , with  $\mathcal{V}_1 = \{v_1, v_2, v_3, v_4\}$ , and  $\mathcal{E}_1 = \{(v_1, v_3), (v_3, v_4), (v_4, v_1), (v_4, v_2)\}$ ; (b) an undirected graph  $G_2 = (\mathcal{V}_2, \mathcal{E}_2)$  with  $\mathcal{V}_2 = \{v_1, v_2, v_3, v_4\}$ , and  $\mathcal{E}_2 = \{(v_1, v_3), (v_3, v_1), (v_3, v_4), (v_4, v_3), (v_4, v_1), (v_1, v_4), (v_4, v_2), (v_2, v_4)\}$ .

between two not necessarily different vertices  $v_i$  and  $v_j$  is an alternating sequence of vertices and edges, say  $v_{i_1}, e_{i_1}, v_{i_2}, e_{i_1}, \dots, v_{i_l}, e_{i_l}, v_{i_{l+1}}$ , where  $v_{i_1} = v_i$ ,  $v_{i_{l+1}} = v_j$ , and  $e_{i_k} = (v_{i_k}, v_{i_{k+1}})$ . A walk is usually shortly written as  $W = v_{i_1}v_{i_2}\dots v_{i_{l+1}}$  since from this form it is clear where are the edges in the sequences. The walk  $W$  has the vertex set  $\mathcal{V}(W) = \{v_{i_k} | k = 1, \dots, l+1\}$ , the edge set  $\mathcal{E}(W) = \{e_{i_k} | k = 1, \dots, l\}$ , and the length  $l$ . If all the vertices in  $\mathcal{V}(W)$  are distinct,  $W$  is called a *path*. Meanwhile, if  $l \geq 3$ ,  $v_{i_1} = v_{i_{l+1}}$  and  $v_{i_k} \neq v_{i_m}, \forall 1 \leq k \neq m \leq l$ , we call this walk a *cycle*. Further, we use  $C_l$  to denote a cycle graph of length  $l$ .

A vertex  $v_i$  is a *out-root (in-root)*, if for every  $v_j \in \mathcal{V}, j \neq i$ , there exists a path joining  $v_i$  to  $v_j$  ( $v_j$  to  $v_i$ ). A graph having only one out-root (in-root) is *rooted out-branching (rooted in-branching)*. Further, a *directed out-tree (directed in-tree)* is a rooted out-branching graph (rooted in-branching graph), where every vertex, except the out-root (in-root), has exactly a parent vertex (child vertex). A *spanning out-tree (spanning tree)* of  $G$  is a directed tree formed by the edges in  $\mathcal{E}$  that connects all the vertices in  $\mathcal{V}$ . A digraph is *strongly connected* if for every pair of vertices, there exists a path connecting them. In this case, all vertices of  $G$  are roots.

Let the edges in  $\mathcal{E}$  be indexed in an order, one can write  $\mathcal{E} = \{e_{k_{ij}}\}_{k=1,\dots,m}$ , where  $m = |\mathcal{E}|$ . If

it is unimportant to specify the end-vertices explicitly, the subscript  $ij$  is dropped out and one writes  $e_k$  with the understanding that  $e_k \equiv e_{kij} \equiv (v_i, v_j)$ . The *incidence matrix*  $\mathbf{H} = [h_{ki}] \in \mathbb{R}^{m \times n}$  of the graph  $G$  characterizes the relation between the vertex set and the edge set and is defined as follows:

$$h_{ki} = \begin{cases} -1, & \text{if vertex } i \text{ is the tail of } e_k, \\ 1, & \text{if vertex } i \text{ is the head of } e_k, \\ 0, & \text{otherwise.} \end{cases}$$

Note that the edges in  $\mathcal{E}$  can only describe the connectivity between the vertices. In order to quantify the strength of these connections, we introduce a (scalar) weight set  $\mathcal{A} = \{a_{ij} \geq 0 | 1 \leq i, j \leq n\}$ , where  $a_{ij} > 0$  ( $a_{ij} = 0$ ) if and only if  $e_{ij} \in \mathcal{E}$  ( $e_{ij} \notin \mathcal{E}$ , respectively). A graph  $G$  with a weight set  $\mathcal{A}$  is referred to as a *weighted digraph* and is denoted by  $G = (\mathcal{V}, \mathcal{E}, \mathcal{A})$ . Define the *adjacency matrix* of the graph  $G$  as  $\mathbf{A} = [a_{ij}] \in \mathbb{R}^{n \times n}$ . The degree of a vertex  $v_i$  in a weighted digraph is defined as  $d_i = \sum_{j=1}^n a_{ij} = \sum_{j \in \mathcal{N}_i} a_{ij}$ . The matrix  $\mathbf{D} = \text{diag}([d_1, \dots, d_n]) \in \mathbb{R}^{n \times n}$  is called the *degree matrix*. The *Laplacian matrix* of  $G$  is defined as  $\mathbf{L} = \mathbf{D} - \mathbf{A} \in \mathbb{R}^{n \times n}$ . If  $G$  has a spanning tree, then  $\text{rank}(\mathbf{L}) = n - 1$ , and  $\mathcal{N}(\mathbf{L}) = \mathcal{N}(\mathbf{H}) = \mathcal{R}(\mathbf{1}_n)$  [121, 126].

A graph  $G$  is *undirected* if  $(v_i, v_j) \in \mathcal{E}$  implies that  $(v_j, v_i) \in \mathcal{E}$ , and  $a_{ij} = a_{ji}, \forall 1 \leq i, j \leq n$ . It follows that  $\mathbf{A}$  is symmetric, i.e.,  $\mathbf{A} = \mathbf{A}^\top$ . A graph is connected if for every pair of vertices, there exists a path connecting them. The Laplacian matrix of a connected graph is symmetric, positive semidefinite, and has a unique zero eigenvalue with the corresponding (right) eigenvector  $\mathbf{1}_n$ .

## 2.2 Bearing rigidity theory

Bearing rigidity theory in  $\mathbb{R}^d$  has been recently proposed and found its applications in the bearing-only formation control and network localization problems [49, 73].

Consider a group of  $n$  noncollocated points in the  $d$ -dimensional space. In the global coordinate system  $\Sigma$ , let  $\mathbf{p}_i \in \mathbb{R}^d$  denote the absolute position of the  $i$ -th point. A *framework* in  $\mathbb{R}^d$  is denoted

by  $G(\mathbf{p})$ , where  $G = (\mathcal{V}, \mathcal{E})$  is a graph of  $n$  vertices and  $m$  edges, and  $\mathbf{p} = [\mathbf{p}_1^\top, \dots, \mathbf{p}_n^\top]^\top \in \mathbb{R}^{dn}$  a realization of the  $n$ -point set in the space.

For  $1 \leq i, j \leq n$  and  $i \neq j$ , we define  $\mathbf{z}_{ij} = \mathbf{p}_j - \mathbf{p}_i$  as the *displacement* between two points  $i$  and  $j$ , and we use  $d_{ij} = \|\mathbf{z}_{ij}\|$  to denote the *Euclidean distance* between them. The *bearing vector*  $\mathbf{g}_{ij}$  from  $i$  to  $j$  is the unit vector obtained from the displacement by normalizing its length [17], i.e.,

$$\mathbf{g}_{ij} \triangleq \frac{\mathbf{p}_j - \mathbf{p}_i}{\|\mathbf{p}_j - \mathbf{p}_i\|} = \frac{\mathbf{z}_{ij}}{\|\mathbf{z}_{ij}\|} = \frac{\mathbf{z}_{ij}}{d_{ij}}. \quad (2.1)$$

Note that  $\mathbf{g}_{ij}$  contains the directional information from  $i$  to  $j$  and  $\|\mathbf{g}_{ij}\| = 1$ . The *orthogonal projection matrix* corresponding to  $\mathbf{g}_{ij}$  is defined as  $\mathbf{P}_{\mathbf{g}_{ij}} = \mathbf{I}_d - \mathbf{g}_{ij}\mathbf{g}_{ij}^\top \in \mathbb{R}^{d \times d}$ . The matrix  $\mathbf{P}_{\mathbf{g}_{ij}}$  is symmetric, idempotent, and positive semidefinite, i.e.,  $\mathbf{P}_{\mathbf{g}_{ij}} = \mathbf{P}_{\mathbf{g}_{ij}}^\top = \mathbf{P}_{\mathbf{g}_{ij}}^2 \geq 0$ . Moreover,  $\mathcal{N}(\mathbf{P}_{\mathbf{g}_{ij}}) = \mathcal{R}(\mathbf{g}_{ij})$  and the eigenvalues of  $\mathbf{P}_{\mathbf{g}_{ij}}$  are  $\{0, \underbrace{1, 1, \dots, 1}_{n-1 \text{ elements}}\}$ . Thus, it follows that  $\mathbf{P}_{\mathbf{g}_{ij}}\mathbf{g}_{ij} = \mathbf{P}_{\mathbf{g}_{ij}}\mathbf{z}_{ij} = \mathbf{0}_d$ , and  $\mathbf{z}_{ij}^\top \mathbf{P}_{\mathbf{g}_{ij}} = \mathbf{g}_{ij}^\top \mathbf{P}_{\mathbf{g}_{ij}} = \mathbf{0}_d^\top$ .

Let the edges in  $\mathcal{E}$  be indexed by  $\{e_k\}_{k=1,\dots,m}$ . For each edge  $e_k \in \mathcal{E}$ , we denote the corresponding displacement and bearing vector as  $\mathbf{z}_k$  and  $\mathbf{g}_k$ , respectively. Also, we define  $\mathbf{z} = [\mathbf{z}_1^\top, \dots, \mathbf{z}_m^\top]^\top \in \mathbb{R}^{dm}$ , and  $\mathbf{g} = [\mathbf{g}_1^\top, \dots, \mathbf{g}_m^\top]^\top \in \mathbb{R}^{dm}$ . The *bearing rigidity matrix* is defined as follows [49]:

$$\mathbf{R}_b(\mathbf{p}) \triangleq \frac{\partial \mathbf{g}}{\partial \mathbf{p}} = \text{blkdiag} \left( \frac{\mathbf{P}_{\mathbf{g}_k}}{\|\mathbf{z}_k\|} \right) \bar{\mathbf{H}}. \quad (2.2)$$

In equation (2.2),  $\mathbf{R}_b \in \mathbb{R}^{dm \times dn}$ ,  $\text{blkdiag}(\cdot)$  is a block diagonal matrix,  $\bar{\mathbf{H}} = \mathbf{H} \otimes \mathbf{I}_d \in \mathbb{R}^{dm \times dn}$ , and “ $\otimes$ ” denotes the Kronecker product. For any bearing rigidity matrix, it can be checked that  $\mathcal{R}([\mathbf{1}_n \otimes \mathbf{I}_d, \mathbf{p}]) = \mathcal{R}([\mathbf{1}_n \otimes \mathbf{I}_d, \mathbf{p} - \mathbf{1}_n \otimes \mathbf{p}_c]) \subseteq \mathcal{N}(\mathbf{R}_b)$ , where  $\mathbf{p}_c \triangleq (\sum_{i=1}^n \mathbf{p}_i)/n = (\mathbf{1}_n \otimes \mathbf{I}_d)^\top \mathbf{p}/n$  is the group’s centroid. Consequently,  $r(\mathbf{R}_b) \leq dn - d - 1$ . A framework  $G(\mathbf{p})$  is said to be *infinitesimally bearing rigid* (IBR) if and only if  $r(\mathbf{R}_b) = dn - d - 1$ .

**Lemma 2.1** [49, Theorem 4] A framework  $G(\mathbf{p})$  is infinitesimally bearing rigid if and only if  $\mathcal{N}(\mathbf{R}_b) = \mathcal{R}([\mathbf{1}_n \otimes \mathbf{I}_d, \mathbf{p} - \mathbf{1}_n \otimes \mathbf{p}_c])$ .

An IBR framework can be uniquely determined up to a translation and a scaling factor. The matrix  $\mathbf{L}_b(\mathbf{p}) \triangleq \mathbf{R}_b^\top \mathbf{R}_b \in \mathbb{R}^{dn \times dn}$  is referred to as the *bearing Laplacian*. Since  $\mathcal{N}(\mathbf{L}_b) = \mathcal{N}(\mathbf{R}_b)$ , a framework is infinitesimally bearing rigid if and only if  $r(\mathbf{L}_b) = dn - d - 1$ .

### 2.3 Almost global input-to-state stability

This section recalls some existing results on almost global input-to-state stability theory [87, 88]. Recall that a function  $A : [0, +\infty) \rightarrow [0, +\infty)$  is of class  $\mathcal{K}$  if continuous, strictly increasing, and  $A(0) = 0$ . A function  $V$  is proper provided  $V^{-1}(\mathcal{A})$  is compact for all compacts  $\mathcal{A}$  included in the domain of  $V$ .

**Assumption 2.1** *Let  $\mathcal{M}$  be an  $n$ -dimensional  $C^2$  connected and orientable Riemannian manifold without boundary, and let  $\mathbf{f} : \mathcal{M} \times \mathcal{D} \rightarrow T_x \mathcal{M}$  be a  $C^1$ -Lipschitz function and  $\mathcal{D}$  be a closed subset of  $\mathbb{R}^m$ .*

Consider the nonlinear systems of the following type:

$$\dot{\mathbf{x}}(t) = \mathbf{f}(\mathbf{x}, \mathbf{d}), \quad (2.3)$$

where  $\mathbf{x} \in \mathcal{M}$ . Denote  $X(t, \mathbf{x}, t_0; \mathbf{d})$  as the solution of (2.3) and we call the following system the unperturbed system:

$$\dot{\mathbf{x}}(t) = \mathbf{f}(\mathbf{x}(t), \mathbf{0}) \triangleq \mathbf{f}_0(\mathbf{x}(t)). \quad (2.4)$$

We further suppose that the following assumptions hold.

**Assumption 2.2** *There exists a nonnegative and proper  $C^1$  function  $V : \mathcal{M} \rightarrow \mathbb{R}$  such that:*

$$\dot{V}(\mathbf{x}) = \frac{\partial V(\mathbf{x})}{\partial \mathbf{x}} \mathbf{f}_0(\mathbf{x}) < 0, \quad \forall \mathbf{x} \in \mathcal{M} : \mathbf{f}_0(\mathbf{x}) \neq \mathbf{0}. \quad (2.5)$$

**Assumption 2.3** Any equilibrium  $\mathbf{x}_l$  which is not asymptotically stable, is isolated and such that at least one eigenvalue of  $d\mathbf{f}_0(\mathbf{x}_l) : T_{\mathbf{x}_l}\mathcal{M} \rightarrow T_{\mathbf{x}_l}\mathcal{M}$  has strictly positive real part, where  $d\mathbf{f}_0(\mathbf{x})$  denotes the differential of  $\mathbf{f}_0(\mathbf{x})$  at  $\mathbf{x}$ .

**Definition 2.2** [88, Definition 1] A system as in (2.3) is said to be almost globally Input-to-State Stable (ISS) with respect to a compact subset  $\mathcal{A} \subset \mathcal{M}$  if  $\mathcal{A}$  is locally asymptotically stable for  $\mathbf{d} \equiv \mathbf{0}$  and there exists  $B(\cdot) \in \mathcal{K}$  such that for each locally essentially bounded and measurable perturbation  $\mathbf{d} : \mathbb{R} \rightarrow \mathcal{D}$ , there exists a zero volume set  $\tilde{\mathcal{B}}_d \subset \mathcal{M}$  such that, for all  $\mathbf{x} \in \mathcal{M} \setminus \tilde{\mathcal{B}}_d$ , it holds

$$\lim_{t \rightarrow +\infty} \sup \delta(X(t, \mathbf{x}, \mathbf{0}; \mathbf{d}), \mathcal{A}) \leq B(\|\mathbf{d}\|_\infty),$$

where  $\delta(\mathbf{x}, \mathbf{y})$  denotes the Riemannian distance between  $\mathbf{x}$  and  $\mathbf{y}$  in  $\mathcal{M}$ .

**Lemma 2.3** [88, Proposition 3] Consider a system as in (2.3), and assume that  $W : \mathcal{M} \rightarrow \mathbb{R}_{\geq 0}$  exists, of class  $C^1$ , proper and satisfying

$$\dot{W}(\mathbf{x}) \leq -A(W(\mathbf{x})) + c + B(\|\mathbf{d}\|), \quad \forall \mathbf{x} \in \mathcal{M}, \mathbf{d} \in \mathcal{D}, \quad (2.6)$$

where functions  $A(\cdot), B(\cdot) \in \mathcal{K}$ . Then, system (2.3) fulfills the ultimate boundedness property.

**Lemma 2.4** [88, Proposition 2] Consider a system as in (2.3) which fulfills Assumptions 2.1 to 2.3. Assume in addition, that the set of asymptotically stable equilibria of (2.4), denoted by  $\mathcal{E}_s$ , be finite. If ultimate boundedness holds, then, (2.3) is almost globally ISS with respect to the set  $\mathcal{E}_s$ .

**Lemma 2.5** [87, Theorem 2] Consider the cascade system

$$\begin{aligned} \dot{\mathbf{x}} &= \mathbf{f}(\mathbf{x}, \mathbf{y}) \\ \dot{\mathbf{y}} &= \mathbf{g}(\mathbf{y}) \end{aligned} \quad (2.7)$$

with state  $\mathbf{z} = [\mathbf{x}^\top, \mathbf{y}^\top]^\top \in \mathcal{M} \times \mathcal{N}$ . Assume that  $\mathbf{f}$  and  $\mathbf{g}$  satisfy  $\mathbf{f}(\mathbf{0}_\mathcal{M}, \mathbf{0}_\mathcal{N}) = \mathbf{0}_\mathcal{M}$  and  $\mathbf{g}(\mathbf{0}_\mathcal{N}) = \mathbf{0}_\mathcal{N}$ , for some points  $\mathbf{0}_\mathcal{M} \in \mathcal{M}$  and  $\mathbf{0}_\mathcal{N} \in \mathcal{N}$ . Let the  $\mathbf{x}$ -subsystem be almost globally ISS with respect

to the equilibrium  $\mathbf{0}_{\mathcal{M}}$  and the input  $\mathbf{y}$  and the  $\mathbf{y}$ -subsystem be almost globally asymptotically stable (GAS) at  $\mathbf{0}_{\mathcal{N}}$ . Then, the interconnection (2.7) is almost GAS at  $\mathbf{0}_{\mathcal{M} \times \mathcal{N}} \triangleq \mathbf{0}_{\mathcal{M}} \times \mathbf{0}_{\mathcal{N}}$ .

## 2.4 Finite-time stability theory

Let  $\mathbf{x} = [x_1, \dots, x_d]^T$  denote a column vector in  $\mathbb{R}^d$  ( $d \geq 1$ ). We denote  $|\mathbf{x}| = [|x_1|, \dots, |x_d|]^T$  and  $\|\mathbf{x}\|_1 = \sum_{i=1}^d |x_i|$ . For  $\alpha \in \mathbb{R}$ , the function  $\text{sig}(\cdot)^\alpha : \mathbb{R}^d \rightarrow \mathbb{R}^d$  is defined as  $\text{sig}(\mathbf{x})^\alpha = [\text{sgn}(x_1)|x_1|^\alpha, \dots, \text{sgn}(x_d)|x_d|^\alpha]^T$  [123]. The following inequality will be used later in this thesis.

**Lemma 2.6** [127] If  $\xi_1, \dots, \xi_d \geq 0$  and  $0 \leq p \leq 1$ , then

$$\left( \sum_{i=1}^d \xi_i \right)^p \leq \sum_{i=1}^d \xi_i^p.$$

A condition for finite-time convergence of a continuous time system is given by the following lemma.

**Lemma 2.7** [123] Suppose there exists a continuous function  $V(\mathbf{x}) : \mathcal{D} \rightarrow \mathbb{R}$  such that the following conditions hold

- i)  $V(\mathbf{x})$  is positive definite,
- ii) If there exist  $\kappa > 0$ ,  $\alpha \in (0, 1)$ , and an open neighborhood  $\mathcal{U}_0 \in \mathcal{D}$  of the origin such that

$$\dot{V}(\mathbf{x}) + \kappa(V(\mathbf{x}))^\alpha \leq 0, \forall \mathbf{x} \in \mathcal{U}_0 \setminus \{\mathbf{0}\},$$

then  $V(\mathbf{x})$  will reach zero in finite time with the settling time  $T \leq V(0)^{1-\alpha}/(\kappa(1-\alpha))$ .

## 2.5 Some useful lemmas

**Lemma 2.8** [128] Let  $\mathbf{B}_i$ ,  $i = 1, \dots, n$ , be  $n$  positive semidefinite matrices and  $\mathbf{B} = \sum_{i=1}^n \mathbf{B}_i$ . Then,  $\mathcal{N}(\mathbf{B}) = \bigcap_{i=1}^n \mathcal{N}(\mathbf{B}_i)$  and  $\mathcal{N}(\mathbf{B}) \subseteq \mathcal{N}(\mathbf{B}_i)$ .

**Lemma 2.9** Let  $\mathbf{g}_1, \dots, \mathbf{g}_m$  be  $m \geq 2$  bearing vectors in  $\mathbb{R}^d$ . If there exist  $i, j \in \{1, \dots, m\}$ ,  $i \neq j$ , such that  $\mathbf{g}_i \neq \pm \mathbf{g}_j$ , then the matrix  $\mathbf{M} = \sum_{k=1}^m \mathbf{P}_{\mathbf{g}_k}$  is positive definite.

*Proof:* Observe that  $\mathbf{P}_{\mathbf{g}_k}$  is symmetric positive semidefinite, so  $\mathbf{M}$  is also symmetric positive semidefinite. From Lemma 2.8,  $\mathcal{N}(\mathbf{M}) = \bigcap_{k=1}^m \mathcal{N}(\mathbf{P}_{\mathbf{g}_k}) = \bigcap_{k=1}^m \mathcal{R}(\mathbf{g}_k)$ . Since there exist  $i, j \in \{1, \dots, m\}$ ,  $i \neq j$ , such that  $\mathbf{g}_i \neq \pm \mathbf{g}_j$ , it follows that  $\mathcal{R}(\mathbf{g}_i) \cap \mathcal{R}(\mathbf{g}_j) = \{\mathbf{0}_d\}$ . Thus,  $\mathcal{N}(\mathbf{M}) = \{\mathbf{0}_d\}$ , which implies that  $\mathbf{M}$  is positive definite.  $\blacksquare$

**Lemma 2.10** Let  $\mathbf{g}_i, \mathbf{g}_{i,1}, \mathbf{g}_{i,2} \in \mathbb{R}^3$  be a set of three orthonormal vectors. There holds:

$$\mathbf{P}_{\mathbf{g}_i} = \mathbf{I}_3 - \mathbf{g}_i \mathbf{g}_i^\top = \mathbf{g}_{i,1} \mathbf{g}_{i,1}^\top + \mathbf{g}_{i,2} \mathbf{g}_{i,2}^\top. \quad (2.8)$$

*Proof:* Consider an arbitrary vector  $\mathbf{u} \in \mathbb{R}^3$ . From the definition of the three unit vectors  $\mathbf{g}_i$ ,  $\mathbf{g}_{i,1}$  and  $\mathbf{g}_{i,2}$ , these vectors form a basis in  $\mathbb{R}^3$ . Thus, we can write  $\mathbf{u} = m_1 \mathbf{g}_i + m_2 \mathbf{g}_{i,1} + m_3 \mathbf{g}_{i,2}$ , where  $m_l \in \mathbb{R}$ , for  $l = 1, 2, 3$ . Observe that

$$\begin{aligned} (\mathbf{g}_i \mathbf{g}_i^\top + \mathbf{g}_{i,1} \mathbf{g}_{i,1}^\top + \mathbf{g}_{i,2} \mathbf{g}_{i,2}^\top) \mathbf{u} &= (\mathbf{g}_i \mathbf{g}_i^\top + \mathbf{g}_{i,1} \mathbf{g}_{i,1}^\top + \mathbf{g}_{i,2} \mathbf{g}_{i,2}^\top)(m_1 \mathbf{g}_i + m_2 \mathbf{g}_{i,1} + m_3 \mathbf{g}_{i,2}) \\ &= m_1 \mathbf{g}_i \mathbf{g}_i^\top \mathbf{g}_i + m_2 \mathbf{g}_{i,1} \mathbf{g}_{i,1}^\top \mathbf{g}_{i,1} + m_3 \mathbf{g}_{i,2} \mathbf{g}_{i,2}^\top \mathbf{g}_{i,2} \\ &= m_1 \mathbf{g}_i + m_2 \mathbf{g}_{i,1} + m_3 \mathbf{g}_{i,2} = \mathbf{u}. \end{aligned} \quad (2.9)$$

Since (2.9) holds for any arbitrary  $\mathbf{u} \in \mathbb{R}^3$ , one has  $\mathbf{g}_i \mathbf{g}_i^\top + \mathbf{g}_{i,1} \mathbf{g}_{i,1}^\top + \mathbf{g}_{i,2} \mathbf{g}_{i,2}^\top = \mathbf{I}_3$ , and (2.8) follows immediately.  $\blacksquare$

Similarly, Lemma 2.10 can be extended to an arbitrary  $d$ -dimensional space ( $d \geq 2$ ).

**Lemma 2.11** Let  $\mathbf{g}_i$  and  $\mathbf{g}_{i,1}, \dots, \mathbf{g}_{i,d-1}$  be an orthonormal basis in  $\mathbb{R}^d$  ( $d \geq 2$ ). The following expression holds:

$$\mathbf{P}_{\mathbf{g}_i} = \mathbf{I}_d - \mathbf{g}_i \mathbf{g}_i^\top = \sum_{k=1}^{d-1} \mathbf{g}_{i,k} \mathbf{g}_{i,k}^\top. \quad (2.10)$$

## **Part II**

# **Bearing-Based Formation Control**

# Chapter 3

## Bearing-Based Control of Leader-First Follower Formations

This chapter compises of results from [57, 58, 82, 129]. In Section 3.1, the bearing-based Henneberg construction is introduced and some properties of the LFF formations are investigated. Then, various bearing-only control laws for LFF formations are proposed under two main themes: with and without a global reference frame. In Section 3.2, when a global reference frame is available, bearing-only almost global/global stabilization control laws and a finite-time control law are studied. In Section 3.3, when the agents do not have access to the global reference frame, two formation control strategies are proposed based on orientation alignment and orientation estimation. Strategies to rotate and to rescale the target formation are discussed in Section 3.5. Section 3.6 provides numerical simulations to support the analysis. Finally, experiments on quadrotor systems are reported in Section 3.7.

### 3.1 Bearing-based Henneberg construction

#### 3.1.1 Bearing assignment for formation control

Consider the task of controlling a group of  $n$  autonomous agents in a  $d$ -dimensional space to take up a formation shape that is bearing congruent to a prescribed configuration  $\mathbf{p}^* \in \mathbb{R}^{dn}$ . Here, bearing congruency means that the formation and the target formation are differ only by a dilation and a translation [49]. Let  $\Gamma \triangleq \{\mathbf{g}_{ij}^* | i, j = 1, \dots, n, i \neq j\}$  be the set of all bearing vectors in the target configuration  $\mathbf{p}^*$ . Supposing that all agents have access to a global reference frame, in order to guarantee bearing congruence between the formation with the configuration  $\mathbf{p}^*$ , it is unnecessary to control all bearing vectors. In fact, based on bearing rigidity theory [49], when a certain subset of

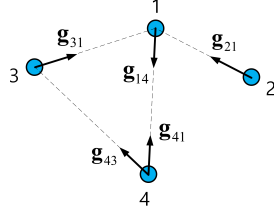


Figure 3.1. An example of bearing constraint assignment: agents 2 and 3 control their bearings toward agent 1; agents 1 and 4 both control the bearing between them; agent 4 controls two bearings with regard to agents 1 and 3.

desired bearing vectors in  $\Gamma$  is achieved, the target formation shape will be attained.

Therefore, the formation control task is shared to every agent in the group, and each agent must only maintain one or more local bearing vectors with regard to other agents in the system. The directed graph  $G$  is used to describe this task assignment. We refer to  $G(p)$  as a formation. A directed edge  $e_{ij}$  in  $\mathcal{E}$  implies that the task of controlling  $g_{ij}$  is assigned to agent  $i$  while a double-edge  $e_{ij}$  and  $e_{ji}$  means that two agents  $i$  and  $j$  are assigned to control  $g_{ij}$  and  $g_{ji}$ , respectively. An example of task allocation on a group of four agents is illustrated in Fig. 3.1.

Besides achieving the group's task, in formation control, it is desirable that the control scheme has a scalability property and should be cost effective. A possible design strategy is minimizing the number of bearing vectors that have to be controlled. Let all agents have access to a common global reference frame; then it holds  $g_{ij} = -g_{ji}$ . Thus, the role of controlling a bearing vector between two agents  $i$  and  $j$  can be assigned to only one of the two agents, for example, to agent  $i$ , and then agent  $j$  moves without awareness of this task. The rest of this chapter will focus on a task distribution strategy in a special structure termed “leader-first follower” or “two-leader formation” [46, 75].

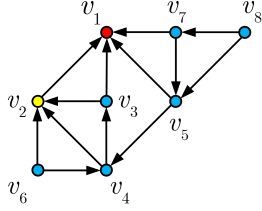


Figure 3.2. An LFF graph of eight vertices: vertex  $v_1$  (the leader) has no neighbor, vertex  $v_2$  (the first follower) has one neighbor, and each vertex  $v_i$  ( $i = 3, \dots, 8$ ) has two neighbors.

### 3.1.2 Bearing-based Henneberg construction

The underlying graph of a leader-first follower (LFF) formation is built up from a bearing-based Henneberg construction. For example, an LFF graph of eight vertices is given in Fig. 3.2. The Henneberg construction starts from a directed edge following by a sequence of operations namely *vertex addition* and *edge splitting* and is defined as follows:

**Definition 3.1 (Henneberg construction)** *Start from a pair of vertices  $v_1$  and  $v_2$  and a directed edge  $(v_2, v_1)$  joining them. Define the degree of cascade of a vertex as the length of its longest directed path from this vertex to the vertex  $v_1$ . Then, vertex 1 has degree 0, vertex 2 has degree 1, and we denote  $\text{doc}(v_1) = 0$ ,  $\text{doc}(v_2) = 1$ . In each step, we perform one of the following two operations:*

- **Vertex addition:** Add a new vertex  $v_i$  to the graph, together with two directed edges to two existing vertices  $v_j$ ,  $v_k$  in the graph. The degree of cascade of the new vertex is defined by  $\text{doc}(v_i) = \max[\text{doc}(v_j), \text{doc}(v_k)] + 1$ .
- **Edge splitting:** Consider a vertex  $v_i$  having precisely two neighbors  $v_j$  and  $v_m$  in the graph. Remove an edge  $(v_i, v_j)$  from the graph and add a new vertex  $v_k$  together with three directed edges  $(v_i, v_k)$ ,  $(v_k, v_j)$ , and  $(v_k, v_m)$  where  $\text{doc}(v_l) \leq \text{doc}(v_i)$ . Then, update the degrees of cascade of  $v_k$  and all its parent vertices in the new graph:  $\text{doc}(v_k) = \max[\text{doc}(v_j), \text{doc}(v_l)] + 1$ .

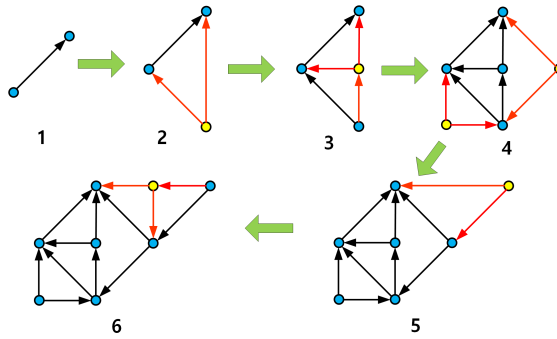


Figure 3.3. An example of Henneberg construction. In each step, the added vertex and added edges are in yellow and red, respectively. Vertex addition is used in steps 2, 4, and 5 while edge splitting is used in steps 3 and 6.

$$1, \text{doc}(v_i) = \max[\text{doc}(v_k), \text{doc}(v_m)] + 1, \dots$$

Figure 3.3 depicts an example on constructing the eight-vertex graph in Fig. 3.2. Any graph  $G = (\mathcal{V}, \mathcal{E})$  of  $n$  vertices obtained using a Henneberg construction defined above is acyclic and rooted in-branching. Further,  $G$  has exactly  $2n - 3$  directed edges [2, 28] and except for vertices  $v_1$  and  $v_2$ , each vertex in  $G$  has precisely two neighbor vertices. It is not difficult to see that in each of the above steps, the degree of the new vertex is two, and the degree of existing vertices in the graph before and after the step is unaltered. An induction argument then shows that all vertices other than  $v_1$  and  $v_2$  have degree two.

Let each vertex in  $\mathcal{V}$  represent an agent in the group and each edge in  $\mathcal{E}$  represent a bearing vector assignment. There is an agent 1 (the leader) with no neighbor. Agent 2 is the first follower, which is supposed to control one bearing vector to the leader. Agent 3 (the second follower) has to control exactly two bearing vectors to the leader and the first follower. Similarly, each agent  $i$  ( $3 \leq i \leq n$ ) has to control two bearing vectors to two agents  $j, k \in \{1, \dots, i-1\}$ . The Henneberg construction together with a bearing assignment is referred to as a *bearing-based Henneberg construction*.

Consider an  $n$ -agent formation in  $\mathbb{R}^d$ ; we examine the degrees of freedom specifying the formation shape. With  $n$  agents, there are  $dn$  coordinates, from which  $d + 1$  ( $d$  accounting for position of the centroid and 1 for the scale) should be subtracted. Thus,  $dn - d - 1$  scalar values specify the formation shape.

Now, consider an LFF formation constructed from a bearing-based Henneberg construction. Consider agent 2 which is assigned only one unit bearing vector  $\mathbf{g}_{21}^* \in \mathbb{R}^d$ . Note that any vector in  $\mathbb{R}^d$  contains  $d$  pieces of data. Since one constraint  $\|\mathbf{g}_{21}^*\| = 1$  was used, there are  $d - 1$  independent pieces of bearing data<sup>1</sup> in  $\mathbf{g}_{21}^*$ . Next, consider agent 3, which is assigned two bearing vectors  $\mathbf{g}_{31}^*$  and  $\mathbf{g}_{32}^*$  as depicted in Fig. 3.4. The two vectors  $\mathbf{g}_{31}^*$  and  $\mathbf{g}_{32}^*$  cannot be chosen arbitrarily. If we choose  $\mathbf{g}_{31}^*$  first, since  $\mathbf{g}_{31}^* \neq \pm \mathbf{g}_{21}^*$  and  $\|\mathbf{g}_{31}^*\| = 1$ , we have  $d - 1$  independent pieces of bearing data in  $\mathbf{g}_{31}^*$ . Now because positions of three agents 1, 2 and 3 define a plane, it follows that  $\mathbf{g}_{31}^*$  and  $\mathbf{g}_{21}^*$  define the same plane, call it,  $\mathcal{P}_1$  in  $\mathbb{R}^d$ . Next, we choose  $\mathbf{g}_{32}^*$ . Besides the norm constraint  $\|\mathbf{g}_{32}^*\| = 1$ ,  $\mathbf{g}_{32}^*$  must be additionally restricted to the plane  $\mathcal{P}_1$ , which is called *coplanarity restriction*, and  $\mathbf{g}_{32}^* \neq \pm \mathbf{g}_{31}^*$  and  $\mathbf{g}_{32}^* \neq \pm \mathbf{g}_{21}^*$ . By choosing a direction in a plane, we have only one degree of freedom. This implies that only one piece of bearing data in  $\mathbf{g}_{32}^*$  can be freely chosen. Thus, there are totally  $d$  (i.e.,  $(d - 1) + 1$ ) independent pieces of bearing data chosen by agent 3. From a similar argument, for each agent  $i > 3$  with two neighbors  $1 \leq j < k < i$ , there are  $d$  independent pieces of bearing data from  $\mathbf{g}_{ij}^*$  and  $\mathbf{g}_{ik}^*$ . Hence, for the overall LFF formation with  $2n - 3$  bearing vectors, there are exactly  $(d - 1) + d(n - 2) = dn - d - 1$  pieces of independent bearing data that can be chosen.

**Remark 3.2** *For planar LFF formations ( $d = 2$ ), each bearing vector contains exactly one in-*

---

<sup>1</sup>When we measure a relative bearing vector in  $\mathbb{R}^d$ , we obtain  $d - 1$  scalar pieces of information, which we term bearing data. As far as a single measurement is concerned, they are all independent, in the sense that no relation is implied among them. When a collection of such measurements is obtained for a number of agents in a general formation, relations may exist, and then the data would not be independent.

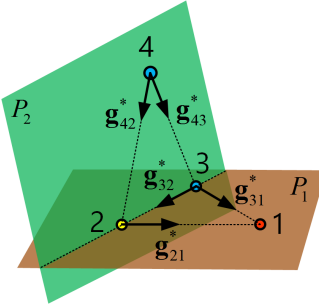


Figure 3.4. Since agents 1, 2, 3 are in the same plane  $\mathcal{P}_1$ , the two desired bearing vectors  $\mathbf{g}_{31}^*$  and  $\mathbf{g}_{32}^*$  of agent 3 must be in the same plane with  $\mathbf{g}_{21}^*$ . The position  $\mathbf{p}_3^*$  in  $\mathbb{R}^d$  can be uniquely determined from  $\mathbf{p}_1^*$ ,  $\mathbf{p}_2^*$  and  $\mathbf{g}_{31}^*$ ,  $\mathbf{g}_{32}^*$ .

*dependent bearing data. Thus, the number of independent bearing data specifying the formation ( $dn - d - 1 = 2n - 3$ ) matches the number of edges in the graph ( $|\mathcal{E}| = m = 2n - 3$ ). Hence,  $2n - 3$  is the minimal number of bearing vectors to specify a formation in the plane. This observation is consistent with the discussion in [46].*

For an LFF formation in  $\mathbb{R}^d$ , there are totally  $2n - 3$  bearing vectors that specify the formation. For  $d \geq 3$ , the  $2n - 3$  bearing vectors gives rise to more pieces of data than degrees of freedom due to the coplanarity restriction, i.e. there is redundant data in the collection of bearing vectors. Determining whether or not  $2n - 3$  is also the minimal number of bearing vectors to specify a formation with general directed graph in  $\mathbb{R}^d$ ,  $d \geq 3$  is beyond the scope of this section. We refer readers to [130] for a further discussion on this topic. Henceforth, we will assume that all specifications of bearings are consistent with the coplanarity restriction described above.

### 3.1.3 Properties of LFF formations

This section studies some properties of LFF formations constructed from a bearing-based Henneberg construction.

**Lemma 3.3 (Uniqueness of the target formation)** Consider an LFF formation with the position of the leader  $\mathbf{p}_1^*$ , the distance  $d_{21}^* = \|\mathbf{p}_2^* - \mathbf{p}_1^*\|$  and the set of bearing vectors  $\{\mathbf{g}_{ij}^*\}_{e_{ij} \in \mathcal{E}}$ . If each agent  $i$  ( $i \geq 3$ ) has two neighbors  $1 \leq j, k < i$ ,  $j \neq k$  with  $\mathbf{g}_{ij}^* \neq \mathbf{g}_{ik}^*$ , the location  $\mathbf{p}_i^*$  is uniquely determined from its neighbors' positions and the desired bearing vectors. More specifically,  $\mathbf{p}_i^*$  is calculated iteratively by

$$\mathbf{p}_i^* = \left( \sum_{j \in \mathcal{N}_i} \mathbf{P}_{\mathbf{g}_{ij}^*} \right)^{-1} \left( \sum_{j \in \mathcal{N}_i} \mathbf{P}_{\mathbf{g}_{ij}^*} \mathbf{p}_j^* \right). \quad (3.1)$$

*Proof:* For agent 2, since  $\mathbf{g}_{21}^* = (\mathbf{p}_1^* - \mathbf{p}_2^*)/d_{21}^*$ , we have  $\mathbf{p}_2^* = \mathbf{p}_1^* - d_{21}^* \mathbf{g}_{21}^*$ . Consider agent 3, the position  $\mathbf{p}_3^*$  of agent 3 satisfies two bearing vectors  $\mathbf{g}_{31}^*$  and  $\mathbf{g}_{32}^*$  as depicted in Fig. 3.4. Thus,

$$\mathbf{P}_{\mathbf{g}_{31}^*}(\mathbf{p}_1^* - \mathbf{p}_3^*) = \mathbf{0}, \text{ and } \mathbf{P}_{\mathbf{g}_{32}^*}(\mathbf{p}_2^* - \mathbf{p}_3^*) = \mathbf{0}. \quad (3.2)$$

From (3.2), it follows that

$$(\mathbf{P}_{\mathbf{g}_{31}^*} + \mathbf{P}_{\mathbf{g}_{32}^*})\mathbf{p}_3^* = \mathbf{P}_{\mathbf{g}_{31}^*}\mathbf{p}_1^* + \mathbf{P}_{\mathbf{g}_{32}^*}\mathbf{p}_2^*. \quad (3.3)$$

Consider the matrix  $(\mathbf{P}_{\mathbf{g}_{31}^*} + \mathbf{P}_{\mathbf{g}_{32}^*})$ . Since  $\mathbf{g}_{31}^* \neq \pm \mathbf{g}_{32}^*$ , it follows from Lemma 2.9 that  $(\mathbf{P}_{\mathbf{g}_{31}^*} + \mathbf{P}_{\mathbf{g}_{32}^*})$  is positive definite. Thus,  $\mathbf{p}_3^*$  can be calculated from (3.3) by

$$\mathbf{p}_3^* = (\mathbf{P}_{\mathbf{g}_{31}^*} + \mathbf{P}_{\mathbf{g}_{32}^*})^{-1} (\mathbf{P}_{\mathbf{g}_{31}^*}\mathbf{p}_1^* + \mathbf{P}_{\mathbf{g}_{32}^*}\mathbf{p}_2^*), \quad (3.4)$$

which can be written in a compact form as (3.1). For  $i = 4, \dots, n$ , the position can be calculated in a similar way.  $\blacksquare$

**Lemma 3.4 (Translation of the target formation)** Given  $d_{21}^*$  and  $\{\mathbf{g}_{ij}^*\}_{e_{ij} \in \mathcal{E}}$ , the translation of the leader's position determines the translation of the entire formation.

*Proof:* We only need to prove that if  $\mathbf{p}_1^*$  is changed to  $\mathbf{q}_1^* = \mathbf{p}_1^* + \boldsymbol{\delta}$ , then  $\mathbf{p}_i^*$  for all  $i$  will be changed to  $\mathbf{q}_i^* = \mathbf{p}_i^* + \boldsymbol{\delta}$ . For agent 2, it is obvious that  $\mathbf{q}_2^* = \mathbf{q}_1^* - d_{21}^* \mathbf{g}_{21}^* = \mathbf{p}_1^* + \boldsymbol{\delta} - d_{21}^* \mathbf{g}_{21}^* = \mathbf{p}_2^* + \boldsymbol{\delta}$ .

For agent 3, we have

$$\begin{aligned}
\mathbf{q}_3^* &= (\mathbf{P}_{g_{31}^*} + \mathbf{P}_{g_{32}^*})^{-1} (\mathbf{P}_{g_{31}^*} \mathbf{q}_1^* + \mathbf{P}_{g_{32}^*} \mathbf{q}_2^*) \\
&= (\mathbf{P}_{g_{31}^*} + \mathbf{P}_{g_{32}^*})^{-1} (\mathbf{P}_{g_{31}^*} \mathbf{p}_1^* + \mathbf{P}_{g_{32}^*} \mathbf{p}_2^* + (\mathbf{P}_{g_{31}^*} + \mathbf{P}_{g_{32}^*}) \delta) \\
&= \mathbf{p}_3^* + \delta.
\end{aligned}$$

For agent  $i$  ( $i = 4, \dots, n$ ), the proof is similar.  $\blacksquare$

Although the main goal is achieving a formation shape defined by some desired bearing vectors, it is important to have a measure to compare the size between two LFF formations. To this end, we have the following definition.

**Definition 3.5 (Formation scale)** Consider an LFF formation  $G(\mathbf{p})$ , the formation scale is defined as the average of all the inter-agent distances defined by the edge set,  $\mathcal{E}$ ,

$$\zeta(G(\mathbf{p})) \triangleq \frac{1}{|\mathcal{E}|} \sum_{(v_i, v_j) \in \mathcal{E}} \|\mathbf{p}_i - \mathbf{p}_j\| = \frac{1}{|\mathcal{E}|} \sum_{e_{ij} \in \mathcal{E}} d_{ij}.$$

**Lemma 3.6 (Scale of the target formation)** For an LFF formation, if  $d_{21}^*$  is scaled by  $\alpha$ , the inter-agent distance function is scaled by  $\alpha$ , i.e, the formation scale is determined by  $d_{21}^*$ .

*Proof:* Suppose that  $\mathbf{p}_2^* - \mathbf{p}_1^*$  is changed to  $\alpha(\mathbf{p}_2^* - \mathbf{p}_1^*)$  for  $\alpha \neq 0$ , then for any  $e_{ij} \in \mathcal{E}$ ,  $\mathbf{p}_i^* - \mathbf{p}_j^*$  will be changed to  $\alpha(\mathbf{p}_i^* - \mathbf{p}_j^*)$ . We only consider  $n = 3$  without loss of generality. Since

$$\begin{aligned}
\mathbf{p}_3^* - \mathbf{p}_1^* &= (\mathbf{P}_{g_{31}^*} + \mathbf{P}_{g_{32}^*})^{-1} (\mathbf{P}_{g_{31}^*} \mathbf{p}_1^* + \mathbf{P}_{g_{32}^*} \mathbf{p}_2^*) - \mathbf{p}_1^* \\
&= (\mathbf{P}_{g_{31}^*} + \mathbf{P}_{g_{32}^*})^{-1} (\mathbf{P}_{g_{31}^*} \mathbf{p}_1^* + \mathbf{P}_{g_{32}^*} \mathbf{p}_2^* - (\mathbf{P}_{g_{31}^*} + \mathbf{P}_{g_{32}^*}) \mathbf{p}_1^*) \\
&= (\mathbf{P}_{g_{31}^*} + \mathbf{P}_{g_{32}^*})^{-1} \mathbf{P}_{g_{32}^*} (\mathbf{p}_2^* - \mathbf{p}_1^*).
\end{aligned}$$

It follows that when  $\mathbf{p}_2^* - \mathbf{p}_1^*$  is changed to  $\alpha(\mathbf{p}_2^* - \mathbf{p}_1^*)$ ,  $\mathbf{p}_3^* - \mathbf{p}_1^*$  will be changed to  $\alpha(\mathbf{p}_3^* - \mathbf{p}_1^*)$ . For other displacements, the proof is similar.  $\blacksquare$

### 3.2 Bearing-only control of LFF formations

#### 3.2.1 Problem formulation

Consider a group of  $n$  agents modeled by a single integrator model,

$$\dot{\mathbf{p}}_i = \mathbf{u}_i, \quad i = 1, \dots, n. \quad (3.5)$$

where  $\mathbf{p}_i \in \mathbb{R}^d$  and  $\mathbf{u}_i \in \mathbb{R}^d$  are the position and the control input of agent  $i$  at time instance  $t$ , respectively. All agents in the group have access to a common global reference frame and each agent can sense the relative bearing vectors to its neighbors. We assume that the  $n$ -agent system satisfies the following assumptions.

**Assumption 3.1** *The sensing graph in the group is characterized by a graph  $G = (\mathcal{V}, \mathcal{E})$  generated from a Henneberg construction. Each agent can measure the bearing vectors with regard to its neighbor agents.*

**Assumption 3.2** *The information of a desired formation is given as a set of feasible desired bearing constraints  $\mathcal{B} = \{\mathbf{g}_{ij}^* \in \mathbb{R}^d \mid e_{ij} \in \mathcal{E}\}$ . The feasibility conditions are: (i) there exists a configuration  $\bar{\mathbf{p}} \in \mathbb{R}^{dn}$  such that  $\mathbf{g}_{ij}^* = \frac{\bar{\mathbf{p}}_j - \bar{\mathbf{p}}_i}{\|\bar{\mathbf{p}}_j - \bar{\mathbf{p}}_i\|}, \forall \mathbf{g}_{ij}^* \in \mathcal{B}$ ; (ii) Agent  $i$ 's ( $3 \leq i \leq n$ ) desired position is not collinear with its two neighbor agents  $j, k$  ( $1 \leq j \neq k < i$ ), i.e.,  $\mathbf{g}_{ij}^* \neq \pm \mathbf{g}_{ik}^*$ .*

Note that Assumption 3.2 implies that the desired bearing vectors have been chosen to guarantee the coplanarity condition as discussed in the subsection 3.1.2.

**Assumption 3.3** *Initially, the positions of all agents are not collocated, i.e.,  $\mathbf{p}_i(0) \neq \mathbf{p}_j(0), \forall 1 \leq i \neq j \leq n$ .*

This section aims to solve the following problem.

**Problem 3.1** Under the Assumptions 3.1-3.3, design control laws for the agents using only local bearing information such that all desired bearing vectors in  $\mathcal{B}$  are asymptotically achieved as  $t \rightarrow \infty$ .

### 3.2.2 Almost global stabilization of LFF formations

The following bearing-only control law is proposed for each agent  $i$  ( $i = 1, \dots, n$ ):

$$\dot{\mathbf{p}}_i = \mathbf{u}_i = - \sum_{j \in \mathcal{N}_i} \mathbf{P}_{\mathbf{g}_{ij}} \mathbf{g}_{ij}^*. \quad (3.6)$$

We will prove that the control law (3.6) almost globally stabilizes the  $n$ -agent system to the target formation satisfying all bearing vectors in  $\mathcal{B}$ . Note that almost global stability is understood in the sense that every trajectory starting in  $\mathbb{R}^{dn} \setminus \mathcal{A}$  asymptotically converges to the target formation, where  $\mathcal{A}$  is a set of measure zero in  $\mathbb{R}^{dn}$  [87, 88]. The analysis starts from the leader and the first follower to other followers. Due to the cascade structure of LFF formations, mathematical induction will be invoked to establish almost global stability of the  $n$ -agent LFF formation.

#### 3.2.2.1 The leader and the first follower

Since the leader (agent 1) has no neighbor, from (3.6),  $\dot{\mathbf{p}}_1 = \mathbf{u}_1 = \mathbf{0}$  and the leader's position is fixed at  $\mathbf{p}_1 = \mathbf{p}_1^*$  for all  $t \geq 0$ . The first follower (agent 2) can measure one bearing constraint  $\mathbf{g}_{21}$  and has to asymptotically reach to  $\mathbf{p}_{2a}^* = \mathbf{p}_1^* - d_{21}\mathbf{g}_{21}^*$  corresponding to  $\mathbf{g}_{21} = \mathbf{g}_{21}^*$  (see Fig. 3.5). The control law for agent 2 is proposed as

$$\dot{\mathbf{p}}_2 = \mathbf{u}_2 = -\mathbf{P}_{\mathbf{g}_{21}} \mathbf{g}_{21}^*. \quad (3.7)$$

We have the following result for the equilibrium of the first follower.

**Lemma 3.7** Under Assumptions 3.1-3.3 and control law (3.7): (i)  $d_{21}$  is invariant; (ii) There are two equilibria of (3.7):  $\mathbf{p}_{2a}^* = \mathbf{p}_1^* - d_{21}\mathbf{g}_{21}^*$  where  $\mathbf{g}_{21} = \mathbf{g}_{21}^*$  and  $\mathbf{p}_{2b}^* = \mathbf{p}_1^* + d_{21}\mathbf{g}_{21}^*$  where  $\mathbf{g}_{21} = -\mathbf{g}_{21}^*$ . The equilibrium  $\mathbf{p}_{2a}^*$  is almost globally exponentially stable, while the equilibrium  $\mathbf{p}_{2b}^*$  is unstable.

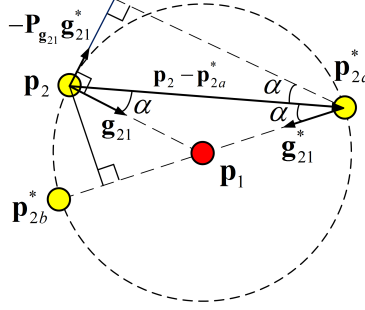


Figure 3.5. Agent 2 adopts the control law (3.7). There are two isolated equilibria  $p_{2a}^*$  and  $p_{2b}^*$  corresponding to  $\mathbf{g}_{21} = \mathbf{g}_{21}^*$  and  $\mathbf{g}_{21} = -\mathbf{g}_{21}^*$ , respectively.

*Proof:* (i) We have

$$\frac{d}{dt} d_{21}^2 = \frac{d}{dt} (\mathbf{z}_{21}^\top \mathbf{z}_{21}) = 2\mathbf{z}_{21}^\top \dot{\mathbf{z}}_{21} = 2\mathbf{z}_{21}^\top (\dot{\mathbf{p}}_1 - \dot{\mathbf{p}}_2) = 2\mathbf{z}_{21}^\top \mathbf{P}_{\mathbf{g}_{21}} \mathbf{g}_{21}^* = 0, \quad (3.8)$$

where the last equality follows from  $\mathbf{z}_{21}^\top \mathbf{P}_{\mathbf{g}_{21}} = \mathbf{0}^\top$ . Thus,  $d_{21}$  is invariant under the control law (3.7).

(ii) It follows from (3.7) and the property of the projection matrix that  $\dot{\mathbf{p}}_2 = \mathbf{0}$  if and only if  $\mathbf{g}_{21} = \mathbf{g}_{21}^*$  or  $\mathbf{g}_{21} = -\mathbf{g}_{21}^*$ . Since  $d_{21}$  is invariant, in  $\mathbb{R}^d$  there are only two equilibrium points:  $p_{2a}^*$  corresponding to  $\mathbf{g}_{21} = \mathbf{g}_{21}^*$  and  $p_{2b}^*$  corresponding to  $\mathbf{g}_{21} = -\mathbf{g}_{21}^*$  as depicted in Fig. 3.5.

Consider the Lyapunov function  $V_b = \frac{1}{2} \|\mathbf{p}_2 - \mathbf{p}_{2b}^*\|^2$ , which is continuously differentiable everywhere since  $d_{21} = d_{21}(0) \neq 0$  for all  $t \geq 0$ . Moreover,  $V_b$  is positive definite and  $V_b = 0$  if and only if  $\mathbf{p}_2 = \mathbf{p}_{2b}^*$ . The derivative of  $V_b$  along a trajectory of system (3.7) is

$$\begin{aligned} \dot{V}_b &= (\mathbf{p}_2 - \mathbf{p}_{2b}^*)^\top \dot{\mathbf{p}}_2 = -(\mathbf{p}_2 - \mathbf{p}_{2b}^*)^\top \mathbf{P}_{\mathbf{g}_{21}} \mathbf{g}_{21}^* \\ &= (\mathbf{p}_2 - \mathbf{p}_{2b}^*)^\top \frac{\mathbf{P}_{\mathbf{g}_{21}}}{d_{21}} (\mathbf{p}_1 - \mathbf{p}_2 + \mathbf{p}_2 - \mathbf{p}_{2b}^*) \\ &= (\mathbf{p}_2 - \mathbf{p}_{2b}^*)^\top \frac{\mathbf{P}_{\mathbf{g}_{21}}}{d_{21}} (\mathbf{p}_2 - \mathbf{p}_{2b}^*) \geq 0, \end{aligned} \quad (3.9)$$

since  $\mathbf{P}_{\mathbf{g}_{21}} \mathbf{z}_{21} = \mathbf{0}$  and  $\mathbf{P}_{\mathbf{g}_{21}}$  is positive semidefinite. Therefore,  $\mathbf{p}_2 = \mathbf{p}_{2b}^*$  is unstable by Chetaev's instability theorem [125][Theorem 4.3].

Similarly, consider the Lyapunov function  $V_a = \frac{1}{2} \|\mathbf{p}_2 - \mathbf{p}_{2a}^*\|^2$ , which is continuously differen-

tiable, radially unbounded. Moreover,  $V_a$  is positive definite,  $V_a = 0$  if and only if  $\mathbf{p}_2 = \mathbf{p}_{2a}^*$ . Along a trajectory of system (3.7),

$$\dot{V}_a = (\mathbf{p}_2 - \mathbf{p}_{2a}^*)^\top \dot{\mathbf{p}}_2 = -(\mathbf{p}_2 - \mathbf{p}_{2a}^*)^\top \mathbf{P}_{g_{21}} \mathbf{g}_{21}^* = -(\mathbf{p}_2 - \mathbf{p}_{2a}^*)^\top \frac{\mathbf{P}_{g_{21}}}{d_{21}} (\mathbf{p}_2 - \mathbf{p}_{2a}^*) \leq 0. \quad (3.10)$$

Note  $\dot{V}_a = 0$  if and only if  $\mathbf{p}_2 = \mathbf{p}_{2a}^*$  or  $\mathbf{p}_2 = \mathbf{p}_{2b}^*$ , see Fig. 3.5. Since  $\mathbf{p}_{2b}^*$  is unstable,  $\mathbf{p}_{2a}^*$  is almost globally asymptotically stable due to LaSalle's invariance principle.

Moreover, consider  $\mathbf{p}_2(0) \neq \mathbf{p}_{2b}^*$ , we can write

$$\dot{V}_a = -\frac{2 \sin^2 \alpha}{d_{21}} V_a \leq -\frac{2 \sin^2 \alpha(0)}{d_{21}} V_a = -\kappa V_a,$$

where  $\alpha$  is the angle as depicted in Fig. 3.5,  $\alpha(0) \in (0, \frac{\pi}{2}]$  for  $\mathbf{p}_2(0) \neq \mathbf{p}_{2b}^*$ , and  $\kappa = 2d_{21}^{-1} \sin^2 \alpha(0) > 0$ . It follows that  $\mathbf{p}_2 \rightarrow \mathbf{p}_{2a}^*$  exponentially fast if  $\mathbf{p}_2(0) \neq \mathbf{p}_{2b}^*$ .  $\blacksquare$

### 3.2.2.2 The second follower

We will analyze the dynamics of agent 3 (the second follower), whose neighbors are agents 1 and 2. The other agent's dynamics can be treated later in a similar way. The dynamics of agent 3 is

$$\dot{\mathbf{p}}_3 = \mathbf{u}_3(\mathbf{p}_3, \mathbf{p}_2) = -\mathbf{P}_{g_{31}} \mathbf{g}_{31}^* - \mathbf{P}_{g_{32}} \mathbf{g}_{32}^*. \quad (3.11)$$

We consider (3.11) as a cascade system with  $\mathbf{p}_2$  being an input to the unforced system

$$\dot{\mathbf{p}}_3 = \mathbf{u}_3(\mathbf{p}_3, \mathbf{p}_{2a}^*) = -\mathbf{P}_{g_{31}} \mathbf{g}_{31}^* - \mathbf{P}_{g_{32}} \mathbf{g}_{32}^*. \quad (3.12)$$

The unforced system (3.12) characterizes the motion of agent 3 when agent 2 is located at its desired position  $\mathbf{p}_{2a}^*$ . However, if agent 2 is initially located at the undesired equilibrium  $\mathbf{p}_2(0) = \mathbf{p}_{2b}^*$ , then  $\dot{\mathbf{p}}_2(t) = \mathbf{0}$  and the dynamics of agent 3 changes to

$$\dot{\mathbf{p}}_3 = \mathbf{u}_3(\mathbf{p}_3, \mathbf{p}_{2b}^*). \quad (3.13)$$

The following lemma characterizes the equilibrium set of (3.12) and (3.13).

**Lemma 3.8** (i) The system (3.12) has a unique equilibrium point

$$\mathbf{p}_{3a}^* = (\mathbf{P}_{\mathbf{g}_{31}^*} + \mathbf{P}_{\mathbf{g}_{32}^*})^{-1} (\mathbf{P}_{\mathbf{g}_{31}^*} \mathbf{p}_1^* + \mathbf{P}_{\mathbf{g}_{32}^*} \mathbf{p}_{2a}^*)$$

corresponding to  $\mathbf{g}_{31} = \mathbf{g}_{31}^*$  and  $\mathbf{g}_{32} = \mathbf{g}_{32}^*$ .

(ii) The system (3.13) has a unique equilibrium point

$$\mathbf{p}_{3b}^* = (\mathbf{P}_{\mathbf{g}_{31}^*} + \mathbf{P}_{\mathbf{g}_{32}^*})^{-1} (\mathbf{P}_{\mathbf{g}_{31}^*} \mathbf{p}_1^* + \mathbf{P}_{\mathbf{g}_{32}^*} \mathbf{p}_{2b}^*)$$

corresponding to  $\mathbf{g}_{31} = -\mathbf{g}_{31}^*$  and  $\mathbf{g}_{32} = -\mathbf{g}_{32}^*$ .

*Proof:* (i) The equilibria of (3.12) satisfy

$$\dot{\mathbf{p}}_3 = -(\mathbf{P}_{\mathbf{g}_{31}} \mathbf{g}_{31}^* + \mathbf{P}_{\mathbf{g}_{32}} \mathbf{g}_{32}^*) = \mathbf{0}. \quad (3.14)$$

Premultiplying  $\mathbf{g}_{31}^\top$  on both sides of (3.14), we have

$$\begin{aligned} \mathbf{g}_{31}^\top (\mathbf{P}_{\mathbf{g}_{31}} \mathbf{g}_{31}^* + \mathbf{P}_{\mathbf{g}_{32}} \mathbf{g}_{32}^*) &= 0 \\ \text{or,} \quad \mathbf{g}_{31}^\top \mathbf{P}_{\mathbf{g}_{32}} \mathbf{g}_{32}^* &= 0. \end{aligned} \quad (3.15)$$

Equation (3.15) is satisfied if and only if  $\mathbf{g}_{31} = \pm \mathbf{g}_{32}$  or  $\mathbf{g}_{32}^* = \pm \mathbf{g}_{31}$ . The condition  $\mathbf{g}_{32} = \pm \mathbf{g}_{31}$  happens if and only if agent 3 is collinear with agent 1 and agent 2. In this case,  $\mathbf{P}_{\mathbf{g}_{31}} = \mathbf{P}_{\mathbf{g}_{32}} = \mathbf{P}_{\mathbf{g}_{12}^*}$ .

Substituting them into (3.14) gives  $\mathbf{P}_{\mathbf{g}_{12}^*} (\mathbf{g}_{31}^* + \mathbf{g}_{32}^*) = \mathbf{0}$ , or equivalently,

$$\mathbf{g}_{32}^* + \mathbf{g}_{31}^* = k \mathbf{g}_{12}^*, \quad (3.16)$$

where  $k$  is a nonzero constant.

On the other hand, from the assumption on feasibility of the target formation, the desired position of agent 3 and two leaders must be coplanar. Thus, there exist positive scalars  $d_{12}^*$ ,  $d_{31}^*$  and  $d_{32}^*$  such that

$$d_{12}^* \mathbf{g}_{12}^* - d_{32}^* \mathbf{g}_{32}^* + d_{31}^* \mathbf{g}_{31}^* = \mathbf{0}. \quad (3.17)$$

Substitute (3.16) into (3.17), it follows that

$$\frac{d_{12}^*}{k}(\mathbf{g}_{31}^* + \mathbf{g}_{32}^*) - d_{32}^*\mathbf{g}_{32}^* + d_{31}^*\mathbf{g}_{31}^* = \mathbf{0}$$

$$\text{or, } (d_{12}^* + kd_{31}^*)\mathbf{g}_{31}^* + (-kd_{32}^* + d_{12}^*)\mathbf{g}_{32}^* = \mathbf{0},$$

which implies  $\mathbf{g}_{31}^*$  is parallel with  $\mathbf{g}_{32}^*$ . This contradicts Assumption 2 that  $\mathbf{g}_{31}^* \neq \pm \mathbf{g}_{32}^*$ . Thus, (i) cannot happen and (3.15) holds if and only if  $\mathbf{g}_{32} = \pm \mathbf{g}_{32}^*$ . Substituting  $\mathbf{g}_{32} = \pm \mathbf{g}_{32}^*$  into (3.12), it follows that  $\mathbf{g}_{31} = \pm \mathbf{g}_{31}^*$ .

The feasibility of  $\mathcal{B}$  guarantees the existence of  $\mathbf{p}_{3a}^*$  where  $\mathbf{g}_{31}^*$  and  $\mathbf{g}_{32}^*$  are both achieved. The equilibrium  $\mathbf{p}_{3a}^*$  is uniquely determined as in Lemma 3.3. It can be seen that when  $\mathbf{p}_2 = \mathbf{p}_{2a}^*$ , the other combinations  $-\mathbf{g}_{31}^*$  and  $\mathbf{g}_{32}^*$ , or  $\mathbf{g}_{31}^*$  and  $-\mathbf{g}_{32}^*$ , or  $-\mathbf{g}_{31}^*$  and  $-\mathbf{g}_{32}^*$  are unrealizable in  $\mathbb{R}^d$ .

(ii) Following the same process as the above, the equilibrium has to satisfy  $\mathbf{g}_{31} = \pm \mathbf{g}_{31}^*$  and  $\mathbf{g}_{32} = \pm \mathbf{g}_{32}^*$ . The existence of  $\mathbf{p}_{3a}^*$  in the case (i) implies the existence of  $\mathbf{p}_{3b}^*$  which is symmetric with  $\mathbf{p}_{3a}^*$  about  $\mathbf{p}_1$  as depicted in Fig. 3.6. At  $\mathbf{p}_{3b}^*$ , the bearing vectors with regard to  $\mathbf{p}_1$  and  $\mathbf{p}_{2b}^*$  are  $\mathbf{g}_{31} = -\mathbf{g}_{31}^*$  and  $\mathbf{g}_{32} = -\mathbf{g}_{32}^*$ , respectively. ■

We discuss on stability of the equilibria of two systems (3.12) and (3.13) in the following lemma.

**Lemma 3.9** (i) The equilibrium  $\mathbf{p}_{3a}^*$  corresponding to  $\mathbf{g}_{31} = \mathbf{g}_{31}^*$  and  $\mathbf{g}_{32} = \mathbf{g}_{32}^*$  of the unforced system (3.12) is globally asymptotically stable. (ii) The equilibrium  $\mathbf{p}_{3b}^*$  corresponding to  $\mathbf{g}_{31} = -\mathbf{g}_{31}^*$  and  $\mathbf{g}_{32} = -\mathbf{g}_{32}^*$  of the unforced system (3.13) is unstable.

*Proof:* (i) Consider the Lyapunov candidate function  $V = \frac{1}{2}\|\mathbf{p}_3 - \mathbf{p}_{3a}^*\|^2$  which is positive

definite, radially unbounded and continuously differentiable. We have

$$\begin{aligned}
\dot{V} &= -(\mathbf{p}_3 - \mathbf{p}_{3a}^*)^\top (\mathbf{P}_{g_{31}} \mathbf{g}_{31}^* + \mathbf{P}_{g_{32}} \mathbf{g}_{32}^*) \\
&= -(\mathbf{p}_3 - \mathbf{p}_{3a}^*)^\top \frac{\mathbf{P}_{g_{31}}}{\|\mathbf{z}_{31}^*\|} (\mathbf{p}_1 - \mathbf{p}_3 + \mathbf{p}_3 - \mathbf{p}_{3a}^*) - (\mathbf{p}_3 - \mathbf{p}_{3a}^*)^\top \frac{\mathbf{P}_{g_{32}}}{\|\mathbf{z}_{32}^*\|} (\mathbf{p}_2 - \mathbf{p}_3 + \mathbf{p}_3 - \mathbf{p}_{3a}^*) \\
&= -(\mathbf{p}_3 - \mathbf{p}_{3a}^*)^\top \underbrace{\left( \frac{\mathbf{P}_{g_{31}}}{\|\mathbf{z}_{31}^*\|} + \frac{\mathbf{P}_{g_{32}}}{\|\mathbf{z}_{32}^*\|} \right)}_{\triangleq \mathbf{M}} (\mathbf{p}_3 - \mathbf{p}_{3a}^*).
\end{aligned} \tag{3.18}$$

Since  $\mathbf{P}_{g_{31}}$  and  $\mathbf{P}_{g_{32}}$  are positive semi-definite matrices,  $\mathbf{M}$  is also positive semi-definite. Thus,

$\dot{V} \leq 0$ . Moreover,  $\dot{V} = 0$  if and only if  $(\mathbf{p}_3 - \mathbf{p}_{3a}^*) \in \mathcal{N}(\mathbf{M})$ . We consider two cases:

- If  $\mathbf{g}_{31} = \pm \mathbf{g}_{32}$  or three agents are in collinear positions, then,  $\mathcal{N}(\mathbf{M}) = \text{span}\{\mathbf{g}_{31}\}$ . Due to Assumption 3.2 on the feasibility of  $\mathcal{B}$ ,  $\mathbf{p}_{3a}^*$  is not collinear with  $\mathbf{p}_1$  and  $\mathbf{p}_{2a}^*$ , that is  $(\mathbf{p}_3 - \mathbf{p}_{3a}^*) \notin \mathcal{N}(\mathbf{M})$ . Therefore,

$$\dot{V} \leq -\gamma \sin^2 \alpha \|\mathbf{p}_3 - \mathbf{p}_{3a}^*\|^2 = -\gamma \sin^2 \alpha V \leq 0,$$

where  $\alpha$  is the angle between the line connecting  $\mathbf{p}_3$  and  $\mathbf{p}_{3a}^*$  and the line connecting  $\mathbf{p}_1$  and  $\mathbf{p}_{2a}^*$  as depicted in Fig. 3.6, and  $\gamma = \|\mathbf{z}_{31}^*\|^{-1} + \|\mathbf{z}_{32}^*\|^{-1}$ . It is easy to see that  $\alpha \in (0, \pi)$ .

- If  $\mathbf{g}_{31} \neq \pm \mathbf{g}_{32}$ ,  $\mathbf{M}$  is positive definite by Lemma 2.9. As a result,

$$\dot{V} \leq -\lambda_{\min}(\mathbf{M}(t)) \|\mathbf{p}_3 - \mathbf{p}_{3a}^*\|^2 = -\lambda_{\min}(\mathbf{M}(t)) V \leq 0,$$

where  $\lambda_{\min}(\mathbf{M}(t)) > 0$  is the smallest eigenvalue of  $\mathbf{M}$  at time  $t$  and  $\dot{V} = 0$  if and only if  $\mathbf{p}_3 = \mathbf{p}_{3a}^*$ .

Choosing  $\kappa = \min\{\inf_t \{\lambda_{\min}(\mathbf{M})\}, \gamma \sin^2 \alpha\} > 0$ , it follows that  $\dot{V} \leq -\kappa V \leq 0$ . As a result,  $\dot{V}$  is negative definite and  $\dot{V} = 0$  if and only if  $\mathbf{p}_3 = \mathbf{p}_{3a}^*$ . Thus,  $\mathbf{p}_3 = \mathbf{p}_{3a}^*$  of (3.12) is globally asymptotically stable [125].

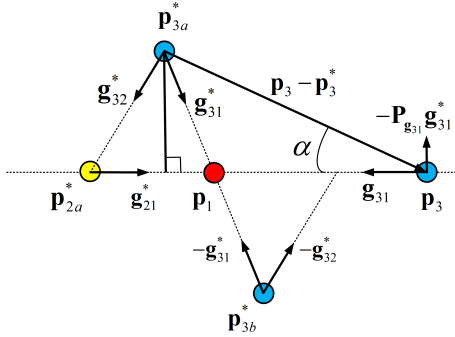


Figure 3.6. Illustration when the position of agent 3,  $\mathbf{p}_3$ , is collinear with  $\mathbf{p}_1$  and  $\mathbf{p}_{2a}^*$ .

(ii) Consider the Lyapunov function  $V = \frac{1}{2}\|\mathbf{p}_3 - \mathbf{p}_{3b}^*\|^2$ . Similar to (i), along a trajectory of system (3.13), there holds

$$\begin{aligned}\dot{V} &= (\mathbf{p}_3 - \mathbf{p}_{3b}^*)^\top (\mathbf{P}_{\mathbf{g}_{31}}(-\mathbf{g}_{31}^*) + \mathbf{P}_{\mathbf{g}_{32}}(-\mathbf{g}_{32}^*)) \\ &= (\mathbf{p}_3 - \mathbf{p}_{3b}^*)^\top \frac{\mathbf{P}_{\mathbf{g}_{31}}}{\|\mathbf{z}_{31}^*\|} (\mathbf{p}_1 - \mathbf{p}_3 + \mathbf{p}_3 - \mathbf{p}_{3b}^*) + (\mathbf{p}_3 - \mathbf{p}_{3b}^*)^\top \frac{\mathbf{P}_{\mathbf{g}_{32}}}{\|\mathbf{z}_{32}^*\|} (\mathbf{p}_2 - \mathbf{p}_3 + \mathbf{p}_3 - \mathbf{p}_{3b}^*) \\ &= (\mathbf{p}_3 - \mathbf{p}_{3b}^*)^\top \left( \frac{\mathbf{P}_{\mathbf{g}_{31}}}{\|\mathbf{z}_{31}^*\|} + \frac{\mathbf{P}_{\mathbf{g}_{32}}}{\|\mathbf{z}_{32}^*\|} \right) (\mathbf{p}_3 - \mathbf{p}_{3b}^*) \\ &= (\mathbf{p}_3 - \mathbf{p}_{3b}^*)^\top \mathbf{M} (\mathbf{p}_3 - \mathbf{p}_{3b}^*) \geq 0.\end{aligned}$$

Thus,  $\dot{V} > 0$  if  $\mathbf{p}_3 \neq \mathbf{p}_{3b}^*$ . The equilibrium  $\mathbf{p}_3 = \mathbf{p}_{3b}^*$  is unstable and  $\|\mathbf{p}_3 - \mathbf{p}_3^*\|$  grows unbounded in this case. Thus,  $\mathbf{p}_2(0) \neq \mathbf{p}_{2b}^*$  is required to avoid the divergence of  $\mathbf{p}_3$ . ■

Since the bearing vectors are undefined when the neighbor agents are collocated, the analysis is valid when collision avoidance is guaranteed. In practice, when each agent is equipped with vision sensors, collision avoidance can be treated independently by vision-based techniques, see [131, 132] and the references therein for examples. A sufficient condition for collision-free between agent 3 and its leaders under the dynamics (3.12) is given in the following lemma.

**Lemma 3.10** *Consider the system (3.12), agent 3 never collides with agents 1 and agent 2 if*

$$\|\mathbf{p}_3(0) - \mathbf{p}_3^*\| < \min\{\|\mathbf{p}_3^* - \mathbf{p}_1^*\|, \|\mathbf{p}_3^* - \mathbf{p}_{2a}^*\|\}. \quad (3.19)$$

*Proof:* Agent 3 never collides with agent 1 if  $\|\mathbf{p}_3 - \mathbf{p}_1\| = \|\mathbf{p}_3 - \mathbf{p}_1^*\| > 0, \forall t \geq 0$ . Since

$$\|\mathbf{p}_3 - \mathbf{p}_1^*\| = \|(\mathbf{p}_3 - \mathbf{p}_3^*) + (\mathbf{p}_3^* - \mathbf{p}_1^*)\| \geq \|\mathbf{p}_3^* - \mathbf{p}_1^*\| - \|\mathbf{p}_3 - \mathbf{p}_3^*\|,$$

and  $\mathbf{p}_3 \rightarrow \mathbf{p}_3^*$  asymptotically (Lemma 3.9(i)), the following condition is sufficient to avoid collision between agent 1 and agent 3

$$\|\mathbf{p}_3(0) - \mathbf{p}_3^*\| < \|\mathbf{p}_3^* - \mathbf{p}_1^*\|.$$

Similarly, a sufficient condition for collision-free between agent 2 and agent 3 is given as

$$\|\mathbf{p}_3(0) - \mathbf{p}_3^*\| < \|\mathbf{p}_3^* - \mathbf{p}_{2a}^*\|.$$

Thus, condition (3.19) guarantees collision-free between agent 3 and its leaders. ■

**Remark 3.11** In [66], a bearing-only navigation problem in a two-dimensional space with three stationary landmarks was studied. The authors in [66] proposed a 2D version of the control law (3.12) to guide an agent to any desired position in  $\mathbb{R}^2$ . Lemma 3.9(i) improved the result in [66, Proposition 1] by showing that it is sufficient to use only two stationary landmarks to reach any position in  $\mathbb{R}^d$  that is not collinear with the two landmarks.

At this stage, we can prove the following result on the stability of the system (3.11).

**Proposition 3.12** The system (3.11) has an almost globally asymptotically stable equilibrium  $\mathbf{p}_3 = \mathbf{p}_{3a}^*$  corresponding to  $\mathbf{g}_{31} = \mathbf{g}_{31}^*$  and  $\mathbf{g}_{32} = \mathbf{g}_{32}^*$ .

*Proof:* It will be first shown that the system (3.11) satisfies the ultimate boundedness property. Consider the Lyapunov function  $V = \frac{1}{2}\|\mathbf{p}_3 - \mathbf{p}_{3a}^*\|^2$  which is positive definite, radially unbounded and continuously differentiable. If  $\mathbf{p}_2(0) \neq \mathbf{p}_{2b}^*$ , the derivative of  $V$  along a trajectory of system

(3.11) is

$$\begin{aligned}
\dot{V} &= -2(\mathbf{p}_3 - \mathbf{p}_3^*)^\top (\mathbf{P}_{\mathbf{g}_{31}} \mathbf{g}_{31}^* + \mathbf{P}_{\mathbf{g}_{32}} \mathbf{g}_{32}^*) \\
&= -(\mathbf{p}_3 - \mathbf{p}_3^*)^\top \left( \frac{\mathbf{P}_{\mathbf{g}_{31}}}{\|\mathbf{z}_{31}^*\|} (\mathbf{p}_1 - \mathbf{p}_3 + \mathbf{p}_3 - \mathbf{p}_{3a}^*) + \frac{\mathbf{P}_{\mathbf{g}_{32}}}{\|\mathbf{z}_{32}^*\|} (\mathbf{p}_{2a}^* - \mathbf{p}_2 + \mathbf{p}_2 - \mathbf{p}_3 + \mathbf{p}_3 - \mathbf{p}_{3a}^*) \right) \\
&= -(\mathbf{p}_3 - \mathbf{p}_3^*)^\top \left( \frac{\mathbf{P}_{\mathbf{g}_{31}}}{\|\mathbf{z}_{31}^*\|} + \frac{\mathbf{P}_{\mathbf{g}_{32}}}{\|\mathbf{z}_{32}^*\|} \right) (\mathbf{p}_3 - \mathbf{p}_3^*) + (\mathbf{p}_3 - \mathbf{p}_3^*)^\top \frac{\mathbf{P}_{\mathbf{g}_{32}}}{\|\mathbf{z}_{32}^*\|} (\mathbf{p}_2 - \mathbf{p}_{2a}^*) \\
&\leq -(\mathbf{p}_3 - \mathbf{p}_3^*)^\top \left( \frac{\mathbf{P}_{\mathbf{g}_{31}}}{\|\mathbf{z}_{31}^*\|} + \frac{\mathbf{P}_{\mathbf{g}_{32}}}{\|\mathbf{z}_{32}^*\|} \right) (\mathbf{p}_3 - \mathbf{p}_3^*) + \|\mathbf{p}_3 - \mathbf{p}_3^*\| \frac{\|\mathbf{P}_{\mathbf{g}_{32}}\|}{\|\mathbf{z}_{32}^*\|} \|\mathbf{p}_2 - \mathbf{p}_{2a}^*\| \\
&\leq -(\mathbf{p}_3 - \mathbf{p}_3^*)^\top \left( \frac{\mathbf{P}_{\mathbf{g}_{31}}}{\|\mathbf{z}_{31}^*\|} + \frac{\mathbf{P}_{\mathbf{g}_{32}}}{\|\mathbf{z}_{32}^*\|} \right) (\mathbf{p}_3 - \mathbf{p}_3^*) + \frac{2d_{21}}{\|\mathbf{z}_{32}^*\|} \|\mathbf{p}_3 - \mathbf{p}_3^*\|. \tag{3.20}
\end{aligned}$$

When  $\|\mathbf{p}_3\|$  is large, the second term in (3.20) is  $\mathcal{O}(\|\mathbf{p}_3 - \mathbf{p}_{3a}^*\|)$  while the first term is  $-\mathcal{O}(\|\mathbf{p}_3 - \mathbf{p}_{3a}^*\|^2)$ . This implies  $\dot{V} < 0$  when  $\|\mathbf{p}_3\|$  is large. Equivalently,  $\|\mathbf{p}_3 - \mathbf{p}_{3a}^*\|$  is ultimately bounded and so is  $\|\mathbf{p}_3\|$ . Since the unforced system (3.12) has a globally asymptotically stable equilibrium  $\mathbf{p}_{3a}^*$  as shown in Lemma 3.9 and satisfies the ultimate boundedness property, the system (3.11) is input-to-state stable (ISS) with regard to the input  $\mathbf{p}_2$ . On the other hand, according to Lemma 3.7, the input  $\mathbf{p}_2$  exponentially converges to  $\mathbf{p}_{2a}^*$  if it is not initially located at  $\mathbf{p}_{2b}^*$ . Thus, the equilibrium  $\mathbf{p}_3 = \mathbf{p}_{3a}^*$  is almost globally asymptotically stable according to Theorem 2.5. ■

By Proposition 3.1, the desired equilibrium  $\mathbf{p}_2 = \mathbf{p}_{2a}^*, \mathbf{p}_3 = \mathbf{p}_{3a}^*$  of the cascade system

$$\begin{aligned}
\dot{\mathbf{p}}_2 &= \mathbf{u}_2(\mathbf{p}_2), \\
\dot{\mathbf{p}}_3 &= \mathbf{u}_3(\mathbf{p}_3, \mathbf{p}_2). \tag{3.21}
\end{aligned}$$

is proved to be almost globally asymptotically stable. All trajectories of (3.21) converge to the desired positions except for those starting at  $\mathbf{p}_2(0) = \mathbf{p}_{2b}^*$ . Moreover, the undesired equilibrium  $\mathbf{p}_2 = \mathbf{p}_{2b}^*, \mathbf{p}_3 = \mathbf{p}_{3b}^*$  is unstable.

### 3.2.2.3 The $n$ -agent system

Consider the LFF formation of  $n$ -agents ( $n \geq 3$ ) satisfying all assumptions in Problem 3.1. From the assumption on the graph  $G$ , each agent  $i$  ( $3 \leq i \leq n$ ) has two neighbors  $1 \leq j \neq k \leq i-1$  and must control two bearing vectors  $\mathbf{g}_{ij}, \mathbf{g}_{ik}$ . The control law for agent  $i$  is explicitly given as

$$\dot{\mathbf{p}}_i = \mathbf{u}_i(\mathbf{p}_i, \mathbf{p}_{i-1}, \dots, \mathbf{p}_2) = -\mathbf{P}_{\mathbf{g}_{ij}} \mathbf{g}_{ij}^* - \mathbf{P}_{\mathbf{g}_{ik}} \mathbf{g}_{ik}^*. \quad (3.22)$$

The dynamics of  $n$  agents can be expressed in the form of a cascade system:

$$\dot{\mathbf{p}} = \begin{bmatrix} \dot{\mathbf{p}}_1 \\ \dot{\mathbf{p}}_2 \\ \dot{\mathbf{p}}_3 \\ \vdots \\ \dot{\mathbf{p}}_i \\ \vdots \\ \dot{\mathbf{p}}_n \end{bmatrix} = \begin{bmatrix} \mathbf{0} \\ \mathbf{u}_2(\mathbf{p}_2) \\ \mathbf{u}_3(\mathbf{p}_3, \mathbf{p}_2) \\ \vdots \\ \mathbf{u}_i(\mathbf{p}_i, \mathbf{p}_{i-1}, \dots, \mathbf{p}_2) \\ \vdots \\ \mathbf{u}_n(\mathbf{p}_n, \mathbf{p}_{n-1}, \dots, \mathbf{p}_2) \end{bmatrix}, \quad (3.23)$$

where  $(\mathbf{p}_{i-1}, \dots, \mathbf{p}_2)$  is considered as an input to the dynamics of an agent  $i$  ( $i = 3, \dots, n$ ). From Lemmas 3.8 and 3.9, for each  $i = 3, \dots, n$ , the equilibrium

$$\mathbf{p}_i = \mathbf{p}_{ia}^* = \left( \sum_{j \in \mathcal{N}_i} \mathbf{P}_{\mathbf{g}_{ij}}^* \right)^{-1} \left( \sum_{j \in \mathcal{N}_i} \mathbf{P}_{\mathbf{g}_{ij}} \mathbf{p}_{ja}^* \right)$$

is a globally asymptotically stable equilibrium of the unforced subsystem

$$\dot{\mathbf{p}}_i = \mathbf{u}_i(\mathbf{p}_i, \mathbf{p}_{(i-1)a}^*, \dots, \mathbf{p}_{2a}^*). \quad (3.24)$$

Based on results on the stability of cascade interconnected systems, we can prove almost global stability of the system (3.23) in the following theorem.

**Theorem 3.13** Under the Assumptions 3.1-3.3 and the proposed control laws, the system (3.23) has two equilibria. The equilibrium  $\mathbf{p}_a^* = [\mathbf{p}_1^{*\top}, \mathbf{p}_{2a}^{*\top}, \dots, \mathbf{p}_{na}^{*\top}]^\top$  satisfying all desired bearings constraints in  $\mathcal{B}$  is almost globally asymptotically stable. The equilibrium  $\mathbf{p}_b^* = [\mathbf{p}_1^\top, \mathbf{p}_{2b}^{*\top}, \dots, \mathbf{p}_{nb}^{*\top}]^\top$  is unstable. All trajectories starting with  $\mathbf{p}_2(0) \neq \mathbf{p}_{2b}^*$  asymptotically converge to  $\mathbf{p}_a^*$ .

*Proof:* We will prove this theorem by mathematical induction. Consider  $\mathbf{p}_2(0) \neq \mathbf{p}_{2b}^*$ . Firstly, for  $l = 2$ , we have  $\mathbf{p}_2 = \mathbf{p}_{2a}^*$  is almost globally asymptotically stable and  $\mathbf{p}_2 = \mathbf{p}_{2b}^*$  is unstable based on Lemma 3.7. Thus, Theorem 3.13 is true for  $l = 2$ . Secondly, Theorem 3.13 is also true for  $l = 3$  based on Proposition 3.12.

Secondly, suppose that the claim of Theorem 3.13 is true for  $l = 3, 4, \dots, i - 1$ . That is,  $\mathbf{p}_i = \mathbf{p}_{ia}^*$  is globally asymptotically stable for all  $3 \leq l \leq i - 1$ . We have to prove that the theorem is also true for  $l = i$ . By following a similar process as in the proof of Lemma 3.9, we can show that  $\mathbf{p}_{ia}^*$  is a globally asymptotically stable equilibrium of the unforced system (3.24).

We will next show that  $\mathbf{p}_i(t)$  is bounded. To this end, suppose  $i$  has two neighbor agents  $j$  and  $k$ ,  $1 \leq j \neq k < i$ . Consider the Lyapunov function  $V = \frac{1}{2}\|\mathbf{p}_i - \mathbf{p}_{ia}^*\|^2$  which is positive definite, radially unbounded and continuously differentiable. The derivative of  $V$  along a trajectory of the system (3.24) is given by

$$\begin{aligned} \dot{V} &= -(\mathbf{p}_i - \mathbf{p}_{ia}^*)^\top (\mathbf{P}_{\mathbf{g}_{ij}} \mathbf{g}_{ij}^* + \mathbf{P}_{\mathbf{g}_{ik}} \mathbf{g}_{ik}^*) \\ &= -(\mathbf{p}_i - \mathbf{p}_{ia}^*)^\top \left( \frac{\mathbf{P}_{\mathbf{g}_{ij}}}{\|\mathbf{z}_{ij}^*\|} (\mathbf{p}_{ja}^* - \mathbf{p}_j + \mathbf{p}_j - \mathbf{p}_i + \mathbf{p}_i - \mathbf{p}_{ia}^*) + \frac{\mathbf{P}_{\mathbf{g}_{ik}}}{\|\mathbf{z}_{ik}^*\|} (\mathbf{p}_{ka}^* - \mathbf{p}_k + \mathbf{p}_k - \mathbf{p}_i + \mathbf{p}_i - \mathbf{p}_{ia}^*) \right) \\ &= -(\mathbf{p}_i - \mathbf{p}_{ia}^*)^\top \left( \frac{\mathbf{P}_{\mathbf{g}_{ij}}}{\|\mathbf{z}_{ij}^*\|} + \frac{\mathbf{P}_{\mathbf{g}_{ik}}}{\|\mathbf{z}_{ik}^*\|} \right) (\mathbf{p}_i - \mathbf{p}_{ia}^*) - (\mathbf{p}_i - \mathbf{p}_{ia}^*)^\top \left( \frac{\mathbf{P}_{\mathbf{g}_{ij}}}{\|\mathbf{z}_{ij}^*\|} (\mathbf{p}_{ja}^* - \mathbf{p}_j) + \frac{\mathbf{P}_{\mathbf{g}_{ik}}}{\|\mathbf{z}_{ik}^*\|} (\mathbf{p}_{ka}^* - \mathbf{p}_k) \right) \\ &\leq -(\mathbf{p}_i - \mathbf{p}_{ia}^*)^\top \mathbf{M}(\mathbf{p}_i - \mathbf{p}_{ia}^*) + \|\mathbf{p}_i - \mathbf{p}_{ia}^*\| \left( \frac{\|\mathbf{P}_{\mathbf{g}_{ij}}\|}{\|\mathbf{z}_{ij}^*\|} \|\mathbf{p}_{ja}^* - \mathbf{p}_j\| + \frac{\|\mathbf{P}_{\mathbf{g}_{ik}}\|}{\|\mathbf{z}_{ik}^*\|} \|\mathbf{p}_{ka}^* - \mathbf{p}_k\| \right) \end{aligned}$$

Because Theorem 3.13 is true for  $l \leq i - 1$ ,  $\|\mathbf{p}_j - \mathbf{p}_{ja}^*\|$  and  $\|\mathbf{p}_k - \mathbf{p}_{ka}^*\|$  are bounded and converge to zero as  $t \rightarrow +\infty$ . It follows that  $\|\mathbf{p}_i - \mathbf{p}_{ia}^*\|$  and thus  $\|\mathbf{p}_i\|$  is bounded. Thus, the equilibrium  $\mathbf{p}_{ia}^*$

is asymptotically stable and all trajectories with  $\mathbf{p}_2(0) \neq \mathbf{p}_{2b}^*$  converge to  $\mathbf{p}_{ia}^*$  (Theorem 2.5). Further, if  $\mathbf{p}_2(0) = \mathbf{p}_{2b}^*$ , the system has an unstable equilibrium  $\mathbf{p}_{ib}^*$  due to Lemma 3.9. Therefore,  $\mathbf{p}_i = \mathbf{p}_{ia}^*$  is almost globally asymptotically stable and Theorem 3.13 is also true for  $l = i$ .

Finally, from mathematical induction, the claim holds for all  $l \geq 3$ . Thus the  $n$ -agent system (3.23) is almost globally asymptotically stable. All trajectories satisfying  $\mathbf{p}_2(0) \neq \mathbf{p}_{2b}^*$  converge to a formation satisfying all desired bearing vectors in  $\mathcal{B}$ . If  $\mathbf{p}_2(0) = \mathbf{p}_{2b}^*$ , the system has an undesired equilibrium where  $\mathbf{g}_{ij} = -\mathbf{g}_{ij}^*$  for all  $\mathbf{g}_{ij}^* \in \mathcal{B}$ . This undesired equilibrium is unstable. ■

### 3.2.3 Global stabilization of LFF formations

In the previous subsection, the fact that instead of the global stabilization we have an almost global stabilization of the overall formation is due to the possibility that  $\mathbf{p}_2(0) = \mathbf{p}_{2b}^*$ , which is an unstable equilibrium. Of course, in practice noise may displace the system from  $\mathbf{p}_{2b}^*$  if it is initialized there. However, instead of relying on noise, we can propose the following modified bearing-only control law for agent 2:

$$\mathbf{u}_2 = -\mathbf{P}_{\mathbf{g}_{21}} \mathbf{g}_{21}^* - k \|\mathbf{g}_{21} - \mathbf{g}_{21}^*\| \mathbf{P}_{\mathbf{g}_{21}} (\text{sgn}(\mathbf{P}_{\mathbf{g}_{21}} \mathbf{g}_{21}^*) + \mathbf{n}). \quad (3.25)$$

In this control law,  $k > 0$  is a control gain,  $\text{sgn}$  denotes the signum function,  $\text{sgn}(\mathbf{P}_{\mathbf{g}_{21}} \mathbf{g}_{21}^*) \triangleq [\text{sgn}([\mathbf{P}_{\mathbf{g}_{21}} \mathbf{g}_{21}^*]_1), \dots, \text{sgn}([\mathbf{P}_{\mathbf{g}_{21}} \mathbf{g}_{21}^*]_d)]^\top$ ;  $\mathbf{n} = \mathbf{n}(t) = [n_1(t), \dots, n_d(t)]$ , where  $n_1(t), \dots, n_d(t)$  are time-varying continuous functions satisfying  $\sum_{k=1}^d n_k^2(t) = c$ , and  $c$  is a constant satisfying  $0 < c < 1$ .<sup>2</sup>

In the control law (3.25), the first term is the same as the control law (3.7) while the last term is added to guarantee global convergence of  $\mathbf{g}_{21}$  to  $\mathbf{g}_{21}^*$ . Note that the adjustment term in (3.25) was

---

<sup>2</sup>When  $d = 2$ , we may choose  $\mathbf{n} = \sqrt{c}[\cos t, \sin t]^\top$ .

originally introduced in another form in [11, 133]. Observe that under the control law (3.25), we have

$$\begin{aligned} \frac{d}{dt} d_{21}^2 &= \frac{d}{dt} (\mathbf{z}_{21}^\top \mathbf{z}_{21}) = 2\mathbf{z}_{21}^\top (\dot{\mathbf{p}}_1 - \dot{\mathbf{p}}_2) \\ &= -2\mathbf{z}_{21}^\top \mathbf{P}_{g_{21}} (\mathbf{g}_{21}^* + k \|\mathbf{g}_{21} - \mathbf{g}_{21}^*\| (\mathbf{sgn}(\mathbf{P}_{g_{21}} \mathbf{g}_{21}^*) + \mathbf{n})) = 0. \end{aligned} \quad (3.26)$$

Thus,  $d_{21}$  is invariant under the control law (3.25). Further, it can be checked that  $\mathbf{p}_{2b}^*$  is not an equilibrium of (3.25) due to the adjustment term. We prove the following result on stability of the agent 2.

**Proposition 3.14** *Under the control law (3.25), the equilibrium  $\mathbf{p}_{2a}^* = \mathbf{p}_1^* - d_{21}\mathbf{g}_{21}^*$  corresponding to  $\mathbf{g}_{21} = \mathbf{g}_{21}^*$  is globally asymptotically stable and almost globally exponentially stable.*

*Proof:* We consider the solution  $\mathbf{p}_2$  of the nonsmooth system (3.25) in the Filippov sense [134, 135]. For almost all time,

$$\dot{\mathbf{p}}_2 \in -\mathbf{P}_{g_{21}} \mathbf{g}_{21}^* - k \|\mathbf{g}_{21} - \mathbf{g}_{21}^*\| \mathbf{P}_{g_{21}} (K[\mathbf{sgn}](\mathbf{P}_{g_{21}} \mathbf{g}_{21}^*) + \mathbf{n}), \quad (3.27)$$

where  $K[\mathbf{f}](x)$  denotes the Filippov set-valued mapping of  $\mathbf{f}(x)$  [134]. Consider the Lyapunov function  $V = \frac{1}{2} \|\mathbf{p}_2 - \mathbf{p}_{2a}^*\|^2$ , which is continuously differentiable, radially unbounded and positive definite. Then at each point  $\mathbf{p}_2 \in \mathbb{R}^d$ ,  $\partial V = (\mathbf{p}_2 - \mathbf{p}_{2a}^*)$ . Based on [134, Theorem 2.2],  $\dot{V}$  exists almost everywhere (a.e.) and  $\dot{V} \in^{a.e.} \dot{V}$ , where

$$\begin{aligned} \dot{V} &= \bigcap_{\xi \in \partial V} \xi^\top \dot{\mathbf{p}}_2 \\ &= -(\mathbf{p}_2 - \mathbf{p}_{2a}^*)^\top \mathbf{P}_{g_{21}} \mathbf{g}_{21}^* - k \|\mathbf{g}_{21} - \mathbf{g}_{21}^*\| (\mathbf{p}_2 - \mathbf{p}_{2a}^*)^\top \mathbf{P}_{g_{21}} (K[\mathbf{sgn}](\mathbf{P}_{g_{21}} \mathbf{g}_{21}^*) + \mathbf{n}) \\ &= -(\mathbf{p}_2 - \mathbf{p}_{2a}^*)^\top \frac{\mathbf{P}_{g_{21}}}{d_{21}} (\mathbf{p}_2 - \mathbf{p}_{2a}^*) - kd_{21} \|\mathbf{g}_{21} - \mathbf{g}_{21}^*\| (\mathbf{P}_{g_{21}} \mathbf{g}_{21}^*)^\top (K[\mathbf{sgn}](\mathbf{P}_{g_{21}} \mathbf{g}_{21}^*) + \mathbf{n}). \end{aligned}$$

Define  $\boldsymbol{\eta} \triangleq \mathbf{P}_{g_{21}} \mathbf{g}_{21}^* = [\eta_1, \dots, \eta_d]^\top$ , we have

$$\dot{V} \leq -(\mathbf{p}_2 - \mathbf{p}_{2a}^*)^\top \frac{\mathbf{P}_{g_{21}}}{d_{21}} (\mathbf{p}_2 - \mathbf{p}_{2a}^*) - kd_{21} \|\mathbf{g}_{21} - \mathbf{g}_{21}^*\| \left( \boldsymbol{\eta}^\top K[\mathbf{sgn}](\boldsymbol{\eta}) - |\boldsymbol{\eta}^\top \mathbf{n}| \right). \quad (3.28)$$

From the property of **sgn** function, we can write

$$\boldsymbol{\eta}^\top K[\text{sgn}](\boldsymbol{\eta}) = \sum_{i=1}^d \eta_i K[\text{sgn}](\eta_i).$$

Recall from [134] that

$$K[\text{sgn}](\eta_i) = \begin{cases} 1 & \eta_i > 0 \\ [-1, 1] & \eta_i = 0 \\ -1 & \eta_i < 0 \end{cases}.$$

Thus,  $\eta_i K[\text{sgn}](\eta_i) = |\eta_i|$  and

$$\boldsymbol{\eta}^\top K[\text{sgn}](\boldsymbol{\eta}) = \sum_{k=1}^d |\eta_k|. \quad (3.29)$$

Moreover,

$$\left| \sum_{k=1}^d \eta_k n_k \right| \leq \sum_{k=1}^d |\eta_k n_k| \leq \sum_{k=1}^d |\eta_k| |n_k| \leq \sqrt{c} \sum_{k=1}^d |\eta_k|,$$

where the last inequality follows from the fact that  $|n_k| \leq \sqrt{\sum_{k=1}^d n_k^2} = \sqrt{c} < 1$ . Therefore,

$$\begin{aligned} \dot{\tilde{V}} &\leq -(\mathbf{p}_2 - \mathbf{p}_{2a}^*)^\top \frac{\mathbf{P}_{\mathbf{g}_{21}}}{d_{21}} (\mathbf{p}_2 - \mathbf{p}_{2a}^*) - k(1 - \sqrt{c}) d_{21} \|\mathbf{g}_{21} - \mathbf{g}_{21}^*\| \sum_{k=1}^d |\eta_k| \\ &\leq -(\mathbf{p}_2 - \mathbf{p}_{2a}^*)^\top \frac{\mathbf{P}_{\mathbf{g}_{21}}}{d_{21}} (\mathbf{p}_2 - \mathbf{p}_{2a}^*) \leq 0. \end{aligned} \quad (3.30)$$

It follows that  $\dot{\tilde{V}} = 0$  if and only if  $\mathbf{p}_2 = \mathbf{p}_{2a}^*$  or  $\mathbf{p}_2 = \mathbf{p}_{2b}^*$ . Since  $\dot{\mathbf{p}}_2|_{\mathbf{p}_2=\mathbf{p}_{2b}^*} \neq \mathbf{0}$ , based on

LaSalle's invariance principle for nonsmooth system [134, Theorem 3.2], every trajectory of (3.27) asymptotically converges to  $\mathbf{p}_{2a}^*$ .

Next, let  $\alpha$  be the angle between  $\mathbf{p}_{2a}^* - \mathbf{p}_2$  and  $\mathbf{g}_{21}^*$  as depicted in Fig. 3.6, we have  $\alpha \in [0, \pi/2]$ .

Further, we can write  $\|\mathbf{P}_{\mathbf{g}_{21}}(\mathbf{p}_2 - \mathbf{p}_{2a}^*)\| = \sin \alpha \|\mathbf{p}_2 - \mathbf{p}_{2a}^*\|$ . For all  $\mathbf{p}_2(0) \neq \mathbf{p}_{2b}^*$ , we have  $\alpha(0) > 0$ .

Since  $\mathbf{p}_2 \rightarrow \mathbf{p}_{2a}^*$  asymptotically, we have  $\alpha(t) \geq \alpha(0) > 0, \forall t > 0$ . It follows from (3.30) that

$$\dot{V} \leq -(\mathbf{p}_2 - \mathbf{p}_{2a}^*)^\top \frac{\mathbf{P}_{\mathbf{g}_{21}}}{d_{12}} (\mathbf{p}_2 - \mathbf{p}_{2a}^*) = -\frac{\sin^2 \alpha}{d_{21}} \|\mathbf{p}_2 - \mathbf{p}_{2a}^*\|^2 \leq -\frac{2 \sin^2 \alpha(0)}{d_{21}} V = -\kappa V \leq 0,$$

where  $\kappa = 2d_{21}^{-1} \sin^2 \alpha(0) > 0$ . Therefore, the equilibrium  $\mathbf{p}_2 = \mathbf{p}_{2a}^*$  is globally asymptotically stable and almost globally exponentially stable. ■

**Theorem 3.15** Under Assumptions 3.1-3.3, if agent 2 adopts the control law (3.25) and agent  $i$  ( $3 \leq i \leq n$ ) adopts the control law (3.22), the formation globally asymptotically reaches the desired formation satisfying all bearing vectors in  $\mathcal{B}$ .

*Proof:* The proof involves the same steps as in Section 3.2.2. The only difference is agent 2 always reaches  $\mathbf{p}_{2a}^*$  from any initial condition. Thus,  $\mathbf{p}_i \rightarrow \mathbf{p}_{ia}^*, \forall 3 \leq i \leq n$ , or i.e, the LFF formation globally asymptotically converges to the desired formation satisfying all bearing vectors in  $\mathcal{B}$ . ■

### 3.2.4 Finite-time bearing-only formation control

In this subsection, we are interested in designing bearing-only control laws to achieve the desired formation in finite time. Finite-time controllers are advantages since it increases convergence rate and provides an upper bound that guarantee the formation is in the desired shape. The following two control laws, for each agent  $i = 2, \dots, n$ , are proposed to solve Problem 3.1:

$$\mathbf{u}_i = - \sum_{j \in \mathcal{N}_i} \frac{\mathbf{P}_{\mathbf{g}_{ij}} \mathbf{g}_{ij}^*}{\|\mathbf{P}_{\mathbf{g}_{ij}} \mathbf{g}_{ij}^*\|^\beta}, \quad (3.31)$$

and

$$\mathbf{u}_i = - \sum_{j \in \mathcal{N}_i} \mathbf{P}_{\mathbf{g}_{ij}} \text{sig}(\mathbf{P}_{\mathbf{g}_{ij}} \mathbf{g}_{ij}^*)^\beta, \quad (3.32)$$

where  $0 < \beta < 1$  is a positive constant. Observe that for  $0 < \beta < 1$ , (3.31) and (3.32) are continuous control laws. Both of the proposed control laws are modified from the bearing-only control law (3.6) in the previous section. The finite-time modifications are inspired from previous works on finite-time consensus [105, 136] and formation control [41, 137, 138].

Since the stability analysis of the LFF formation under (3.31) and (3.32) are more or less similar, we only focus on the control law (3.31). Consider agent 2, the first follower, the following lemma can be proved:

**Lemma 3.16** Under assumptions 3.1–3.3 and the control law (3.31),  $\mathbf{p}_2 \rightarrow \mathbf{p}_{2a}^* = \mathbf{p}_1 - d_{21}\mathbf{g}_{21}^*$  in finite time if initially  $\mathbf{p}_2(0) \neq \mathbf{p}_{2b}^* = \mathbf{p}_1 + d_{21}\mathbf{g}_{21}^*$ .

*Proof:* First of all, since the leader is stationary, the control law for the first follower is written as follows:

$$\dot{\mathbf{p}}_2 = -\frac{\mathbf{P}_{\mathbf{g}_{21}}\mathbf{g}_{21}^*}{\|\mathbf{P}_{\mathbf{g}_{21}}\mathbf{g}_{21}^*\|^\beta}. \quad (3.33)$$

Thus,  $\mathbf{g}_{21}^\top \dot{\mathbf{p}}_2 = 0$  and  $d_{21}$  is time invariant, which implies the formula of  $\mathbf{p}_{2a}^*$  and  $\mathbf{p}_{2b}^*$ . Consider the Lyapunov function  $V_a = \frac{1}{2}\|\mathbf{p}_2 - \mathbf{p}_{2a}^*\|^2$ , which is positive definite, radially unbounded and  $V_a = 0$  if and only if  $\mathbf{p}_2 = \mathbf{p}_{2a}^*$ . Along a trajectory of (3.33), we have

$$\dot{V}_a = -(\mathbf{p}_2 - \mathbf{p}_{2a}^*)^\top \frac{\mathbf{P}_{\mathbf{g}_{21}}\mathbf{g}_{21}^*}{\|\mathbf{P}_{\mathbf{g}_{21}}\mathbf{g}_{21}^*\|^\beta} = -d_{21} \frac{\mathbf{g}_{21}^{*\top} \mathbf{P}_{\mathbf{g}_{21}}\mathbf{g}_{21}^*}{\|\mathbf{P}_{\mathbf{g}_{21}}\mathbf{g}_{21}^*\|^\beta} = -d_{21} \|\mathbf{P}_{\mathbf{g}_{21}}\mathbf{g}_{21}^*\|^{2-\beta}. \quad (3.34)$$

Moreover, using the property  $\mathbf{g}_{21}^{*\top} \mathbf{P}_{\mathbf{g}_{21}}\mathbf{g}_{21}^* = \mathbf{g}_{21}^\top \mathbf{P}_{\mathbf{g}_{21}}^* \mathbf{g}_{21}$ , if  $\mathbf{p}_2(0) \neq \mathbf{p}_{2b}^*$ , it holds

$$\begin{aligned} \dot{V}_a &= -d_{21} \|\mathbf{g}_{21}^\top \mathbf{P}_{\mathbf{g}_{21}}^* \mathbf{g}_{21}\|^{\frac{2-\beta}{2}} \\ &= -\frac{1}{(d_{21})^{1-\beta}} \left( (\mathbf{p}_2 - \mathbf{p}_1)^\top \mathbf{P}_{\mathbf{g}_{21}}^* (\mathbf{p}_2 - \mathbf{p}_1) \right)^{\frac{2-\beta}{2}} \\ &= -\frac{1}{(d_{21})^{1-\beta}} \left( (\mathbf{p}_2 - \mathbf{p}_{2a}^*)^\top \mathbf{P}_{\mathbf{g}_{21}}^* (\mathbf{p}_2 - \mathbf{p}_{2a}^*) \right)^{\frac{2-\beta}{2}} \\ &\leq -\frac{(\sin \alpha(0))^{2-\beta}}{(d_{21})^{1-\beta}} \|\mathbf{p}_2 - \mathbf{p}_{2a}^*\|^{2-\beta} \\ &\leq -\kappa V_a^{\frac{2-\beta}{2}}, \end{aligned} \quad (3.35)$$

where  $\kappa = \frac{(\sin \alpha(0))^{2-\beta}}{(d_{21})^{1-\beta}} > 0$ ,  $\alpha$  is the angle as defined in the previous section, and  $\frac{1}{2} < \frac{2-\beta}{2} < 1$ .

Thus, according to Theorem 2.7, it follows that  $\mathbf{p}_2 = \mathbf{p}_{2a}^*$  is a finite-time stable equilibrium. By considering the Lyapunov function  $V_b = \frac{1}{2}\|\mathbf{p}_2 - \mathbf{p}_{2b}^*\|^2$ , it can be shown that the equilibrium  $\mathbf{p}_2 = \mathbf{p}_{2b}^*$  is exponentially unstable. Thus,  $\mathbf{p}_2 \rightarrow \mathbf{p}_{2a}^*$  in finite time if  $\mathbf{p}_2(0) \neq \mathbf{p}_{2b}^*$ .  $\blacksquare$

Next, consider agent 3. The dynamics of agent 3 is given as follows:

$$\dot{\mathbf{p}}_3 = -\frac{\mathbf{P}_{\mathbf{g}_{31}}\mathbf{g}_{31}^*}{\|\mathbf{P}_{\mathbf{g}_{31}}\mathbf{g}_{31}^*\|^\beta} - \frac{\mathbf{P}_{\mathbf{g}_{32}}\mathbf{g}_{32}^*}{\|\mathbf{P}_{\mathbf{g}_{32}}\mathbf{g}_{32}^*\|^\beta} \quad (3.36)$$

It is not difficult to prove that when  $\mathbf{p}_2 = \mathbf{p}_{2a}^*$ , the equilibrium of (3.36) is  $\mathbf{p}_3 = \mathbf{p}_{3a}^*$  where  $\mathbf{g}_{31} = \mathbf{g}_{31}^*$  and  $\mathbf{g}_{32} = \mathbf{g}_{32}^*$ . The stability of this equilibrium is studied in the following lemma.

**Lemma 3.17** *Under assumptions 3.1–3.3 and the control law (3.31),  $\mathbf{p}_3 \rightarrow \mathbf{p}_{3a}^*$  in finite time if initially  $\mathbf{p}_2(0) \neq \mathbf{p}_{2b}^*$ .*

*Proof:* Since  $\mathbf{p}_2(0) \neq \mathbf{p}_{2b}^*$ , it follows that after a finite time  $T_2$ ,  $\mathbf{p}_2 = \mathbf{p}_{2a}^*$ . Thus, we can study the equation (3.36) for  $t \geq T_2$ . Consider the Lyapunov function  $V = \frac{1}{2}\|\mathbf{p}_3 - \mathbf{p}_{3a}^*\|^2$ , which is radially unbounded and positive definite,  $V = 0$  if and only if  $\mathbf{p}_3 = \mathbf{p}_{3a}^*$ . Moreover, for  $t \geq T_2$ ,

$$\begin{aligned}\dot{V} &= -(\mathbf{p}_3 - \mathbf{p}_{3a}^*)^\top \left( \frac{\mathbf{P}_{\mathbf{g}_{31}} \mathbf{g}_{31}^*}{\|\mathbf{P}_{\mathbf{g}_{31}} \mathbf{g}_{31}^*\|^\beta} + \frac{\mathbf{P}_{\mathbf{g}_{32}} \mathbf{g}_{32}^*}{\|\mathbf{P}_{\mathbf{g}_{32}} \mathbf{g}_{32}^*\|^\beta} \right) \\ &= -d_{31}^* \|\mathbf{P}_{\mathbf{g}_{31}} \mathbf{g}_{31}^*\|^{2-\beta} - d_{32}^* \|\mathbf{P}_{\mathbf{g}_{32}} \mathbf{g}_{32}^*\|^{2-\beta}\end{aligned}\quad (3.37)$$

$$\begin{aligned}&= -(d_{31}^*)^{\beta-1} \|\mathbf{P}_{\mathbf{g}_{31}} (\mathbf{p}_3 - \mathbf{p}_{3a}^*)\|^{2-\beta} - (d_{32}^*)^{\beta-1} \|\mathbf{P}_{\mathbf{g}_{32}} (\mathbf{p}_3 - \mathbf{p}_{3a}^*)\|^{2-\beta} \\ &\leq -\gamma \left( (\mathbf{p}_3 - \mathbf{p}_{3a}^*)^\top \mathbf{P}_{\mathbf{g}_{31}} (\mathbf{p}_3 - \mathbf{p}_{3a}^*) + (\mathbf{p}_3 - \mathbf{p}_{3a}^*)^\top \mathbf{P}_{\mathbf{g}_{32}} (\mathbf{p}_3 - \mathbf{p}_{3a}^*) \right)^{\frac{2-\beta}{2}} \\ &\leq -\gamma \left( (\mathbf{p}_3 - \mathbf{p}_{3a}^*)^\top (\mathbf{P}_{\mathbf{g}_{31}} + \mathbf{P}_{\mathbf{g}_{32}}) (\mathbf{p}_3 - \mathbf{p}_{3a}^*) \right)^{\frac{2-\beta}{2}} \\ &\leq -\gamma \lambda_{\min} (\mathbf{P}_{\mathbf{g}_{31}} + \mathbf{P}_{\mathbf{g}_{32}}) \|\mathbf{p}_3 - \mathbf{p}_{3a}^*\|^{2-\beta} \\ &\leq -\kappa V^{\frac{2-\beta}{2}},\end{aligned}\quad (3.38)$$

where  $\kappa = \gamma \lambda_{\min} (\mathbf{P}_{\mathbf{g}_{31}} + \mathbf{P}_{\mathbf{g}_{32}})$ ,  $\gamma = \min\{(d_{31}^*)^{\beta-1}, (d_{32}^*)^{\beta-1}\}$ , and  $\lambda_{\min} (\mathbf{P}_{\mathbf{g}_{31}} + \mathbf{P}_{\mathbf{g}_{32}}) > 0$  denotes the smallest eigenvalue of  $\mathbf{P}_{\mathbf{g}_{31}} + \mathbf{P}_{\mathbf{g}_{32}}$ . Also, from (3.37) to (3.38), we have applied Lemma 2.6 to derive the inequality  $\dot{V} \leq -\kappa V^{\frac{2-\beta}{2}}$  shows that  $\mathbf{p}_3 = \mathbf{p}_{3a}^*$  is a finite time stable equilibrium.  $\blacksquare$

By a similar analysis, one can prove the main theorem of this subsection:

**Theorem 3.18** *Under assumptions 3.1–3.3 and the control law (3.31),  $\mathbf{p}_i \rightarrow \mathbf{p}_{ia}^*, i = 2, \dots, n$  in finite time if initially  $\mathbf{p}_2(0) \neq \mathbf{p}_{2b}^*$ . That is, the desired formation is achieved in finite time.*

### 3.3 Bearing-based control of LFF formations via orientation alignment

In this section, we design a bearing-based control law for LFF formations when the model of each agent is given in  $\mathbb{R}^3 \times SO(3)$ , thus including both position and orientation of the agent. This setup is more distributed since the agents' orientations are no longer required to be aligned.

#### 3.3.1 Problem formulation

Consider a group of  $n$  autonomous agents in the three-dimensional space  $\mathbb{R}^3$ . The position, linear velocity, and angular velocity of agent  $i$  given in a global reference frame are denoted as  $\mathbf{p}_i, \mathbf{u}_i, \mathbf{w}_i \in \mathbb{R}^3$ , respectively. Each agent  $i$  maintains a local reference frame  ${}^i\Sigma$ ; the linear and the angular velocity of agent  $i$  expressed in  ${}^i\Sigma$  are given by  $\mathbf{u}_i^i = [u_x^i, u_y^i, u_z^i]^\top$  and  $\mathbf{w}_i^i = [w_x^i, w_y^i, w_z^i]^\top$ , respectively. Let  $\mathbf{R}_i \in SO(3)$  be the rotation from  ${}^i\Sigma$  to a global frame  $\Sigma$ ; we have  $\det(\mathbf{R}_i) = 1$  and  $\mathbf{R}_i \mathbf{R}_i^\top = \mathbf{I}_3$ .

The position and orientation dynamics of agent  $i$  in the global reference frame are

$$\dot{\mathbf{p}}_i = \mathbf{R}_i \mathbf{u}_i^i \quad (3.39)$$

$$\dot{\mathbf{R}}_i = \mathbf{R}_i \mathbf{S}_i, \quad (3.40)$$

where

$$\mathbf{S}_i = \begin{bmatrix} 0 & -w_z^i & w_y^i \\ w_z^i & 0 & -w_x^i \\ -w_y^i & w_x^i & 0 \end{bmatrix}$$

is a skew-symmetric matrix. Note that from (3.39)-(3.40), the dynamics of agent  $i$  is now defined in  $\mathbb{R}^3 \times SO(3)$ . Let the Assumptions 3.1-3.3 for Problem 3.1 on sensing graph and initial position of the agents hold. Further, it is assumed that in addition to the local bearings  $\mathbf{g}_{ij}^i = \mathbf{R}_i^\top \mathbf{g}_{ij}$ , agent  $i$  can also obtain the relative orientation  $\mathbf{R}_i^\top \mathbf{R}_j$  with regard to each neighbor agent  $j$ . Finally, the following assumption on the initial orientations of the agents is adopted.

**Assumption 3.4** *The initial orientations of all agents are contained within a closed ball  $\bar{B}_r(\mathbf{R}_1)$  of radius  $r$  less than  $\pi/2$ . Equivalently, the symmetric part of  $\mathbf{R}_1^\top \mathbf{R}_i(0)$  is positive definite,  $\forall i = 2, \dots, n$  [139].*

At this point, we can formulate the following problem.

**Problem 3.2** *Given an  $n$ -agent system with initial positions  $\mathbf{p}(0)$  and orientations  $\{\mathbf{R}_i(0)\}_{i \in \mathcal{V}}$  satisfying Assumptions 3.1-3.4, design  $\mathbf{u}_i^i$  and  $\mathbf{w}_i^i$  for agent  $i \in \mathcal{V}$  based on local bearing measurements and relative orientation measurements such that  $\{\mathbf{R}_i(t)\}_{i=1,\dots,n}$  converges to  $\mathbf{R}_1(0)$  and  $\mathbf{g}_{ij}^i \rightarrow \mathbf{g}_{ij}^*$  for all  $\mathbf{g}_{ij}^* \in \mathcal{B}$ .*

### 3.3.2 Proposed control strategy

To solve Problem 3.2, a two-layer control strategy is proposed for the  $n$ -agent system. The two layers will be referred to as the orientation alignment layer and the formation control layer. On the orientation alignment layer, a consensus algorithm is used to synchronize all agents' orientations. Simultaneously, on the formation control layer, we implement the bearing-only control law proposed earlier in Problem 3.1 in each agent's local frame to achieve the desired formation. This two-layer control strategy was also used in formation control problems with different setups [23, 24, 49, 140].

#### 3.3.2.1 The orientation alignment layer

The following orientation alignment control law for each agent  $i$  ( $1 \leq i \leq n$ ) is adopted:

$$S_i = - \sum_{j \in \mathcal{N}_i} (\mathbf{R}_j^\top \mathbf{R}_i - \mathbf{R}_i^\top \mathbf{R}_j). \quad (3.41)$$

The control law (3.41) is adopted from the attitude synchronization control law in [94, 139, 141]. Since  $\mathbf{R}_j^\top \mathbf{R}_i = (\mathbf{R}_i^\top \mathbf{R}_j)^\top$ , the control law (3.41) requires only the *local relative orientations* of agent  $i$  with regard to its neighbors and no communication between agents is needed [141].

Because the leader has no neighbor, we let  $\dot{\mathbf{R}}_1 = \mathbf{0}$ . Thus the orientation of the leader is time invariant, i.e.,  $\mathbf{R}_1(t) = \mathbf{R}_1(0)$ , for all time  $t > 0$ .

From (3.40), the angular velocity in the global reference frame can be rewritten as follows

$$\dot{\mathbf{R}}_i = -\sum_{j \in \mathcal{N}_i} \mathbf{R}_i (\mathbf{R}_j^\top \mathbf{R}_i - \mathbf{R}_i^\top \mathbf{R}_j). \quad (3.42)$$

Unlike [23, 24, 49, 140] where the interaction graphs are assumed to be undirected, the alignment (3.41) is performed in a directed graph  $G$  built up via a Henneberg construction, i.e., a rooted directed graph with a root at vertex  $v_1$ . This setup leads to a different result. When the interaction graph is bidirectional, the final orientation is determined by all agents' initial orientations [141]. However, when the graph is directed and has a rooted spanning tree, the aligned orientation is determined by the orientations of the agent locating at the root of the graph, as stated in the following lemma.

**Lemma 3.19** [141, 142, Theorem 3.2] *Assume that  $G$  has a rooted spanning tree. If there is  $\mathbf{R} \in SO(3)$ , such that the orientations of all agents initially are contained within a closed ball  $\bar{B}_r(\mathbf{R})$  of radius  $r$  less than  $\pi/2$  centered around  $\mathbf{R}$ , then the controller (3.41) is a synchronization controller, i.e.,  $\mathbf{R}_i^\top \mathbf{R}_j \rightarrow \mathbf{I}_3$  asymptotically for all  $i, j \in \mathcal{V}$ .*

The following result is implied from Lemma 3.19 and Corollary 2 in [139].

**Lemma 3.20** *Under Assumptions 3.4 and the orientation alignment control law (3.40), if the directed graph  $G$  is built up via a Henneberg construction, all agents' orientations will asymptotically converge to the leader's orientation, i.e., for  $i = 2, \dots, n$ ,  $\mathbf{R}_i(t)^\top \mathbf{R}_1 \rightarrow \mathbf{I}_3$  asymptotically, as  $t \rightarrow \infty$ .*

### 3.3.2.2 The formation control layer

In this layer, we use a locally implemented version of the control laws in Section 3.2. The leader is stationary, i.e.,  $\mathbf{u}_1^1 = \mathbf{0}$ . The first follower's position control law written in its local reference frame

is designed as<sup>3</sup>

$$u_2^2 = -P_{g_{21}^i}(I_3 + R_2^\top R_1)g_{21}^*. \quad (3.43)$$

For each follower agent  $i$  ( $3 \leq i \leq n$ ), the position control law in  ${}^i\Sigma$  is

$$\mathbf{u}_i^i = -\sum_{j \in \mathcal{N}_i} P_{g_{ij}^i}(I_3 + R_i^\top R_j)g_{ij}^*, \quad (3.44)$$

where  $P_{g_{ij}^i} = I_3 - g_{ij}^i(g_{ij}^i)^\top$  is the orthogonal projection matrix. Using the following derivation

$$\begin{aligned} R_i P_{g_{ij}^i}(I_3 + R_i^\top R_j)g_{ij}^* &= R_i(I_3 - R_i^\top g_{ij} g_{ij}^\top R_i)(I_3 + R_i^\top R_j)g_{ij}^* \\ &= R_i R_i^\top (I_3 - g_{ij} g_{ij}^\top) R_i (I_3 + R_i^\top R_j) g_{ij}^* \\ &= P_{g_{ij}}(R_i + R_j)g_{ij}^*, \end{aligned}$$

from (3.39) and (3.44), we can express the dynamics of agent 2 in the global frame as follows:

$$\dot{\mathbf{p}}_2 = \underbrace{-2P_{g_{21}}R_1g_{21}^*}_{\triangleq \mathbf{f}_2(\mathbf{p}, t)} + \underbrace{P_{g_{21}}(R_1 - R_2)g_{21}^*}_{\triangleq \mathbf{h}_2(\mathbf{p}, t)}. \quad (3.45)$$

Similarly, from (3.39) and (3.44), the dynamics of an agent  $i$  ( $i = 3, \dots, n$ ) can be expressed as

$$\begin{aligned} \dot{\mathbf{p}}_i &= -\sum_{j \in \mathcal{N}_i} P_{g_{ij}}(R_i + R_j)g_{ij}^* \\ &= \underbrace{-2 \sum_{j \in \mathcal{N}_i} P_{g_{ij}}R_1g_{ij}^*}_{\triangleq \mathbf{f}_i(\mathbf{p}, t)} + \underbrace{\sum_{j \in \mathcal{N}_i} P_{g_{ij}}(2R_1 - R_i - R_j)g_{ij}^*}_{\triangleq \mathbf{h}_i(\mathbf{p}, t)}. \end{aligned}$$

Then, the position dynamics of the  $n$ -agent system can be expressed in the following compact form

$$\dot{\mathbf{p}} = \mathbf{f}(\mathbf{p}) + \mathbf{h}(\mathbf{p}, t), \quad (3.46)$$

where  $\mathbf{f}(\mathbf{p}) = [f_1^\top, \dots, f_n^\top]^\top$ ,  $\mathbf{h}(\mathbf{p}, t) = [h_1^\top, \dots, h_n^\top]^\top$  and  $f_1 = \mathbf{0}$ ,  $h_n = \mathbf{0}$ . We will analyze the

system (3.46) in the next section using the results on almost global ISS stability [88].

---

<sup>3</sup>The global stabilization control law (3.25) cannot be used here since it uses global information.

### 3.3.3 Stability analysis

#### 3.3.3.1 The input to the nominal system

Observe that in the compact form (3.46),  $\mathbf{h}(t)$  can be considered as an input to the nominal system

$$\dot{\mathbf{p}} = \mathbf{f}(\mathbf{p}). \quad (3.47)$$

We have the following lemma on  $\mathbf{h}(t)$ .

**Lemma 3.21** *Under Assumptions 3.1-3.4, the input  $\mathbf{h}(t)$  from the orientation alignment layer to the formation control layer is bounded. Moreover,  $\mathbf{h}(t)$  asymptotically converges to  $\mathbf{0}$  as  $t \rightarrow \infty$ .*

*Proof:* This proof is similar to the proof of [49, Lemma 12] and will be omitted. ■

#### 3.3.3.2 The first follower

The dynamics of agent 2 (the first follower) is given by

$$\dot{\mathbf{p}}_2 = \underbrace{-2\mathbf{P}_{g_{21}}\mathbf{R}_1\mathbf{g}_{21}^*}_{\triangleq \mathbf{f}_2(\mathbf{p}_2)} + \underbrace{\mathbf{P}_{g_{21}}(\mathbf{R}_1 - \mathbf{R}_2)\mathbf{g}_{21}^*}_{\triangleq \mathbf{h}_2(t)} \quad (3.48)$$

$$\dot{\mathbf{R}}_2 = -\mathbf{R}_2(\mathbf{R}_1^\top \mathbf{R}_2 - \mathbf{R}_2^\top \mathbf{R}_1). \quad (3.49)$$

We have the following lemma on the unforced system  $\dot{\mathbf{p}}_2 = \mathbf{f}_2(\mathbf{p}_2)$ , whose proof is similar to the proof of Lemma 3.7.

**Lemma 3.22** *The unforced system  $\dot{\mathbf{p}}_2 = \mathbf{f}_2(\mathbf{p}_2)$  has two equilibria. The first equilibrium  $\mathbf{p}_2 = \mathbf{p}_{2a}^*$  corresponding to  $\mathbf{g}_{21} = \mathbf{R}_1\mathbf{g}_{21}^*$  is almost globally asymptotically stable. The second equilibrium  $\mathbf{p}_2 = \mathbf{p}_{2b}^*$  corresponding to  $\mathbf{g}_{21} = -\mathbf{R}_1\mathbf{g}_{21}^*$  is (exponentially) unstable.*

In fact, every initial condition, other than the unstable equilibrium point, is in the region of convergence of the equilibrium point  $\mathbf{p}_{2a}^*$ .

**Lemma 3.23** *The system (3.48) has two equilibria. The equilibrium  $\mathbf{p}_2 = \mathbf{p}_{2a}^*$  is almost globally asymptotically stable. The equilibrium  $\mathbf{p}_2 = \mathbf{p}_{2b}^*$  is exponentially unstable. All trajectories with  $\mathbf{p}_2(0) \neq \mathbf{p}_{2b}^*$ ,  $\mathbf{R}_2(0) \neq \mathbf{R}_1$  asymptotically converge to the stable equilibrium.*

*Proof:* We first prove the system (3.48) satisfies the ultimate boundedness property. Consider the potential function  $V = \frac{1}{2}\|\mathbf{p}_2 - \mathbf{p}_{2a}^*\|^2$  which is positive definite, radially unbounded and  $V = 0$  if and only if  $\mathbf{p}_2 = \mathbf{p}_{2a}^*$ . Then,

$$\begin{aligned}\dot{V} &= (\mathbf{p}_2 - \mathbf{p}_{2a}^*)^\top \dot{\mathbf{p}}_2 = -2(\mathbf{p}_2 - \mathbf{p}_{2a}^*)^\top \mathbf{P}_{g_{21}} \mathbf{R}_1 \mathbf{g}_{21}^* + (\mathbf{p}_2 - \mathbf{p}_{2a}^*)^\top \mathbf{h}_2 \\ &= -2(\mathbf{p}_2 - \mathbf{p}_{2a}^*)^\top \frac{\mathbf{P}_{g_{21}}}{d_{21}} (\mathbf{p}_2 - \mathbf{p}_{2a}^*) + (\mathbf{p}_2 - \mathbf{p}_{2a}^*)^\top \mathbf{h}_2 \\ &\leq -\frac{2 \sin^2 \alpha(0)}{d_{21}} \|\mathbf{p}_2 - \mathbf{p}_{2a}^*\|^2 + \|\mathbf{p}_2 - \mathbf{p}_{2a}^*\| \|\mathbf{h}_2\| \\ &\leq -\kappa V + 2d_{21} \|\mathbf{h}_2\|,\end{aligned}\tag{3.50}$$

where  $\kappa = 4d_{21}^{-1} \sin^2 \alpha(0)$ , and  $\alpha$  is the angle between  $\mathbf{p}_{2a}^* - \mathbf{p}_2$  and  $\mathbf{g}_{21}^*$ . Since  $\|\mathbf{p}_2 - \mathbf{p}_{2a}^*\|$  is bounded, it follows from equation (3.50) that the system (3.48) is ultimately bounded due to Lemma 2.3.

When  $\mathbf{h}_2(t) = \mathbf{0}$ , the unforced system has two isolated equilibria with properties given in Lemma 3.22. Since the system (3.48) satisfies Assumptions 2.1–2.3 and the ultimate boundedness property, (3.48) is almost globally ISS with respect to the equilibrium  $\mathbf{p}_2 = \mathbf{p}_{2a}^*$  based on Theorem 2.4.

Since  $\mathbf{h}_2(t) \rightarrow \mathbf{0}$  as proved in Lemma 3.21, the equilibrium  $\mathbf{p}_2 = \mathbf{p}_{2a}^*$  of (3.48) is almost globally asymptotically stable (Theorem 2.5). ■

### 3.3.3.3 The second follower

Similar to the first follower, the second follower's dynamics is given by

$$\dot{\mathbf{p}}_3 = \underbrace{-2\mathbf{P}_{g_{31}} \mathbf{R}_1 \mathbf{g}_{31}^* - 2\mathbf{P}_{g_{32}} \mathbf{R}_1 \mathbf{g}_{32}^*}_{\triangleq \mathbf{f}_3(\mathbf{p}_3, \mathbf{p}_2)} + \mathbf{h}_3(t).\tag{3.51}$$

Lemmas 3.24 are about the unforced systems:

$$\dot{\mathbf{p}}_3 = \mathbf{f}_3(\mathbf{p}_3, \mathbf{p}_{2a}^*) \quad (3.52)$$

$$\dot{\mathbf{p}}_3 = \mathbf{f}_3(\mathbf{p}_3, \mathbf{p}_{2b}^*). \quad (3.53)$$

**Lemma 3.24** *The system (3.52) has a globally asymptotically stable equilibrium  $\mathbf{p}_{3a}^*$  where  $\mathbf{g}_{31} = \mathbf{R}_1 \mathbf{g}_{31}^*$  and  $\mathbf{g}_{32} = \mathbf{R}_1 \mathbf{g}_{32}^*$ . The system (3.53) has an unstable equilibrium  $\mathbf{p}_{3b}^*$  where  $\mathbf{g}_{31} = -\mathbf{R}_1 \mathbf{g}_{31}^*$  and  $\mathbf{g}_{32} = -\mathbf{R}_1 \mathbf{g}_{32}^*$ .*

*Proof:* The result follows from Lemma 3.9. ■

**Lemma 3.25** *The cascade system (3.48), (3.51) has two equilibria. The equilibrium  $\mathbf{p}_2 = \mathbf{p}_{2a}^*$ ,  $\mathbf{p}_3 = \mathbf{p}_{3a}^*$  is almost globally asymptotically stable. The equilibrium  $\mathbf{p}_2 = \mathbf{p}_{2b}^*$ ,  $\mathbf{p}_3 = \mathbf{p}_{3b}^*$  is unstable. All trajectories starting out of the undesired equilibrium asymptotically converge to the stable equilibrium.*

*Proof:* As in Lemma 3.23, we firstly prove that the system (3.51) satisfies the ultimate boundedness property if  $\mathbf{p}_2(0) \neq \mathbf{p}_{2b}^*$ . Consider the Lyapunov function  $V = \frac{1}{2} \|\mathbf{p}_3 - \mathbf{p}_{3a}^*\|^2$ , the derivative of  $V$  is given by

$$\begin{aligned} \dot{V} &= -2(\mathbf{p}_3 - \mathbf{p}_3^*)^\top (\mathbf{P}_{\mathbf{g}_{31}} \mathbf{R}_1 \mathbf{g}_{31}^* + \mathbf{P}_{\mathbf{g}_{32}} \mathbf{R}_1 \mathbf{g}_{32}^* - \mathbf{h}_3) \\ &= -2(\mathbf{p}_3 - \mathbf{p}_3^*)^\top \left( \frac{\mathbf{P}_{\mathbf{g}_{31}}}{\|\mathbf{z}_{31}^*\|} + \frac{\mathbf{P}_{\mathbf{g}_{32}}}{\|\mathbf{z}_{32}^*\|} \right) (\mathbf{p}_3 - \mathbf{p}_3^*) + (\mathbf{p}_3 - \mathbf{p}_3^*)^\top \frac{\mathbf{P}_{\mathbf{g}_{32}}}{\|\mathbf{z}_{32}^*\|} (\mathbf{p}_2 - \mathbf{p}_{2a}^*) + (\mathbf{p}_3 - \mathbf{p}_3^*)^\top \mathbf{h}_3 \\ &\leq -2(\mathbf{p}_3 - \mathbf{p}_3^*)^\top \mathbf{M}(\mathbf{p}_3 - \mathbf{p}_3^*) + \|\mathbf{p}_3 - \mathbf{p}_3^*\| \left( \frac{\|\mathbf{P}_{\mathbf{g}_{32}}\|}{\|\mathbf{z}_{32}^*\|} \|\mathbf{p}_2 - \mathbf{p}_{2a}^*\| + \|\mathbf{h}_3\| \right) \\ &\leq -2\kappa \|\mathbf{p}_3 - \mathbf{p}_3^*\|^2 + \|\mathbf{p}_3 - \mathbf{p}_3^*\| \left( \frac{2d_{21}}{\|\mathbf{z}_{32}^*\|} + \|\mathbf{h}_3\| \right), \end{aligned} \quad (3.54)$$

where  $\kappa > 0$  as defined in Lemma 3.9. Further, in equation (3.54), we know that  $\|\mathbf{h}_3\|$  is bounded from Lemma 3.21. Thus, when  $\|\mathbf{p}_3 - \mathbf{p}_{3a}^*\|$  is large enough, the second term is  $\mathcal{O}(\|\mathbf{p}_3 - \mathbf{p}_{3a}^*\|)$  while

the first term is  $\mathcal{O}(-\|\mathbf{p}_3 - \mathbf{p}_{3a}^*\|^2)$ , and  $\dot{V} < 0$ . Consequently,  $\|\mathbf{p}_3 - \mathbf{p}_{3a}^*\|$  is bounded and we can choose  $m_3$  such that  $m_3 > \max_{t \geq 0} \|\mathbf{p}_3 - \mathbf{p}_{3a}^*\|$ . It follows that

$$\dot{V} \leq -2\kappa V + 2d_{21}\|\mathbf{z}_{32}^*\|^{-1}m_3 + m_3\|\mathbf{h}_3\|,$$

or the system (3.51) satisfies the ultimate boundedness property. When  $\mathbf{h}_3(t) = \mathbf{0}$ , the unforced system has two isolated equilibria with properties given in Lemma 3.24. Since the system (3.51) satisfies Assumptions 2.1–2.3 and the ultimate boundedness property in Chapter 2.3, (3.51) is almost globally ISS with respect to the equilibrium  $\mathbf{p}_3 = \mathbf{p}_{3a}^*$  according to Theorem 2.4.

Because  $\mathbf{h}_3(t) \rightarrow \mathbf{0}$  as proved in Lemma 3.21, the equilibrium  $\mathbf{p}_3 = \mathbf{p}_{3a}^*$  of (3.48) is almost globally asymptotically stable Theorem 2.5.  $\blacksquare$

### 3.3.3.4 The overall system

Consider the  $n$ -agent system (3.46)

$$\dot{\mathbf{p}} = \mathbf{f}(\mathbf{p}) + \mathbf{h}(\mathbf{p}, t),$$

We have the following lemma whose proof follows from Lemma 3.22 and repetitively applying Lemma 3.23.

**Lemma 3.26** *The unforced system  $\dot{\mathbf{p}} = \mathbf{f}(\mathbf{p})$  has two equilibria. The first equilibrium  $\mathbf{p} = \mathbf{p}_a^*$  corresponding to  $\mathbf{g}_{ij} = \mathbf{R}_1 \mathbf{g}_{ij}^*$ ,  $\forall \mathbf{g}_{ij}^* \in \mathcal{B}$  is almost globally asymptotically stable. The second equilibrium  $\mathbf{p} = \mathbf{p}_b^*$  corresponding to  $\mathbf{g}_{ij} = -\mathbf{R}_1 \mathbf{g}_{ij}^*$ ,  $\forall \mathbf{g}_{ij}^* \in \mathcal{B}$  is unstable.*

Finally, the main result of this section is given in the following Theorem.

**Theorem 3.27** *Consider the system (3.39)–(3.40). Under Assumptions 3.1–3.4 and the proposed control laws (3.41), (3.43) and (3.44),  $\mathbf{R}_i \rightarrow \mathbf{R}_1$  and  $\mathbf{p} \rightarrow \mathbf{p}_a^*$  ( $i = 1, \dots, n$ ) asymptotically if initially  $\mathbf{R}_2(0) \neq \mathbf{R}_1, \mathbf{p}_2(0) \neq \mathbf{p}_{2b}^*$ .*

*Proof:* We have  $\mathbf{R}_i \rightarrow \mathbf{R}_1$  based on Lemma 3.20. The convergence of  $\mathbf{p}$  to the target formation follows from Lemma 3.23, Lemma 3.25, and by invoking mathematical induction as in Theorem 3.13.

■

### 3.4 Bearing-based control of LFF formations via global orientation estimation

This section proposes another two-layer distributed control strategy for LFF formations. It will be shown that by simultaneously estimating the global orientation [25, 143] and controlling position, the agents can also achieve a target formation.

#### 3.4.1 Problem formulation

This section follows the setup in the Section 3.3, i.e., Assumptions 3.1–3.3 hold and but the agent's dynamics is defined in  $\mathbb{R}^d \times SO(d)$ . The equations of each agent is still given as in Eqs. (3.39)–(3.40), but  $\mathbf{p}_i$  and  $\mathbf{R}_i$  are defined in  $\mathbb{R}^d$  and  $SO(d)$ , respectively. Each agent  $i$ ,  $i = 1, \dots, n$ , can sense the relative orientations and exchange information with its neighbor agents. Specifically, if  $j$  is a neighbor of  $i$ , then  $i$  senses the relative orientation of  $j$ 's local reference frame with regard to the  $i$ 's local reference frame  $\mathbf{R}_{ij}$ , which could be written as  $\mathbf{R}_{ij} = \mathbf{R}_i^{-1} \mathbf{R}_j = \mathbf{R}_i^\top \mathbf{R}_j$ .

From the relative orientation information, each agent  $i$  tries to estimate its own orientation  $\mathbf{R}_i$  with respect to the global reference frame. This estimation is characterized by the matrix  $\hat{\mathbf{R}}_i \in SO(d)$ . The directed weighted graph  $G_o = (\mathcal{V}_o, \mathcal{E}_o, \mathcal{A}_o)$  characterizes the (relative) orientation sensing between agents in the system. Note that  $\mathcal{V}_o = \{v_1, \dots, v_n\}$ ,  $\mathcal{E}_o \subseteq \mathcal{V}_o \times \mathcal{V}_o$  and  $\mathcal{A}_o$  is a set of positive scalar weights  $a_{ij}$  corresponding to each edge  $(v_i, v_j) \in \mathcal{E}_o$ . Let  $\mathbf{L}_o \in \mathbb{R}^{n \times n}$  be the graph Laplacian of  $G_o$ . The following assumption is imposed on the orientation sensing graph:

**Assumption 3.5** *The orientation sensing graph  $G_o$  is rooted out-branching.*

Suppose that each agent can sense some bearing vectors toward its neighbor agents. That is, if agent  $j$  is a neighbor of agent  $i$  and their positions are not collocated, agent  $i$  can sense the bearing vector  $\mathbf{g}_{ij}^i$  in  ${}^i\Sigma$ . The bearing sensing graph is given by an LFF graph  $G = (\mathcal{V}, \mathcal{E})$ . The target formation shape is given by the set of desired bearing vectors  $\mathcal{B} = \{\mathbf{g}_{ij}^*\}_{e_{ij} \in \mathcal{E}}$ . Each agent  $i$  is given  $\mathbf{g}_{ij}^*$  and can sense all bearing vectors  $\mathbf{g}_{ij}^i, \forall j \in \mathcal{N}_i$ . The bearing-based formation control problem with global orientation estimation can be stated as follows:

**Problem 3.3** Consider the system of  $n$  agents with dynamics (3.39)–(3.40). Under Assumptions 3.1–3.3, 3.5 and for a common reference frame  ${}^c\Sigma$  identified by  $\mathbf{R}^* \in SO(d)$ , design a control strategy for each agent using only local bearings and relative orientation information such that the system almost globally asymptotically achieves a target formation shape up to a translation and a rotation identified by  $\mathbf{R}^*$ .

In other words, the objective of Problem 3.3 is achieving a formation with  $\frac{\mathbf{p}_j - \mathbf{p}_i}{\|\mathbf{p}_j - \mathbf{p}_i\|} \rightarrow \mathbf{R}^* \mathbf{g}_{ij}^*$ ,  $\forall e_{ij} \in \mathcal{E}$ , as  $t \rightarrow \infty$ .

### 3.4.2 Global orientation estimation

Define the matrix  $\mathbf{Q}_i \in SO(d)$  as  $\mathbf{Q}_i := \mathbf{R}_i^\top \mathbf{X}$ ,  $\forall i = 1, \dots, n$ , where  $\mathbf{X} \in SO(d)$  and  $\mathbf{X}$  is a constant matrix. Since  $\mathbf{R}_{ij} = \mathbf{R}_i^{-1} \mathbf{R}_j = \mathbf{R}_i^\top \mathbf{R}_j$ , it follows that

$$\mathbf{Q}_i = \mathbf{R}_{ij} \mathbf{Q}_j, \quad \forall e_{ij} \in \mathcal{E}_o. \quad (3.55)$$

Finding the steady-state solution of  $\hat{\mathbf{R}}_i$  is equivalent to finding  $\mathbf{Q}_i$  satisfying the equality (3.55). An algorithm to find  $\mathbf{Q}_i : [0, \infty) \rightarrow \mathbb{R}^{d \times d}$  that achieves the following two goals

1.  $\mathbf{Q}_i(t) \in SO(d), \forall t \in [0, \infty)$ ,
2.  $\mathbf{Q}_i(t) \rightarrow \mathbf{R}_{ij} \mathbf{Q}_j(t)$ , as  $t \rightarrow \infty, \forall e_{ij} \in \mathcal{E}_o$ .

has been recently proposed in [26, 143]. The algorithm is given as follows:

Suppose that each agent  $i$  generates  $d$  auxiliary variables  $\mathbf{z}_{i,k} \in \mathbb{R}^d$ ,  $k = 1, \dots, d$ . Let  $\mathbf{Q}_i$  be represented as  $\mathbf{Q}_i = [\mathbf{q}_{i,1}, \mathbf{q}_{i,2}, \dots, \mathbf{q}_{i,d}]$  where  $\mathbf{q}_{i,k} \in \mathbb{R}^d$ ,  $k = 1, \dots, d$ , is a column vector of  $\mathbf{Q}_i$ . The orthonormal column vectors of  $\mathbf{Q}_i$  can be constructed based on the following Gram-Schmidt process with any independent vectors  $\mathbf{z}_{i,k}$ ,  $k = 1, \dots, d$ , as follows:

$$\begin{aligned}\mathbf{v}_{i,1} &\triangleq \mathbf{z}_{i,1}, & \mathbf{q}_{i,1} &\triangleq \frac{\mathbf{v}_{i,1}}{\|\mathbf{v}_{i,1}\|}, \\ \mathbf{v}_{i,2} &\triangleq \mathbf{z}_{i,2} - (\mathbf{z}_{i,2}^T \mathbf{q}_{i,1}) \mathbf{q}_{i,1}, & \mathbf{q}_{i,2} &\triangleq \frac{\mathbf{v}_{i,2}}{\|\mathbf{v}_{i,2}\|}, \\ &\vdots & &\vdots \\ \mathbf{v}_{i,d} &\triangleq \mathbf{z}_{i,d} - \sum_{k=1}^{d-1} (\mathbf{z}_{i,d}^T \mathbf{q}_{i,k}) \mathbf{q}_{i,k}, & \mathbf{q}_{i,d} &\triangleq \sigma \frac{\mathbf{v}_{i,d}}{\|\mathbf{v}_{i,d}\|},\end{aligned}\tag{3.56}$$

where

$$\sigma \triangleq \text{sgn} \left( \det \left( \left[ \mathbf{q}_{i,1}, \dots, \mathbf{q}_{i,d-1}, \frac{\mathbf{v}_{i,d}}{\|\mathbf{v}_{i,d}\|} \right] \right) \right).\tag{3.57}$$

Note that  $\sigma$  is chosen such that  $\det(\mathbf{Q}_i) = +1$  and subsequently  $\mathbf{Q}_i \in SO(d)$ .

Consider now the second goal, an estimation law for the auxiliary variables is proposed as follows:

$$\dot{\mathbf{z}}_{i,k}(t) = \sum_{j \in \mathcal{N}_i} a_{ij} (\mathbf{R}_{ij} \mathbf{z}_{j,k}(t) - \mathbf{z}_{i,k}(t)),\tag{3.58}$$

where  $\mathbf{R}_{ij} = \mathbf{R}_i^\top \mathbf{R}_j$  is available from relative orientation measurements. Note that each agent  $i$  is simultaneously running  $d$  estimation laws for the  $d$  auxiliary variables  $\mathbf{z}_{i,1}, \dots, \mathbf{z}_{i,d}$ . Let  $\mathbf{z}_k(t) = [\mathbf{z}_{1,k}^\top, \dots, \mathbf{z}_{n,k}^\top]^\top \in \mathbb{R}^{dn}$ , the estimation law (3.58) can be rewritten in the matrix form as

$$\dot{\mathbf{z}}_k(t) = \mathbf{N} \mathbf{z}_k(t),\tag{3.59}$$

with  $\mathbf{N} = -\mathbf{D}(\mathbf{L}_o \otimes \mathbf{I}_d)\mathbf{D}^{-1} \in \mathbb{R}^{dn \times dn}$ , where  $\mathbf{D} = \text{diag}(\mathbf{R}_1^\top, \dots, \mathbf{R}_n^\top)$ . Notice that  $\mathbf{D}^{-1} = \mathbf{D}^\top = \text{diag}(\mathbf{R}_1, \dots, \mathbf{R}_n)$  due to properties of the rotation matrix.

By introducing a coordinate transformation  $\mathbf{z}_{i,k} = \mathbf{R}_i \mathbf{y}_{i,k}$ , and let  $\mathbf{y}_k(t) = [\mathbf{y}_{1,k}^\top, \dots, \mathbf{y}_{n,k}^\top]^\top \in \mathbb{R}^{dn}$ , we have  $\mathbf{z} = \mathbf{D}^{-1} \mathbf{y}$ . Thus, (3.59) can be rewritten as follows:

$$\dot{\mathbf{y}}_k(t) = -(\mathbf{L}_o \otimes \mathbf{I}_d) \mathbf{y}_k(t), \quad \forall k = 1, \dots, n.\tag{3.60}$$

Let  $\mathcal{Q}_{\mathbf{y}_k} := \{\mathbf{y}_k \in \mathbb{R}^{dn} \mid \mathbf{y}_{1,k} = \mathbf{y}_{2,k} = \dots = \mathbf{y}_{n,k}\}$ . For the estimation of orientation, we have to avoid the convergence of variables  $\mathbf{y}_k$  to zero. Thus, the desired equilibrium set is defined by  $\mathcal{S}_{\mathbf{y}_k} := \mathcal{Q}_{\mathbf{y}} \setminus \{\mathbf{0}\}$ . The following theorems about the global orientation estimation dynamics can be stated. Their proofs can be found in [26, 143].

**Theorem 3.28** *Consider the system (3.60), under Assumption 3.5, there exists a finite point  $\mathbf{y}_k^\infty \in \mathcal{S}_{\mathbf{y}_k}$  ( $k = 1, \dots, d$ ) such that  $\mathbf{y}_k$  exponentially converges if and only if the initial value  $\mathbf{y}_k(0)$  ( $k = 1, \dots, d$ ) is not in  $\mathcal{R}(\mathbf{L}_o \otimes \mathbf{I}_d)$ .*

Theorem 3.28 implies  $\lim_{t \rightarrow \infty} \mathbf{z}_k = \mathbf{D}\mathbf{y}_k^\infty, \forall k = 1, \dots, d$ . Since  $\mathbf{Q}_i \in SO(d)$  is derived from  $\mathbf{z}_{i,k}, \forall k = 1, \dots, d$ , there exists  $\mathbf{Q}_i^\infty \in SO(d)$  to which  $\mathbf{Q}_i$  converges.

**Theorem 3.29** *Let  $\mathbf{Q}_i \in SO(d)$  for the  $i$ -th agent be derived from procedures (3.56) and (3.58). There exists a common matrix  $\mathbf{R}_i^* \in SO(d)$  such that  $\mathbf{Q}_i$  converges to  $\mathbf{R}_i^* \mathbf{R}_i^*$  as  $t \rightarrow \infty$  for all  $i = 1, \dots, n$ .*

**Remark 3.30** *As pointed out by Theorem 3.28, the existence of the estimated solution depends on the initial values of auxiliary variables  $\mathbf{z}_{i,k}, i = 1, \dots, n, k = 1, \dots, d$ . Since the set of initial auxiliary variables resulting in nonexistence of solution is a set of Lebesgue measure zero in  $\mathbb{R}^{dn}$ , the estimation law (3.58) converges almost globally asymptotically.*

**Corollary 3.31** *Suppose that the graph  $G_o$  is rooted-out branching and the root node (say node 1) has information about a common global coordinate frame  $\Sigma$ , and thus does not update its orientation  $\dot{\mathbf{z}}_{1,k} = \mathbf{0}$  while other nodes follows the orientation estimation (3.58), then the estimated orientation  $\mathbf{Q}_i$  converges to  $\mathbf{R}_i^* \mathbf{R}_1$  as  $t \rightarrow \infty$ , for all  $i = 1, \dots, n$ .*

*Proof:* The proof can be found in [58] and will be omitted. ■

### 3.4.3 Distributed bearing-based formation control

To solve Problem 3.3, the following bearing-only distributed control law is proposed for each agent  $i$  ( $i = 1, \dots, n$ ):

$$\mathbf{u}_i^i = - \sum_{j \in \mathcal{N}_i} \mathbf{P}_{\mathbf{g}_{ij}^i} \mathbf{Q}_i \mathbf{g}_{ij}^*, \quad (3.61)$$

where  $\mathbf{Q}_i$  is the estimated orientation matrix obtained at time  $t$  based on (3.58),  $\mathbf{P}_{\mathbf{g}_{ij}^i} = \mathbf{I}_d - \mathbf{g}_{ij}^i (\mathbf{g}_{ij}^i)^\top$  is the projection matrix obtained from bearing measurements in  ${}^i\Sigma$ , and  $\mathcal{N}_i$  denotes the set of neighbor of agent  $i$  in the bearing sensing graph  $G$ .

Note that  $\mathbf{P}_{\mathbf{g}_{ij}^i} = \mathbf{R}_i^T \mathbf{P}_{\mathbf{g}_{ij}} \mathbf{R}_i$ . Further, since  $\mathbf{Q}_i$  is a rotation matrix, we can write  $\mathbf{Q}_i = \mathbf{R}_i^\top \mathbf{R}_{\Delta i} \mathbf{R}^*$ , where  $\mathbf{R}_{\Delta i} \in SO(d)$  is the rotation error during the estimation procedure at time  $t \geq 0$ .

Since the dynamics of each agent  $i$  written in the global reference frame is given by

$$\dot{\mathbf{p}}_i = \mathbf{R}_i \mathbf{u}_i^i, \quad i = 1, \dots, n, \quad (3.62)$$

from (3.61), we can write

$$\begin{aligned} \dot{\mathbf{p}}_i &= -\mathbf{R}_i \sum_{j \in \mathcal{N}_i} \mathbf{P}_{\mathbf{g}_{ij}^i} \mathbf{Q}_i \mathbf{g}_{ij}^* \\ &= -\mathbf{R}_i \sum_{j \in \mathcal{N}_i} \mathbf{R}_i^T \mathbf{P}_{\mathbf{g}_{ij}} \mathbf{R}_i \mathbf{R}_i^\top \mathbf{R}_{\Delta i} \mathbf{R}^* \mathbf{g}_{ij}^* \\ &= -\sum_{j \in \mathcal{N}_i} \mathbf{P}_{\mathbf{g}_{ij}} \mathbf{R}_{\Delta i} \mathbf{R}^* \mathbf{g}_{ij}^* \\ &= -\underbrace{\sum_{j \in \mathcal{N}_i} \mathbf{P}_{\mathbf{g}_{ij}} \mathbf{R}^* \mathbf{g}_{ij}^*}_{\triangleq \mathbf{f}_i(\mathbf{p})} + \underbrace{\sum_{j \in \mathcal{N}_i} \mathbf{P}_{\mathbf{g}_{ij}} (\mathbf{I}_d - \mathbf{R}_{\Delta i}) \mathbf{R}^* \mathbf{g}_{ij}^*}_{\triangleq \mathbf{h}_i(t)}, \end{aligned} \quad (3.63)$$

where  $\mathbf{g}_{ij}^\infty = \mathbf{R}^* \mathbf{g}_{ij}^*$ , and  $\mathbf{h}_i(t) = \sum_{j \in \mathcal{N}_i} \mathbf{P}_{\mathbf{g}_{ij}} (\mathbf{I}_d - \mathbf{R}_{\Delta i}) \mathbf{R}^* \mathbf{g}_{ij}^*$ . Let  $\mathbf{p} = [\mathbf{p}_1^\top, \dots, \mathbf{p}_n^\top]^\top \in \mathbb{R}^{dn}$ ,  $\mathbf{h}(t) = [\mathbf{h}_1^\top, \dots, \mathbf{h}_n^\top]^\top \in \mathbb{R}^{dn}$ , and  $\mathbf{g}^\infty = [(\mathbf{g}_1^\infty)^\top, \dots, (\mathbf{g}_m^\infty)^\top]^\top \in \mathbb{R}^{dn}$ . From equation (3.63), we can write the overall dynamics as follows:

$$\dot{\mathbf{p}} = \mathbf{f}(\mathbf{p}) + \mathbf{h}(t), \quad (3.64)$$

where  $\mathbf{f}(\mathbf{p}) = -\bar{\mathbf{H}}^T \text{blkdiag}(\mathbf{P}_{\mathbf{g}_k}) \mathbf{g}^\infty$ , and  $\mathbf{h}(t)$  is an input to the unforced system:

$$\dot{\mathbf{p}} = \mathbf{f}(\mathbf{p}) = -\bar{\mathbf{H}}^T \text{blkdiag}(\mathbf{P}_{\mathbf{g}_k}) \mathbf{g}^\infty, \quad (3.65)$$

The following lemma can be proved:

**Lemma 3.32** *The input  $\mathbf{h}(t)$  is bounded. Moreover,  $\mathbf{h}(t) \rightarrow \mathbf{0}$  exponentially.*

*Proof:* Since  $\|\mathbf{h}_i(t)\| \leq \sum_{j \in \mathcal{N}_i} \|\mathbf{P}_{\mathbf{g}_i}\| \|\mathbf{I}_d - \mathbf{R}_{\Delta i}\| \|\mathbf{R}^*\| \|\mathbf{g}_{ij}^*\|$  and each component in the left hand side is bounded,  $\|\mathbf{h}_i(t)\|$  is also bounded. Based on Theorem 3.29,  $\mathbf{R}_{\Delta i} \rightarrow \mathbf{I}_d$  exponentially as  $t \rightarrow \infty$ . Thus  $\|\mathbf{h}_i(t)\| \rightarrow 0$  exponentially. ■

Next, recalling from Section 3.2 that the unforced system (3.65) has two equilibrium points: the equilibrium  $\mathbf{p} = \mathbf{p}_d^\infty$  corresponding to  $\mathbf{g}_{ij} = \mathbf{g}_{ij}^\infty, \forall e_{ij} \in \mathcal{E}$  is almost globally exponentially stable; the equilibrium  $\mathbf{p} = \mathbf{p}_u^\infty$  corresponding to  $\mathbf{g}_{ij} = -\mathbf{g}_{ij}^\infty, \forall e_{ij} \in \mathcal{E}$  is exponentially unstable. The main result in this section is stated in the following theorem, whose proof is similar to the proof of Theorem 3.27 and will be omitted.

**Theorem 3.33** *Under Assumptions 3.1, 3.2, 3.3 and 3.5, the equilibrium  $\mathbf{p} = \mathbf{p}_d^\infty$  corresponding to  $\mathbf{g}_{ij} = \mathbf{g}_{ij}^\infty, \forall e_{ij} \in \mathcal{E}$  of the system (3.64) is almost globally asymptotically stable.*

**Corollary 3.34** *If there exists an agent satisfying the hypothesis of the Corollary 3.31, then any trajectory of the system 3.64 almost globally asymptotically converges to a desired equilibrium  $\mathbf{p} = \mathbf{p}_d$  where  $\mathbf{g}_{ij} = \mathbf{g}_{ij}^*, \forall e_{ij} \in \mathcal{E}$ .*

*Proof:* From the result of Corollary 3.31, all agents can estimate its exact orientation, i.e.  $\mathbf{Q}_i(t) \rightarrow \mathbf{R}_i^T$  as  $t \rightarrow \infty$ . This implies  $\mathbf{R}^* = \mathbf{I}_d$ , and thus  $\mathbf{g}^\infty = \mathbf{g}^*$ . The remaining proof follows from Theorem 3.33. ■

### 3.5 Regulating the target formation

This section studies two strategies to regulate the LFF formations given that the  $n$ -agent system starts from a formation which is bearing congruent to the desired formation. First, a strategy is proposed to control the formation's orientation by switching the leader's orientation. Second, it is shown that by controlling the distance between the leader and the first follower, one can control the formation's scale.

#### 3.5.1 Controlling the formation's orientation

As proved in Section 3.3, under the two-layer control strategy, the  $n$ -agent system (3.39)-(3.40) almost globally asymptotically converges to the desired formation  $\mathbf{p}_a^*$  corresponding to  $\mathbf{g}_{ij} = \mathbf{R}_1 \mathbf{g}_{ij}^*$ . The desired formation's orientation with regard to the global reference frame is thus determined by the leader's orientation. When the actual formation is identical with the desired formation  $\mathbf{g}_{ij} = \mathbf{g}_{ij}^*$ ,  $\mathbf{R}_i = \mathbf{R}_1$  for all  $1 \leq i \leq n$ , the leader can control the overall formation's orientation with regard to the global reference frame by switching its orientation  $\mathbf{R}_1$  to a new orientation  $\mathbf{R}'_1$ . The new orientation must satisfy the following assumption.

**Assumption 3.6** *The new orientation  $\mathbf{R}'_1$  is contained within a closed ball  $\bar{B}_r(\mathbf{R}_1)$  of radius  $r$  less than  $\pi/2$ , or equivalently, the symmetric part of  $(\mathbf{R}'_1)^\top \mathbf{R}_1$  is positive definite.*

**Corollary 3.35** *Under Assumptions 3.1–3.3 and control laws 3.42–(3.44), if initially, the formation is at a desired equilibrium satisfying  $\mathbf{g}_{ij}(0) = \mathbf{R}_1 \mathbf{g}_{ij}^*$ ,  $\forall \mathbf{g}_{ij}^* \in \mathcal{B}$ ,  $\mathbf{R}_i(0) = \mathbf{R}_1$ ,  $\forall i = 1, \dots, n$ , and agent 1 switches its orientation to  $\mathbf{R}'_1$  satisfying Assumption 3.6, the formation asymptotically converges to a formation with the same formation scale satisfying  $\mathbf{g}_{ij} = \mathbf{R}'_1 \mathbf{g}_{ij}^*$ ,  $\forall \mathbf{g}_{ij}^* \in \mathcal{B}$ .*

*Proof:* Since the new orientation  $\mathbf{R}'_1$  satisfies Assumption 3.6, after the leader switches its orientation, the convergence of all other agents' orientations to  $\mathbf{R}'_1$  is guaranteed and thus  $\mathbf{R}_i \rightarrow \mathbf{R}'_1$ ,

$2 \leq i \leq n$ .

The new desired formation has to satisfy  $\mathbf{g}_{ij} = \mathbf{R}'_1 \mathbf{g}_{ij}^*$ ,  $\forall \mathbf{g}_{ij}^* \in \mathcal{B}$ . Because  $\mathbf{g}_{21}(0) = \mathbf{R}_1 \mathbf{g}_{21}^*$ ,  $\mathbf{R}_2(0) = \mathbf{R}_1$ , after the leader switches its orientation, agent 2 cannot be at the new undesired equilibrium, i.e.,  $\mathbf{g}_{21}(0) \neq -\mathbf{R}'_1 \mathbf{g}_{21}^*$ ,  $\mathbf{R}_2(0) \neq \mathbf{R}'_1$ . Therefore, the convergence of the formation to the new desired formation follows immediately from Theorem 3.27. ■

### 3.5.2 Rescaling the formation

In practice, it may be desired to control the scale of the formation. If only the bearing information is measured, there is apparently no basis to control the size of the overall formation. Suppose the formation is its desired shape. Further, assume that one distance,  $d_{12}$ , between the leader and first follower, for which there is an associated desired distance constraint  $d^*$ , can be measured by the leader. It turns out that by controlling  $d_{12}$ , the whole other distances in the LFF formation will be controlled. The scale adjustment control law is proposed as

$$\dot{\mathbf{p}}_1 = \alpha_1(d_{12}^2 - (d^*)^2)(\mathbf{p}_2 - \mathbf{p}_1), \quad (3.66)$$

where  $\alpha_1 > 0$  is a control gain.

**Proposition 3.36** *Under Assumptions 3.1-3.3, if the LFF formation is initially in a desired formation, agent 1 moves under the control law (3.66) and other agents move under the bearing-only control law (3.43)-(3.44), the LFF formation asymptotically converges to a new desired formation with formation scale specified by  $d^*$ .*

*Proof:* Since the formation is initially at a desired formation, all local orientations are aligned and will not be changed with time. Moreover, as  $\mathbf{g}_{21}(0) = \mathbf{R}_1 \mathbf{g}_{21}^*$ , and the first follower will not

move ( $\dot{\mathbf{p}}_2 = \mathbf{0}$ ) because the motion of the leader preserves  $\mathbf{g}_{21}$ . This fact follows from

$$\frac{\partial \mathbf{g}_{21}}{\partial \mathbf{p}_1} \dot{\mathbf{p}}_1 = \frac{\mathbf{P}_{\mathbf{g}_{21}}}{d_{12}} \alpha_1 (d_{12}^2 - (d^*)^2) (\mathbf{p}_2 - \mathbf{p}_1) = \alpha_1 \frac{d_{12}^2 - (d^*)^2}{d_{12}} \mathbf{P}_{\mathbf{g}_{21}} \mathbf{z}_{12} = \mathbf{0}. \quad (3.67)$$

It is easy to prove that  $d_{21}$  converges to  $d^*$  exponentially fast by considering the Lyapunov function  $V = \frac{1}{4}(d_{12}^2 - (d^*)^2)^2$  [57]. The remaining proof for convergence of other followers is similar to the proof of Theorem 3.13.

Finally, the formation scale asymptotically converges to the desired one, which is fully determined by the distance between the leader and the first follower according to Lemma 3.6. ■

### 3.6 Simulation results

In this section, an eight-agent system with an LFF graph as depicted in Fig. 3.2 is considered. The desired bearing vectors were chosen to satisfy Assumption 3. The desired formation is a cube in  $\mathbb{R}^3$ .

#### 3.6.1 Simulation 1: Achieving the desired formation

The leader's initial conditions are  $\mathbf{p}_1(0) = [0, 0, 0]^\top$ ,  $\mathbf{R}_1(0) = \mathbf{I}_3$ . Other agents' orientations were randomly chosen such that Assumption 3.4 is satisfied. Agent 2's initial position is chosen at  $\mathbf{p}_2(0) = [1, \sqrt{3}, 0]^\top$ , which is not an undesired equilibrium.

Figure 3.7 depicts trajectories and orientations of eight agents. The initial orientations and the final orientations are colored black and red, respectively. Observe that agent 1 does not move in this simulation, and  $d_{21}(t) = d_{21}(0) = 2, \forall t \geq 0$ . In the final formation, all orientations are aligned and all desired bearing vectors are satisfied. Thus, the simulation result is consistent with Theorem 3.27.

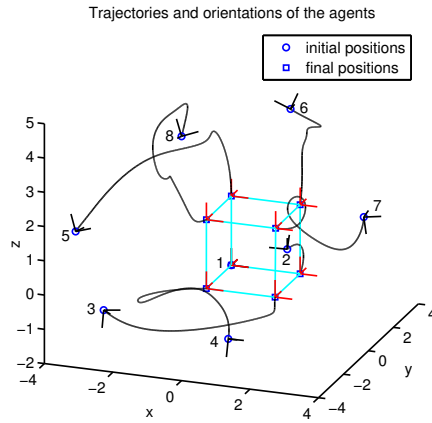


Figure 3.7. Simulation 1: Achieving the desired formation with orientation alignment.

### 3.6.2 Simulation 2: Rotating formation by switching leader's orientation

This simulation continues from the end of Simulation 1, i.e. eight agents have taken up the desired formation shape described in the previous simulation. Agent 1 switches its orientation from  $I_3$  to

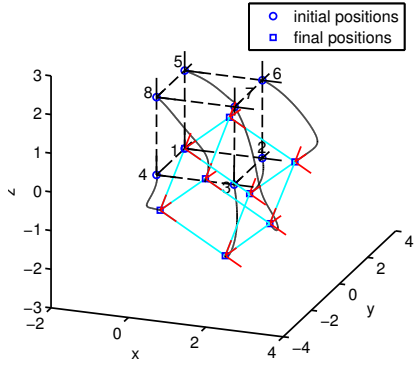
$$\mathbf{R}'_1 = \begin{bmatrix} 0.7071 & 0 & 0.7071 \\ 0.3536 & 0.8660 & -0.3536 \\ -0.6124 & 0.5000 & 0.6124 \end{bmatrix},$$

which satisfies Assumption 3.6. Figure 3.8a depicts trajectories and orientations of eight agents after agent 1 switched its orientation. The final formation is rotated by  $\mathbf{R}'_1$  from the initial formation and all agent's local orientations converge to  $\mathbf{R}'_1$ . Agent 1 does not move in this simulation. Also, the formation's scale does not change during the system's evolution and  $d_{21}(t) = 2$ , for all  $t \geq 0$ .

### 3.6.3 Simulation 3: Rescaling the formation

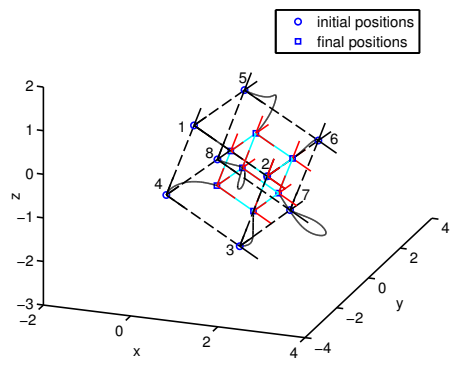
This simulation continues from the end of Simulation 2. The leader starts to control the scale. It is shown in Fig. 3.8b that the formation is rescaled to the desired formation scale, and  $d_{21}(t) \rightarrow d^* = 1$ . Agent 1 moves along a straight line toward agent 2 while agent 2 does not move since its bearing

Trajectories and orientations of the agents after switching



(a) Simulation 2: Rotating the target formation by switching the leader's orientation.

Trajectories and orientations of the agents during rescaling



(b) Simulation 3: Rescaling the target formation by controlling the distance  $d_{12}$ .

Figure 3.8. Regulating the target formation

constraint  $\mathbf{g}_{21}^*$  is always satisfied. Thus, the simulation result is consistent with Proposition 3.36.

### 3.7 Implementation on quadrotor systems

An LFF formation is implemented in quadrotor systems. Consider a three-agent LFF formations consisting of a leader, a first follower and a second follower with a setup depicted in Fig. 3.9. The desired formation shape is an isosceles right triangle.

The quadrotor system is equipped with GPS and IMU for navigation, and a zigbee module for communication. The bearing vectors are calculated from GPS signals, which contain the positional information. That is, quadrotor 2 receives the position  $\mathbf{p}_1$  of quadrotor 1, and calculates the bearing vector  $\mathbf{g}_{21} = (\mathbf{p}_1 - \mathbf{p}_2)/\|\mathbf{p}_1 - \mathbf{p}_2\|$  to quadrotor 1; quadrotor 3 receives  $\mathbf{p}_1$  and  $\mathbf{p}_2$  from quadrotors 1 and 2, and calculates the bearing vectors  $\mathbf{g}_{31} = (\mathbf{p}_1 - \mathbf{p}_3)/\|\mathbf{p}_1 - \mathbf{p}_3\|$  and  $\mathbf{g}_{32} = (\mathbf{p}_2 - \mathbf{p}_3)/\|\mathbf{p}_2 - \mathbf{p}_3\|$ , respectively. The bearing-only control law (3.6) is modified a little bit as follows:

$$\mathbf{u}_i = -k_c(\|\mathbf{g}_{ij} - \mathbf{g}_{ij}^*\|) \sum_{j \in \mathcal{N}_i} P_{\mathbf{g}_{ij}} \mathbf{g}_{ij}^*, \quad (3.68)$$

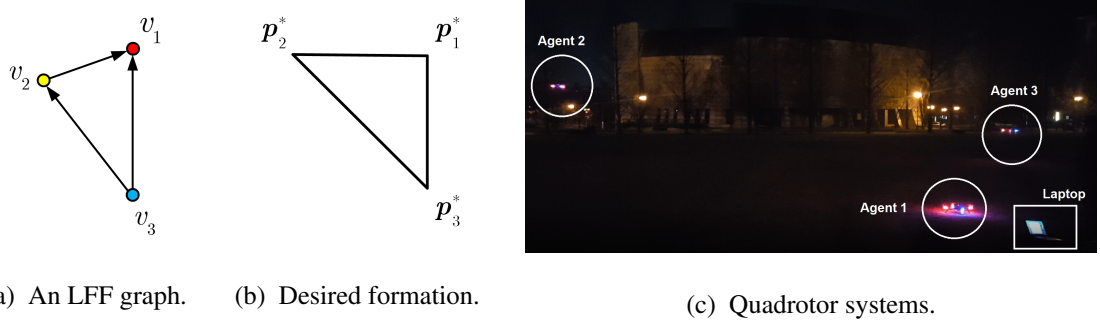
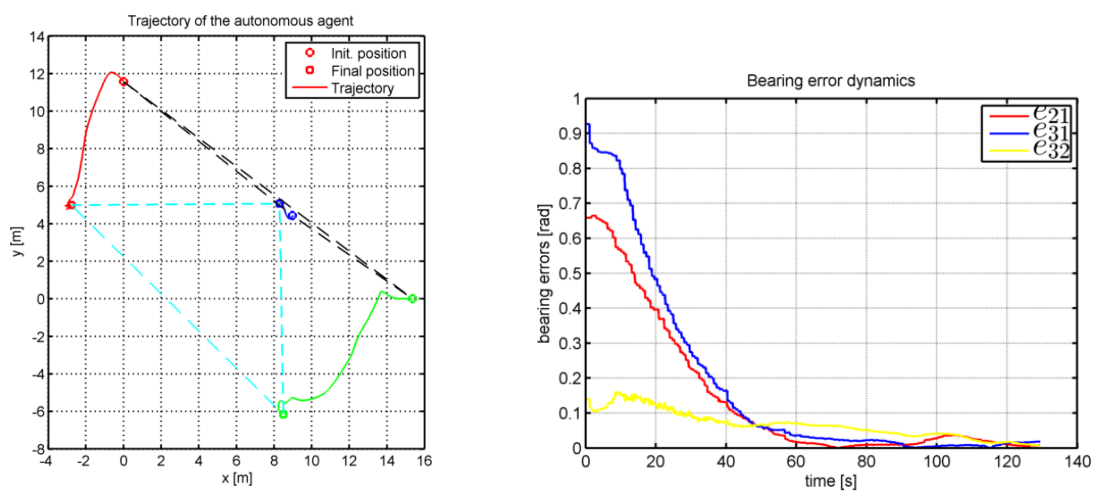


Figure 3.9. Experiment setup

where  $k_c(\|\mathbf{g}_{ij} - \mathbf{g}_{ij}^*\|) > 0$  is piece-wise constant gains. The control gain  $k_c(\|\mathbf{g}_{ij} - \mathbf{g}_{ij}^*\|)$  has been designed such that  $\|\mathbf{u}_i\|$  does not become too small when  $\|\mathbf{g}_{ij} - \mathbf{g}_{ij}^*\|$  becomes small. Note that on one hand, a small error in bearing error could lead to a big distortion in the final formation shape. On the other hand, nearby the equilibrium, the magnitude of  $\|\mathbf{u}_i\|$  becomes so small in compare with the GPS errors and the wind. Thus, the gain  $k_c(\|\mathbf{g}_{ij} - \mathbf{g}_{ij}^*\|)$  is scheduled to guarantee a better performance nearby the equilibrium by some logic functions in the navigation program.

The control law (3.68) is implemented onboard from each quadrotor. Also, the quadrotors' GPS positions are sent to a laptop to collect and analyze the flying data.

Trajectories of three quadrotors are reported in Fig. 3.10 (blue - quadrotor 1, red - quadrotor 2, and green - quadrotor 3). It can be observed that the quadrotors asymptotically form the desired isosceles right triangular formation. Quadrotor 1 does not move, but its GPS is floating a little bit in time. The bearing errors  $e_{ij} = \|\mathbf{g}_{ij} - \mathbf{g}_{ij}^*\|$  decay asymptotically until reaching a lower bound small error less than 0.05. Also, it is observed that the distance between agent 1 and 2 cannot be invariant in time because of the wind and GPS error. However, the variation is quite small regarding the possible error of few meters of GPS signals. Thus, the experimental trajectories are consistent with the analysis and numerical simulation presented in the previous sections.



(a) Trajectories: blue - agent 1, red - agent 2,

(b) Bearing errors vs time.

green - agent 3.

Figure 3.10. Experiment results.

# Chapter 4

## Formations on Directed Cycles with Bearing-Only Measurements

This chapter studies a bearing-only formation control problem with a directed cycle sensing graph. More specifically, the  $n$ -agent formation in the plane and the three-agent formation in the three dimensional space with directed cycles sensing graphs are studied. In Section 4.1, some preliminary results on bearing-only formation are described and the main problem is formulated. Section 4.2 presents the main stability results pertaining to bearing-only formation control using cyclic pursuit in the plane. Section 4.3 extends the analysis of directed triangular formations to the three dimensional space. Finally, in Section 4.4, simulations validate the theoretical developments.

### 4.1 Problem formulation and the proposed control law

#### 4.1.1 Problem formulation

Consider a formation of  $n$  ( $n \geq 3$ ) autonomous agents in  $\mathbb{R}^d$  ( $d = 2$  or  $3$  and will be clear from the context). The dynamics of each agent is given by a single-integrator model,

$$\dot{\mathbf{p}}_i = \mathbf{u}_i, \quad \forall i \in \mathcal{I} \triangleq \{1, \dots, n\}, \quad (4.1)$$

where  $\mathbf{p}_i, \mathbf{u}_i \in \mathbb{R}^d$  are the position and the control input of the agent  $i$  expressed in the global coordinate frame, respectively.

Directed graphs are used to describe the sensing and controlling topology between agents in the formation [32, 91]. A directed graph is described by  $G = (\mathcal{V}, \mathcal{E})$ , where  $\mathcal{V} = \{v_1, \dots, v_n\}$  is the set

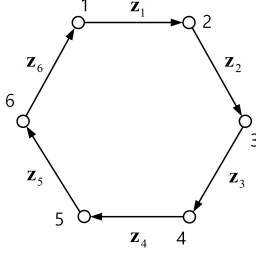


Figure 4.1. A directed cycle graph with six nodes.

of vertices and  $\mathcal{E} = \{(v_i, v_j) | i, j \in \mathcal{I}\}$  is the set of directed edges. A vertex  $v_j$  is called a neighbor of vertex  $v_i$  if and only if  $(v_i, v_j) \in \mathcal{E}$ . Let  $\mathcal{N}_i = \{j \in \mathcal{I} | (v_i, v_j) \in \mathcal{E}\}$ . A *directed cycle* with  $n$  vertices (and also  $n$  edges), denoted by  $C_n$ , is a directed graph where vertex  $v_{i+1} \equiv v_{(i+1)(\text{modulo } n)}$  is the only neighbor of vertex  $v_i$ , i.e.,  $\mathcal{N}_i = \{i + 1(\text{modulo } n)\}$ .

A directed cycle of six nodes is illustrated in Fig. 4.1. The relative position vector is defined as  $\mathbf{z}_i = \mathbf{p}_{i+1} - \mathbf{p}_i$ , for  $i \in \mathcal{I}$ . The variable  $\mathbf{z}_i$  is sometimes referred to as the edge  $(v_i, v_{i+1})$  in the Euclidean space. Further,  $d_i = \|\mathbf{z}_i\|$  is the distance between two agents  $i$  and  $i + 1$ . Also, let the absolute and relative positions be stacked as vectors  $\mathbf{p} = [\mathbf{p}_1^\top, \dots, \mathbf{p}_n^\top]^\top \in \mathbb{R}^{dn}$  and  $\mathbf{z} = [\mathbf{z}_1^\top, \dots, \mathbf{z}_n^\top]^\top \in \mathbb{R}^{dn}$ , respectively.

Assume that agent  $i$  can measure the bearing with respect to agent  $i + 1$  (modulo  $n$ ). Based on bearing measurements, agent  $i$  can obtain the relative bearing vector [66],

$$\mathbf{g}_i = \frac{\mathbf{p}_{i+1} - \mathbf{p}_i}{\|\mathbf{p}_{i+1} - \mathbf{p}_i\|} = \frac{\mathbf{z}_i}{\|\mathbf{z}_i\|}. \quad (4.2)$$

The unit vector  $\mathbf{g}_i$  contains the direction information from agent  $i$  to agent  $i + 1$ . Suppose agent  $i$  also knows a desired bearing vector  $\mathbf{g}_i^*$  and the control objective is to asymptotically reduce the bearing error between  $\mathbf{g}_i$  and  $\mathbf{g}_i^*$  to zero. The following definition describes admissible desired bearings.

**Definition 4.1** *The set  $\mathcal{B}_n = \{\mathbf{g}_i^*\}_{i \in \mathcal{I}}$  is called a feasible bearing vector set if and only if for each  $i \in \mathcal{I}$ ,  $\mathbf{g}_i^* \neq \pm \mathbf{g}_{i+1}^*$  and there exist strictly positive scalars  $d_i$  such that  $\sum_{i=1}^n d_i \mathbf{g}_i^* = \mathbf{0}$ .*

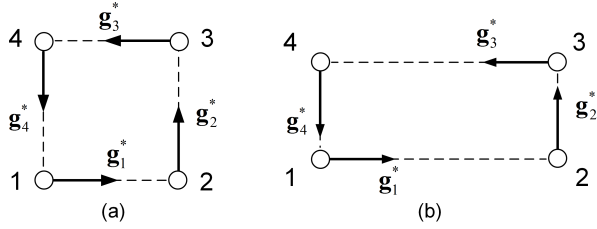


Figure 4.2. Both configurations (a) and (b) satisfy all desired bearing vectors  $\mathbf{g}_i^*, i = 1, \dots, 4$  but are not similar.

It follows from Definition 4.1 that when the desired bearing vectors belong to the set  $\mathcal{B}_n$ , there does not exist three consecutive agents  $i - 1, i$  and  $i + 1$  whose desired positions are collinear. The condition  $\sum_{i=1}^n d_i \mathbf{g}_i^* = \mathbf{0}$  implies that the desired formation of the agents is a closed polygon because each vector of the form  $d_i \mathbf{g}_i^*$  is essentially an edge of the desired polygon, connecting agents  $i$  and  $i + 1$ , with  $\mathbf{g}_i^*$  being the desired bearing of agent  $i$  with respect to its leader, agent  $i + 1$ . The scalar  $d_i$  is the length of the edge between agents  $i$  and  $i + 1$  and is thus the distance between agents  $i$  and  $i + 1$  in Euclidean space corresponding to a feasible formation.

For  $n = 3$ , every triangular formation, satisfying a given desired bearing configuration in  $\mathcal{B}_3$ , is related by translations and a dilation to another feasible formation. For  $n > 3$ , this property is generally not true. To see this, consider a four-agent formation as shown in Fig. 4.2. There are two configurations in  $\mathbb{R}^2$  with sensing graph  $C_4$ . The desired bearing vectors are given by  $\mathbf{g}_1^* = [1, 0]^\top$ ,  $\mathbf{g}_2^* = [0, 1]^\top$ ,  $\mathbf{g}_3^* = [-1, 0]^\top$ , and  $\mathbf{g}_4^* = [0, -1]^\top$ . Although both Figs. 4.2(a) and 4.2(b) satisfy the desired bearings, the formation shapes are not similar. Similarity between formations can only be achieved if the *infinitesimal bearing rigidity* conditions in [49] are satisfied. However, for  $n > 3$  such conditions do not hold for a cycle digraph and so the formation shape is not fixed for a given set of desired bearing vectors.

Let  $\mathbf{J} = \begin{bmatrix} 0 & -1 \\ 1 & 0 \end{bmatrix}$  denote the perpendicular operator, with the property  $\mathbf{J}^\top = -\mathbf{J}$ . Then,  $\mathbf{g}_i^\perp = \mathbf{J}\mathbf{g}_i$  is the unit vector perpendicular to  $\mathbf{g}_i$  in the counterclockwise direction. The following result characterizes a condition for feasibility of a set  $\mathcal{B}_n$  in  $\mathbb{R}^2$ :

**Lemma 4.2** *In  $\mathbb{R}^2$ , the set  $\mathcal{B}_n$  is a feasible bearing vector set if and only if for all  $i \in \mathcal{I}$ :  $\mathbf{g}_i^* \neq \pm \mathbf{g}_{i+1}^*$ , and there exist  $j, k \in \mathcal{I} \setminus \{i\}$  such that  $(\mathbf{g}_j^*)^\top \mathbf{g}_i^{*\perp} < 0$  and  $(\mathbf{g}_k^*)^\top \mathbf{g}_i^{*\perp} > 0$ .*

*Proof:* (Necessity) Suppose  $\mathcal{B}_n$  is a feasible bearing vector set. There exist positive scalars  $d_i$  such that

$$\sum_{i=1}^n d_i \mathbf{g}_i^* = \mathbf{0}. \quad (4.3)$$

One shall prove that there exist  $j, k \in \mathcal{I} \setminus \{i\}$  such that  $(\mathbf{g}_j^*)^\top \mathbf{g}_i^{*\perp} < 0$  and  $(\mathbf{g}_k^*)^\top \mathbf{g}_i^{*\perp} > 0$  by contradiction.

Suppose there does not exist any  $j \in \mathcal{I} \setminus \{i\}$  such that  $(\mathbf{g}_j^*)^\top \mathbf{g}_i^{*\perp} < 0$ . Then rewriting equation (4.3) as

$$-\frac{1}{d_i} \sum_{l \neq i, l=1}^n d_l \mathbf{g}_l^* = \mathbf{g}_i^*, \quad (4.4)$$

and pre-multiplying both sides of (4.4) with  $(\mathbf{g}_i^{*\perp})^\top$ , we have

$$-\frac{1}{d_i} \sum_{l \neq i, l=1}^n d_l (\mathbf{g}_i^{*\perp})^\top \mathbf{g}_l^* = (\mathbf{g}_i^{*\perp})^\top \mathbf{g}_i^* = 0. \quad (4.5)$$

Since  $(\mathbf{g}_i^{*\perp})^\top \mathbf{g}_l^* \geq 0$ , for all  $l \neq i$ , the left hand side of (4.5) is nonpositive. In fact, since  $\mathbf{g}_{i+1}^* \neq \pm \mathbf{g}_i^*$ , we have  $(\mathbf{g}_i^{*\perp})^\top \mathbf{g}_{i+1}^* \neq 0$ , which implies that the left hand side of (4.5) is negative. However, the right hand side of (4.5) is zero. This contradiction implies that there exists at least one  $j \in \mathcal{I} \setminus \{i\}$  such that  $(\mathbf{g}_j^*)^\top \mathbf{g}_i^{*\perp} < 0$ . Similarly, the existence of at least some  $k \in \mathcal{I} \setminus \{i\}$  such that  $(\mathbf{g}_k^*)^\top \mathbf{g}_i^{*\perp} > 0$  is also necessary for a feasible bearing set.

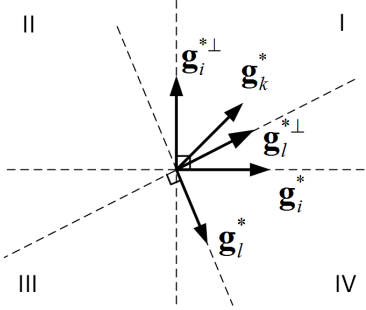


Figure 4.3. Four regions separated by two lines containing two vectors  $\mathbf{g}_i^*$  and  $\mathbf{g}_i^{*\perp}$ .

(*Sufficiency*) Suppose that for all  $i \in \mathcal{I}$ :  $\mathbf{g}_i^* \neq \pm \mathbf{g}_{i+1}^*$ , and there are  $j, k \in \mathcal{I} \setminus \{i\}$  such that  $(\mathbf{g}_j^*)^\top \mathbf{g}_i^{*\perp} < 0$  and  $(\mathbf{g}_k^*)^\top \mathbf{g}_i^{*\perp} > 0$ . We shall prove that there exist positive scalars  $d_i$  such that (4.3) is satisfied. The proof contains the following steps.

Step 1: If  $\mathbf{g}_k^* \neq -\mathbf{g}_j^*$ , we go to Step 2. Otherwise, if  $\mathbf{g}_k^* = -\mathbf{g}_j^*$ , we shall show that there exists

$l \in \mathcal{I} \setminus \{i, j, k\}$ , such that  $\mathbf{g}_l^* \neq \pm \mathbf{g}_j^*$ . Suppose that there does not exist such an  $l$ , then

$(\mathbf{g}_m^*)^\top \mathbf{g}_j^{*\perp} = 0$  for all  $m \in \mathcal{I} \setminus \{i, j\}$  and  $(\mathbf{g}_i^*)^\top \mathbf{g}_j^{*\perp} = -(\mathbf{g}_j^*)^\top \mathbf{g}_i^{*\perp} > 0$ . Thus, there does not exist any vector  $\mathbf{g}_m^* \in \mathcal{B}_n$  such that  $(\mathbf{g}_m^*)^\top \mathbf{g}_j^{*\perp} < 0$ , which contradicts the sufficiency assumption. This contradiction implies the existence of  $l \in \mathcal{I} \setminus \{i, j, k\}$ , such that  $\mathbf{g}_l^* \neq \pm \mathbf{g}_j^*$  and  $(\mathbf{g}_l^*)^\top \mathbf{g}_j^{*\perp} < 0$ .

There are three possibilities: (i)  $(\mathbf{g}_l^*)^\top \mathbf{g}_i^{*\perp} < 0$ , we reindex  $j \leftrightarrow l$  and move to Step 2; (ii)

$(\mathbf{g}_l^*)^\top \mathbf{g}_i^{*\perp} > 0$ , we reindex  $k \leftrightarrow l$  and move to Step 2; (iii)  $(\mathbf{g}_l^*)^\top \mathbf{g}_i^{*\perp} = 0$ , or i.e.,  $\mathbf{g}_l^* = \pm \mathbf{g}_i^*$ .

Because  $(\mathbf{g}_l^*)^\top \mathbf{g}_j^{*\perp} < 0$  and  $(\mathbf{g}_i^*)^\top \mathbf{g}_j^{*\perp} > 0$ , we have  $\mathbf{g}_l^* = -\mathbf{g}_i^*$ . Choosing  $d_i = d_l = 1$ , we write

$$\mathbf{g}_i^* + \mathbf{g}_l^* = \mathbf{0}, \quad (4.6)$$

and move to Step 3.

Step 2: Since  $\mathbf{g}_j^* \neq -\mathbf{g}_k^*$ , two linearly independent vectors  $\mathbf{g}_j^*$  and  $\mathbf{g}_k^*$  form a basis for  $\mathbb{R}^2$ . Thus, we can write:

$$\mathbf{g}_i^* = m_1 \mathbf{g}_j^* + m_2 \mathbf{g}_k^*, \quad (4.7)$$

where  $m_1, m_2$  are scalars. Premultiplying both sides of the above equation with  $(\mathbf{g}_i^{*\perp})^\top$  yields

$$0 = m_1(\mathbf{g}_i^{*\perp})^\top \mathbf{g}_j^* + m_2(\mathbf{g}_i^{*\perp})^\top \mathbf{g}_k^*. \text{ Thus}$$

$$m_2 = m_1(-(\mathbf{g}_i^{*\perp})^\top \mathbf{g}_j^*) / ((\mathbf{g}_i^{*\perp})^\top \mathbf{g}_k^*),$$

which implies  $\operatorname{sgn}(m_1) = \operatorname{sgn}(m_2)$ . Thus, there are two cases:

- Case 1:  $m_1 < 0, m_2 < 0$ . Thus, we can write  $\mathbf{g}_i^* + r_1 \mathbf{g}_j^* + r_2 \mathbf{g}_k^* = \mathbf{0}$ , where  $r_1 = -m_1 > 0$  and  $r_2 = -m_2 > 0$ .
- Case 2:  $m_1 > 0, m_2 > 0$ . In this case, we will prove that there always exists at least two vectors  $\mathbf{g}_{j_1}^*, \mathbf{g}_{k_1}^*, j_1, k_1 \in \mathcal{I} \setminus \{i\}$  such that  $\mathbf{g}_i^* + r_1 \mathbf{g}_{j_1}^* + r_2 \mathbf{g}_{k_1}^* = \mathbf{0}$  where  $r_1 > 0, r_2 > 0$ .

In fact, two vectors  $\mathbf{g}_i^*$  and  $\mathbf{g}_i^{*\perp}$  separate the plane into four regions I - IV as shown in Fig. 4.3.

If there does not exist even a single such pair  $j_1$  and  $k_1$ , from (4.7) all desired bearing vectors must be contained in two regions I and IV. Then, one can choose the index  $l$  corresponding to the vector  $\mathbf{g}_l^*$  such that it minimizes the inner product  $(\mathbf{g}_l^*)^\top \mathbf{g}_i^{*\perp}$  (which is clearly negative from the assumption of the sufficiency proof). It follows that for any vector  $\mathbf{g}_k^* \in \mathcal{B}_n$ , there are  $c_1, c_2 \geq 0$  such that  $\mathbf{g}_k^* = c_1 \mathbf{g}_l^* + c_2 \mathbf{g}_i^{*\perp}$ , and

$$(\mathbf{g}_k^*)^\top \mathbf{g}_l^{*\perp} = (c_1 \mathbf{g}_l^* + c_2 \mathbf{g}_i^{*\perp})^\top \mathbf{g}_l^{*\perp} = c_2 (\mathbf{g}_i^{*\perp})^\top \mathbf{g}_l^{*\perp} = c_2 (\mathbf{g}_i^*)^\top \mathbf{J}^\top \mathbf{J} \mathbf{g}_l^* = c_2 (\mathbf{g}_i^*)^\top \mathbf{g}_l^* \geq 0.$$

Thus, there does not exist any  $\mathbf{g}_k^* \in \mathcal{B}_n$  such that  $(\mathbf{g}_k^*)^\top \mathbf{g}_l^{*\perp} < 0$ . This contradicts our assumption and thus there must exist  $j_1, k_1 \in \mathcal{I} \setminus \{i\}$  such that  $\mathbf{g}_i^* + r_1 \mathbf{g}_{j_1}^* + r_2 \mathbf{g}_{k_1}^* = \mathbf{0}$ , where  $r_1, r_2 > 0$ .

From both cases, it follows that for any  $\mathbf{g}_i^*$ , one can always find two vectors  $\mathbf{g}_j^*, \mathbf{g}_k^*$  and scalars  $r_1, r_2 > 0$  such that

$$\mathbf{g}_i^* + r_1 \mathbf{g}_j^* + r_2 \mathbf{g}_k^* = \mathbf{0}. \quad (4.8)$$

Step 3: Taking the summation over all  $i$  as expressed in the form of (4.6) and (4.8), one will obtain an expression in form of (4.3), which concludes the proof.

■

In this chapter, the control objective for the general  $n$ -agent scenario is to achieve a formation that satisfies a given set of desired bearings for the agents and not necessarily a fixed shape. As discussed earlier, only for  $n = 3$ , one gets a fixed shape corresponding to a given set of desired bearing vectors, though the scale of the formation is not fixed in this case. Hence, the 3-agent scenario is studied in some detail. Before stating the main problem, the main assumptions are now summarized.

**Assumption 4.1** *All agents' local reference frames are aligned, and the dynamics of each agent is given as in (4.1).*

Note that Assumption 4.1 is common in bearing-based formation control problem. To relax this assumption, we could adopt some orientation alignment strategies simultaneously with the main control law (see e.g. [23, 24, 49]).

**Assumption 4.2** *Each agent  $i$  ( $i \in \mathcal{I}$ ) is given a desired bearing vector,  $\mathbf{g}_i^* \in \mathcal{B}_n$ , with respect to its leader. Moreover, the set of desired bearing vector  $\mathcal{B}_n$  is feasible.*

The following problem can be now stated.

**Problem 4.1** *Given a group of  $n$  agents in a plane, satisfying Assumptions 4.1-4.2, and a feasible set of desired bearing vectors  $\mathcal{B}_n$ , design control laws for the agents using only bearing measurements such that  $\mathbf{g}_i \rightarrow \mathbf{g}_i^*$  asymptotically,  $\forall \mathbf{g}_i^* \in \mathcal{B}_n$ .*

### 4.1.2 The bearing-only control law

To address the main problem, the bearing-only control law proposed in [49] is adopted. Specifically, the control law for each agent  $i$ ,  $i \in \mathcal{I}$ , is given by

$$\dot{\mathbf{p}}_i = \mathbf{u}_i = -\mathbf{P}_{g_i} \mathbf{g}_i^*, \quad (4.9)$$

where  $\mathbf{P}_{g_i}$  is the projection matrix associated with the measured bearing vector  $\mathbf{g}_i \in \mathbb{R}^d$ , and is explicitly given by  $\mathbf{P}_{g_i} = \mathbf{I}_d - \mathbf{g}_i \mathbf{g}_i^\top$ . For each agent  $i$ , the control law (4.9) requires only a local bearing measurement  $\mathbf{g}_i$  and a desired bearing vector  $\mathbf{g}_i^*$ .

Intuitively, if agent  $i + 1$  is stationary, the control law (4.9) asymptotically drives agent  $i$  to a position that satisfies  $\mathbf{g}_i = \mathbf{g}_i^*$  while preserving the initial distance between two agents [82, Lemma 1]. Note that the projection matrix  $\mathbf{P}_{g_i}$  in  $\mathbb{R}^2$  can be rewritten as  $\mathbf{P}_{g_i} = \mathbf{g}_i^\perp (\mathbf{g}_i^\perp)^\top$  [66]. As a result, the control law (4.9) can be expressed as

$$\dot{\mathbf{p}}_i = -\mathbf{g}_i^\perp (\mathbf{g}_i^\perp)^\top \mathbf{g}_i^*. \quad (4.10)$$

## 4.2 The directed cycle formation in the plane

This section studies planar formations under the bearing-only control law (4.9). A special case in this class, formation of three agents, is investigated. The triangular formations in  $\mathbb{R}^2$  possess a special property, as discussed earlier. Their formation shapes are uniquely determined by specifying the desired bearing vectors and are only different up to a scaling factor. A sufficient condition on initial conditions for the three-agent system is obtained such that the agents asymptotically achieve the desired bearing. Then, the general  $n$ -agent formations are discussed as a natural extension.

### 4.2.1 The three agent formations

The equations of motion for the three-agent system can be explicitly written as follows:

$$\dot{\mathbf{p}}_1 = -\mathbf{P}_{\mathbf{g}_1} \mathbf{g}_1^* \quad (4.11a)$$

$$\dot{\mathbf{p}}_2 = -\mathbf{P}_{\mathbf{g}_2} \mathbf{g}_2^* \quad (4.11b)$$

$$\dot{\mathbf{p}}_3 = -\mathbf{P}_{\mathbf{g}_3} \mathbf{g}_3^*. \quad (4.11c)$$

Define the following sets:

$$\mathcal{Q}_3 \triangleq \{\mathbf{p} \in \mathbb{R}^6 | \mathbf{g}_i = \pm \mathbf{g}_i^*, i = 1, 2, 3\},$$

$$\mathcal{D}_3 \triangleq \{\mathbf{p} \in \mathbb{R}^6 | \mathbf{g}_i = \mathbf{g}_i^*, i = 1, 2, 3\},$$

$$\mathcal{U}_3 \triangleq \mathcal{Q}_3 \setminus \mathcal{D}_3.$$

The set  $\mathcal{Q}_3$  contains all equilibria of (4.11) and can be partitioned into  $\mathcal{D}_3$  which contains all desired formations, and  $\mathcal{U}_3$  containing the undesired ones. Figure 4.4 depicts an example of two different triangular formations in  $\mathcal{Q}_3$ . Since  $\mathcal{B}_3$  is feasible,  $\mathcal{D}_3 \neq \emptyset$ , and there exists a triangle specified by three desired bearing vectors  $\mathbf{g}_1^*$ ,  $\mathbf{g}_2^*$ , and  $\mathbf{g}_3^*$ . Thus, there exist positive scalars  $m_1, m_2, m_3$  such that

$$m_1 \mathbf{g}_1^* + m_2 \mathbf{g}_2^* + m_3 \mathbf{g}_3^* = \mathbf{0}. \quad (4.12)$$

Dividing both sides of (4.12) by  $m_1 > 0$ , one obtains

$$\mathbf{g}_1^* = -\frac{m_2}{m_1} \mathbf{g}_2^* - \frac{m_3}{m_1} \mathbf{g}_3^* = -n_2 \mathbf{g}_2^* - n_3 \mathbf{g}_3^*, \quad (4.13)$$

where  $n_2 = m_2/m_1 > 0$ , and  $n_3 = m_3/m_1 > 0$ . We examine the set of undesired equilibria  $\mathcal{U}_3$  next.

**Lemma 4.3** *The set  $\mathcal{U}_3$  contains all points  $\mathbf{p} \in \mathbb{R}^6$  such that  $\mathbf{g}_i = -\mathbf{g}_i^*, i = 1, 2, 3$ .*

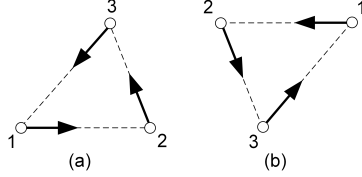


Figure 4.4. The formation (a) is a desired formation where  $\mathbf{g}_i = \mathbf{g}_i^*, i = 1, 2, 3$ , while the formation (b) is an undesired one where  $\mathbf{g}_i = -\mathbf{g}_i^*, i = 1, 2, 3$ .

*Proof:* Consider a point  $\mathbf{p} \in \mathcal{U}_3$  where distances between three agents are  $d_1, d_2, d_3 > 0$ . Since  $\sum_{i=1}^3 \mathbf{z}_i = \sum_{i=1}^3 (\mathbf{p}_{i+1} - \mathbf{p}_i) = 0$  and  $\mathbf{z}_i = d_i \mathbf{g}_i$ , we have  $d_1 \mathbf{g}_1 + d_2 \mathbf{g}_2 + d_3 \mathbf{g}_3 = \mathbf{0}$ , or equivalently,  $\mathbf{g}_1 = -\frac{d_2}{d_1} \mathbf{g}_2 - \frac{d_3}{d_1} \mathbf{g}_3$ . Without loss of generality, assume that at  $\mathbf{p}$ , we have  $\mathbf{g}_1 = -\mathbf{g}_1^*$ . Then,

$$\mathbf{g}_1^* = \frac{d_2}{d_1} \mathbf{g}_2 + \frac{d_3}{d_1} \mathbf{g}_3. \quad (4.14)$$

Since  $\mathbf{p} \in \mathcal{U}_3 \subset \mathcal{Q}_3$ , it follows  $\mathbf{g}_2 = \pm \mathbf{g}_2^*, \mathbf{g}_3 = \pm \mathbf{g}_3^*$ . There are four possibilities: (i)  $\mathbf{g}_2 = -\mathbf{g}_2^*, \mathbf{g}_3 = -\mathbf{g}_3^*$ ; (ii)  $\mathbf{g}_2 = \mathbf{g}_2^*, \mathbf{g}_3 = -\mathbf{g}_3^*$ ; (iii)  $\mathbf{g}_2 = \mathbf{g}_2^*, \mathbf{g}_3 = -\mathbf{g}_3^*$ ; and (iv)  $\mathbf{g}_2 = \mathbf{g}_2^*, \mathbf{g}_3 = \mathbf{g}_3^*$ . Upon substituting these values of  $\mathbf{g}_2$  and  $\mathbf{g}_3$  for the four cases, in (4.14), we get a unique representation of  $\mathbf{g}_1^*$  in terms of  $\mathbf{g}_2^*$  and  $\mathbf{g}_3^*$  in each case because  $\mathbf{g}_2^*, \mathbf{g}_3^*$ , being linearly independent by definition, form a basis for  $\mathbb{R}^2$ . In other words, the representation of  $\mathbf{g}_1^*$  in terms of  $\mathbf{g}_2^*$  and  $\mathbf{g}_3^*$  over the field of real numbers is unique. Further, from (4.13) we know that both of these scalars are negative. Hence, by comparing the representation (4.14) with (4.13), it follows that only case (i) is possible for a feasible triangle. Therefore, we conclude that  $\mathcal{U}_3 = \{\mathbf{p} \in \mathbb{R}^6 | \mathbf{g}_i = -\mathbf{g}_i^*, i = 1, 2, 3\}$ . ■

Consider a triangular formation in  $\mathbb{R}^2$ . Let  $\alpha_i$  be the magnitude of the angle between  $\mathbf{g}_i$  and  $\mathbf{g}_i^*$  as depicted in Fig. 4.5 ( $0 \leq \alpha_i \leq \pi$ ). Then, at any equilibrium point of (4.11) in  $\mathcal{D}_3$ ,  $\alpha_i = 0, \forall i = 1, 2, 3$ , while at any equilibrium point in  $\mathcal{U}_3$ ,  $\alpha_i = \pi, \forall i = 1, 2, 3$ . Thus, the convergence of  $\mathbf{p}$  to a point in  $\mathcal{D}_3$  (correspondingly  $\mathcal{U}_3$ ) is equivalent to the convergence of  $\boldsymbol{\alpha} = [\alpha_1, \alpha_2, \alpha_3]^\top$  to  $[0, 0, 0]^\top$  (correspondingly  $[\pi, \pi, \pi]^\top$ ). Let  $\beta_i$  ( $0 \leq \beta_i \leq \pi$ ) be the magnitude of the angle between  $\mathbf{g}_{i+1}$  and

$\mathbf{g}_i$ . In order to analyze the system's stability, the position dynamics (4.11) is firstly changed into the angle dynamics. Since

$$\cos \alpha_i = (\mathbf{g}_i^*)^\top \mathbf{g}_i, \quad (4.15)$$

taking the derivative with respect to time on both sides of (4.15) and noting that

$$\frac{\partial \mathbf{g}_i}{\partial \mathbf{z}_i} = \frac{\partial}{\partial \mathbf{z}_i} \left( \frac{\mathbf{z}_i}{\|\mathbf{z}_i\|} \right) = \frac{\|\mathbf{z}_i\| \mathbf{I}_2 - \mathbf{z}_i \frac{\mathbf{z}_i^\top}{\|\mathbf{z}_i\|^2}}{\|\mathbf{z}_i\|^2} = \frac{\mathbf{I}_2 - \mathbf{g}_i \mathbf{g}_i^\top}{\|\mathbf{z}_i\|} = \frac{\mathbf{P}_{\mathbf{g}_i}}{d_i},$$

one gets

$$\dot{\alpha}_i \sin \alpha_i = -(\mathbf{g}_i^*)^\top \frac{\mathbf{P}_{\mathbf{g}_i}}{d_i} (\dot{\mathbf{p}}_{i+1} - \dot{\mathbf{p}}_i). \quad (4.16)$$

Substituting  $\dot{\mathbf{p}}_i$  from (4.10) and using the idempotent property of the projection matrix,  $\mathbf{P}_{\mathbf{g}_i} = \mathbf{P}_{\mathbf{g}_i}^2 = \mathbf{g}_i^\perp (\mathbf{g}_i^\perp)^\top$  in (4.16), it follows that

$$\begin{aligned} d_i \dot{\alpha}_i \sin \alpha_i &= (\mathbf{g}_i^*)^\top \mathbf{g}_i^\perp (\mathbf{g}_i^\perp)^\top \mathbf{g}_{i+1}^\perp (\mathbf{g}_{i+1}^\perp)^\top \mathbf{g}_{i+1}^* - (\mathbf{g}_i^*)^\top \mathbf{g}_i^\perp (\mathbf{g}_i^\perp)^\top \mathbf{g}_i^* \\ &= (\pm \sin \alpha_i)(\cos \beta_i)(\pm \sin \alpha_{i+1}) - \sin^2 \alpha_i, \end{aligned}$$

where the last step is reached by using  $(\mathbf{g}_i^*)^\top \mathbf{g}_i^\perp = \pm \sin \alpha_i$  and  $(\mathbf{g}_i^\perp)^\top \mathbf{g}_{i+1}^\perp = \mathbf{g}_i^\top \mathbf{J}^\top \mathbf{J} \mathbf{g}_{i+1} =$

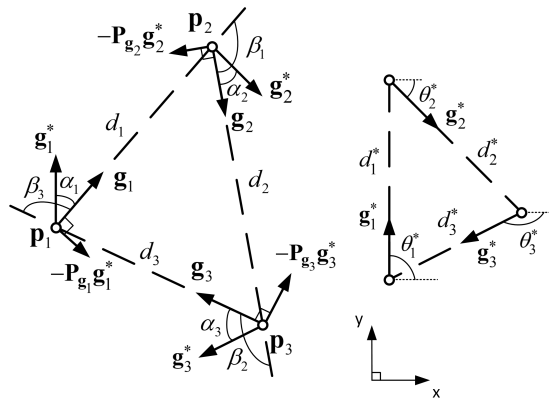


Figure 4.5. The directed triangle formation under control law (4.11) (left); a desired formation (right).

$\mathbf{g}_i^\top \mathbf{g}_{i+1} = \cos \beta_i$ . Thus, the dynamics in terms of angles can be explicitly written as

$$\dot{\alpha}_1 = -\frac{\sin \alpha_1}{d_1} \pm \frac{\sin \alpha_2 \cos \beta_1}{d_1}, \quad (4.17a)$$

$$\dot{\alpha}_2 = -\frac{\sin \alpha_2}{d_2} \pm \frac{\sin \alpha_3 \cos \beta_2}{d_2}, \quad (4.17b)$$

$$\dot{\alpha}_3 = -\frac{\sin \alpha_3}{d_3} \pm \frac{\sin \alpha_1 \cos \beta_3}{d_3}. \quad (4.17c)$$

Let  $\theta_i^*$  be the absolute angle between the vector  $\mathbf{g}_i^*$  and the  $x$ -axis of the global coordinate frame.

It follows that the angle between  $\mathbf{g}_i$  and the  $x$ -axis is  $\theta_i^* \pm \alpha_i$ . As a result,  $\beta_i = (\theta_i^* \pm \alpha_i) - (\theta_{i+1}^* \pm \alpha_{i+1})$

is dependent on  $\alpha_i$  and  $\alpha_{i+1}$  only. Thus, the following relations follow:

$$\frac{\partial \dot{\alpha}_i}{\partial \alpha_i} = -\frac{\cos \alpha_i}{d_i} + \frac{\sin \alpha_i \pm \sin \alpha_{i+1} \cos \beta_i}{d_i^2} \frac{\partial d_i}{\partial \alpha_i} \pm \frac{\sin \alpha_{i+1} \sin \beta_i}{d_i} \frac{\partial \beta_i}{\partial \alpha_i}, \quad (4.18a)$$

$$\frac{\partial \dot{\alpha}_i}{\partial \alpha_{i+1}} = \left( \pm \frac{\cos \alpha_{i+1} \cos \beta_i}{d_i} + \frac{\sin \alpha_i \pm \sin \alpha_{i+1} \cos \beta_i}{d_i^2} \frac{\partial d_i}{\partial \alpha_{i+1}} \pm \frac{\sin \alpha_{i+1} \sin \beta_i}{d_i} \frac{\partial \beta_i}{\partial \alpha_{i+1}} \right), \quad (4.18b)$$

$$\frac{\partial \dot{\alpha}_i}{\partial \alpha_j} = \frac{\sin \alpha_i \pm \sin \alpha_{i+1} \cos \beta_i}{d_i^2} \frac{\partial d_i}{\partial \alpha_j}, \quad j \neq i, i+1. \quad (4.18c)$$

These aid in the linearization of the system (4.17) about the equilibria and subsequent local stability analysis. Toward the same end, a refinement of Gershgorin' theorem in accordance with [128] will now be stated.

**Lemma 4.4** Suppose  $G(\mathbf{A})$  is the union of the  $n$  Gershgorin discs for a matrix  $\mathbf{A} \in \mathbb{R}^{n \times n}$ . If the union of  $k$  of the  $n$  discs that comprise  $G(\mathbf{A})$  forms a set  $G_k(\mathbf{A})$  that is disjoint from the remaining  $n - k$  discs, then  $G_k(\mathbf{A})$  contains exactly  $k$  eigenvalues of  $\mathbf{A}$ , counted according to their algebraic multiplicities.

Next, the local stability of the system described by (4.17) is investigated.

**Lemma 4.5** *The equilibria corresponding to  $\mathcal{D}_3$  are locally asymptotically stable and the ones corresponding to  $\mathcal{U}_3$  are unstable.*

*Proof:* At each equilibrium in  $\mathcal{D}_3$ ,  $\alpha_i = 0$ , while, at each equilibrium in  $\mathcal{U}_3$ ,  $\alpha_i = \pi, \forall i = 1, 2, 3$ .

By linearizing equation (4.17), near the equilibrium  $\boldsymbol{\alpha} = [\alpha_1, \alpha_2, \alpha_3]^\top = \mathbf{0}$ ,

$$\mathbf{A}_1 = \frac{\partial \dot{\boldsymbol{\alpha}}}{\partial \boldsymbol{\alpha}} \Big|_{\boldsymbol{\alpha}=\mathbf{0}} = \begin{bmatrix} -\frac{1}{d_1^*} & \pm \frac{\cos \beta_1^*}{d_1^*} & 0 \\ 0 & -\frac{1}{d_2^*} & \pm \frac{\cos \beta_2^*}{d_2^*} \\ \pm \frac{\cos \beta_3^*}{d_3^*} & 0 & -\frac{1}{d_3^*} \end{bmatrix}.$$

Since the desired formation is not a straight line,  $\beta_i^* \neq 0, \pi$  and the matrix  $\mathbf{A}_1$  is strictly diagonally dominant. Thus, by Gershgorin's theorem [128],  $\mathbf{A}_1$  is Hurwitz. It follows that the equilibria in  $\mathcal{D}_3$  are locally exponentially stable.

Similarly, near the equilibrium  $\boldsymbol{\alpha} = [\alpha_1, \alpha_2, \alpha_3]^\top = [\pi, \pi, \pi]^\top = \pi \mathbf{1}$ , we have

$$\mathbf{A}_2 = \frac{\partial \dot{\boldsymbol{\alpha}}}{\partial \boldsymbol{\alpha}} \Big|_{\boldsymbol{\alpha}=\pi \mathbf{1}} = \begin{bmatrix} \frac{1}{d_1^*} & \pm \frac{\cos \beta_1^*}{d_1^*} & 0 \\ 0 & \frac{1}{d_2^*} & \pm \frac{\cos \beta_2^*}{d_2^*} \\ \pm \frac{\cos \beta_3^*}{d_3^*} & 0 & \frac{1}{d_3^*} \end{bmatrix}.$$

In this case,  $\mathbf{A}_2$  is again strictly diagonally dominant, and so all its eigenvalues are in the right half of the complex plane. It follows that all equilibria in  $\mathcal{U}_3$  are unstable. ■

**Theorem 4.6** *In  $\mathbb{R}^2$ , suppose that  $0 \leq \alpha_i(0) \leq \frac{\pi}{2}$  for  $i = 1, 2, 3$ . Under Assumptions 4.1-4.2 and the control law (4.9),  $\boldsymbol{\alpha} \rightarrow \mathbf{0}$  asymptotically, i.e. the agents asymptotically converge to a formation satisfying all the desired bearing vectors.*

*Proof:* Let  $V = \|\boldsymbol{\alpha}\|_\infty = \alpha_{max} = \max_{i=1,2,3} \alpha_i$  which is continuous and positive definite. Since  $V$  is not continuously differentiable, Clark's generalized gradient and LaSalle's invariance principle for nonsmooth systems [134] are employed to analyze the system given by (4.17).

Firstly, without loss of generality, assume that for an interval  $t \in [T_1, T_2]$ ,  $\alpha_1 > \alpha_2 \geq \alpha_3 \geq 0$ .

Then,  $V = \max_{i=1,2,3} \alpha_i = \alpha_1$  and, in this interval, from (4.17), one has

$$\begin{aligned}\dot{V} = \dot{\alpha}_1 &= -\frac{1}{d_1}(\sin \alpha_1 \pm \sin \alpha_2 \cos \beta_1) \\ &\leq -\frac{1}{d_1}(\sin \alpha_1 - \sin \alpha_2 |\cos \beta_1|) \\ &< -\frac{1}{d_1} \sin \alpha_2(1 - |\cos \beta_1|) \leq 0,\end{aligned}\tag{4.19}$$

The last inequality holds as  $\sin(\cdot)$  is strictly increasing in its argument in  $[0, \pi/2]$ . Next, consider the following case:

$$\max_i \alpha_i = \begin{cases} \alpha_1 & t \in [T_1, T_2), \\ \alpha_1 = \alpha_2 > \alpha_3 & t = T_2, \\ \alpha_2 & t \in (T_2, T_3]. \end{cases}$$

Based on the notation of Clark's generalized gradient [134],  $\partial V(\boldsymbol{\alpha}) = [1, 0, 0]^\top$  for  $t \in [T_1, T_2)$ ,  $\partial V(\boldsymbol{\alpha}) = [0, 1, 0]^\top$  for  $t \in (T_2, T_3]$ , and at  $t = T_2$ ,

$$\partial V(\boldsymbol{\alpha}) = \overline{\text{co}} \left\{ [1, 0, 0]^\top, [0, 1, 0]^\top \right\} = \{[\eta_1, \eta_2, 0]^\top | \eta_i \in [0, 1], \eta_1 + \eta_2 = 1\},$$

where  $\overline{\text{co}}\{a, b\}$  denotes the convex closure of  $a$  and  $b$ . Thus,  $\dot{V}$  exists almost everywhere (a.e.) and at  $t = T_2$ , we have  $\dot{V} \in \dot{\tilde{V}}$ , where

$$\begin{aligned}\dot{\tilde{V}} &= \bigcap_{\boldsymbol{\eta} \in \partial V} \boldsymbol{\eta}^\top \dot{\boldsymbol{\alpha}} = \eta_1 \dot{\alpha}_1 + \eta_2 \dot{\alpha}_2 + 0 \cdot \dot{\alpha}_3 \\ &= -\frac{\eta_1}{d_1}(\sin \alpha_1 \pm \sin \alpha_2 \cos \beta_1) - \frac{\eta_2}{d_2}(\sin \alpha_2 \pm \sin \alpha_3 \cos \beta_2) \\ &< -\frac{\eta_1}{d_1} \sin \alpha_2(1 - |\cos \beta_1|) - \frac{\eta_2}{d_2} \sin \alpha_3(1 - |\cos \beta_2|) \leq 0,\end{aligned}$$

for all  $\eta_1 \in [0, 1]$ ,  $\eta_2 \in [0, 1]$  and  $\eta_1 + \eta_2 = 1$ .

Similarly, consider the case

$$\max_i \alpha_i = \begin{cases} \alpha_1 & t \in [T_1, T_2), \\ \alpha_1 = \alpha_3 > \alpha_2 & t = T_2, \\ \alpha_3 & t \in (T_2, T_3]. \end{cases}$$

one has  $\partial V(\boldsymbol{\alpha}) = [1, 0, 0]^\top$  for  $t \in [T_1, T_2)$ ,  $\partial V(\boldsymbol{\alpha}) = [0, 0, 1]^\top$  for  $t \in (T_2, T_3]$ , and at  $t = T_2$ ,

$$\partial V(\boldsymbol{\alpha}) = \overline{co} \left\{ [1, 0, 0]^\top, [0, 0, 1]^\top \right\} = \{ [\eta_1, 0, \eta_3]^\top \mid \eta_i \in [0, 1], \eta_1 + \eta_3 = 1 \}.$$

Thus,  $\dot{V}$  exists a.e., and at  $t = T_2$ ,  $\dot{V} \in \dot{V}$ , where

$$\begin{aligned} \dot{V} &= \bigcap_{\boldsymbol{\eta} \in \partial V} \boldsymbol{\eta}^\top \dot{\boldsymbol{\alpha}} = \eta_1 \dot{\alpha}_1 + 0 \cdot \dot{\alpha}_2 + \eta_3 \dot{\alpha}_3 \\ &= -\frac{\eta_1}{d_1} (\sin \alpha_1 \pm \sin \alpha_2 \cos \beta_1) - \frac{\eta_3}{d_3} (\sin \alpha_3 \pm \sin \alpha_1 \cos \beta_3) \\ &= -\frac{\eta_1}{d_1} (\sin \alpha_1 \pm \sin \alpha_2 \cos \beta_1) - \frac{\eta_3}{d_3} (\sin \alpha_1 \pm \sin \alpha_1 \cos \beta_3) \\ &< -\frac{\eta_1}{d_1} \sin \alpha_2 (1 - |\cos \beta_1|) - \frac{\eta_3}{d_3} \sin \alpha_1 (1 - |\cos \beta_3|) \leq 0. \end{aligned}$$

Thirdly, suppose that at  $t = T_4$ ,  $\alpha_1 = \alpha_2 = \alpha_3$ . Then, Clark's generalized gradient of  $V$  at

$t = T_4$  is given by

$$\partial V(\boldsymbol{\alpha}) = \overline{co} \left\{ [1, 0, 0]^\top, [0, 1, 0]^\top, [0, 0, 1]^\top \right\} = \{ [\eta_1, \eta_2, \eta_3]^\top \mid \eta_i \in [0, 1], \eta_1 + \eta_2 + \eta_3 = 1 \}.$$

Then,  $\dot{V} \in \dot{V}$  and since  $\dot{\alpha}_i$  is continuous at  $t = T_4$ ,

$$\begin{aligned} \dot{V} &= \bigcap_{\boldsymbol{\eta} \in \partial V} \boldsymbol{\eta}^\top \dot{\boldsymbol{\alpha}} = \eta_1 \dot{\alpha}_1 + \eta_2 \dot{\alpha}_2 + \eta_3 \dot{\alpha}_3 \\ &= -\frac{\eta_1}{d_1} (\sin \alpha_1 \pm \sin \alpha_2 \cos \beta_1) - \frac{\eta_2}{d_2} (\sin \alpha_2 \pm \sin \alpha_3 \cos \beta_2) - \frac{\eta_3}{d_3} (\sin \alpha_3 \pm \sin \alpha_1 \cos \beta_3) \\ &\leq -\sin \alpha_1 \sum_{i=1}^3 \frac{\eta_i}{d_i} (1 - |\cos \beta_i|) \leq 0, \end{aligned} \tag{4.20}$$

for all  $\eta_i \in [0, 1]$ ,  $\eta_1 + \eta_2 + \eta_3 = 1$ .

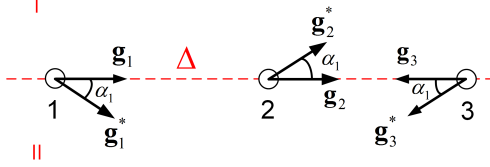


Figure 4.6. Three agents are collinear and  $\alpha_1 = \alpha_2 = \alpha_3 > 0$ .

From the above cases, one can conclude that  $V$  is a non-increasing function of time and  $0 \leq \alpha_i \leq \alpha_{\max} \leq \alpha_{\max}(0) \leq \pi/2, \forall t \geq 0$ . Further,  $\dot{V} = 0$  can occur if and only if  $\alpha_1 = \alpha_2 = \alpha_3$  and one of the following conditions holds:

- $\alpha_1 = \alpha_2 = \alpha_3 = 0$ .
- There exists  $i$  such that  $\beta_i = k\pi, k \in \{0, 1\}$  and  $\alpha_i \neq 0$ . Without loss of generality, let  $i = 1$ .

Then, the agents 1, 2, 3 are collinear in that order along a line  $\Delta$  as illustrated in Fig. 4.6. In this case,  $\beta_1 = 0$  and  $\beta_2 = \beta_3 = \pi$ . The line  $\Delta$  separates the plane into two regions I and II. Suppose  $\mathbf{g}_3^*$  points towards region II. Since  $\alpha_1 = \alpha_3$  and  $\mathbf{g}_1^* \neq \pm \mathbf{g}_3^*$ , it follows that  $\mathbf{g}_1^*$  must also point towards region II. Now consider agent 2, if  $\mathbf{g}_2^*$  points towards region I, since  $\alpha_2 = \alpha_3$ , it follows  $\mathbf{g}_2^* = -\mathbf{g}_3^*$  which is a contradiction. On the other hand, if  $\mathbf{g}_2^*$  points towards region II, since  $\alpha_3 = \alpha_1$ , it follows that  $\mathbf{g}_2^* = \mathbf{g}_1^*$  which is also a contradiction. Thus, it is ruled out.

Consequently,  $\dot{\tilde{V}} < 0$  whenever there exists  $i$  such that  $\alpha_i > 0$  and  $\dot{\tilde{V}} = 0$  if and only if  $\alpha_i = 0, \forall i = 1, 2, 3$ . It follows that  $\alpha_i \rightarrow 0$  asymptotically [134]. ■

#### 4.2.2 The $n$ -agent formations

Similar to the three-agent case, define the following sets:

$$\mathcal{Q}_n \triangleq \{\mathbf{p} \in \mathbb{R}^{2n} | \mathbf{g}_i = \pm \mathbf{g}_i^*, i \in \mathcal{I}\},$$

$$\mathcal{D}_n \triangleq \{\mathbf{p} \in \mathbb{R}^{2n} | \mathbf{g}_i = \mathbf{g}_i^*, i \in \mathcal{I}\},$$

$$\mathcal{U}_n \triangleq \mathcal{Q}_n \setminus \mathcal{D}_n.$$

$\mathcal{Q}_n$  is the set of all equilibria of (4.9) that can be partitioned into  $\mathcal{D}_n$  – the set of desired equilibria, and  $\mathcal{U}_n$  – the set of undesired equilibria. Unlike the three agent case, the undesired equilibrium set  $\mathcal{U}_n$  may admit different possibilities and not just the set  $\{\mathbf{p} \in \mathbb{R}^{2n} | \mathbf{g}_i = -\mathbf{g}_i^*, i \in \mathcal{I}\}$ . Thus, Lemma 4.3 cannot be generalized for  $n$ -agents. Figure 4.7 shows a four-agent formation to illustrate this.

Consider a directed cycle formation in  $\mathbb{R}^2$ . As in case of a triangle, let  $\alpha_i$  be the magnitude of the angle between  $\mathbf{g}_i$  and  $\mathbf{g}_i^*$  as shown in Fig. 4.8, and note that  $0 \leq \alpha_i \leq \pi$ . Each equilibrium  $\mathbf{p}^* \in \mathcal{D}$  corresponds to  $\alpha_i = 0$ ,  $i \in \mathcal{I}$ . For each equilibrium  $\mathbf{p}^* \in \mathcal{U}$ , there exists at least an index  $i$ ,  $i \in \mathcal{I}$ , such that  $\alpha_i = \pi$ . Let  $\beta_i$  be the magnitude of the angle between  $\mathbf{g}_i$  and  $\mathbf{g}_{i+1}$  and  $d_i = \|\mathbf{z}_i\|$  be the distance between agents  $i$  and  $i + 1$ . The dynamics in terms of angles are given by

$$\dot{\alpha}_i = -\frac{\sin \alpha_i}{d_i} \pm \frac{\sin \alpha_{i+1} \cos \beta_i}{d_i}, \quad i \in \mathcal{I}. \quad (4.21)$$

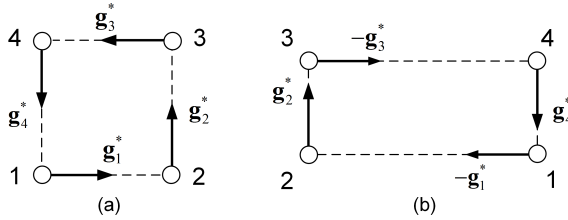


Figure 4.7. A desired formation is given in (a). An undesired formation is given in (b), where  $\mathbf{g}_1 = -\mathbf{g}_1^*$ ,  $\mathbf{g}_2 = \mathbf{g}_2^*$ ,  $\mathbf{g}_3 = -\mathbf{g}_3^*$ , and  $\mathbf{g}_4 = \mathbf{g}_4^*$ .

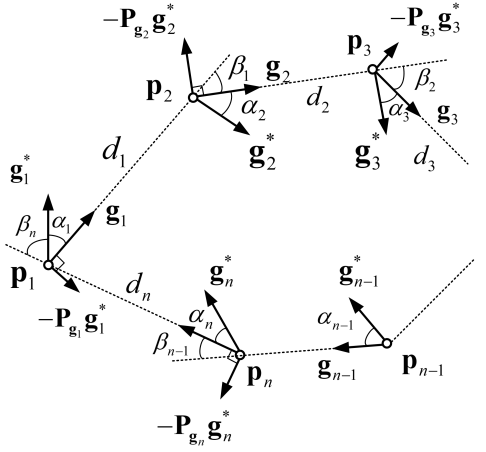


Figure 4.8. Formation of  $n$  agents under control law (4.9).

**Lemma 4.7** *The equilibria corresponding to  $\mathcal{D}_n$  are locally asymptotically stable, while those corresponding to  $\mathcal{U}_n$  are unstable.*

*Proof:* The proof is similar to that of Lemma 4.5. By linearizing (4.21), it turns out that at a desired equilibrium,

$$\left. \frac{\partial \dot{\alpha}}{\partial \alpha} \right|_{\alpha=0} = \begin{bmatrix} -\frac{1}{d_1^*} & \pm \frac{\cos \beta_1^*}{d_1^*} & 0 & \dots & 0 \\ \vdots & \ddots & \ddots & \ddots & \vdots \\ \vdots & \vdots & \ddots & -\frac{1}{d_{m-1}^*} & \pm \frac{\cos \beta_{m-1}^*}{d_{m-1}^*} \\ \pm \frac{\cos \beta_m^*}{d_m} & 0 & \dots & 0 & -\frac{1}{d_m^*} \end{bmatrix}$$

is Hurwitz according to Gershgorin's theorem, unless  $\cos \beta_i^* = 1$ ,  $\forall i \in \mathcal{I}$ . But this possibility is ruled out near an equilibrium, since we know that for a feasible formation  $\beta_i^* \neq 0$  for any  $i$ . On the other hand, for any equilibrium  $\alpha = \alpha^*$  in  $\mathcal{U}_n$ , there exists at least some  $i$ ,  $i \in \mathcal{I}$ , such that  $\alpha_i^* = \pi$ .

Thus, we have

$$\frac{\partial \dot{\alpha}}{\partial \alpha} \Big|_{\alpha=\alpha^*} = \begin{bmatrix} -\frac{1}{d_1^*} & \pm \frac{\cos \beta_1^*}{d_1^*} & 0 & \cdots & 0 \\ 0 & \ddots & \ddots & \ddots & \vdots \\ \vdots & \ddots & \frac{1}{d_i^*} & \pm \frac{\cos \beta_i^*}{d_i^*} & 0 \\ 0 & \ddots & \ddots & \ddots & \ddots \\ \pm \frac{\cos \beta_m^*}{d_m^*} & 0 & \cdots & 0 & -\frac{1}{d_m^*} \end{bmatrix}$$

and observe that there always exists at least one Gershgorin disc in the open right half plane (corresponding to  $i$ -th row). If there are more such rows with positive diagonal entries, then the discs corresponding to all such rows will be contained in the right half plane. Moreover, all such discs in the right half plane disc are disjoint from the discs in the left half plane. Using the refinement stated in Lemma 4.4, it follows that there must be at least one eigenvalue with a positive real part if there is at least one positive diagonal entry in the Jacobian above. Thus,  $\alpha^*$  is an unstable equilibrium. Hence, any undesired equilibrium in  $\mathcal{U}_n$  is unstable. ■

**Theorem 4.8** *In  $\mathbb{R}^2$ , suppose that  $0 \leq \alpha_i(0) \leq \frac{\pi}{2}$ ,  $i \in \mathcal{I}$ . Under Assumptions 4.1-4.2 and the control law (4.9),  $\alpha \rightarrow \mathbf{0}$  asymptotically, i.e. the agents asymptotically converge to a formation satisfying all the desired bearing vectors.*

*Proof:* Consider the Lyapunov function  $V = \|\alpha\|_{\max} = \max_{i=1,\dots,n} \alpha_i$ . By similar arguments as in Theorem 4.6,  $V$  is a decreasing function of time and  $0 \leq \alpha_i \leq \alpha_{\max} \leq \alpha_{\max}(0) \leq \pi/2$ ,  $\forall t \geq 0$ . Further,  $\dot{V} = 0$  if and only if  $\alpha_i = \alpha_j \forall i, j \in \mathcal{I}$  and one of the following conditions holds: (i)  $\alpha_i = \alpha_j = 0, \forall i, j \in \mathcal{I}$ ; or (ii) There exists a straight line in 2-D such that all desired bearing vectors  $\mathbf{g}_i^*$  are equally inclined with it by an angle  $\alpha$ . Below we will prove that (ii) cannot happen and thus (i) is the only possible equilibrium.

Suppose that the agents have all aligned themselves in a straight line formation. Clearly, for a

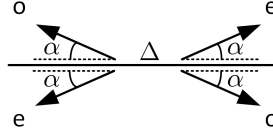


Figure 4.9. Four possible directions that the desired bearing vector makes an angle  $\alpha$  with the line  $\Delta$ .

given  $\alpha$ , there are only four possible directions as illustrated in Fig. 4.9. Without loss of generality, if one of the direction marked ‘e’ corresponds to an agent  $i$ , such that  $i$  is even, then agent  $(i + 1)$  must have  $g_{i+1}^*$  along one of the direction marked ‘o’ due to the requirement that  $g_i^* \neq \pm g_{i+1}^*$ . Now, by mathematical induction it follows that all agents with odd indices must be along one of the direction marked ‘o’ and all even indexed agents bearings must be along the directions marked ‘e’. We split up the situation into two cases

Case 1.  $n$  is odd.

Consider the agent indexed  $n$ . Since  $n$  is odd, it must have its desired bearing  $g_n^*$  along one of the direction marked ‘o’. But agent  $n + 1$  (modulo  $n$ ), or agent 1, also points along one of the direction marked ‘o’. Thus, for  $n$  odd, we cannot have this scenario without violating Assumption 4.2.

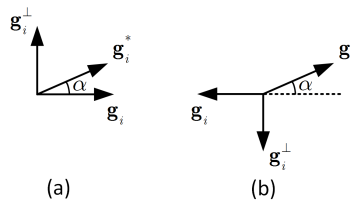


Figure 4.10. The vector  $g_i^*$  points North East (NE).

Case 2.  $n$  is even.

Suppose  $n$  is even. Clearly, this does not pose the same problem as for odd number of agents. So, it is possible that agents do line up along a straight line  $\Delta$ . But we need to investigate if such a straight

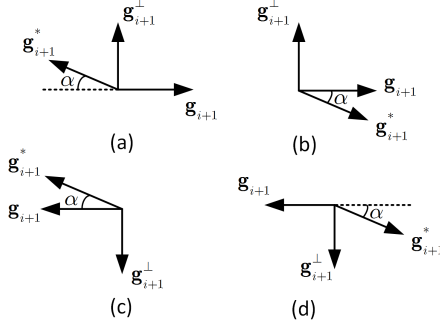


Figure 4.11. Four possible configurations of agent ( $i+1$ )'s bearings.

line formation is sustained. Consider the equation

$$d_i \sin \alpha_i \dot{\alpha}_i = (\mathbf{g}_i^*)^\top (\mathbf{g}_i^\perp)^\top (\mathbf{g}_{i+1}^\perp)^\top \mathbf{g}_{i+1}^* - ((\mathbf{g}_i^*)^\top \mathbf{g}_i^\perp)^2,$$

when the agents are aligned along a straight line. Without loss of generality, we further suppose that the desired bearing of agent  $i$  is pointing toward North East (NE) as shown in Fig. 4.10. In Fig. 4.10(a),  $(\mathbf{g}_i^*)^\top \mathbf{g}_i^\perp = +\sin \alpha$  and in Fig. 4.10(b),  $(\mathbf{g}_i^*)^\top \mathbf{g}_i^\perp = -\sin \alpha$ .

Now, consider the agent  $(i+1)$ . Figure 4.11 depicts four possible configurations of agent  $(i+1)$ 's bearings. Clearly, in Fig. 4.11(a) and 4.11(d),  $(\mathbf{g}_{i+1}^*)^\top \mathbf{g}_{i+1}^\perp = +\sin \alpha$  while in Fig. 4.11(b) and 4.11(c),  $(\mathbf{g}_{i+1}^*)^\top \mathbf{g}_{i+1}^\perp = -\sin \alpha$ .

Now, for Fig. 4.10(a), Fig. 4.11(a) and Fig. 4.11(b) taken together,  $\cos \beta_i = (\mathbf{g}_i^\perp)^\top \mathbf{g}_{i+1}^\perp = \mathbf{g}_i^\top \mathbf{g}_{i+1} = \cos 0 = 1$ ; and for Fig. 4.10(a), Fig. 4.11(c) and Fig. 4.11(d) taken together,  $\cos \beta_i = \cos \pi = -1$ . Similarly, for Fig. 4.10(b), Fig. 4.11(a) and Fig. 4.11(b),  $\cos \beta_i = -1$ ; and for Fig. 4.10(b), Fig. 4.11(c) and Fig. 4.11(d) taken together,  $\cos \beta_i = 1$ .

Keeping these in mind, it turns out that for  $\mathbf{g}_i^*$  as in Fig. 4.10(a),

$$\dot{\alpha}_i = \begin{cases} 0 & \text{for } \mathbf{g}_{i+1}^* \text{ as in Figs. 4.11(a) and (c)} \\ -\frac{2 \sin \alpha}{d_i} & \text{for } \mathbf{g}_{i+1}^* \text{ as in Figs. 4.11(b) and (d).} \end{cases}$$

Similarly, for  $\mathbf{g}_i^*$  as in Fig. 4.10(b),

$$\dot{\alpha}_i = \begin{cases} 0 & \text{for } \mathbf{g}_{i+1}^* \text{ as in Figs. 4.11(a) and (c)} \\ -\frac{2 \sin \alpha}{d_i} & \text{for } \mathbf{g}_{i+1}^* \text{ as in Figs. 4.11(b) and (d).} \end{cases}$$

Thus, if  $\mathbf{g}_i^*$  points North East,  $\mathbf{g}_{i+1}^*$  must point North West (NW) for  $\dot{\alpha}_i = 0$ .

By a similar procedure, it may be shown that if  $\mathbf{g}_{i+1}^*$  points NW then  $\mathbf{g}_{i+2}^*$  must point NE for  $\dot{\alpha}_{i+1} = 0$ .

Combining these facts, it turns out that if  $\dot{\alpha}_i = 0, \forall i \in \mathcal{I}$ , at the straight line formation is to hold true, then the sequence of desired bearings must be  $\dots - \text{NE} - \text{NW} - \text{NE} - \text{NW} - \dots$ . As a result, all desired bearing vectors are contained in a half plane on the North side of the line  $\Delta$ . This clearly violates Lemma 4.2 for feasible desired bearing set. Hence, we conclude that at the straight line configuration, there must be some  $i$  such that  $\dot{\alpha}_i \neq 0$ . Similar reasoning may be applied for  $\mathbf{g}_i^*$  along any direction other than NE.

Hence, we conclude that if the agents happen to align along a straight line for  $t = t_1$ , they cannot remain in this configuration  $\forall t > t_1$ . ■

### 4.3 The triangular formation in the three dimensional space

This Section extends the analysis on directed triangular formations to the three-dimensional space. The directed triangular formations in three-dimensional space exhibit both similarities and uniqueness properties just as in the planar case. This extension also illustrates the challenges in analyzing system dynamics in a higher dimensional space and also when the number of agents,  $n$ , is greater than three.

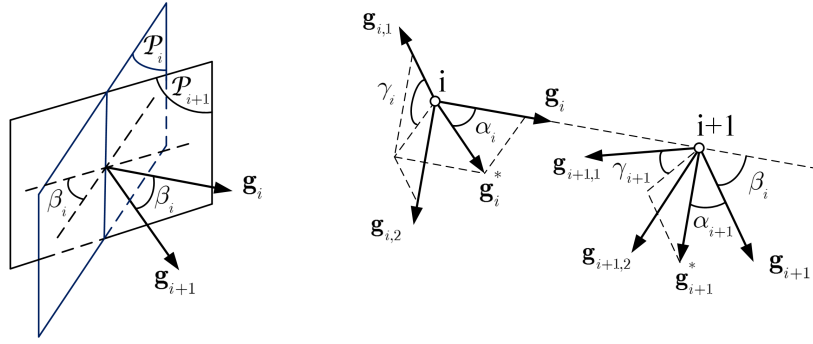


Figure 4.12. The sensing model of an agent  $i$  in the 3D space.

#### 4.3.1 Preliminary results

Consider a group of three autonomous agents in  $\mathbb{R}^3$ . Each agent follows the bearing-only control law (4.9), where  $P_{\mathbf{g}_i} \in \mathbb{R}^{3 \times 3}$  is the projection matrix, and  $\mathbf{g}_i^* \in \mathbb{R}^3$  is the desired bearing vector of agent  $i$ .

Since the set of desired bearing vectors  $\mathcal{B}_3 = \{\mathbf{g}_i^* \in \mathbb{R}^3 \mid \|\mathbf{g}_i^*\| = 1, i = 1, 2, 3\}$  is *feasible*, there exist positive constants  $d_1, d_2, d_3$  such that

$$d_1 \mathbf{g}_1^* + d_2 \mathbf{g}_2^* + d_3 \mathbf{g}_3^* = \mathbf{0}. \quad (4.22)$$

Note that equation (4.22) implies three desired bearing vectors  $\mathbf{g}_1^*$ ,  $\mathbf{g}_2^*$ , and  $\mathbf{g}_3^*$  are *coplanar*.

Next, we study the set of equilibria of (4.9) for the three agent case. Define the following sets:

$$\bar{\mathcal{Q}}_3 \triangleq \{\mathbf{p} \in \mathbb{R}^9 \mid \mathbf{g}_i = \pm \mathbf{g}_i^*, i = 1, 2, 3\},$$

$$\bar{\mathcal{D}}_3 \triangleq \{\mathbf{p} \in \mathbb{R}^9 \mid \mathbf{g}_i = \mathbf{g}_i^*, i = 1, 2, 3\},$$

$$\bar{\mathcal{U}}_3 \triangleq \mathcal{Q}_3 \setminus \mathcal{D}_3,$$

where the set  $\bar{\mathcal{Q}}_3$  contains all equilibria of (4.9), which includes  $\bar{\mathcal{D}}_3$  – the set of all desired formations, and  $\bar{\mathcal{U}}_3$  – the set of undesired formations. As before,  $\bar{\mathcal{D}}_3 \neq \emptyset$ , and there exists a triangle specified by the three desired bearing vectors  $\mathbf{g}_1^*$ ,  $\mathbf{g}_2^*$ , and  $\mathbf{g}_3^*$  since they comprise a feasible desired bearing set.

We have the following Lemma about the set of undesired equilibrium. The proof is similar to that of Lemma 4.5 by treating the plane on which the desired formation lies as  $\mathbb{R}^2$ .

**Lemma 4.9** *The set  $\bar{\mathcal{U}}_3$  contains all points  $\mathbf{p} \in \mathbb{R}^9$  such that  $\mathbf{g}_i = -\mathbf{g}_i^*$ ,  $i = 1, 2, 3$ .*

**Remark 4.10** *Note that the directed cycle graph with four agents,  $C_4$ , in  $\mathbb{R}^3$  can also be bearing rigid (see [130] for a discussion) and is the counterpart of the triangle in  $\mathbb{R}^2$ . However, in the following subsection, we provide a result on local stability of general directed cycle formations in  $\mathbb{R}^3$  and study asymptotic stability of the triangular formations in detail. The stability analysis of the three agent formation illustrates the challenges involved in analyzing the stability of more general formations in three dimensions.*

### 4.3.2 The dynamical model

Let  $\alpha_i$  be the magnitude of the angle between  $\mathbf{g}_i$  and  $\mathbf{g}_i^*$ , for  $i = 1, 2, 3$ . Since the three desired bearing vectors define a plane in  $\mathbb{R}^3$ , the shape of the triangle, and the plane on which it lies are fixed whenever all three desired bearing vectors are satisfied. Thus, according to Lemma 4.9, the equilibria can be equivalently classified into two sets based on the angles  $\alpha_i$ :  $\bar{\mathcal{D}}_3 = \{\mathbf{p} \in \mathbb{R}^9 \mid \alpha_i = 0, i = 1, 2, 3\}$  and  $\bar{\mathcal{U}}_3 = \{\mathbf{p} \in \mathbb{R}^9 \mid \alpha_i = \pi, i = 1, 2, 3\}$ . Given a formation  $\mathbf{p}(0) \in \mathbb{R}^9$ , instead of the position dynamics (4.9), we can study the angle dynamics in terms of  $\alpha_i$ . Toward this end, we transform (4.9) into the angle dynamics. Figure 4.12 depicts the sensing model of agent  $i$ . It may be noted that although the desired triangle is a planar polygon, the trajectories of the agents do not necessarily evolve along the plane on which the desired formation lies. In Fig. 4.12, we denote

- $\alpha_i$ : the magnitude of the angle between  $\mathbf{g}_i$  and  $\mathbf{g}_i^*$ ,  $0 \leq \alpha_i \leq \pi$ .
- $\mathcal{P}_i$ : the plane having two tangent vectors  $\mathbf{g}_{i,1}$  and  $\mathbf{g}_{i,2}$ , or in other words, the plane having  $\mathbf{g}_i$  as its normal vector.

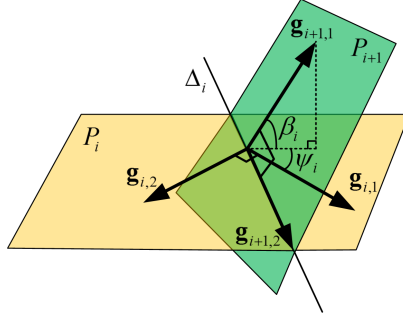


Figure 4.13. Illustration of vectors  $\mathbf{g}_{i,1}$ ,  $\mathbf{g}_{i,2}$ ,  $\mathbf{g}_{i+1,1}$ , and  $\mathbf{g}_{i+1,2}$ .

- $\nabla_i = \mathcal{P}_i \cap \mathcal{P}_{i+1}$ : the intersection between planes  $\mathcal{P}_i$  and  $\mathcal{P}_{i+1}$ .
- $\gamma_i$ : the angle between the orthogonal projection of  $\mathbf{g}_i^*$  into the plane  $\mathcal{P}_i$  and  $\mathbf{g}_{i,1}$ ,  $0 \leq \gamma_i < 2\pi$ .
- $\beta_i$ : the magnitude of the angle between  $\mathbf{g}_i$  and  $\mathbf{g}_{i+1}$ ,  $0 \leq \beta_i \leq \pi$ .

For each  $\alpha_i$ ,  $i = 1, 2, 3$ , we can write

$$\cos \alpha_i = (\mathbf{g}_i^*)^\top \mathbf{g}_i. \quad (4.23)$$

Taking the derivative of both sides of (4.23), it follows that  $\sin \alpha_i \dot{\alpha}_i = -\mathbf{g}_i^{*\top} \frac{P_{\mathbf{g}_i}}{d_i} (\dot{\mathbf{p}}_{i+1} - \dot{\mathbf{p}}_i) = -\mathbf{g}_i^{*\top} \frac{P_{\mathbf{g}_i}}{d_i} (-P_{\mathbf{g}_{i+1}} \mathbf{g}_{i+1}^* + P_{\mathbf{g}_i} \mathbf{g}_i^*) = \mathbf{g}_i^{*\top} \frac{P_{\mathbf{g}_i} P_{\mathbf{g}_{i+1}}}{d_i} \mathbf{g}_{i+1}^* - \mathbf{g}_i^{*\top} \frac{P_{\mathbf{g}_i}}{d_i} \mathbf{g}_i^*$ . Note that

$$\begin{aligned} \mathbf{g}_i^{*\top} P_{\mathbf{g}_i} \mathbf{g}_i^* &= \mathbf{g}_i^{*\top} (\mathbf{g}_{i,1} \mathbf{g}_{i,1}^\top + \mathbf{g}_{i,2} \mathbf{g}_{i,2}^\top) \mathbf{g}_i^* = (\mathbf{g}_{i,1}^\top \mathbf{g}_i^*)^2 + (\mathbf{g}_{i,2}^\top \mathbf{g}_i^*)^2 \\ &= \sin^2 \alpha_i \cos^2 \gamma_i + \sin^2 \alpha_i \sin^2 \gamma_i = \sin^2 \alpha_i (\cos^2 \gamma_i + \sin^2 \gamma_i) = \sin^2 \alpha_i, \end{aligned}$$

and

$$\begin{aligned} \mathbf{g}_i^{*\top} P_{\mathbf{g}_i} P_{\mathbf{g}_{i+1}} \mathbf{g}_{i+1}^* &= \mathbf{g}_i^{*\top} (\mathbf{g}_{i,1} \mathbf{g}_{i,1}^\top + \mathbf{g}_{i,2} \mathbf{g}_{i,2}^\top) (\mathbf{g}_{i+1,1} \mathbf{g}_{i+1,1}^\top + \mathbf{g}_{i+1,2} \mathbf{g}_{i+1,2}^\top) \mathbf{g}_{i+1}^* \\ &= (\mathbf{g}_i^{*\top} \mathbf{g}_{i,1} \mathbf{g}_{i,1}^\top + \mathbf{g}_i^{*\top} \mathbf{g}_{i,2} \mathbf{g}_{i,2}^\top) (\mathbf{g}_{i+1,1} \mathbf{g}_{i+1,1}^\top \mathbf{g}_{i+1}^* + \mathbf{g}_{i+1,2} \mathbf{g}_{i+1,2}^\top \mathbf{g}_{i+1}^*) \\ &= \pm (\sin \alpha_i \cos \gamma_i \mathbf{g}_{i,1}^\top + \sin \alpha_i \sin \gamma_i \mathbf{g}_{i,2}^\top) (\mathbf{g}_{i+1,1} \sin \alpha_{i+1} \cos \gamma_{i+1} + \mathbf{g}_{i+1,2} \sin \alpha_{i+1} \sin \gamma_{i+1}) \\ &= \pm \sin \alpha_i \sin \alpha_{i+1} h_i, \end{aligned} \quad (4.24)$$

where

$$h_i = \mathbf{w}_{i,1}^\top \mathbf{w}_{i,2} = (\cos \gamma_i \mathbf{g}_{i,1} + \sin \gamma_i \mathbf{g}_{i,2})^\top (\cos \gamma_{i+1} \mathbf{g}_{i+1,1} + \sin \gamma_{i+1} \mathbf{g}_{i+1,2}). \quad (4.25)$$

To ease the calculation of  $h_i$ , we choose  $\mathbf{g}_{i+1,1}$  perpendicular to the line  $\nabla_i$  and  $\mathbf{g}_{i+1,2}$  lies along  $\nabla_i$  as depicted in Fig. 4.13. Let  $\psi_i$  be the angle between  $\mathbf{g}_{i,1}$  and the orthogonal projection of  $\mathbf{g}_{i+1,1}$  on the plane  $\mathcal{P}_i$ , then  $0 \leq \psi_i < 2\pi$ . We thus have,  $\mathbf{g}_{i,1}^\top \mathbf{g}_{i+1,1} = |\cos \beta_i| \cos \psi_i$ ,  $\mathbf{g}_{i,1}^\top \mathbf{g}_{i+1,2} = \sin \psi_i$ ,  $\mathbf{g}_{i,2}^\top \mathbf{g}_{i+1,1} = |\cos \beta_i| \cos(\psi_i + \frac{\pi}{2}) = -|\cos \beta_i| \sin \psi_i$ , and  $\mathbf{g}_{i,2}^\top \mathbf{g}_{i+1,2} = \cos \psi_i$ . Substituting these into Eq. (4.25), it follows

$$\begin{aligned} h_i &= |\cos \beta_i| \cos \gamma_i \cos \gamma_{i+1} \cos \psi_i + \cos \gamma_i \sin \gamma_{i+1} \sin \psi_i \\ &\quad - |\cos \beta_i| \sin \gamma_i \cos \gamma_{i+1} \sin \psi_i + \sin \gamma_i \sin \gamma_{i+1} \cos \psi_i \\ &= |\cos \beta_i| \cos \gamma_{i+1} (\cos \gamma_i \cos \psi_i - \sin \gamma_i \sin \psi_i) + \sin \gamma_{i+1} (\cos \gamma_i \sin \psi_i + \sin \gamma_i \cos \psi_i) \\ &= |\cos \beta_i| \cos \gamma_{i+1} \cos(\gamma_i + \psi_i) + \sin \gamma_{i+1} \sin(\gamma_i + \psi_i). \end{aligned} \quad (4.26)$$

In (4.26), applying the Cauchy-Schwarz inequality  $(AX + BY)^2 \leq (A^2 + B^2)(X^2 + Y^2)$ , it follows

$$\begin{aligned} h_i^2 &\leq (\cos^2 \beta_i \cos^2 \gamma_{i+1} + \sin^2 \gamma_{i+1})(\cos^2(\gamma_i + \psi_i) + \sin^2(\gamma_i + \psi_i)) \\ &\leq (1. \cos^2 \gamma_{i+1} + \sin^2 \gamma_{i+1}) \cdot 1 = 1, \end{aligned} \quad (4.27)$$

with equality holding when  $A/X = B/Y$ . But, since  $\sqrt{X^2 + Y^2} = 1$ , for  $|h_i| = 1$ , we also require  $\sqrt{A^2 + B^2} = 1$ . Hence, from (4.26)-(4.27), for  $|h_i| = 1$ , it is necessary that either (i)  $|\cos \beta_i| = 1$  and  $\gamma_{i+1} = \psi_i + \gamma_i$ , or (ii)  $|\cos \beta_i| \neq 1$  and  $\sin \gamma_{i+1} = \sin(\gamma_i + \psi_i) = 1$ . Condition (i) implies  $\beta_i = 0, \pi$  i.e.,  $\mathbf{g}_i = \pm \mathbf{g}_{i+1}$ . Condition (ii) implies  $\gamma_{i+1} = \text{either } \frac{\pi}{2} \text{ or } \frac{3\pi}{2}$  for each  $i$ , and it follows further from (4.26) that  $\sin(\gamma_i + \psi_i) = 1$ , or i.e.,  $\psi_i = 0, \pi$ .

Overall, we can write the dynamical equation of  $\alpha_i$ , for the three agent scenario, as follows:

$$\dot{\alpha}_i = -\frac{\sin \alpha_i}{d_i} \pm h_i \frac{\sin \alpha_{i+1}}{d_i}, \quad (4.28)$$

where  $|h_i| \leq 1$ ,  $\forall i = 1, 2, 3$ . It may be pointed out that, though equation (4.28) involves more angle variables to describe the dynamics in three dimensions, it has a form similar to the two-dimensional version (4.17) in Section 4.2.

### 4.3.3 Stability analysis

We shall now study the system (4.28). As before, we note that

$$\frac{\partial \dot{\alpha}_i}{\partial \alpha_i} = -\frac{\cos \alpha_i}{d_i} + \frac{\sin \alpha_i \pm \sin \alpha_{i+1} h_i}{d_i^2} \frac{\partial d_i}{\partial \alpha_i} + \frac{\sin \alpha_{i+1}}{d_i} \frac{\partial h_i}{\partial \alpha_i}, \quad (4.29a)$$

$$\frac{\partial \dot{\alpha}_i}{\partial \alpha_{i+1}} = \pm \frac{\cos \alpha_{i+1} h_i}{d_i} + \frac{\sin \alpha_i \pm \sin \alpha_{i+1} h_i}{d_i^2} \frac{\partial d_i}{\partial \alpha_{i+1}} + \frac{\sin \alpha_{i+1}}{d_i} \frac{\partial h_i}{\partial \alpha_{i+1}}, \quad (4.29b)$$

$$\frac{\partial \dot{\alpha}_i}{\partial \alpha_j} = \frac{\sin \alpha_i \pm \sin \alpha_{i+1} h_i}{d_i^2} \frac{\partial d_i}{\partial \alpha_j} \pm \frac{\sin \alpha_{i+1}}{d_i} \frac{\partial h_i}{\partial \alpha_j}, \quad j \neq i, i+1. \quad (4.29c)$$

We are now equipped to prove the following result on local stability.

**Lemma 4.11** *The equilibria corresponding to  $\bar{\mathcal{D}}_3$  are locally asymptotically stable and the ones corresponding to  $\bar{\mathcal{U}}_3$  are unstable.*

*Proof:* At each equilibrium in  $\bar{\mathcal{D}}_3$ ,  $\alpha_i = 0$ , while, at each equilibrium in  $\bar{\mathcal{U}}_3$ ,  $\alpha_i = \pi$ ,  $\forall i = 1, 2, 3$ .

Denote  $\boldsymbol{\alpha} = [\alpha_1, \alpha_2, \alpha_3]^\top$ . Linearizing equation (4.28), for 3 agents, at the equilibrium  $\boldsymbol{\alpha} = \mathbf{0}$ ,

$$\mathbf{A}_1 = \left. \frac{\partial \dot{\boldsymbol{\alpha}}}{\partial \boldsymbol{\alpha}} \right|_{\boldsymbol{\alpha}=\mathbf{0}} = \begin{bmatrix} -\frac{1}{d_1^*} & \pm \frac{h_1^*}{d_1^*} & 0 \\ 0 & -\frac{1}{d_2^*} & \pm \frac{h_2^*}{d_2^*} \\ \pm \frac{h_3^*}{d_3^*} & 0 & -\frac{1}{d_3^*} \end{bmatrix}.$$

In order to use Gershgorin's theorem, we have to ensure that  $|h_i^*| < 1$  at the equilibrium point.

But the diagonally dominant Jacobian,  $\mathbf{A}_1$ , satisfies the ‘SC-property’ as mentioned in [128]. Thus, according to Theorem 6.2.8 and Corollary 6.2.9 in [128], if the Jacobian  $\mathbf{A}_1$  has to have an eigenvalue at the origin, then  $|h_i| = 1 \forall i$  is required. So it suffices to ensure that  $|h_i| = 1$  cannot hold for at least some  $i$ . However, we can, in fact, show that  $|h_i| < 1 \forall i$ . From the Assumption that  $\mathbf{g}_i^* \neq \mathbf{g}_{i+1}^*$ ,

$\forall i = 1, 2, 3$ , it follows that  $|\cos \beta_i^*| \neq 1$  or condition (i) cannot occur for all  $i$ , i.e.  $\beta_i^* = 0, \pi$  cannot hold for any  $i$ . Moreover, condition (ii) also cannot hold because at the equilibrium,  $\gamma_i = 0 \forall i$ . This is true since the projection of  $\mathbf{g}_i = \mathbf{g}_i^*$  on the plane  $\mathcal{P}_i$  is zero for all  $i$ . Thus, from (4.25) and the discussion following it, at equilibrium  $\boldsymbol{\alpha} = \mathbf{0}$ , and we have  $|h_i^*| = |\cos \beta_i^* \cos \psi_i^*| < 1 \forall i$ . In fact, for a triangle (a planar polygon), at equilibrium we have  $\psi_i^* = 0 \forall i$  and so the off-diagonal entries of  $\mathbf{A}_1$  are the same as that obtained for the two dimensional case. Thus, the matrix  $\mathbf{A}_1$  is strictly diagonally dominant with negative diagonal entries and is therefore Hurwitz, by Gershgorin's theorem. It follows that the equilibrium  $\boldsymbol{\alpha} = \mathbf{0}$  is locally exponentially stable.

Similarly, at the equilibrium  $\boldsymbol{\alpha} = [\alpha_1, \alpha_2, \alpha_3]^\top = [\pi, \pi, \pi]^\top = \pi\mathbf{1}$ , we have

$$\mathbf{A}_2 = \frac{\partial \dot{\boldsymbol{\alpha}}}{\partial \boldsymbol{\alpha}} \Big|_{\boldsymbol{\alpha}=\pi\mathbf{1}} = \begin{bmatrix} \frac{1}{d_1^*} & \pm \frac{h_1^*}{d_1^*} & 0 \\ 0 & \frac{1}{d_2^*} & \pm \frac{h_2^*}{d_2^*} \\ \pm \frac{h_3^*}{d_3^*} & 0 & \frac{1}{d_3^*} \end{bmatrix}.$$

In this case,  $\mathbf{A}_2$  is again strictly diagonally dominant, and so all its eigenvalues are in the right half of the complex plane. It follows that all equilibria in  $\mathcal{U}_3$  are unstable.  $\blacksquare$

We shall now state another Lemma that will aid in the analysing the region of attraction of the desired equilibria.

**Lemma 4.12** Suppose three coplanar unit vectors  $\mathbf{v}_i \in \mathbb{R}^3$ ,  $i = 1, 2, 3$ , that are pairwise linearly independent, satisfy  $\sum_{i=1}^3 \lambda_i \mathbf{v}_i = 0$  for  $\lambda_i \in \mathbb{R}_+$ . A fourth unit vector  $\mathbf{v} \in \mathbb{R}^3$  that subtends equal angles with each  $\mathbf{v}_i$  must be normal to the plane containing the three vectors.

*Proof:* Consider  $\mathbf{v}^\top \sum_{i=1}^3 \lambda_i \mathbf{v}_i = 0$ . Now,  $|\mathbf{v}^\top \mathbf{v}_i| = c \in \mathbb{R}_+ \forall i$ . Thus, we have  $c(\pm \lambda_1 \pm \lambda_2 \pm \lambda_3) = 0$ . Since  $\mathbf{v}_i$  are pairwise linearly independent and satisfy  $\sum_{i=1}^3 \lambda_i \mathbf{v}_i = 0$ , these vectors define triangles in their common plane each of whose sides have lengths equal to or proportional to  $\lambda_i$ , with the constant of proportionality describing the size of the particular triangle. Further, we



(a) All planes  $\mathcal{P}_i$  intersect on the line  $\nabla$ .

(b)  $\mathbf{g}_i, \mathbf{g}_{i-1}$ , and  $\mathbf{g}_{i+1}$  are perpendicular to  $\nabla$ .

Figure 4.14. Illustration of the proof of Theorem 4.13.

know that for a triangle, the sum of the length of two sides is always greater than the third. Therefore,

$(\pm \lambda_1 \pm \lambda_2 \pm \lambda_3) \neq 0$ . Thus,  $c = 0$ . Hence, the result.  $\blacksquare$

**Theorem 4.13** In  $\mathbb{R}^3$ , suppose that  $0 \leq \alpha_i(0) \leq \frac{\pi}{2}$  for  $i = 1, 2, 3$ . Under the control law (4.9),

$\boldsymbol{\alpha} \rightarrow \mathbf{0}$  asymptotically, i.e. the agents asymptotically converge to a formation satisfying all the desired bearing vectors.

*Proof:* Consider the Lyapunov function  $V = \|\boldsymbol{\alpha}\|_\infty = \max_{i=1,2,3} \alpha_i$ , by similar arguments as in Theorem 4.6,  $V$  is a decreasing function of time and  $0 \leq \alpha_i \leq \alpha_{\max} \leq \alpha_{\max}(0) \leq \pi/2, \forall t \geq 0$ .

Further,  $\dot{V} = 0$  if and only if  $\alpha_1 = \alpha_2 = \alpha_3$  and one of the following conditions holds:

(i)  $\alpha_1 = \alpha_2 = \alpha_3 = 0$ ;

(ii) There exists a configuration such that  $|h_i| = 1, \forall i$ . Then the following possibilities emerge:

(a)  $\beta_i = 0$  or  $\pi$ , and  $\gamma_{i+1} = \gamma_i + \psi_i$  for all  $i$ .

(b)  $\gamma_i$  = either  $\frac{\pi}{2}$  or  $\frac{3\pi}{2}$  and  $\psi_i = 0, \pi$  for each  $i$ .

(c)  $\beta_i = 0$  or  $\pi$ , and  $\gamma_{i+1} = \gamma_i + \psi_i$  for some  $i$ , while  $\gamma_j = \frac{\pi}{2}$  or  $\frac{3\pi}{2}$  and  $\psi_j = 0$ , or  $\pi$  for the remaining  $j \in \mathcal{I}, j \neq i$ .

It will be proved that each of the cases (a), (b) and (c) cannot hold.

(a) In this case three agents are collinear due to  $\beta_i = 0$  or  $\pi$  for  $i = 1, 2, 3$ . Further, the three desired bearing vectors are coplanar (because they are feasible) and  $\alpha_1 = \alpha_2 = \alpha_3 = \alpha \neq 0$ . Now, following Lemma 4.12, we may conclude that  $\alpha = \pi/2$  and the agents are aligned along the normal to the plane containing the desired bearing vectors. Thus, the planes  $\mathcal{P}_i$  are identical for all  $i$ . This is also the same plane on which all the desired bearing vectors lie. Now, consider the expression for  $h_i$  in (4.25). From the definition of  $\gamma_i$ , it is clear that in this case the vectors  $\mathbf{w}_{i,1}$  and  $\mathbf{w}_{i,2}$  are the unit vectors  $\mathbf{g}_i^*$  and  $\mathbf{g}_{i+1}^*$ , respectively because the orthogonal projections of  $\mathbf{g}_i^*$  and  $\mathbf{g}_{i+1}^*$  on  $\mathcal{P}_i$  (or  $\mathcal{P}_{i+1}$ ) are the vectors  $\mathbf{g}_i^*$  and  $\mathbf{g}_{i+1}^*$  themselves. Since,  $\mathbf{g}_i^* \neq \pm \mathbf{g}_{i+1}^*$  for a feasible formation, we conclude that  $|h_i|$ , which is the inner product of two linearly independent unit vectors, must be less than unity for all  $i$ . Alternately, we could arrive at the same conclusion about  $|h_i|$  by observing that the requirement  $\gamma_{i+1} = \gamma_i + \psi_i$  also leads to  $\mathbf{g}_i^* = \pm \mathbf{g}_{i+1}^*$  because now  $\mathbf{g}_{i,1}$  and  $\mathbf{g}_{i+1,1}$ , being coplanar, are separated by the angle  $\psi_i$ . This is clearly infeasible, leading to a contradiction.

(b) In this case, it is clear from Fig. 4.13 that  $\psi_i = 0, \pi \forall i$  leads to  $\mathbf{g}_{i,2} = \pm \mathbf{g}_{i+1,2} \forall i$ . Since we have chosen  $\mathbf{g}_{i+1,2}$  to lie along  $\nabla_i$ , the line of intersection of  $\mathcal{P}_i$  and  $\mathcal{P}_{i+1}$ , it immediately follows that all the planes  $\mathcal{P}_i$  intersect along the same line, say  $\nabla$ , as shown in Fig. 4.14a. Also, since  $\gamma_i =$  either  $\frac{\pi}{2}$  or  $\frac{3\pi}{2}$  for each  $i$ , we conclude from the definition of  $\gamma_i$  that the three vectors  $\mathbf{g}_i^*, \mathbf{g}_i$  and  $\mathbf{g}_{i,2}$  are all orthogonal to  $\mathbf{g}_{i,1}$  and hence coplanar for all  $i$ . It may be remarked that even if  $\gamma_i = \frac{\pi}{2}$ , while  $\gamma_{i+1} = \frac{3\pi}{2}$ , the coplanarity of  $\mathbf{g}_i^*, \mathbf{g}_i$  and  $\mathbf{g}_{i,2}$  still holds. In other words, all  $\gamma_i$  need not necessarily be equal but so long as they are either  $\frac{\pi}{2}$  or  $\frac{3\pi}{2}$  individually, our conclusion about the coplanarity is unaffected.

Denote the plane containing the triplet  $\mathbf{g}_i^*, \mathbf{g}_i$  and  $\mathbf{g}_{i,2}$  as  $\mathcal{P}_i^\perp$ . Note that all such planes  $\mathcal{P}_i^\perp$  also intersect along the common line  $\nabla$ , containing  $\mathbf{g}_{i,2}$ . Since  $\alpha_i = \alpha \neq 0 \forall i$ , we may now deduce that for each  $i$ ,  $\mathbf{g}_i^*$  has two possible orientations on the plane  $\mathcal{P}_i^\perp$ , for a given  $\mathbf{g}_i$ . This is illustrated in Fig. 4.14b. For one of these orientations,  $\mathbf{g}_{1,2}^T \mathbf{g}_i^* > 0$  while for the other  $\mathbf{g}_{1,2}^T \mathbf{g}_i^* < 0$ . Since there

exist scalars  $d_i > 0$  such that  $\sum_{i=1}^3 d_i \mathbf{g}_i^* = 0$ , it follows  $\mathbf{g}_{1,2}^\top \mathbf{g}_i^*$  cannot all be positive or negative because otherwise,  $\mathbf{g}_{i,2}^\top (\sum_{i=1}^3 d_i \mathbf{g}_i^*) \neq 0$  for any choice of the scalars  $d_i$ . Thus the desired bearings  $\mathbf{g}_i^*$  can neither all be pointing towards  $\mathbf{g}_i^{*+}$  nor can they all point toward  $\mathbf{g}_i^{*-}$  in Fig. 4.14b. In other words, we may conclude that in (4.24) the orthogonal projection of  $\mathbf{g}_i^*$  on  $\mathcal{P}_i$ , i.e.  $\mathbf{P}_{\mathbf{g}_i} \mathbf{g}_i^*$  and that of  $\mathbf{g}_{i+1}^*$  on  $\mathcal{P}_{i+1}$ , i.e.  $\mathbf{P}_{\mathbf{g}_{i+1}} \mathbf{g}_{i+1}^*$ , both of which lie on the line  $\nabla$  that is common to all the planes  $\mathcal{P}_i$ , cannot point along the same direction for all  $i$ . Hence, the inner product of these two projections,  $\mathbf{g}_i^{*\top} \mathbf{P}_{\mathbf{g}_i} \mathbf{P}_{\mathbf{g}_{i+1}} \mathbf{g}_{i+1}^*$ , must be negative for some  $i$ . Thus, for some  $i$  the product  $\pm \sin \alpha_i \sin \alpha_{i+1}$  must be  $-\sin \alpha_i \sin \alpha_{i+1} = -\sin^2 \alpha$ . This is because there must be some  $i$  such that  $\mathbf{g}_i^*$  points along  $\mathbf{g}_i^{*+}$  while  $\mathbf{g}_{i+1}^*$  is along  $\mathbf{g}_{i+1}^{*-}$ , or vice versa. At the same time, for three agents, there will also be some  $j$  such that the product  $\pm \sin \alpha_j \sin \alpha_{j+1}$  must be  $+\sin \alpha_j \sin \alpha_{j+1} = +\sin^2 \alpha$ . Hence, there exists  $i$  such that its dynamics will be

$$\dot{\alpha}_i = \frac{2 \sin \alpha}{d_i} \neq 0.$$

and also  $j$  such that its dynamics will be

$$\dot{\alpha}_j = 0.$$

This nonzero derivative of  $\alpha_i$  will cause it to change the value of  $\alpha_i$  while the zero derivative of  $\alpha_j$  will cause  $\alpha_j$  to remain unchanged. This will violate the condition  $\alpha_i = \alpha \forall i$  and thus  $\dot{V}$  will not remain zero.

(c) In this case, since there are only three agents,  $\beta_i = 0$  again implies that three agents are collinear. Thus, it reduces to the same scenario as in (a).

From above arguments, (ii) cannot happen and thus  $\dot{V} = 0$  if and only if (i) happens, or three agent are at the desired formation. It follows from LaSalle Invariance Principle that the desired equilibrium is asymptotically stable. ■

#### 4.3.4 The $n$ -agent case

The  $n$ -agent system in  $\mathbb{R}^3$  will now be briefly discussed. Defining the following sets:

$$\bar{\mathcal{Q}}_n = \{\mathbf{p} \in \mathbb{R}^{3n} \mid \mathbf{g}_i = \pm \mathbf{g}_i^*, \forall i \in \mathcal{I}\},$$

$$\bar{\mathcal{D}}_n = \{\mathbf{p} \in \mathbb{R}^{3n} \mid \mathbf{g}_i = \mathbf{g}_i^*, \forall i \in \mathcal{I}\},$$

$$\bar{\mathcal{U}}_n = \bar{\mathcal{Q}}_n \setminus \bar{\mathcal{D}}_n.$$

The following lemma is about local stability of equilibrium sets  $\bar{\mathcal{D}}_n$  and  $\bar{\mathcal{U}}_n$ .

**Lemma 4.14** *The equilibria corresponding to  $\bar{\mathcal{D}}_n$  are locally asymptotically stable and the ones corresponding to  $\bar{\mathcal{U}}_n$  are unstable.*

*Proof:* The proof follows from linearizing equation (4.28). ■

**Remark 4.15** *It is not straightforward to prove the asymptotic stability of the equilibrium in  $\bar{\mathcal{D}}_n$ .*

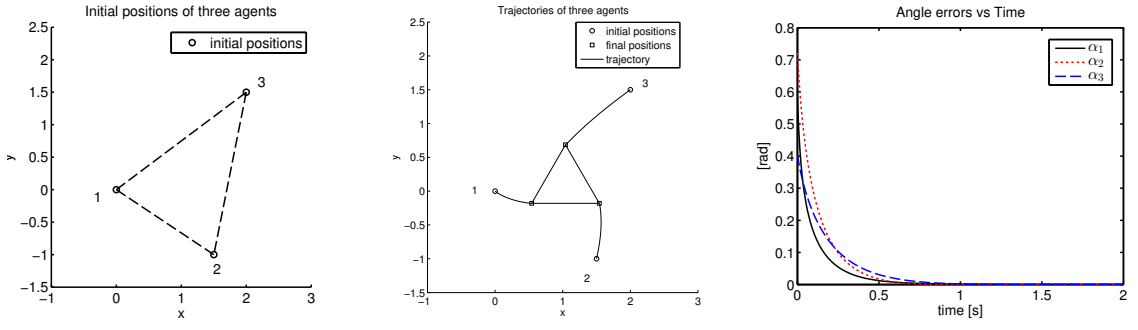
*Consider the Lyapunov function  $V = \max_{i=1,\dots,n} \alpha_i$ , we can process in a similar manner as in Theorem 4.13 until the step of examining all possibilities that may lead to  $\dot{V} = 0$ . At that point, we cannot deduce collinearity of the  $n$  agent formation as in case (c) in the proof of Theorem 4.13.*

#### 4.4 Simulations

##### 4.4.1 Simulation 1: A three-agent formation in the plane

In this simulation, we consider three agents. The desired formation is an equilateral triangle. The initial positions of the agents are  $\mathbf{p}_1(0) = [0, 0]^\top$ ,  $\mathbf{p}_2(0) = [1.5, -1]^\top$ , and  $\mathbf{p}_3(0) = [2, 1.5]^\top$  as shown in Fig. 4.15a. It may be verified that the condition for convergence is satisfied.

The trajectories of the three agents are shown in Fig. 4.15b. The agents asymptotically form an equilateral triangle as desired. Observe from Fig. 4.15c that the angle  $\alpha_i \rightarrow 0$  asymptotically.



(a) The initial formation. (b) Trajectories and final formation. (c) The angles  $\alpha_i$  vs. Time [s].

Figure 4.15. Simulation results of a three-agent formation under the bearing-only control law (4.9).

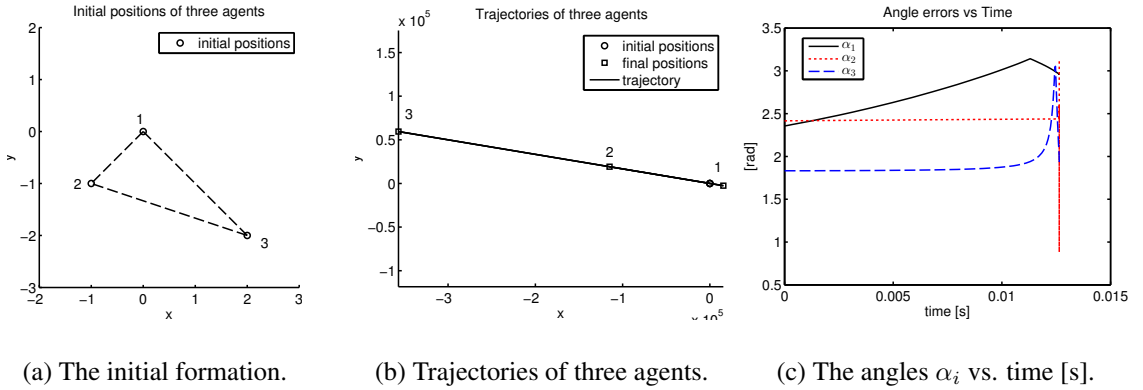


Figure 4.16. The three-agent formation under the control law (4.9) with another initial condition.

For the same system with another initial condition that does not satisfy our condition  $\alpha_i \leq \frac{\pi}{2} \forall i$ , it is shown in Fig. 4.16 that instability can occur. Thus, the simulation results are consistent with our analysis in Section 4.2.1.

#### 4.4.2 Simulation 2: A six-agent formation in the plane

Next, we consider a six-agent system with the measurement graph as depicted in Figure 4.1. The desired bearing vectors are chosen to obtain a regular hexagon. The initial positions of the agents are chosen such that they are not too far from the desired bearings.

Two simulations with different initial conditions, both satisfying  $\alpha_i \leq \frac{\pi}{2} \forall i$ , are shown in Fig. 4.17

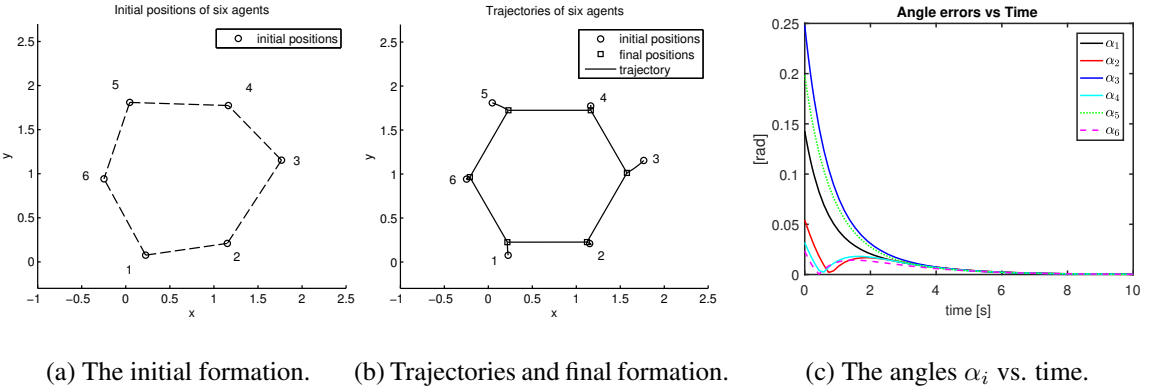


Figure 4.17. Simulation results of a six-agent formation under the bearing-only control law (4.9).

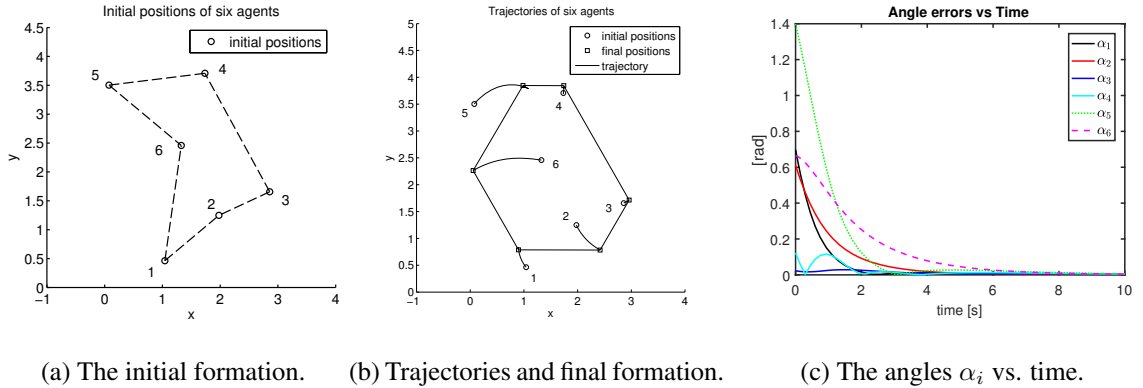
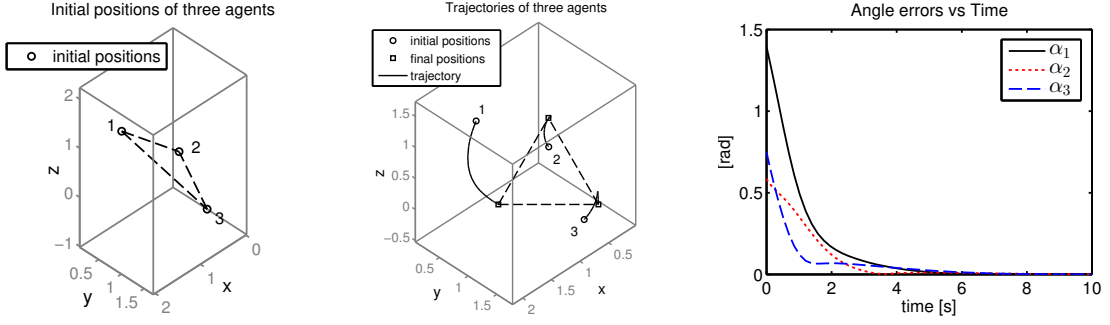


Figure 4.18. Simulation results of the six-agent formation for a different set of initial conditions.

and Fig. 4.18. In both simulations, the agents asymptotically converge to a formation that satisfies desired bearing vector set  $\mathcal{B}_n$ . The maximum angle  $\alpha_{\max}$  asymptotically decays, as can be seen from Fig. 4.17c and Fig. 4.18c. Observe from Fig. 4.17b and Fig. 4.18b that the final formation shape is not fixed. This further shows that for  $n > 3$ , the shape of the  $C_n$ -formation is not uniquely determined by specifying bearings alone.

#### 4.4.3 Simulation 3: A three-agent formation in the three-dimensional space

We simulate a three agent formation in  $\mathbb{R}^3$ . The desired formation is an equilateral triangle whose desired bearing vectors are given by  $\mathbf{g}_1^* = [-\sqrt{2}/2, 0, \sqrt{2}/2]^T$ ,  $\mathbf{g}_2^* = [0, \sqrt{2}/2, -\sqrt{2}/2]^T$ , and  $\mathbf{g}_3^* =$



(a) The initial formation. (b) Trajectories and final formation. (c) The angles  $\alpha_i$  vs. time [s].

Figure 4.19. Three agents form an equilateral triangular formation under the control law (4.9).

$$[\sqrt{2}/2, -\sqrt{2}/2, 0]^T.$$

Simulation results are shown in Fig. 4.19. The initial positions of the three agents are not parallel to the plane specified by the desired bearing vectors. The initial angle errors satisfy the condition  $0 \leq \alpha_i \leq \frac{\pi}{2}, \forall i$ . From the agents' trajectories depicted in Fig. 4.19b, we observe that three agents asymptotically reach the desired plane and achieve the desired formation shape. Thus, we conclude that the simulation result is consistent with our analysis in Section 4.3.

## **Part III**

# **The Pointing Consensus Problem**

# Chapter 5

## Pointing Consensus and Bearing-Based Solutions to the Fermat-Weber Location Problem

The content of this chapter is from [144]. Section 5.1 formulates the bearing-based pointing consensus problem. Next, in Section 5.2, a control strategy is proposed to solve the pointing consensus problem. For illustration, a specific problem is studied where the target is the centroid of all agents' formation. Then, the Fermat-Weber location problem is reformulated and two solutions are proposed in 5.3. Finally, simulation results are provided in Section 5.4.

### 5.1 Problem formulation

Consider an  $n$ -agent system ( $n \geq 3$ ) in a three-dimensional ambient space. The system may represent a group of satellites, or a camera network. The location of each agent is unknown to itself and other agents. However, these agents' local reference frames are assumed to be aligned.<sup>1</sup> Let  $\mathbf{p}_i \in \mathbb{R}^3$ ,  $i \in \mathcal{I} \triangleq \{1, \dots, n\}$  be the position vector of the stationary agent  $i$ . Each agent  $i$  has a heading direction given by a unit vector  $\mathbf{b}_i \in \mathbb{R}^3$ ,  $\|\mathbf{b}_i\| = 1$  as depicted in Fig. 5.1.

Suppose that each agent can control its own heading direction by rotating its heading direction around the point  $\mathbf{p}_i$  with an angular velocity  $\omega_i$  and along an immediate rotation axis  $\mathbf{a}_i$ , as illustrated in Fig. 5.1. Let  $\mathbf{p}'_i = \mathbf{p}_i + \mathbf{b}_i$ , the rotational motion of the heading direction  $\mathbf{b}_i$  is equivalent to the motion of the point  $\mathbf{p}'_i$  around the sphere of length 1 centered at  $\mathbf{p}_i$ . The orthogonal projection matrix corresponding to  $\mathbf{b}_i$  is defined as  $\mathbf{P}_{\mathbf{b}_i} \triangleq \mathbf{I}_3 - \mathbf{b}_i \mathbf{b}_i^\top$ .

---

<sup>1</sup>This assumption can be satisfied by employing a orientation alignment or orientation estimation strategy [23, 25].

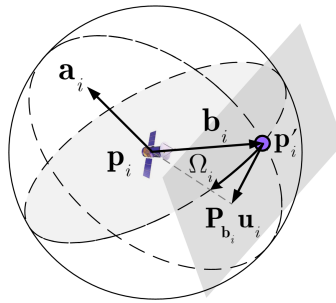


Figure 5.1. The rotational velocity  $\Omega_i$  of the agent  $i$ 's heading direction can be equivalently represented as the velocity  $\mathbf{u}_i = \mathbf{P}_{\mathbf{b}_i} \mathbf{u}_i$  of the head point  $p'_i$ .

Using these notations, one can study the dynamics of the heading direction. The control effort to change  $\mathbf{b}_i$  is given as

$$\dot{\mathbf{p}}'_i = \mathbf{P}_{\mathbf{b}_i} \mathbf{u}_i, \quad (5.1)$$

where  $\mathbf{u}_i \in \mathbb{R}^3$  is the control input to be designed. It follows that

$$\dot{\mathbf{b}}_i = \frac{d}{dt} \left( \frac{\mathbf{p}'_i - \mathbf{p}_i}{\|\mathbf{p}'_i - \mathbf{p}_i\|} \right) = \mathbf{P}_{\mathbf{b}_i} \mathbf{u}_i, \quad (5.2)$$

where one has used the fact that  $\dot{\mathbf{p}}_i = \mathbf{0}$ . Note that the equivalent rotation of the heading vector can be found from the following formulas:  $\|\mathbf{P}_{\mathbf{b}_i} \mathbf{u}_i\| = |\Omega_i| \|\mathbf{b}_i\| = |\Omega_i|$ , and  $\mathbf{a}_i = \mathbf{b}_i \wedge \mathbf{P}_{\mathbf{b}_i} \mathbf{u}_i$ , where “ $\wedge$ ” denotes the cross product.

In many applications, all agents' headings are desired to target a common point in the space. The common point may be a target object, the centroid of all agents, or a location that minimizes a logistic function. The pointing consensus problem without position information has been shown to be a hard problem. To remedy the lack of position information, it is assumed that each agent can sense the directional information (or the bearing vectors) with regard to select neighboring agents. The bearing vector could be obtained, for example, from an on-board camera. This chapter firstly formulates a specific problem, in which all agents' headings are desired to target the group's centroid. The solution to this specific problem can be extended to the general pointing consensus problem

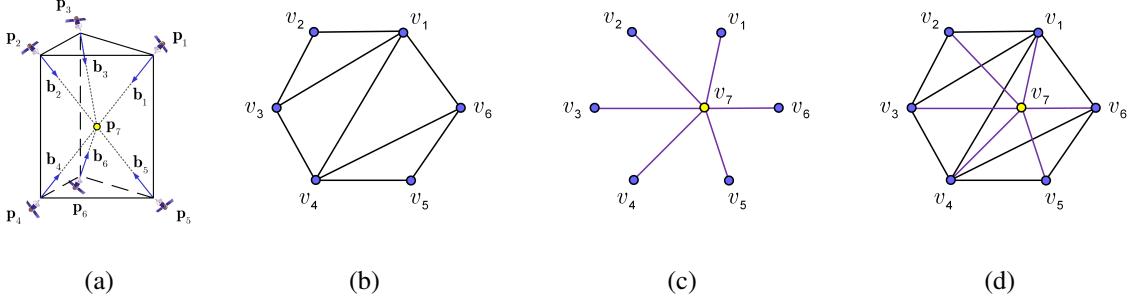


Figure 5.2. Example: A six-agent system and a common target. (a) The agents consent their heading direction into a common point  $p^*$ . (b) The information graph  $G$ . (c) The pointing graph (objective graph). (d) The union graph  $\bar{G}$ .

without much efforts.

The undirected graph  $G = (\mathcal{V}, \mathcal{E})$  is used to characterize the bearing sensing and information exchange graph between  $n$  agents, with the vertex set  $\mathcal{V} = \{v_i | i \in \mathcal{I}\}$  and the edge set  $\mathcal{E} = \{e_{ij} = (v_i, v_j) | i, j \in \mathcal{I}, v_i \neq v_j\}$ . There is no self-edge in the graph  $((v_i, v_i) \notin \mathcal{E})$  since each agent cannot sense the direction to itself. Consider an arbitrary indexing of all edges  $\mathcal{E} = \{e_1, \dots, e_m\}$ , where the following equivalent notations are used for the same edge  $e_{k_{ij}} \equiv e_k \equiv e_{ij}$ . The incidence matrix  $\mathbf{H} \in \mathbb{R}^{m \times n}$  characterizes the relationship between vertices and edges in  $G$ .

If there is an edge  $e_{ij} \in \mathcal{E}$ , two agents  $i$  and  $j$  can sense the bearing vectors ( $\mathbf{g}_{ij}$  and  $\mathbf{g}_{ji}$  in  $\mathbb{R}^3$ ) and exchange information with regard to each other. In order to define the bearing vector  $\mathbf{g}_{ij}$ , two agents  $i$  and  $j$  must not be collocated, i.e.,  $\mathbf{p}_i \neq \mathbf{p}_j, \forall i, j \in \mathcal{I}$ . Let  $\mathbf{p} = [\mathbf{p}_1^\top, \dots, \mathbf{p}_n^\top]^\top \in \mathbb{R}^{3n}$  be the stacked vector of all agents' position vectors. Then,  $\mathbf{p}$  is called a configuration of the graph  $G$ , and  $G(\mathbf{p})$  a framework in  $\mathbb{R}^3$ . Let  $\mathbf{g} = [\dots, \mathbf{g}_{k_{ij}}^\top, \dots]^\top = [\mathbf{g}_1^\top, \dots, \mathbf{g}_m^\top]^\top \in \mathbb{R}^{3m}$  be the stacked bearing measurement vector. The bearing rigidity matrix  $\mathbf{R}_b(\mathbf{p})$  in this setup is of dimension  $3m \times 3n$ .

Assuming that the framework  $G(\mathbf{p})$  is infinitesimally bearing rigid (IBR), i.e., the rank of the

bearing rigidity matrix is  $r(\mathbf{R}(\mathbf{p})) = 3n - 4$ . For an IBR framework, the nullspace of  $\mathbf{R}(\mathbf{p})$  is

$$\mathcal{N}(\mathbf{R}_b(\mathbf{p})) = \mathcal{R}([\mathbf{1}_n \otimes \mathbf{I}_3, \mathbf{p}]) = \mathcal{R}([\mathbf{1}_n \otimes \mathbf{I}_3, \mathbf{p} - \mathbf{1}_n \otimes \mathbf{p}_c]),$$

where  $\mathbf{p}_c \triangleq \sum_{i=1}^n \mathbf{p}_i/n$  is the group's centroid. The bearing Lalacian matrix  $\mathbf{L}_b = \mathbf{R}_b^\top(\mathbf{p})\mathbf{R}_b(\mathbf{p}) \in \mathbb{R}^{3n \times 3n}$  has  $\mathcal{N}(\mathbf{L}_b) = \mathcal{N}(\mathbf{R}_b(\mathbf{p}))$ . Furthermore, a three-dimensional framework is infinitesimally bearing rigid if and only if  $r(\mathbf{L}_b) = 3n - 4$ .

Before stating the main problem, the assumptions are summarized as follows:

**Assumption 5.1** *The  $n$  agents' local reference frames are aligned. Their clocks are synchronized.*

*Each agent can control its heading vector according to equation (5.2).*

**Assumption 5.2** *The agents can exchange the information via a fixed, undirected information graph  $G$ . Moreover, the framework  $G(\mathbf{p})$  is infinitesimally bearing rigid.*

The next section is devoted to study the following problem:

**Problem 5.1** *Given an  $n$ -agent system embedded in a three-dimensional ambient space satisfying Assumptions 5.1-5.2. Design a decentralized control law for each agent using the bearing measurements such that all agents' headings asymptotically target the group's centroid.*

## 5.2 The pointing consensus strategy

This section studies the Problem 5.1. It will be firstly shown that if the  $n$ -agent framework is IBR, then so is the combined framework of  $n$  agents and the target. Then, a control strategy is proposed to direct all the agents' headings toward the group's centroid. Finally, it will be proved that the proposed strategy solves Problem 5.1 for almost all initial conditions.

### 5.2.1 Bearing rigidity and the pointing consensus problem

Consider the  $n$ -agent system ( $n \geq 3$ ) with a corresponding framework  $G(\mathbf{p})$  embedded in a three dimensional space. Let  $\mathbf{p}_{n+1}$  be the desired point that all agents' heading are pointing toward. Define the pointing graph  $\mathcal{P}$  with the vertex set  $\bar{\mathcal{V}} = \mathcal{V} \cup \{v_{n+1}\}$  and the edge set  $\mathcal{E}(\mathcal{P}) = \{(v_i, v_{n+1}) | i \in \mathcal{I}\}$ . The pointing graph  $\mathcal{P}$  describes the group's objective, that is, each edge  $(v_i, v_{n+1})$  implies that agent  $i$  need to point toward the point  $\mathbf{p}_{n+1}$ . Further, we define the graph  $\bar{G} = \{\bar{\mathcal{V}}, \bar{\mathcal{E}}\}$ , where  $\bar{\mathcal{E}} = \mathcal{E} \cup \mathcal{E}(\mathcal{P}) = \mathcal{E} \cup \{(v_i, v_{n+1}) | i \in \mathcal{I}\}$  as depicted in Fig. 5.2. Also, let  $\bar{\mathbf{p}} = [\mathbf{p}^\top, \mathbf{p}_{n+1}^\top]^\top$ . Observe that  $\bar{G}$  is a union graph of the bearing measurement graph  $G$  and the pointing graph. Recall that since the agents have access to only the relative bearing vectors  $\{\mathbf{g}_{ij}\}_{e_{ij} \in \mathcal{E}}$ , translations and scalings of the configuration are unobservable. One has the following result on the union framework  $\bar{G}(\bar{\mathbf{p}})$ :

**Lemma 5.1** *Suppose that  $G(\mathbf{p})$  is infinitesimally bearing rigid. Then the union framework  $\bar{G}(\bar{\mathbf{p}})$  is also infinitesimally bearing rigid.*

*Proof:* Let  $\mathbf{L}_b$  and  $\mathbf{L}'_b$  denote the bearing Laplacian of the framework  $G(\mathbf{p})$  and  $\bar{G}(\bar{\mathbf{p}})$ , respectively. Since  $G(\mathbf{p})$  is infinitesimally bearing rigid,  $r(\mathbf{L}_b) = 3n - 4$ . Consider the framework  $\bar{G}(\bar{\mathbf{p}})$ , we can write the bearing Laplacian of  $\bar{G}(\bar{\mathbf{p}})$  as follows:

$$\mathbf{L}'_b = \begin{bmatrix} \mathbf{L}_b + \mathbf{D} & \mathbf{F} \\ \mathbf{F}^\top & \mathbf{E} \end{bmatrix}, \quad (5.3)$$

where  $\mathbf{D} = \text{blkdiag}(\mathbf{P}_{b_k})$ ,  $\mathbf{F}^\top = -[\mathbf{P}_{b_1}, \dots, \mathbf{P}_{b_n}]$ , and  $\mathbf{E} = \sum_{k=1}^n \mathbf{P}_{b_k}$ . Using Schur complement, we can write

$$r(\mathbf{L}'_b) = r(\mathbf{E}) + r(\mathbf{L}_b + \mathbf{D} - \mathbf{F}\mathbf{E}^{-1}\mathbf{F}^\top). \quad (5.4)$$

Since  $G(\mathbf{p})$  is infinitesimally bearing rigid, the  $n$  ( $n \geq 3$ ) bearing vectors  $\mathbf{b}_1, \dots, \mathbf{b}_n$ , cannot all be collinear. It follows that  $\mathbf{E}$  is positive definite. Further, the matrices  $\mathbf{L}_b$  and  $\mathbf{D} - \mathbf{F}\mathbf{E}^{-1}\mathbf{F}^\top$  are

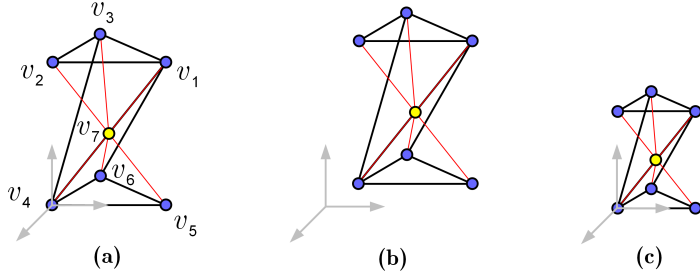


Figure 5.3. Example: A six-agent system and a common target. (a) A configuration of the union framework  $\bar{G}(\bar{p})$ . The configuration  $\bar{p}$  after (b) a translation, (c) a dilation. For both cases (b) and (c), the agents' headings still point toward a common point.

positive semidefinite based on [130, Lemma 4]. It follows from (5.4) that

$$\begin{aligned} r(\mathbf{L}'_b) &\geq r(\mathbf{E}) + \max\{r(\mathbf{L}_b), r(\mathbf{D} - \mathbf{F}\mathbf{E}^{-1}\mathbf{F}^\top)\} \\ &\geq 3 + 3n - 4 = 3(n+1) - 4. \end{aligned} \quad (5.5)$$

Because  $\mathbf{L}'_b$  is a bearing Laplacian,  $r(\mathbf{L}'_b) \leq 3(n+1) - 4$ . Combining with (5.5), we have  $r(\mathbf{L}'_b) = 3(n+1) - 4$ , or i.e.,  $\bar{G}(\bar{p})$  is infinitesimally bearing rigid. ■

Based on Lemma 5.1, when all agents' heading vectors point toward a common point, they maintain their heading vectors towards the common point even when the union framework  $G(\bar{p})$  is translated or dilated. This argument is illustrated in Fig. 5.3. Thus, if the agents can somehow estimate their positions up to a translation and a dilation from the bearing measurements, they can control their heading vectors toward a common point determined by some distributed protocols between them, and the pointing consensus problem is solved. It is worth remarking that a bearing-based network localization problem has been studied in [73]. In [73], the authors assumed that there are several beacon nodes which have access to their absolute locations and proposed a different network localization algorithm. Due to the existence of the beacon nodes, all other nodes can estimate their precise locations under the proposed algorithm in [73]. In the setup of this work, since we assume no beacon node, the

agents can only estimate their positions up to a translation and a dilation. It will be shown later that the agents do not need their absolute positions to solve the Problem 5.1.

**Remark 5.2** *In many existing works in the literature, rigidity is a property of a network/formation and is studied separately from other objectives. For examples, the ideas of adding vertices and edges to an existing rigid framework to build a larger rigid one for studying formation control/network localization were presented in [2, 130]. The result in this subsection shows that rigidity is important to both network localization and pointing objectives. Further, the two objectives can be combined and considered simultaneously. The heading vectors can be treated as the bearing vectors in constructing the union framework  $\bar{G}(\bar{\mathbf{p}})$  since they have similar mathematical properties.*

### 5.2.2 The proposed strategy

Let each agent  $i$  in the system store an estimation of its position  $\hat{\mathbf{p}}_i \in \mathbb{R}^3$ . Through the information graph  $G$ , the each agent exchanges the current estimation with their neighbors. From the exchanged estimations and bearing measurements, the agent  $i$  updates its position estimate under the following bearing-based estimation dynamics:

$$\dot{\hat{\mathbf{p}}}_i(t) = - \sum_{j \in \mathcal{N}_i} \mathbf{P}_{\hat{\mathbf{g}}_{ij}} \mathbf{g}_{ij} - \sum_{j \in \mathcal{N}_i} \|\hat{\mathbf{g}}_{ij} - \mathbf{g}_{ij}\| \mathbf{P}_{\hat{\mathbf{g}}_{ij}} (\text{sgn}(\mathbf{P}_{\hat{\mathbf{g}}_{ij}} \mathbf{g}_{ij}) + \mathbf{n}_{ij}(t)), \quad (5.6)$$

Note that in Eq. (5.6),  $\hat{\mathbf{z}}_{ij} = \hat{\mathbf{p}}_j - \hat{\mathbf{p}}_i$ ,  $\hat{\mathbf{g}}_{ij} = \hat{\mathbf{z}}_{ij} / \|\hat{\mathbf{z}}_{ij}\|$ , and  $\mathbf{P}_{\hat{\mathbf{g}}_{ij}} = \mathbf{I}_3 - \hat{\mathbf{g}}_{ij} \hat{\mathbf{g}}_{ij}^\top$  can be calculated by agent  $i$  from the its estimation and its neighbors' estimations, while  $\mathbf{g}_{ij}$  is the measured bearing vector from agent  $i$ . The additive disturbance term  $\mathbf{n}_{ij}(t) = [n_{ij1}, n_{ij2}, n_{ij3}]^\top$  is a continuous time-varying vector satisfying  $\|\mathbf{n}_{ij}(t)\|_2 = \rho < 1$ , and  $\mathbf{n}_{ij} = -\mathbf{n}_{ji}$  for all  $e_{ij} \in \mathcal{E}$ .

The bearing-based estimation law (5.6) consists of two parts: the first part  $-\sum_{j \in \mathcal{N}_i} \mathbf{P}_{\hat{\mathbf{g}}_{ij}} \mathbf{g}_{ij}$  is the duality of the formation control law introduced in [49], and the remaining part is an adjustment term introduced to guarantee a global convergence of the estimation to the desired value. The second term

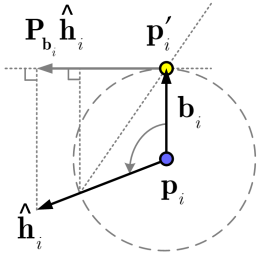


Figure 5.4. Suppose that the vector  $\hat{h}_i$  is fixed, the control law (5.8) rotates  $b_i$  to align with  $\hat{h}_i$  exponentially fast.

vanishes if there is no error between the sensed and estimated bearing vectors  $\|\hat{g}_{ij} - g_{ij}\| = 0, \forall j \in \mathcal{N}_i$ .

**Remark 5.3** There are many possible choices for the additive disturbance term  $\mathbf{n}_{ij}(t)$  [57]. For example, we can choose  $\mathbf{n}_{ij}(t) = \rho_{ij}[\cos(\sigma_{ij}t), \sin(\sigma_{ij}t)\cos(\sigma t), \sin(\sigma_{ij}t)\sin(\sigma t)]^\top$ . The parameters  $\rho_{ij}$ ,  $\{\sigma_{ij}\}_{j \in \mathcal{N}_i}$ , and  $\sigma$  are assumed to be available to agent  $i$ . By designing the parameters such that  $\rho_{ij} = -\rho_{ji}$ ,  $0 < |\rho_{ij}| = \rho < 1$ ,  $\sigma_{ij} = \sigma_{ji}, \forall (i, j) \in \mathcal{E}$ , it is not difficult to check that  $\|\mathbf{n}_{ij}(t)\|_2 = \rho < 1$ , and  $\mathbf{n}_{ij} = -\mathbf{n}_{ji}$  for all  $e_{ij} \in \mathcal{E}$ .

Depending on applications, the agents may choose to consent their heading vectors toward any point in space. In this section, suppose that all agents want to point toward the group's centroid. To this end, the following decentralized centroid estimation and pointing consensus dynamics is proposed for each agent  $i \in \mathcal{I}$ :

$$\dot{\mathbf{q}}_i(t) = \sum_{j \in \mathcal{N}_i} (\mathbf{q}_j(t) - \mathbf{q}_i(t)), \quad \mathbf{q}_i(0) = \hat{\mathbf{p}}_i(0), \quad (5.7)$$

$$\dot{\mathbf{b}}_i(t) = \mathbf{P}_{\mathbf{b}_i}(\mathbf{q}_i(t) - \hat{\mathbf{p}}_i(t)). \quad (5.8)$$

The dynamics (5.7) is simply a consensus protocol used to estimate the centroid of  $n$  points  $\hat{\mathbf{p}}_i(0)$ ,  $i = 1, \dots, n$ . Meanwhile, the pointing dynamics (5.8) guides each heading vector  $\mathbf{b}_i$  toward

the estimated centroid of  $n$  agents. In (5.8),  $\hat{\mathbf{h}}_i(t) = (\mathbf{q}_i - \hat{\mathbf{p}}_i)$  is the estimation of the displacement vector from the agent toward the centroid and is time-varying. The control law (5.8) was inspired from [82, 100] and its principle is illustrated in Fig. 5.4.

### 5.2.3 Stability analysis

In this subsection, we will show that the proposed strategy (5.6), (5.7), (5.8) asymptotically drives all agents' headings toward their centroid. Let each agent initialize a random position estimation  $\hat{\mathbf{p}}_i(0)$ . Without loss of generality, we can assume that these initial estimated values are all different. Let  $\hat{\mathbf{p}} = [\hat{\mathbf{p}}_1^\top, \dots, \hat{\mathbf{p}}_n^\top]^\top$ ,  $\mathbf{g} = [\mathbf{g}_1^\top, \dots, \mathbf{g}_m^\top]^\top$ , and  $\bar{\mathbf{H}} = \mathbf{H} \otimes \mathbf{I}_3$ , we can rewrite (5.6) in the following compact form:

$$\begin{aligned}\dot{\hat{\mathbf{p}}} &= \bar{\mathbf{H}}^\top \text{blkdiag}(\mathbf{P}_{\hat{\mathbf{g}}_k}) \mathbf{g} + \bar{\mathbf{H}}^\top \text{blkdiag}(\mathbf{P}_{\hat{\mathbf{g}}_k} \|\hat{\mathbf{g}}_k - \mathbf{g}_k\|) (\mathbf{sgn}(\text{blkdiag}(\mathbf{P}_{\hat{\mathbf{g}}_k}) \mathbf{g}) + \mathbf{n}) \\ &= \tilde{\mathbf{R}}_b(\hat{\mathbf{p}})^\top (\mathbf{g} + \text{blkdiag}(\|\hat{\mathbf{g}}_k - \mathbf{g}_k\| \mathbf{I}_3) (\mathbf{sgn}(\text{blkdiag}(\mathbf{P}_{\hat{\mathbf{g}}_k}) \mathbf{g}) + \mathbf{n})),\end{aligned}\quad (5.9)$$

where  $\tilde{\mathbf{R}}_b = \text{blkdiag}(\|\mathbf{z}_k\| \mathbf{I}_3) \mathbf{R}_b$ . Define  $\hat{\mathbf{p}}_c = (\sum_{i=1}^n \hat{\mathbf{p}}_i)/n$  and  $\hat{s} = \sqrt{\sum_{i=1}^n \|\hat{\mathbf{p}}_i - \hat{\mathbf{p}}_c\|^2/n}$  as the estimated group's centroid and scale, respectively.

**Lemma 5.4** *Under the estimation dynamics (5.6), the group's centroid and scale are invariant.*

*Proof:* Note that  $\mathcal{N}(\tilde{\mathbf{R}}_b) = \mathcal{N}(\mathbf{R}_b)$ . Thus, from (5.9) and properties of the bearing rigidity matrix  $\mathbf{R}(\hat{\mathbf{p}})$ , we have  $\dot{\hat{\mathbf{p}}} \perp \mathcal{R}([\mathbf{1}_n \otimes \mathbf{I}_3, \hat{\mathbf{p}} - \mathbf{1}_n \otimes \mathbf{p}_c])$ . By writing  $\hat{\mathbf{p}}_c = (\mathbf{1}_n^\top \otimes \mathbf{I}_3) \hat{\mathbf{p}}/n$  and  $\hat{s} = \|\hat{\mathbf{p}} - \mathbf{1}_n \otimes \hat{\mathbf{p}}_c\|/\sqrt{n}$ , it follows that

$$\begin{aligned}\dot{\hat{\mathbf{p}}}_c &= (\mathbf{1}_n^\top \otimes \mathbf{I}_3) \dot{\hat{\mathbf{p}}}/n = \mathbf{0}, \\ \dot{\hat{s}} &= \frac{1}{\sqrt{n}} \frac{(\hat{\mathbf{p}} - \mathbf{1}_n \otimes \hat{\mathbf{p}}_c)^\top}{\|\hat{\mathbf{p}} - \mathbf{1}_n \otimes \hat{\mathbf{p}}_c\|} \dot{\hat{\mathbf{p}}} = 0.\end{aligned}$$

Thus, the estimated group's centroid and scale are invariant. ■

There are three observations from Lemma 5.4. Firstly, since the sum  $\sum_{i=1}^n \hat{p}_i(0)$  is time invariant under (5.6), one can initiate  $\mathbf{q}_i(0) = \hat{\mathbf{p}}_i(0)$  in (5.7) without worrying about the dynamics (5.6). Secondly, invariance of the estimated group's centroid and scale gives a constraint on the number of equilibria of (5.6). Finally, since the estimated group's centroid  $\hat{\mathbf{p}}_c$  and the estimated scale  $\hat{s}$  (which is mathematically the mean of deviation of the estimations  $\hat{p}_i$  with regard to the group centroid) are time invariant, the estimation values will not diverge when evolving under (5.6).

Next, the convergence of the estimation law (5.6) is studied. Since (5.6) is a nonsmooth control law, the solution of (5.9) is studied in the Filippov sense [134]. For brevity, let  $\boldsymbol{\eta} = \text{blkdiag}(\mathbf{P}_{\hat{\mathbf{g}}_k})\mathbf{g} = [\boldsymbol{\eta}_1^\top, \dots, \boldsymbol{\eta}_m^\top]^\top$ , where each  $\boldsymbol{\eta}_k = [\eta_{k1}, \eta_{k2}, \eta_{k3}]^\top$  is a vector in  $\mathbb{R}^3$ . Then, for almost all time,

$$\dot{\hat{\mathbf{p}}} \in \bar{\mathbf{H}}^\top \text{blkdiag}(\mathbf{P}_{\hat{\mathbf{g}}_k})(\boldsymbol{\eta} + \text{blkdiag}(\|\hat{\mathbf{g}}_k - \mathbf{g}_k\| \mathbf{I}_3)(K[\mathbf{sgn}](\boldsymbol{\eta}) + \mathbf{n})), \quad (5.10)$$

where  $K[\mathbf{f}](\mathbf{x})$  is the Filippov set-valued mapping of  $\mathbf{f}(\mathbf{x})$ , “ $\in$ ” denotes the differential inclusion,  $\mathbf{n} = [\mathbf{n}_1^\top, \dots, \mathbf{n}_m^\top]^\top$  is the perturbation vector with  $\mathbf{n}_k = [n_{k1}, n_{k2}, n_{k3}]^\top \in \mathbb{R}^3$ ,  $k = 1, \dots, m$ .

Let  $\mathbf{p}^* = [\mathbf{p}_1^{*\top}, \dots, \mathbf{p}_n^{*\top}]^\top \in \mathbb{R}^{3n}$  be a point satisfying: (i) centroid:  $(\mathbf{1}_n^\top \otimes \mathbf{I}_3)\mathbf{p}^*/n = \hat{\mathbf{p}}_c$ , (ii) scale:  $s(\mathbf{p}^*) = s(\hat{\mathbf{p}})$ , and (iii) at  $\mathbf{p}^*$ , the bearing vectors are  $\hat{\mathbf{g}}_{ij} = \mathbf{g}_{ij}, \forall e_{ij} \in \mathcal{E}$ . It can be checked that  $\mathbf{p}^*$  uniquely exists and is an equilibrium of (5.9). One has the following theorem:

**Theorem 5.5** *Suppose that assumptions 5.1–5.2 are satisfied. Under the estimation law (5.6),  $\hat{\mathbf{p}}$  globally asymptotically converges to  $\mathbf{p}^*$ .*

*Proof:* Consider the Lyapunov function  $V = \frac{1}{2}\|\hat{\mathbf{p}} - \mathbf{p}^*\|^2$ , which is positive definite, continuously differentiable and radially unbounded. At each point  $\hat{\mathbf{p}}$ , there holds  $\partial V = (\hat{\mathbf{p}} - \mathbf{p}^*)$ . Then,  $\dot{V}$

exists almost everywhere (a.e.) and  $\dot{V} \in^{a.e.} \dot{\tilde{V}}$ , where

$$\begin{aligned}\dot{\tilde{V}} &= \bigcap_{\xi \in \partial V} \xi^\top \dot{\hat{p}} = (\hat{p} - p^*)^\top \bar{H}^\top \text{blkdiag}(\mathbf{P}_{\hat{g}_k}) (\boldsymbol{\eta} + \text{blkdiag}(\|\hat{g}_k - g_k\| \mathbf{I}_3) (K[\mathbf{sgn}](\boldsymbol{\eta}) + \mathbf{n})) \\ &= -\boldsymbol{\eta}^\top \text{blkdiag}(\|\hat{z}_k\| \mathbf{I}_3) (\boldsymbol{\eta} + \text{blkdiag}(\|\hat{g}_k - g_k\| \mathbf{I}_3) (K[\mathbf{sgn}](\boldsymbol{\eta}) + \mathbf{n})) \\ &\leq -\sum_{k=1}^m \|\hat{z}_k\| \left( \boldsymbol{\eta}_k^\top \boldsymbol{\eta}_k + \|\hat{g}_k - g_k\| (\boldsymbol{\eta}_k^\top K[\mathbf{sgn}](\boldsymbol{\eta}_k) - |\boldsymbol{\eta}_k^\top \mathbf{n}_k|) \right).\end{aligned}$$

From property of the sgn function, one has  $\boldsymbol{\eta}_k^\top K[\mathbf{sgn}](\boldsymbol{\eta}_k) = \sum_{l=1}^3 |\eta_{kl}| = \|\boldsymbol{\eta}_k\|_1$ . Further, for  $\mathbf{n}_k = [n_{k1}, n_{k2}, n_{k3}]$ , it holds  $|n_{kl}| \leq \sqrt{\sum_{l=1}^3 n_{kl}^2} = \|\mathbf{n}_k\|$ ,  $\forall l = 1, 2, 3$ . Thus,  $|\boldsymbol{\eta}_k^\top \mathbf{n}_k| \leq \sum_{l=1}^3 |\eta_{kl} n_{kl}| \leq \sum_{l=1}^3 |\eta_{kl}| \|\mathbf{n}_k\| \leq \rho \sum_{l=1}^3 |\eta_{kl}| = \rho \|\boldsymbol{\eta}_k\|_1$ . By combining these inequalities, it follows that:

$$\dot{\tilde{V}} \leq -\sum_{k=1}^m \|\hat{z}_k\| \boldsymbol{\eta}_k^\top \boldsymbol{\eta}_k - \sum_{k=1}^m (1-\alpha) \|\hat{z}_k\| \|\hat{g}_k - g_k\| \|\boldsymbol{\eta}\|_1 \leq -\sum_{k=1}^m \|\hat{z}_k\| \boldsymbol{\eta}_k^\top \boldsymbol{\eta}_k \leq 0. \quad (5.11)$$

Note that  $\dot{\tilde{V}} = 0$  if and only if  $\hat{g}_k = g_k$ ,  $\forall k = 1, \dots, m$  or  $\hat{g}_k = -g_k$ ,  $\forall k = 1, \dots, m$ . However, the configuration corresponding to  $\hat{g}_k = -g_k$ ,  $\forall k = 1, \dots, m$  is not an equilibrium of (5.10) due to the adjustment term. Therefore, based on LaSalle's Invariance Principle for nonsmooth system, one can conclude that  $\hat{p}$  globally asymptotically converges to  $p^*$ . ■

**Theorem 5.6** *Under assumptions 5.1–5.2,  $\hat{p} = p^*$  is an almost globally exponentially stable equilibrium of (5.9).*

*Proof:* From the inequality (5.11), one can follow a similar steps as in [49, Theorem 11] to prove the claim. ■

Next, consider the centroid estimation dynamics (5.7), the following result is canonical:

**Theorem 5.7** *Under Assumptions 5.1–5.2,  $\mathbf{q}_i(t)$  converges to  $\hat{\mathbf{p}}_c$  exponentially fast for all  $i \in \mathcal{I}$ .*

*Proof:* Under Assumption 5.2,  $G(\mathbf{p})$  is IBR. This implies that  $G$  is connected. Thus, under the consensus protocol (5.7),  $\mathbf{q}_i(t)$  converges to  $\sum_{i=1}^n \mathbf{q}_i(0)/n = \sum_{i=1}^n \hat{\mathbf{p}}_i(0)/n = \hat{\mathbf{p}}_c$  exponentially fast [91]. ■

Consider the pointing dynamics (5.8). Let  $\mathbf{h}_i^* \triangleq \hat{\mathbf{p}}_c - \mathbf{p}_i^*$ , we can rewrite (5.8) as follows:

$$\dot{\mathbf{b}}_i = \underbrace{\mathbf{P}_{\mathbf{b}_i} \mathbf{h}_i^*}_{\triangleq \mathbf{f}_i(\mathbf{b}_i)} + \underbrace{\mathbf{P}_{\mathbf{b}_i} (-\mathbf{h}_i^* + \hat{\mathbf{h}}_i(t))}_{\triangleq \mathbf{r}_i(t)}. \quad (5.12)$$

From (5.12), the control input used to change each agent's heading consists of two parts: the first part,  $\mathbf{f}_i(\mathbf{b}_i)$ , depends only on  $\mathbf{b}_i$ ; and the second part,  $\mathbf{r}_i(t)$ , depends on the estimation dynamics (5.6)-(5.7). The following lemma states that the inputs only change the direction, and not the magnitude, of the heading vector  $\mathbf{b}_i$ .

**Lemma 5.8** *Under the dynamics (5.6)–(5.8),  $\|\mathbf{b}_i(t)\| = 1$  for all  $i \in \mathcal{I}$  and all time  $t \geq 0$ .*

*Proof:* It can be verified that  $\mathbf{b}_i^\top \dot{\mathbf{b}}_i = \mathbf{b}_i^\top \mathbf{P}_{\mathbf{b}_i} \hat{\mathbf{h}}_i = 0$  since  $\mathbf{b}_i^\top \mathbf{P}_{\mathbf{b}_i} = \mathbf{0}_d^\top$ . As a result,  $\|\mathbf{b}_i(t)\| = \|\mathbf{b}_i(0)\| = 1$  for all  $t \geq 0$ . ■

The next lemma is about the external input  $\mathbf{r}(t)$ .

**Lemma 5.9** *Suppose that assumptions 5.1–5.2 holds. Then under the dynamics (5.6)–(5.12), the input  $\mathbf{r}(t)$  is bounded and  $\|\mathbf{r}(t)\| \rightarrow 0$  exponentially fast.*

*Proof:* To show the boundedness property, the following inequality is employed  $\|\mathbf{r}(t)\| = \|\mathbf{P}_{\mathbf{b}_i}(-\mathbf{h}_i^* + \hat{\mathbf{h}}_i)\| \leq \|\mathbf{P}_{\mathbf{b}_i}\|(\|\mathbf{h}_i^*\| + \|\hat{\mathbf{h}}_i\|)$ . Note that  $\|\mathbf{P}_{\mathbf{b}_i}\| = 1$ ,  $\|\mathbf{h}_i^*\|$  is bounded, and  $\|\hat{\mathbf{h}}_i\| \leq \|\mathbf{q}_i\| + \|\hat{\mathbf{p}}_i\|$  is also bounded due to Theorems 5.5 and 5.7. Thus,  $\mathbf{r}(t)$  bounded. Moreover, it follows from Theorems 5.5–5.7 that  $\hat{\mathbf{h}}_i(t) = \mathbf{q}_i - \hat{\mathbf{p}}_i \rightarrow \hat{\mathbf{p}}_c - \mathbf{p}_i^* = \mathbf{h}_i^*$ , exponentially as  $t \rightarrow \infty$ . Consequently,  $\|\mathbf{r}(t)\| = \|\hat{\mathbf{h}}_i - \mathbf{h}_i^*\| \rightarrow 0$  as  $t \rightarrow \infty$  and the convergence is exponentially fast. ■

Next, consider the system

$$\dot{\mathbf{b}}_i = \mathbf{f}(\mathbf{b}_i) = \mathbf{P}_{\mathbf{b}_i} \mathbf{h}_i^*, \quad (5.13)$$

which is the system (5.12) without the input  $\mathbf{r}(t)$ . For  $\mathbf{h}_i^* \neq 0$ , one has the following lemma whose proof is similar to the proof of [100, Lemma 3.1] and will be omitted:

**Lemma 5.10** *The system (5.13) has two equilibria  $\mathbf{b}_i = \pm \mathbf{b}_i^*$ , where  $\mathbf{b}_i^* = \mathbf{h}_i^*/\|\mathbf{h}_i^*\|$ . The equilibrium  $\mathbf{b}_i = \mathbf{b}_i^*$  is almost globally exponentially stable and the equilibrium  $\mathbf{b}_i = -\mathbf{b}_i^*$  is (exponentially) unstable.*

The main result of this section is stated in the following theorem:

**Theorem 5.11** *Suppose that Assumptions 5.1–5.2 hold. Under the control strategy (5.6), (5.7), (5.8) all agents' headings asymptotically point toward the group's centroid from almost all initial positions.*

*Proof:* Based on Lemma 5.9, for the heading vector  $\mathbf{b}_i$  to remain at the undesired equilibrium point  $\mathbf{b}_i(t) \equiv -\mathbf{b}_i^*$ , it is required that  $\mathbf{r}_i(t) \equiv \mathbf{0}$  and  $\mathbf{b}_i(0) = -\mathbf{b}_i^*$ . Next,  $\mathbf{r}_i \equiv \mathbf{0}$  implies  $\dot{\mathbf{q}}_i \equiv \mathbf{0}$ ,  $\dot{\mathbf{p}}_i \equiv \mathbf{0}$  and either  $\mathbf{q}_i - \hat{\mathbf{p}}_i \in \mathcal{R}(\mathbf{b}_i^*)$  or  $\mathbf{q}_i = \hat{\mathbf{p}}_i$ . Notice that  $\dot{\mathbf{q}}_i \equiv \mathbf{0}$  implies that  $\mathbf{q}_i(0) = \mathbf{p}_c$ , and  $\dot{\mathbf{p}}_i \equiv \mathbf{0}$  implies  $\hat{\mathbf{p}}_i(0) = \mathbf{p}_i^*$ . Thus, there are two cases (i)  $\mathbf{q}_i(0) = \hat{\mathbf{p}}_c$  and  $\hat{\mathbf{p}}_i(0) = \mathbf{p}_i^*$ , or (ii)  $\mathbf{q}_i(0) = \mathbf{p}_i^*$  and  $\hat{\mathbf{p}}_i(0) = \mathbf{p}_i^*$ . Since only  $\hat{\mathbf{p}}_i(0) \neq \hat{\mathbf{p}}_j(0)$  for all  $i, j \in \mathcal{I}$  is considered, both cases (i) and (ii) lead to contradictions and thus  $\mathbf{b}_i$  will not stay at the undesired equilibrium  $\mathbf{b}_i = -\mathbf{b}_i^*$ .

Consider the Lyapunov function  $V = \frac{1}{2}\|\mathbf{b}_i - \mathbf{b}_i^*\|^2$  which is positive definite and continuously differentiable. At any point  $\mathbf{b}_i \in \mathbb{R}^3$ , it holds:

$$\begin{aligned} \dot{V} &= (\mathbf{b}_i - \mathbf{b}_i^*)^\top \mathbf{P}_{\mathbf{b}_i} \mathbf{h}_i^* + (\mathbf{b}_i - \mathbf{b}_i^*)^\top \mathbf{P}_{\mathbf{b}_i} (\hat{\mathbf{h}}_i(t) - \mathbf{h}_i^*) \\ &= -\mathbf{b}_i^{*\top} \mathbf{P}_{\mathbf{b}_i} \mathbf{h}_i^* - \mathbf{b}_i^{*\top} \mathbf{P}_{\mathbf{b}_i} (\hat{\mathbf{h}}_i(t) - \mathbf{h}_i^*) \\ &\leq -\|\mathbf{h}_i^*\| \|\mathbf{b}_i^{*\top} \mathbf{P}_{\mathbf{b}_i} \mathbf{b}_i^*\| + \|\mathbf{b}_i^{*\top} \mathbf{P}_{\mathbf{b}_i} (\hat{\mathbf{h}}_i(t) - \mathbf{h}_i^*)\| \\ &\leq -\beta_i \mathbf{b}_i^{*\top} \mathbf{P}_{\mathbf{b}_i} \mathbf{b}_i^* + \|\mathbf{b}_i^{*\top} \mathbf{P}_{\mathbf{b}_i}\| \|\hat{\mathbf{h}}_i(t) - \mathbf{h}_i^*\|, \end{aligned} \quad (5.14)$$

where  $\beta_i = \|\mathbf{h}_i^*\| > 0$ . It follows from Lemma 5.9 that there exist  $\delta_i, \gamma_i > 0$  such that  $\|\hat{\mathbf{h}}_i(t) - \mathbf{h}_i^*\| \leq \beta_i \delta_i e^{-\gamma_i t}$ . Thus,

$$\dot{V} \leq -\beta_i \|\mathbf{P}_{\mathbf{b}_i} \mathbf{b}_i^*\| (\|\mathbf{P}_{\mathbf{b}_i} \mathbf{b}_i^*\| - \delta_i e^{-\gamma_i t}) \leq \frac{1}{4} \beta_i \delta_i^2 e^{-2\gamma_i t},$$

where the inequality holds if and only if  $\|\mathbf{P}_{\mathbf{b}_i} \mathbf{b}_i^*\| = \frac{\delta_i}{2} e^{-\gamma_i t}$ . Thus,

$$V(\infty) - V(0) \leq \int_0^\infty \frac{1}{4} \beta_i \delta_i^2 e^{-2\gamma_i \tau} d\tau = \frac{\beta_i \delta_i^2}{2\gamma_i}, \quad (5.15)$$

which shows that  $V$  is bounded. Consider the function

$$W = \int_0^t \mathbf{b}_i^{*\top} \mathbf{P}_{\mathbf{b}_i} (\hat{\mathbf{h}}_i(\tau) - \mathbf{h}_i^*) d\tau, \quad (5.16)$$

which is bounded because

$$\begin{aligned} \|W\| &\leq \left\| \int_0^t \mathbf{b}_i^{*\top} \mathbf{P}_{\mathbf{b}_i} (\hat{\mathbf{h}}_i(\tau) - \mathbf{h}_i^*) d\tau \right\| \\ &\leq \int_0^t \|\mathbf{b}_i^{*\top} \mathbf{P}_{\mathbf{b}_i} (\hat{\mathbf{h}}_i(\tau) - \mathbf{h}_i^*)\| d\tau \\ &\leq \int_0^t \|\mathbf{b}_i^{*\top} \mathbf{P}_{\mathbf{b}_i}\| \|\hat{\mathbf{h}}_i(\tau) - \mathbf{h}_i^*\| d\tau \\ &\leq \int_0^t 1. \beta_i \delta_i e^{-\gamma_i \tau} d\tau \leq \frac{\beta_i \delta_i}{\gamma_i} (1 - e^{-\gamma_i t}). \end{aligned} \quad (5.17)$$

Consider  $U = V + W$ , then  $U$  is lower bounded, and

$$\dot{U} = \dot{V} + \dot{W} = -\beta_i \|\mathbf{P}_{\mathbf{b}_i} \mathbf{b}_i^*\|^2 \leq 0. \quad (5.18)$$

Since  $\|\dot{\mathbf{b}}_i\| = \|\mathbf{P}_{\mathbf{b}_i} \mathbf{b}_i^*\| \leq \|\mathbf{P}_{\mathbf{b}_i}\| \|\mathbf{b}_i^*\| = 1$ ,  $\dot{\mathbf{b}}_i$  is bounded and thus so is  $\ddot{U}$ . By Barbalat's lemma,  $\lim_{t \rightarrow \infty} \dot{U} = 0$ . Thus,  $\|\mathbf{P}_{\mathbf{b}_i} \mathbf{b}_i^*\| \rightarrow 0$ , or i.e.,  $\mathbf{b}_i \rightarrow \pm \mathbf{b}_i^*$  as  $t \rightarrow \infty$ . However, the system (5.8) could not stay at  $\mathbf{b}_i = -\mathbf{b}_i^*$  according to the discussion at the beginning of the proof. Therefore, we conclude that  $\mathbf{b}_i \rightarrow \mathbf{b}_i^*$  as  $t \rightarrow \infty$ . ■

**Remark 5.12** As the agents do not have information on their global positions, they cannot localize the correct position of  $\mathbf{p}_c$ . However, they can determine precisely the direction toward  $\mathbf{p}_c$  and point toward it. If there are few agents having their absolute positions and acting as anchor nodes, then they can locate the absolute position of  $\mathbf{p}_c$ .

**Remark 5.13** From the proposed strategy, if one replaces the heading dynamics (5.8) by

$$\dot{\boldsymbol{b}}_i = \mathbf{P}_{\boldsymbol{b}_i} \boldsymbol{q}_i, \quad (5.19)$$

all agents' headings will asymptotically point to the same direction  $\boldsymbol{p}_c / \|\boldsymbol{p}_c\|$  as  $t \rightarrow \infty$ .

#### 5.2.4 Discussion on the desired target point

In this subsection, we discuss the target point in the pointing consensus problem. In general, the dynamics (5.7) can be replaced by a generic target decision dynamics, which estimates  $\hat{\boldsymbol{p}}_{n+1}$ -an estimation of the target point  $\boldsymbol{p}_{n+1}$ . The target point  $\boldsymbol{p}_{n+1}$  satisfies a set of predefined constraints. To guarantee that the agents can consent their headings toward  $\boldsymbol{p}_{n+1}$  asymptotically under our proposed pointing consensus strategy, the set of constraints cannot be arbitrarily chosen.

When the estimation dynamics (5.9) is at its equilibrium, the agents can estimate the configuration  $\boldsymbol{p}$  up to a translation and a scaling. Thus, we can write

$$\boldsymbol{p} = k_s(\boldsymbol{p}^* - \boldsymbol{\Delta} \otimes \mathbf{1}_n), \quad (5.20)$$

where  $\boldsymbol{p}^*$  is the desired equilibrium of the estimation dynamics 5.9,  $0 \neq k_s \in \mathbb{R}$  denotes a scale factor and  $\boldsymbol{\Delta} \in \mathbb{R}^3$  is a translation vector. Moreover, as the union framework  $\bar{\mathcal{G}}(\bar{\boldsymbol{p}})$  is IBR, it follows that

$$\bar{\boldsymbol{p}} = k_s(\bar{\boldsymbol{p}}^* - \boldsymbol{\Delta} \otimes \mathbf{1}_{n+1}), \quad (5.21)$$

where  $\bar{\boldsymbol{p}}^* = [\boldsymbol{p}_1^{*\top}, \dots, \boldsymbol{p}_n^{*\top}, \boldsymbol{p}_{n+1}^{*\top}]^\top \in \mathbb{R}^{3(n+1)}$ .

Let  $\mathbf{f}(\bar{\boldsymbol{p}}) = \mathbf{f}(\boldsymbol{p}_1, \dots, \boldsymbol{p}_n, \boldsymbol{p}_{n+1}) = \mathbf{0}$  be the set of constraints that the target point needs to satisfy and assume that the constraints are sufficient to solve for  $\boldsymbol{p}_{n+1}$ , the following result holds:

**Theorem 5.14** The agents can determine the directions toward the designed target if and only if the set of constraints  $\mathbf{f}(\bar{\boldsymbol{p}}) = \mathbf{0}$  that the target point needs to hold is invariant with respect to a translation and a scaling of the whole framework  $\bar{\mathcal{G}}(\bar{\boldsymbol{p}})$ , or. i.e., the set of constraints satisfies equation (5.21).

*Proof:* (*Necessity*). Let the constraints  $\mathbf{f}(\bar{\mathbf{p}}) = \mathbf{0}$  be invariant with respect to a translation and a scaling of the whole framework. Then,  $\mathbf{f}(\bar{\mathbf{p}}) = \mathbf{f}(k_s(\bar{\mathbf{p}}^* - \Delta \otimes \mathbf{1}_{n+1})) = \mathbf{f}(\bar{\mathbf{p}}^*) = \mathbf{0}$ . Thus, the estimated target point  $\mathbf{p}_{n+1}^*$  satisfies  $\mathbf{f}(\bar{\mathbf{p}}^*) = \mathbf{0}$ . This implies that the agents can determine  $\mathbf{p}_{n+1}^*$  from the estimated positions  $\mathbf{p}_i^*, i \in \mathcal{I}$  and the constraint  $\mathbf{f}(\bar{\mathbf{p}}^*) = \mathbf{0}$ .

(*Sufficiency*). Suppose that the agents can determine the directions to the designed target. Since the agents can estimate their positions  $\mathbf{p}_i^*, i \in \mathcal{I}$ , differing from the precise positions by a translation and a scale factor, the target  $\mathbf{p}_{n+1}^*$  is estimated by solving  $\mathbf{f}(\bar{\mathbf{p}}^*) = \mathbf{f}(\mathbf{p}_1^*, \dots, \mathbf{p}_n^*, \mathbf{p}_{n+1}^*) = \mathbf{0}$ . Suppose that  $\mathbf{f}(\bar{\mathbf{p}}) = \mathbf{0}$  is not invariant with respect to a translation and a scaling of the framework, or i.e.,  $\mathbf{f}(\bar{\mathbf{p}}^*) = \mathbf{f}(\mathbf{p}_1^*, \dots, \mathbf{p}_n^*, \mathbf{p}_{n+1}^*) \neq \mathbf{0}$ . Then, the agents cannot correctly determine  $\mathbf{p}_{n+1}^*$ , which implies that they cannot point toward the designed target. This leads to a contradiction. Thus,  $\mathbf{f}(\bar{\mathbf{p}}) = \mathbf{0}$  needs to hold with respect to a translation and a scaling of the whole framework to guarantee that the agents can determine precisely the directions toward the designed target. ■

Two special classes of the target point are given to illustrate Theorem 5.14. First, consider the following linear constraint

$$\mathbf{f}(\bar{\mathbf{p}}) = \sum_{i=1}^{n+1} a_i \mathbf{p}_i = \mathbf{0}, \text{ with } \sum_{i=1}^{n+1} a_i = 0, \quad (5.22)$$

where  $a_i \in \mathbb{R}, i = 1, \dots, n + 1$ , the following theorem can be proved:

**Theorem 5.15** *The constraint (5.22) is invariant with respect to a translation, a scaling and a rotation of the whole framework.*

*Proof:* Observe that the equation (5.22) is linear, we can separately check the invariance of (5.22) with respect to each operator.

- Translation: Let  $\mathbf{p}_i^* = \mathbf{p}_i + \Delta, \forall i = 1, \dots, n + 1$ . Then,

$$\mathbf{f}(\bar{\mathbf{p}}^*) = \sum_{i=1}^{n+1} a_i \mathbf{p}_i^* = \sum_{i=1}^{n+1} a_i \mathbf{p}_i^* + \left( \sum_{i=1}^{n+1} a_i \right) \Delta = \mathbf{0}.$$

- Scaling: Let  $\bar{\mathbf{p}}^* = k_s(\bar{\mathbf{p}} - \Delta \otimes \mathbf{1}_{n+1})$ . It follows that

$$\mathbf{f}(\bar{\mathbf{p}}^*) = \sum_{i=1}^{n+1} a_i \mathbf{p}_i^* = k_s \sum_{i=1}^{n+1} a_i \mathbf{p}_i + k_s \left( \sum_{i=1}^{n+1} a_i \right) \Delta = \mathbf{0}.$$

- Rotation: Without loss of generality, consider the rotation about  $\mathbf{p}_1$  by the rotation matrix

$\mathbf{Q} \in SO(3)$ . One has  $\mathbf{p}_i^* - \mathbf{p}_1^* = \mathbf{Q}(\mathbf{p}_i - \mathbf{p}_1)$ ,  $i = 1, \dots, n+1$ . Then,

$$\mathbf{f}(\bar{\mathbf{p}}^*) = \sum_{i=1}^{n+1} a_i (\mathbf{p}_1^* + \mathbf{Q}(\mathbf{p}_i - \mathbf{p}_1)) = \left( \sum_{i=1}^{n+1} a_i \right) \mathbf{p}_1^* + \mathbf{Q} \mathbf{f}(\bar{\mathbf{p}}) - \mathbf{Q} \left( \sum_{i=1}^{n+1} a_i \right) \mathbf{p}_1 = \mathbf{0}.$$

Thus, the constraint (5.22) is invariant with respect to a translation, a scaling and a rotation of the whole framework. ■

Two remarks follow from Theorem 5.15. First, suppose further in (5.22) that  $a_i > 0, \forall i \in \mathcal{I}$  and the position estimation dynamics (5.6) is at equilibrium  $\hat{\mathbf{p}} = \mathbf{p}^*$ . Let the target decision dynamics (5.7) in our proposed pointing consensus strategy be replaced by:

$$a_i \dot{\mathbf{q}}_i(t) = \sum_{j \in \mathcal{N}_i} (\mathbf{q}_j(t) - \mathbf{q}_i(t)), \quad \mathbf{q}_i(0) = \mathbf{p}_i^*, \quad \forall i \in \mathcal{I}. \quad (5.23)$$

From [108][Corollary 3], we have  $\sum_{i=1}^n a_i \mathbf{q}_i(t) = \sum_{i=1}^n a_i \mathbf{q}_i(0) = \sum_{i=1}^n a_i \mathbf{p}_i^* = -a_{n+1} \mathbf{p}_{n+1}^*$ ,  $\forall t \geq 0$ , and

$$\mathbf{q}_i(t) \rightarrow \frac{\sum_{i=1}^n a_i \mathbf{q}_i(0)}{\sum_{i=1}^n a_i} = \frac{-a_{n+1} \mathbf{p}_{n+1}^*}{-a_{n+1}} = \mathbf{p}_{n+1}^*,$$

as  $t \rightarrow \infty$ . Thus, the dynamics (5.23) can asymptotically determine the target satisfying the constraint (5.22). If the position estimation dynamics (5.7) is not at equilibrium, the dynamic average consensus proposed in [145] or [146] can be used instead. Second, the class of constraints

$$\mathbf{f}(\bar{\mathbf{p}}) = \sum_{i=1}^{n+1} a_i \mathbf{p}_i + \mathbf{c} = \mathbf{0}, \quad \text{with } \sum_{i=1}^{n+1} a_i = 0, \quad (5.24)$$

where  $a_i \in \mathbb{R}$ ,  $i = 1, \dots, n+1$ ,  $\mathbf{0} \neq \mathbf{c} \in \mathbb{R}^3$ , is not invariant under translation and scaling. Due to the bias term  $\mathbf{c}$ , the estimated target point will have an offset depending on both the initial value  $\hat{\mathbf{p}}(0)$  and  $\mathbf{c}$ .

Next, consider the following bearing-only dependent constraint:

$$\mathbf{f}(\bar{\mathbf{p}}) = \mathbf{f}(\bar{\mathbf{b}}), \quad (5.25)$$

where  $\bar{\mathbf{b}} = [\dots, \mathbf{b}_{ij}^\top, \dots]^\top$  such that  $(i, j) \in \bar{\mathcal{E}}$ . One also has the following theorem:

**Theorem 5.16** *The constraint (5.25) is invariant with respect to a translation and a scaling of the whole framework.*

*Proof:* Due to the IBR property of  $\bar{G}(\bar{\mathbf{p}})$  and according to Theorem 5.5, it follows that  $\mathbf{g}_{ij}^* = \mathbf{g}_{ij}, \forall (i, j) \in \bar{\mathcal{E}}$ . It follows that  $\mathbf{f}(\bar{\mathbf{p}}^*) = \mathbf{f}(\bar{\mathbf{b}}^*) = \mathbf{f}(\bar{\mathbf{b}}) = \mathbf{f}(\bar{\mathbf{p}})$ . Thus, the invariant properties of (5.25) are trivially satisfied. ■

Before ending this subsection, we show that the group's centroid is an example of (5.22). The equation of the group's centroid is written as follows:  $\mathbf{p}_{n+1} \equiv \mathbf{p}_c = \frac{1}{n} \sum_{i=1}^n \mathbf{p}_i$ . This equation is equivalent to

$$\frac{1}{n} \sum_{i=1}^n \mathbf{p}_i - 1 \cdot \mathbf{p}_{n+1} = \mathbf{0}.$$

Let  $a_i = \frac{1}{n}, \forall i \in \mathcal{I}$ , and  $a_{n+1} = -1$ , then  $\sum_{i=1}^{n+1} a_i = 0$ . Thus, the group centroid is a particular case of the class of constraints (5.22).

### 5.3 A decentralized bearing-based solution to the Fermat-Weber location problem

The control strategy in the previous section provides a framework to solve the pointing consensus problem in general. In this section, the applicability of the pointing consensus strategy is illustrated in solving the well-known Fermat-Weber location problem (FWLP) based on only bearing measurements. First, the FWLP is introduced and reformulated into a decentralized setup. Second, two decentralized solutions to the FWLP are proposed based on the framework (5.6), (5.7), (5.8) studied

in the previous section. Finally, mathematical analysis are provided on convergence of the proposed control laws.

### 5.3.1 The Fermat-Weber location problem

Consider  $n$  non-collocated points in a three-dimensional space, with position  $\mathbf{p}_i \in \mathbb{R}^3$  for  $i \in \mathcal{I}$ . For a set of positive weights  $\omega_i > 0$ ,  $i \in \mathcal{I}$ , the Fermat-Weber location problem (FWLP) [106] is stated as follows: “Find the point in  $\mathbb{R}^3$  which minimizes the weighted distance sum  $f(\mathbf{q}) = \sum_{i=1}^n \omega_i \|\mathbf{q} - \mathbf{p}_i\|$ .” Equivalently, it is required to find  $\mathbf{q}^* \in \mathbb{R}^3$  such that:

$$\mathbf{q}^* = \arg \min_{\mathbf{q} \in \mathbb{R}^3} f(\mathbf{q}). \quad (5.26)$$

If  $\omega_i = 1, \forall i \in \mathcal{I}$ , the solution  $\mathbf{q}^*$  of (5.26) is called the geometric median of  $n$  points. A large literature on solving the FWLP can be found in the literature; see [102–104] for examples. The following lemma is about the existence and uniqueness of the solution of the FWLP.

**Lemma 5.17 ([102])** *There exists a unique  $\mathbf{q}^*$  minimizing the function  $f(\mathbf{q})$ . This minimum is characterized by the following optimality conditions:*

1. *If there exists  $\mathbf{q}^*$ , different from all  $\mathbf{p}_i$  ( $i = 1, \dots, n$ ), for which*

$$\sum_{i=1}^n \omega_i \frac{\mathbf{q}^* - \mathbf{p}_i}{\|\mathbf{q}^* - \mathbf{p}_i\|} = \mathbf{0}, \quad (5.27)$$

*then this  $\mathbf{q}^*$  is the minimum.*

2. *If for some  $j \in \{1, \dots, n\}$ , there holds*

$$\left\| \sum_{i=1; i \neq j}^n \omega_i \frac{\mathbf{p}_j - \mathbf{p}_i}{\|\mathbf{p}_j - \mathbf{p}_i\|} \right\| \leq \omega_j, \quad (5.28)$$

*then this  $\mathbf{p}_j$  is the minimum.*

### 5.3.2 A decentralized formulation of the FWLP

Consider a multi-agent system consisting of  $n$  individual agents satisfying Assumptions 5.1–5.2.

The following assumption is imposed on the solution to the Fermat-Weber location problem.

**Assumption 5.3** *Each agent  $i$  is given a positive weight  $\omega_i$ . The unique minimum  $\mathbf{q}^* \in \mathbb{R}^3$  of  $f(\mathbf{q})$  satisfies the condition (5.27).*

Remark that Assumption 5.3 is to assure that the minimum point  $\mathbf{q}^* \in \mathbb{R}^3$  is located in the convex hull of  $\mathbf{p}_i, i \in \mathcal{I}$  and is different for each  $\mathbf{p}_i, i \in \mathcal{I}$ . We can now state a decentralized version of the FWLP using only bearing measurements as follows:

**Problem 5.2** *Given an  $n$ -agent system satisfying Assumptions 5.1, 5.2, and 5.3, design a decentralized control law using only bearing information such that all agents' headings  $\mathbf{b}_i \forall i \in \mathcal{I}$ , asymptotically point into the solution  $\mathbf{q}^*$  of the FWLP.*

In other words, the objective is designing a decentralized bearing-based pointing consensus control law such that  $\mathbf{b}_i \rightarrow \mathbf{b}_i^* = \frac{\mathbf{q}^* - \mathbf{p}_i}{\|\mathbf{q}^* - \mathbf{p}_i\|}, \forall i \in \mathcal{I}$ , and the vectors  $\mathbf{b}_i^*, i \in \mathcal{I}$  satisfy  $\sum_{i=1}^n \omega_i \mathbf{b}_i^* = \mathbf{0}$ .

Note that in Problem 5.2, the constraint (5.27) is bearing-only dependent and thus it belongs to the class of constraints (5.25). Moreover, let  $\mathbf{p}_{n+1} \equiv \mathbf{q}^*$  and  $a_i = \frac{\omega_i}{\|\mathbf{p}_{n+1} - \mathbf{p}_i\|}, \forall i \in \mathcal{I}$ , (5.27) is rewritten as follows:

$$\begin{aligned} \sum_{i=1}^n \frac{\omega_i}{\|\mathbf{p}_{n+1} - \mathbf{p}_i\|} (\mathbf{p}_{n+1} - \mathbf{p}_i) &= \mathbf{0} \\ \sum_{i=1}^n a_i \mathbf{p}_i - \left( \sum_{i=1}^n a_i \right) \mathbf{p}_{n+1} &= \mathbf{0}. \end{aligned} \tag{5.29}$$

By denoting  $a_{n+1} = -\sum_{i=1}^n a_i$ , it follows that  $\sum_{i=1}^{n+1} a_i = 0$ . The equation (5.27) has form of the constraint (5.22), however, it does not belong to the class (5.22) since  $a_i = a_i(\mathbf{p}_i, \mathbf{p}_{n+1})$  depends on the position vectors.

### 5.3.3 The proposed solutions

In the literature, a well-known solution for the FWLP is the Weiszfeld's algorithm, which is a discrete time iterative algorithm [102, 103]. The Weiszfeld's algorithm is centralized since it requires all positions  $\mathbf{p}_i, \forall i \in \mathcal{I}$ . A continuous-time control law to reach to the minimum using only local bearing measurements was introduced in [107]. Other than [107], we are not aware of any other decentralized solutions to the FWLP in the literature.

Two decentralized solutions for pointing toward the minimum of the function  $f$  are proposed. First, all agents estimate their positions  $\hat{\mathbf{p}}_i$  under the control law (5.6). Then, instead of (5.7), the agents adopt the estimated target point  $\hat{\mathbf{q}}$  by a decentralized version of the Weiszfeld's algorithm or the gradient-descent control law in [107]. Finally, the agents control their heading under the control law (5.8).

The two decentralized algorithms to determine the Fermat-Weber point are given as follows:

#### **Algorithm 1: The decentralized Weiszfeld's algorithm**

- Initially, all agents have the same estimation of the minimum:  $\hat{\mathbf{q}}_i[0] = \hat{\mathbf{q}}[0] \neq \hat{\mathbf{p}}_i, \forall i \in \mathcal{I}$ .
- At step  $k$ , we need to estimate two quantities:

$$\bar{\mathbf{r}}[k] = \frac{1}{n} \sum_{i=1}^n \omega_i \frac{\hat{\mathbf{p}}_i}{\|\hat{\mathbf{p}}_i - \hat{\mathbf{r}}_i[k]\|} \quad (5.30)$$

$$\bar{r}[k] = \frac{1}{n} \sum_{i=1}^n \frac{\omega_i}{\|\hat{\mathbf{p}}_i - \hat{\mathbf{q}}_i[k]\|} \quad (5.31)$$

Since correct estimations are required before moving to step  $k + 1$ , we employ the following finite-time consensus protocol for estimating the quantities  $\bar{\mathbf{r}}[k]$  and  $\bar{r}[k]$ :

$$\dot{\mathbf{x}}_i(t) = k_x \sum_{j \in \mathcal{N}_i} \text{sig}(\mathbf{x}_j(t) - \mathbf{x}_i(t))^\alpha. \quad (5.32)$$

Here,  $0 < \alpha < 1$  is a parameter required for finite-time convergence,  $k_x > 0$  is a control gain, and  $t \in (0, \Delta T]$  with  $\Delta T$  the convergence time of the algorithm. To estimate the vector  $\bar{r}[k]$ , in (5.32), we initialize  $x_i(0) = r_i(0) = \omega_i \frac{\hat{p}_i}{\|\hat{p}_i - \hat{q}_i[k]\|}$ ,  $\forall i \in \mathcal{I}$ . Meanwhile, to estimate the scalar  $\bar{r}[k]$ , we set  $x_i(0) = r_i(0) = \frac{\omega_i}{\|\hat{p}_i - \hat{q}_i[k]\|}$ ,  $\forall i \in \mathcal{I}$ . After the time  $\Delta T$ , the consensus dynamics have settled to their average, i.e.,  $r_i(t) = \bar{r}[k]$  and  $r_i(t) = \bar{r}[k]$ , and each agent updates its estimation:

$$\hat{q}_i[k+1] = \frac{r_i(t)}{r_i(t)} = \frac{\bar{r}[k]}{\bar{r}[k]} = \frac{\sum_{i=1}^n \omega_i \frac{\hat{p}_i}{\|\hat{p}_i - \hat{q}_i[k]\|}}{\sum_{i=1}^n \frac{\omega_i}{\|\hat{p}_i - \hat{q}_i[k]\|}}, \quad (5.33)$$

which is precisely the formula of the Weiszfeld's algorithm in [102, 103].

- Let  $k \leftarrow k + 1$  and repeat that procedure.

### Algorithm 2: The decentralized gradient-descent algorithm

- Initially, all agents have the same estimation of the minimum:  $\hat{q}_i[0] = q[0] \neq \hat{p}_i, \forall i \in \mathcal{I}$ .
- At step  $k \geq 1$ , we first estimate the quantity

$$\bar{r}[k] = \frac{1}{n} \sum_{i=1}^n \omega_i \frac{\hat{p}_i[k] - \hat{q}_i[k]}{\|\hat{p}_i[k] - \hat{q}_i[k]\|}$$

by employing the finite-time consensus protocol (5.32). For estimation of  $\bar{r}[k]$ , each agent  $i \in \mathcal{I}$  initializes  $x_i(0) = r_i(0) = \omega_i \frac{\hat{p}_i[k] - \hat{q}_i[k]}{\|\hat{p}_i[k] - \hat{q}_i[k]\|}, \forall i \in \mathcal{I}$ . After a time  $\Delta T$ , the consensus dynamics have converged to the average, i.e.,  $r_i(t) = \bar{r}[k]$ . Then, each agent updates its estimate,

$$\hat{q}_i[k] = \hat{q}_i[k-1] + k_q r_i = \hat{q}_i[k-1] + \frac{k_q}{n} \sum_{i=1}^n \omega_i \frac{\hat{p}_i[k] - \hat{q}_i[k]}{\|\hat{p}_i[k] - \hat{q}_i[k]\|}, \quad (5.34)$$

where  $k_q > 0$  is a constant update gain. It can be checked that (5.34) is the discrete-time version of the control law in [107].

- Let  $k \leftarrow k + 1$  and repeat that procedure.

Due to the Algorithms 1 and 2, the right-hand-side of (5.8) are discontinuous. We rewrite (5.8) as follows:

$$\dot{\mathbf{b}}_i(t) = k_b \mathbf{P}_{\mathbf{b}_i} (\hat{\mathbf{q}}_i[k] - \hat{\mathbf{p}}_i), \quad (5.35)$$

for  $k\Delta T \leq t < (k+1)\Delta T$ ,  $k = 0, 1, 2, \dots$ , and  $k_b > 0$  is a constant control gain.

Thus, our proposed control strategies includes the position estimation (5.6), Algorithm 1 or 2, and the heading vector dynamics (5.35).

### 5.3.4 Stability analysis

In this subsection, we will prove that two control strategies (i) (5.6), Algorithm 1, (5.35), and (ii) (5.6), Algorithm 2, (5.35) asymptotically solve the Problem 5.2. In both strategies, the finite-time consensus protocol (5.32) plays a crucial role for updating the estimation in Algorithms 1 and 2.

We have the following result on the finite time consensus protocol (5.32).

**Lemma 5.18** *Under the control law (5.32),  $\dot{\mathbf{x}}_i \rightarrow \frac{1}{n} \sum_{i=1}^n \alpha_i \mathbf{b}_i[t_k]$ ,  $\forall i \in \mathcal{I}$  in a finite time  $T$  satisfying*

*ing*

$$T \leq \frac{V(0)^{1-\alpha/2}}{\kappa(1-\alpha/2)} = \frac{2V(0)^{(2-\alpha)/2}}{\kappa(2-\alpha)}. \quad (5.36)$$

*Proof:* Rewrite the equation (5.32) in vector form,

$$\dot{\mathbf{x}} = -k_x \bar{\mathbf{H}}^\top \text{sig}(\bar{\mathbf{H}} \mathbf{x})^\alpha, \quad (5.37)$$

where  $\mathbf{x} = [\mathbf{x}_1^\top, \dots, \mathbf{x}_n^\top]^\top \in \mathbb{R}^{3n}$ . Denote  $\boldsymbol{\delta}_i = \mathbf{x}_i - \bar{\mathbf{x}}$ , where  $\bar{\mathbf{x}} = (\sum_{i=1}^n \mathbf{x}_i(0)) / n = (\mathbf{1}_n \otimes \mathbf{I}_3)^\top \mathbf{x}(0) / n$ , and let  $\boldsymbol{\delta} = [\boldsymbol{\delta}_1^\top, \dots, \boldsymbol{\delta}_n^\top]^\top$ . It follows that  $\boldsymbol{\delta} = \mathbf{x} - \mathbf{1}_n \otimes \bar{\mathbf{x}}$ . Since  $\mathbf{H}\mathbf{1}_n = \mathbf{0}$ , we have  $\bar{\mathbf{H}}\mathbf{x} = \bar{\mathbf{H}}\boldsymbol{\delta}$ . Thus, we can write

$$\dot{\boldsymbol{\delta}} = -k_x \bar{\mathbf{H}}^\top \text{sig}(\bar{\mathbf{H}} \boldsymbol{\delta})^\alpha. \quad (5.38)$$

Consider the Lyapunov function  $V = \frac{1}{2}\|\boldsymbol{\delta}\|^2$  which is positive definite, radially unbounded and continuously differentiable. Along a trajectory of (5.38),

$$\begin{aligned}\dot{V} &= -k_x \boldsymbol{\delta}^\top \bar{\mathbf{H}}^\top \text{sig}(\bar{\mathbf{H}}\boldsymbol{\delta})^\alpha = -k_x \sum_{k=1}^{3m} |[\bar{\mathbf{H}}\boldsymbol{\delta}]_k|^\alpha \\ &= -k_x \sum_{k=1}^{3m} |[\bar{\mathbf{H}}\boldsymbol{\delta}]_k^2|^{\frac{\alpha}{2}}\end{aligned}\quad (5.39)$$

$$\begin{aligned}&\leq -k_x \left( \sum_{k=1}^{3m} |[\bar{\mathbf{H}}\boldsymbol{\delta}]_k^2| \right)^{\frac{\alpha}{2}} \\ &= -k_x (\|\bar{\mathbf{H}}\boldsymbol{\delta}\|^2)^{\frac{\alpha}{2}} = -k_x (\boldsymbol{\delta}^\top \bar{\mathbf{L}}\boldsymbol{\delta})^{\frac{\alpha}{2}} \\ &\leq -k_x (2\lambda_2(\mathbf{L}))^{\frac{\alpha}{2}} \left( \frac{\|\boldsymbol{\delta}\|^2}{2} \right)^{\frac{\alpha}{2}} = -\kappa V^{\frac{\alpha}{2}},\end{aligned}\quad (5.40)$$

where  $\mathbf{L}$  is the Laplacian matrix of  $G$ ,  $\bar{\mathbf{L}} = \mathbf{L} \otimes \mathbf{I}_3$ ,  $\lambda_2(\mathbf{L}) > 0$  is the second smallest eigenvalue of  $\mathbf{L}$ , and  $\kappa = k_x (2\lambda_2(\mathbf{L}))^{\frac{\alpha}{2}}$ . Note that in (5.39), we have used the inequality in Lemma 2.6 to get (5.40).

It follows from (5.41) and Lemma 2.7 that  $\boldsymbol{\delta} \rightarrow \mathbf{0}$  or  $\mathbf{x}_i \rightarrow \bar{\mathbf{x}}$  in finite time  $T$  satisfying (5.36). ■

**Lemma 5.19** *In the estimation step of Algorithm 2,*

$$\mathbf{x}_i(t) = \bar{\mathbf{r}}[k] = \frac{1}{n} \sum_{i=1}^n \omega_i \frac{\hat{\mathbf{p}}_i[k] - \hat{\mathbf{q}}_i[k]}{\|\hat{\mathbf{p}}_i[k] - \hat{\mathbf{q}}_i[k]\|}, \forall i \in \mathcal{I}$$

for  $t \geq T$  with

$$T \leq 2 \left( 2 \sum_{i=1}^n \omega_i^2 \right)^{\frac{2-\alpha}{2}} / (\kappa(2-\alpha)). \quad (5.42)$$

*Proof:* Let  $\boldsymbol{\beta}_i[k] = \frac{\hat{\mathbf{p}}_i[k] - \hat{\mathbf{q}}_i[k]}{\|\hat{\mathbf{p}}_i[k] - \hat{\mathbf{q}}_i[k]\|}$ ,  $\forall i \in \mathcal{I}$ , it follows that  $\|\boldsymbol{\beta}_i[k]\| = 1$ . We have

$$\|\boldsymbol{\delta}_i(0)\|^2 = \|\mathbf{x}_i(0) - \bar{\mathbf{x}}(0)\|^2 \leq 2(\|\mathbf{x}_i(0)\|^2 + \|\bar{\mathbf{x}}(0)\|^2) = 2 \left( \omega_i^2 + \left\| \sum_{i=1}^n \omega_i \boldsymbol{\beta}_i[k] \right\|^2 / n^2 \right).$$

Moreover,

$$\left\| \sum_{i=1}^n \omega_i \boldsymbol{\beta}_i[k] \right\|^2 \leq \sum_{i=1}^n \omega_i^2 \sum_{i=1}^n \|\boldsymbol{\beta}_i[k]\|^2 = n \sum_{i=1}^n \omega_i^2.$$

Thus,  $\|\delta_i(0)\|^2 \leq 2(\omega_i^2 + \sum_{i=1}^n \omega_i^2/n)$ ,  $\forall i \in \mathcal{I}$ . Summing up these inequalities, we get

$$V(0) = \|\delta(0)\|^2/2 \leq 2 \sum_{i=1}^n \omega_i^2. \quad (5.43)$$

Therefore, the inequality (5.42) follows immediately from (5.43) and (5.36).  $\blacksquare$

**Remark 5.20** *The upper bound of  $T$  provides a conservative lower bound for choosing the time step in implementing the Algorithm 2, i.e., we can implement Algorithms 2 with*

$$\Delta T \geq 2 \left( 2 \sum_{i=1}^n \alpha_i^2 \right)^{2-\alpha} / (\kappa(2-\alpha))$$

*to guarantee that  $x_i[\Delta T] = \bar{x}[\Delta T]$ ,  $\forall i \in \mathcal{I}$ .*

*Unfortunately, we cannot find an explicit lower bound which is independent on  $\hat{p}_i$  for choosing the time step in Algorithm 1. However, if  $\hat{q}_i[k] \neq \hat{p}_i$  for all time, it can be proved that there exists a lower bound for choosing the time step. Thus, when implementing Algorithm 1, it is recommended to choose  $\Delta T$  sufficiently large depending on the size of the initial estimation  $\hat{p}_i$ .*

The next lemma is about the convergence of the estimation  $\hat{q}_i$ .

**Lemma 5.21** *Under the Algorithms 1 or 2, all agents' estimations  $\hat{q}_i[k]$  asymptotically converge to the minimum  $\hat{q}^*$  of  $f(\hat{q}) = \sum_{i=1}^n \omega_i \|\hat{q} - \hat{p}_i\|$  if  $\hat{q}_i[k] \neq \hat{p}_i$  for all time.*

*Proof:* The update law (5.33) is the same as the Weisfeld's algorithm. Thus, as shown in [102], under the Algorithm 1, the estimation  $\hat{q}_i[k] \rightarrow \hat{q}^*$  as  $k\Delta T \rightarrow \infty$  for almost all initial conditions.

The update law (5.34) is a gradient descent law of  $f$ . Since  $f$  is a strictly convex function for  $\hat{q}_i[k] \neq \hat{p}_i$ ,  $\forall i \in \mathcal{I}$  [107] and the minimum is unique (Lemma (5.17)), it follows that the estimation  $\hat{q}_i[k] \rightarrow \hat{q}^*$  asymptotically.

Finally, both algorithms fail to find the minimum if and only if  $\hat{q}_i[k] = \hat{p}_i$  for some time [102, 103].  $\blacksquare$

We can now state the main result of this section:

**Theorem 5.22** Suppose that Assumptions 5.1, 5.2 and 5.3 hold. If  $\hat{q}[k] \neq \hat{p}_i, \forall i \in \mathcal{I}, \forall k = 0, 1, 2, \dots, \infty$ , the two proposed control strategies solve Problem 5.2, i.e., all heading vectors asymptotically point toward the minimum point  $\mathbf{q}^*$  of  $f(\mathbf{c})$ .

*Proof:* First, the position estimation dynamics give a solution of  $\hat{p}_i$  for all cases. Second, the Algorithms 1 and 2 asymptotically give the solution  $\hat{q}^*$ .

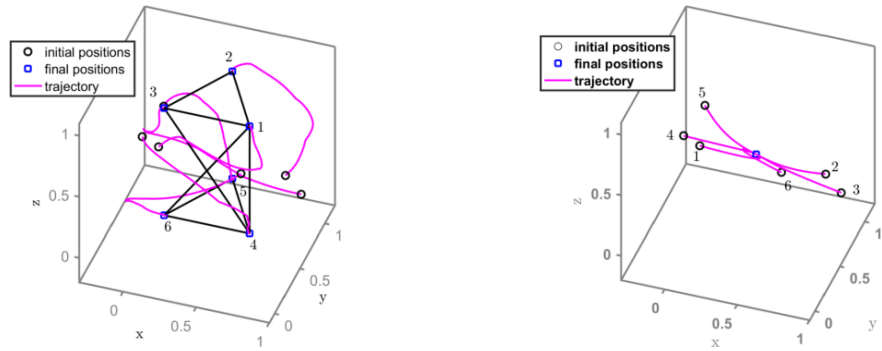
It is remained to prove that the pointing dynamics (5.8) guides all heading vectors to point to  $\mathbf{q}^*$ . Due to the implementation of Algorithms 1 and 2, the right-hand-side of (5.8) is discontinuous at  $t = k\Delta T$ , where  $k = 0, 1, 2, \dots$ . However, for any time  $t$ ,  $\mathbf{b}_i(t)^T \dot{\mathbf{b}}_i(t) = \mathbf{b}_i(t)^T \mathbf{P}_{\mathbf{b}_i}(\hat{q}_i[k] - \hat{p}_i) = 0$  and thus  $\|\mathbf{b}_i(t)\| = 1$ . It shows that during the evolution of  $\hat{q}_i[k]$ , the trajectory of (5.8) is bounded and will not diverge. Thus, if  $\hat{q}_i[k] \rightarrow \hat{q}^*$  asymptotically, by a similar argument as in Theorem 5.11,  $\mathbf{b}_i(t) \rightarrow \frac{\hat{q}^* - \hat{p}_i}{\|\hat{q}^* - \hat{p}_i\|} = \frac{\mathbf{q}^* - \mathbf{p}_i}{\|\mathbf{q}^* - \mathbf{p}_i\|}$  as  $t \rightarrow \infty$ , for all  $i \in \mathcal{I}$ .  $\blacksquare$

## 5.4 Simulation results

In this section, we conduct numerical simulations to verify our analysis in the previous sections. A simulation is about the pointing consensus problem and the others are for solving the FWLP.

### 5.4.1 Simulation 1: Pointing toward the centroid

Consider a six-agent system whose information graph  $G$  is given in Fig. 5.2. Six agents are positioned at  $\mathbf{p}_1 = [3, 0, \frac{9}{2}]^T$ ,  $\mathbf{p}_2 = [\frac{3}{2}, \frac{3\sqrt{3}}{2}, \frac{9}{2}]^T$ ,  $\mathbf{p}_3 = [0, 0, \frac{9}{2}]^T$ ,  $\mathbf{p}_4 = [3, 0, 0]^T$ ,  $\mathbf{p}_5 = [\frac{3}{2}, \frac{3\sqrt{3}}{2}, 0]^T$ , and  $\mathbf{p}_6 = [0, 0, 0]^T$ , respectively. The position estimation control law (5.6) were chosen according to Remark 5.3, with the parameters given as follows:  $\sigma_{12} = 0.1, \sigma_{13} = 0.15, \sigma_{14} = 0.05, \sigma_{16} = 0.02, \sigma_{23} = 0.03, \sigma_{34} = 0.07, \sigma_{45} = 0.075, \sigma_{46} = 0.11, \sigma_{56} = 0.065, \sigma = 0.2$ , and  $k = 0.01$ . The



(a) Trajectories of  $\hat{p}_i$ ,  $i \in \mathcal{I}$  under the position estimation law (5.6). The estimated configuration protocol (5.7). All  $\hat{q}_i$ ,  $i \in \mathcal{I}$  asymptotically reach  $\hat{p}$  differs from  $p$  by a translation and a scale factor.

(b) Trajectories of  $\hat{q}_i$ ,  $i \in \mathcal{I}$  under the consensus protocol law (5.7), all  $\hat{q}_i$ ,  $i \in \mathcal{I}$  asymptotically converges to a consensus, which is the average of  $\hat{p}_i(0)$ .

initial estimates  $\hat{p}_i(0)$  and the initial heading directions  $b_i(0)$   $i \in \mathcal{I}$  were randomly generated.

The six-agent system is simulated under the control strategy (5.6), (5.7), (5.8). Simulation results are given in Figs. 5.5a, 5.5b, and 3.7. From Fig. 5.5a, it can be observed that the estimations asymptotically take up a configuration  $\hat{p}$  differ from the real configuration  $p$  by a translation and a scale factor. Meanwhile, under the consensus protocol law (5.7), all  $\hat{q}_i$ ,  $i \in \mathcal{I}$ , asymptotically converges to the estimated centroid  $\hat{p}_c$ . This makes  $\hat{q}_i - \hat{p}_i$  gradually align with the direction from agent  $i$  toward the centroid. Consequently, after about 20s, the heading vectors of six agents pointed toward the centroid as depicted in Figs. 5.6a–5.6g. Thus, simulation results are consistent with our analysis in the Section 5.2.

#### 5.4.2 Simulation 2: Pointing toward the Fermat-Weber point

We use the same six-agent system as in Simulation 1. The simulations in this section are conducted after each agent has already had an estimation  $\hat{p}_i^*$ . The parameters of the cost function  $f$  are chosen as follows:  $\omega_1 = \omega_2 = \omega_3 = \frac{1}{5}$ ,  $\omega_4 = \omega_5 = \omega_6 = \frac{1}{8}$ . We simulate the system under two control strategies to compare their performance.

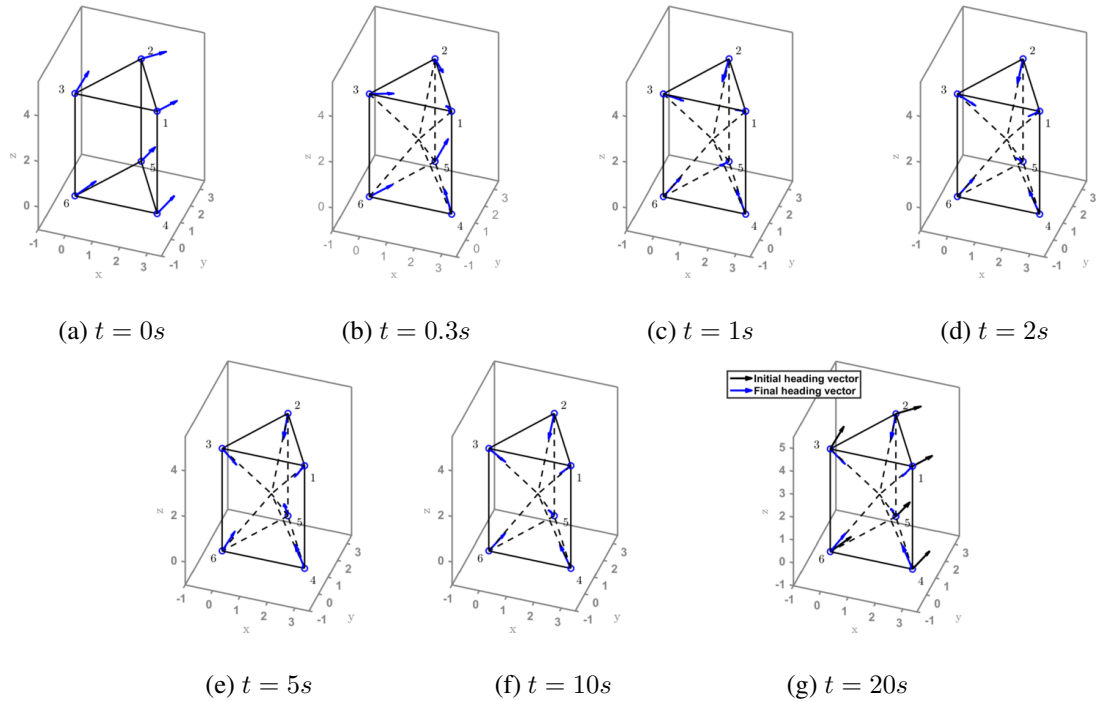


Figure 5.6. Simulation 1: The heading vectors of six agents under the proposed control laws (5.6), (5.7), (5.8). All heading vectors asymptotically point toward the centroid of the formation of six agents after 20s.

**Simulation 2a (Algorithm 1):** The initial estimate of the Fermat-Weber point is chosen to be  $\hat{q}_i[0] = [12.9669, 1.2199, 7.7389]^T$ . This estimation corresponds to the initial states  $r_i[0] = [0.8466, 0.0796, 0.5052]^T$  and  $r_i[0] = 0.0653, \forall i \in \mathcal{I}$ . The chosen control gains are  $k_x = 0.15$  and  $k_b = 0.5$ . The time-step between two updates of  $\hat{q}_i[k]$  in Algorithm 1 is  $\Delta T = 5s$ .

Simulation results are given in Fig. 5.7. The agents can point the heading vectors very close to the Fermat-Weber point in about 40s. Due to the fast convergence of Algorithm 1, the agents can approximate quite precisely the direction to the Fermat-Weber point in a short time. After 20s (three updates of Algorithm 1), the agents point toward  $q_i[3] = [1.6105, 0.8606, 2.9308]^T$ , which is quite close to the Fermat-Weber point ( $[1.500, 0.8666, 3.3451]^T$ ). It is also observed that the pointing dynamics (5.35) is able track the target in the interval between two updates.

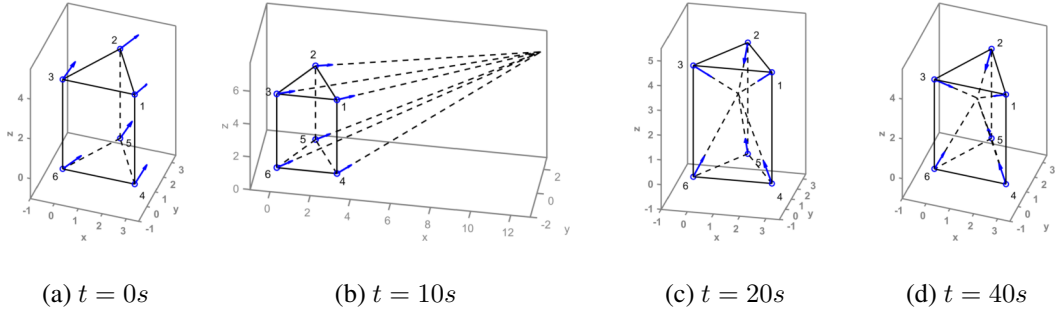


Figure 5.7. Simulation 2a: The headings of six agents under control laws (5.6), Algorithm 1, (5.35).

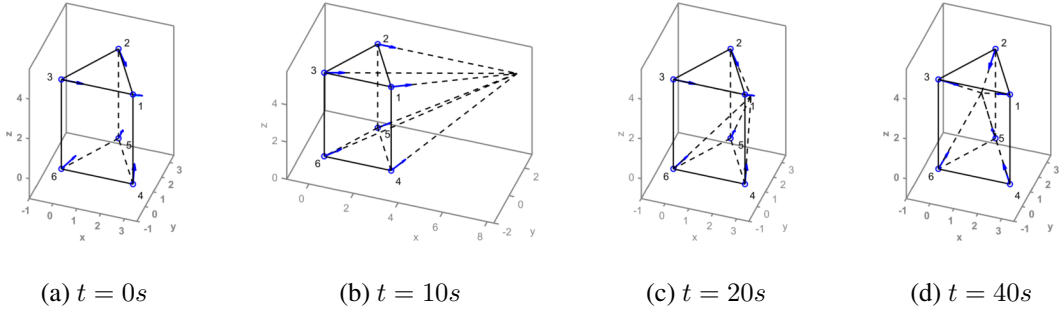


Figure 5.8. Simulation 2b: The headings of six agents under control laws (5.6), Algorithm 2, (5.35).

**Simulation 2b (Algorithm 2):** The initial estimate of the Fermat-Weber point is also chosen to be  $\hat{\mathbf{q}}_i[0] = [12.9669, 1.2199, 7.7389]^T$ . The time step between two updates of  $\hat{\mathbf{q}}_i[k]$  in Algorithm 2 is  $\Delta T = 2s$ . The chosen control gains are  $k_x = 0.15$  and  $k_b = 0.75$ , and the update rate in (5.34) is  $k_q = 8$ .

Simulation results are given Fig. 5.8. After about 40s, the agents' heading vectors point toward  $\mathbf{q}_i[19] = [1.4932, 0.8842, 3.5526]^T$ , which is close to the Fermat-Weber point. As can be observed from Fig. 5.8, the convergence rate of this strategy is slower than the previous strategy. The convergence time of the first control strategy mostly depends on time step between two updates (convergence time of the finite-time consensus protocol (5.32)). Meanwhile, the convergence time of the second control strategy depends on the convergence time of the Algorithm 2 (i.e., the gradient descent update law (5.34)).

## **Part IV**

# **Matrix-Weighted Consensus**

# Chapter 6

## Matrix-Weighted Consensus and Its Applications

The content of this chapter is mainly from [147, 148]. In Section 6.1, we define basic terminologies and introduce the matrix-weighted consensus algorithm. The algebraic condition for globally reaching a consensus in undirected networks is presented in Section 6.2. Section 6.3 further studies the consensus and clustered consensus phenomena under the matrix-weighted consensus algorithm. Finally, Section 6.4 provides two applications of the proposed algorithm.

### 6.1 Preliminaries and problem formulation

#### 6.1.1 Matrix-weighted graphs

This subsection sets a framework for introducing the matrix-weighted consensus protocol and the main analysis of this chapter. Most definitions are analogous to the definitions of algebraic graph theory [121].

A fixed undirected graph with matrix weights is denoted by  $G$ . The graph  $G$  is characterized by a triple  $(\mathcal{V}, \mathcal{E}, \mathcal{A})$ . Here,  $\mathcal{V} = \{v_1, \dots, v_n\}$  denotes the set of  $|\mathcal{V}| = n$  vertices,  $\mathcal{E} = \{e_{ij} = (v_i, v_j) | v_i, v_j \in \mathcal{V}, \text{ and } v_i \neq v_j\}$  denotes the set of  $|\mathcal{E}| = m$  edges, and  $\mathcal{A} = \{\mathbf{A}_{ij} \in \mathbb{R}^{d \times d} | (v_i, v_j) \in \mathcal{E}, \mathbf{A}_{ij} = \mathbf{A}_{ij}^T \geq 0\}$  denotes the set of matrix weights, one for each edge in  $\mathcal{E}$ .<sup>1</sup> The dimension  $d$  ( $d \geq 1$ ) of the matrix weights in  $\mathcal{A}$  depends on the problem. Clearly, if  $d = 1$ , the graph  $G$  becomes an usual undirected scalar-weighted graph.

Depending on the matrix weights, the interconnection between vertices in  $G$  are classified into

---

<sup>1</sup>From the definition,  $(v_i, v_j)$  and  $(v_j, v_i)$  denote the same connection between two vertices  $v_i$  and  $v_j$ .

two types. If the matrix weight  $A_{ij}$  corresponding to edge  $(v_i, v_j) \in \mathcal{E}$  is positive definite, we say that  $(v_i, v_j)$  is a positive definite edge and  $v_i$  and  $v_j$  are connected via a positive definite connection. If the weight matrix  $A_{ij}$  corresponding to an edge  $(v_i, v_j) \in \mathcal{E}$  is positive semidefinite, we say that  $(v_i, v_j)$  is a positive semidefinite edge and  $i$  and  $j$  are connected via a positive semidefinite connection. Apparently, if  $v_i$  and  $v_j$  are disconnected,  $A_{ij} = \mathbf{0}$ . We also assume that the interconnections between any two vertices are symmetric, i.e.,  $A_{ij} = A_{ji}, \forall (v_i, v_j) \in \mathcal{E}$ .

A path is a sequence of vertices in  $G$ , denoted by  $\mathcal{P} = v_{i_1} v_{i_2} \dots v_{i_l}$ , such that  $v_{i_k} \neq v_{i_l}, \forall v_{i_k}, v_{i_l} \in \mathcal{P}$ , and each edge  $(v_{i_k}, v_{i_{k+1}})$ ,  $k = 1, \dots, l - 1$ , is a positive definite or a positive semidefinite connection. The graph  $G$  is *positive semiconnected* if and only if there exists a path between any two vertices in  $G$ . Otherwise,  $G$  is disconnected. We only focus on positively semiconnected graphs. Graphs with disconnected components can be studied similarly. Assuming that  $G$  is positive semiconnected, one can make the following definitions.

**Definition 6.1 (Positive path)** *A positive path is a sequence of vertices and edges in  $G$ , denoted by  $\mathcal{P} = v_{i_1} v_{i_2} \dots v_{i_l}$ , such that  $v_{i_k} \neq v_{i_l}, \forall v_{i_k}, v_{i_l} \in \mathcal{P}$ , and each edge  $(v_{i_k}, v_{i_{k+1}})$ ,  $k = 1, \dots, l - 1$ , is a positive definite edge.*

A tree is an undirected graph containing at least one vertex in which any two vertices are connected by exactly one path. We have the following definition.

**Definition 6.2 (Positive tree)** *A positive tree  $\mathcal{T}$  is a tree contained in  $\mathcal{V}$  having all positive connections.*

Equivalently, for all  $v_i, v_j \in \mathcal{T}$ , there exists a positive path in  $\mathcal{T}$  connecting  $v_i$  and  $v_j$ .

**Definition 6.3 (Positive spanning tree)** *A positive spanning tree  $\mathcal{T}$  of  $G$  is a positive tree containing all vertices in  $\mathcal{V}$ .*

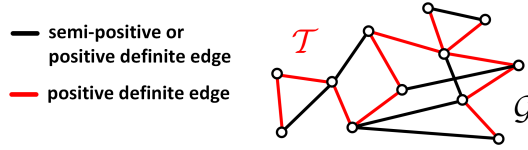


Figure 6.1.  $\mathcal{T}$  is a positive spanning tree of  $G$ . The edges in  $\mathcal{E}(\mathcal{T})$  are in red color.

Note that a tree of  $k$  vertices ( $k \geq 1$ ) contains exactly  $k - 1$  edges. Thus, a positive spanning tree of  $G$  contains exactly  $n - 1$  positive connections. An example of positive spanning tree is depicted in Figure 6.1. Next, we define several algebraic structures corresponding to the matrix weighted graph  $G$ . The *matrix-weighted adjacency matrix* of  $G$  is defined as follows:

$$\mathbf{A} = \begin{bmatrix} \mathbf{0} & \mathbf{A}_{12} & \cdots & \mathbf{A}_{1n} \\ \mathbf{A}_{21} & \mathbf{0} & \ddots & \vdots \\ \vdots & \ddots & \ddots & \mathbf{A}_{n-1,n} \\ \mathbf{A}_{n1} & \cdots & \mathbf{A}_{n,n-1} & \mathbf{0} \end{bmatrix} \in \mathbb{R}^{dn \times dn}. \quad (6.1)$$

Since  $G$  is undirected and  $\mathbf{A}_{ij} = \mathbf{A}_{ji}$ , it is easy to see that  $\mathbf{A}$  is symmetric. For each vertex  $v_i$ , the neighbor set of vertex  $v_i$  is defined as  $\mathcal{N}_i = \{j \in \{1, \dots, n\} | v_j \in \mathcal{V} \text{ and } (v_i, v_j) \in \mathcal{E}\}$ . Let the matrix  $\mathbf{D}_i = \sum_{j \in \mathcal{N}_i} \mathbf{A}_{ij}$  be the *degree matrix* of the vertex  $v_i$ . Further, we define  $\mathbf{D} = \text{blkdiag}(\mathbf{D}_i)$ , the block diagonal matrix of all vertices, as the degree matrix of the graph  $G$ . The *matrix-weighted Laplacian* is defined as  $\mathbf{L} = \mathbf{D} - \mathbf{A} \in \mathbb{R}^{dn \times dn}$ . Consider an arbitrary index of the edges of  $G$ . The edge set and the matrix-weight set can be given as  $\mathcal{E} = \{e_{k_{ij}}\}_{k=1, \dots, m}$  and  $\mathcal{A} = \{\mathbf{A}_{k_{ij}}\}_{k=1, \dots, m}$ , correspondingly. From now on, if it is not important to specify the end-vertices explicitly, the subscript  $ij$  will be dropped out and write  $e_k$  and  $\mathbf{A}_k$  without ambiguity.

Let  $\mathbf{H} = [h_{ij}] \in \mathbb{R}^{m \times n}$  denote the incidence matrix corresponding to an arbitrary orientation of the edges in  $\mathcal{E}$  as defined in Section 2.1. An edge  $e_k$  is called adjacent to a vertex  $v_i$  if and only if  $v_i$  is a head or a tail of  $e_k$ , and this adjacency relationship is denoted by  $e_k \sim v_i$ . We can state the

following results whose proofs can be found in [147].

**Lemma 6.4** *The matrix-weighted Laplacian can be written in the following form:*

$$\mathbf{L} = \bar{\mathbf{H}}^\top \text{blkdiag}(\mathbf{A}_k) \bar{\mathbf{H}}. \quad (6.2)$$

**Corollary 6.5** *For any vector  $\mathbf{v} = [\mathbf{v}_1^\top, \dots, \mathbf{v}_n^\top]^\top \in \mathbb{R}^{dn}$ ,*

$$\mathbf{v}^\top \mathbf{L} \mathbf{v} = \sum_{(i,j) \in \mathcal{E}} (\mathbf{v}_i - \mathbf{v}_j)^\top \mathbf{A}_{ij} (\mathbf{v}_i - \mathbf{v}_j).$$

### 6.1.2 Matrix-weighted consensus protocols

Consider a networked dynamic system consisting of  $n$  agents. Each agent  $i$  in the system has a state vector  $\mathbf{x}_i = [x_{i1}, \dots, x_{id}]^\top \in \mathbb{R}^d$ , where  $d \geq 1$ . The overall system's states are described by a stacked column vector  $\mathbf{x} = [\mathbf{x}_1^\top, \dots, \mathbf{x}_d^\top]^\top \in \mathbb{R}^{dn}$ .

The matrix-weighted undirected graph  $G = (\mathcal{V}(G), \mathcal{E}(G), \mathcal{A}(G))$  describes the interconnection between the agents in the system. Assume that  $G$  is positive semi-connected. An edge  $e_{ij} \in \mathcal{E}$  exists if and only if agent  $i$  and agent  $j$  can sense their relative state information in at least one state variable.

Consider the agents with single-integrator model, each agents updates its states under the following protocol:

$$\dot{\mathbf{x}}_i = \sum_{j \in \mathcal{N}_i} \mathbf{A}_{ij} (\mathbf{x}_j - \mathbf{x}_i), \quad \forall i = 1, \dots, n, \quad (6.3)$$

where  $\mathbf{x}_i \in \mathbb{R}^d$  is the state and the right-hand side of (6.3) is the control input of agent  $i$ ,  $i = 1, \dots, n$ , at time instance  $t \geq 0$ . Using the matrix-weighted Laplacian, we can express the dynamics of  $n$  agents in the following matrix form:

$$\dot{\mathbf{x}} = -\mathbf{L}\mathbf{x}. \quad (6.4)$$

Let us take a closer look the matrices  $\mathbf{A}_{ij}$ . Since  $\mathbf{A}_{ij}$  is symmetric and nonnegative, we can always decompose it into  $\mathbf{A}_{ij} = \mathbf{U}_{ij} \mathbf{D}_{ij} \mathbf{U}_{ij}^\top$ , where  $\mathbf{D}_{ij} \in \mathbb{R}^{d \times d}$  is a diagonal matrix with nonnegative

entries, which are the eigenvalues of  $\mathbf{A}_{ij}$ , and  $\mathbf{U}_{ij} \in \mathbb{R}^{d \times d}$  is an unitary matrix ( $\mathbf{U}_{ij}\mathbf{U}_{ij}^T = \mathbf{I}_d$ ). Thus, we may understand the physical meaning of the equation (6.3) as follows:  $(\mathbf{x}_i(t) - \mathbf{x}_j(t))$  describes the difference in the opinion of two agents at time  $t$ . The matrix  $\mathbf{D}_{ij}$  characterizes that different topics are not considered equally and even few of them are fully ignored. The fact that the eigenvalues of  $\mathbf{D}_{ij}$  are nonnegative characterizes that two agents are friends and they constructively consider the opinion of the other. The matrix  $\mathbf{U}_{ij}$  describes the fact that the difference between their opinions may not be perfectly conceived, and is polarized due to their communication abilities. In the light of this explanation, if the social interaction between  $i$  and  $j$  is perfect, then  $\mathbf{A}_{ij} = \mathbf{I}_d$ .

We have the following definitions:

**Definition 6.6 (Consensus)** *The  $n$ -agent system is said to achieve a consensus if and only if  $\mathbf{x}_i = \mathbf{x}_j$ , for all  $v_i, v_j \in \mathcal{V}$ ,  $v_i \neq v_j$ .*

Define  $\mathcal{R} \triangleq \mathcal{R}(\mathbf{1}_n \otimes \mathbf{I}_d)$  as the consensus space. A consensus of the  $n$ -agent system is globally/locally asymptotically achieved if and only if  $\mathbf{x}(t)$  globally/locally asymptotically approaches  $\mathcal{R}$ . Although consensus is important objective, in some applications, the agents' states are desired to converge to some different values. Under the consensus protocol (6.3), clustering behaviors appear naturally. This phenomenon is due to the existence of some positive semidefinite edges in the graph. A partition of  $\mathcal{V}(G)$  is given by  $\mathcal{C}_1, \dots, \mathcal{C}_l$ , ( $1 \leq l \leq n$ ) satisfying two properties: (i)  $\mathcal{C}_i \cap \mathcal{C}_j = \emptyset$ , for  $i \neq j$ , and (ii)  $\bigcup_{k=1}^l \mathcal{C}_k = \mathcal{V}(G)$ . This leads to the following definition.

**Definition 6.7 (Cluster Consensus)** *The  $n$ -agent system is said to achieve a clustered consensus if there exists a partition  $\mathcal{C}_1, \dots, \mathcal{C}_l$ , such that all agents belonging to the same partition achieve consensus, while for any two agents  $i$  and  $j$  belonging to two different partitions,  $\mathbf{x}_i \neq \mathbf{x}_j$ . Each  $\mathcal{C}_i$ ,  $i = 1, \dots, l$ , is referred to as a cluster.*

## 6.2 Algebraic condition for reaching a consensus

This section aims to find an algebraic condition of the matrix-weighted Laplacian for reaching consensus. We firstly state several properties of the matrix-weighted Laplacian and the dynamical system (6.4).

**Lemma 6.8** *The matrix-weighted Laplacian  $\mathbf{L}$  is symmetric, positive semidefinite, and  $\mathcal{N}(\mathbf{L}) = \text{span}\{\mathbf{1}_n \otimes \mathbf{I}_d, \{\mathbf{v} = [\mathbf{v}_1^\top, \dots, \mathbf{v}_n^\top]^\top \in \mathbb{R}^{dn} | (\mathbf{v}_j - \mathbf{v}_i) \in \mathcal{N}(\mathbf{A}_{ij}), \forall (v_i, v_j) \in \mathcal{E}\}\}$ .*

*Proof:* The symmetric property of  $\mathbf{L}$  follows immediately from its definition. From (6.2), we can write

$$\mathbf{L} = \bar{\mathbf{H}}^\top \text{blkdiag}(\mathbf{A}_k) \bar{\mathbf{H}} = \bar{\mathbf{H}}^\top \text{blkdiag}(\mathbf{A}_k^{1/2}) \text{blkdiag}(\mathbf{A}_k^{1/2}) \bar{\mathbf{H}} = \mathbf{M}^\top \mathbf{M}, \quad (6.5)$$

where  $\mathbf{M} = \text{blkdiag}(\mathbf{A}_k^{1/2}) \bar{\mathbf{H}}$ . Equation (6.5) shows that  $\mathbf{L}$  is positive semidefinite. Moreover, we have  $\mathcal{N}(\mathbf{L}) = \mathcal{N}(\mathbf{M}^\top \mathbf{M}) = \mathcal{N}(\mathbf{M})$ . As a result,  $\mathcal{N}(\mathbf{L}) = \mathcal{N}(\mathbf{M}) \supseteq \mathcal{N}(\bar{\mathbf{H}}) = \mathcal{R}$ . Consider  $\mathbf{v} = [\mathbf{v}_1^\top, \dots, \mathbf{v}_n^\top]^\top \notin \mathcal{R}$  such that  $\mathbf{L}\mathbf{v} = \mathbf{0}$ . It follows  $\mathbf{v}^\top \mathbf{L}\mathbf{v} = 0$ . Thus, from Corollary 6.5, one has

$$\sum_{(v_i, v_j) \in \mathcal{E}} (\mathbf{v}_i - \mathbf{v}_j)^\top \mathbf{A}_{ij} (\mathbf{v}_i - \mathbf{v}_j) = 0. \quad (6.6)$$

Since  $\mathbf{A}_{ij}$  is symmetric and positive semidefinite, (6.6) implies that  $(\mathbf{v}_i - \mathbf{v}_j) \in \mathcal{N}(\mathbf{A}_{ij})$ , for all  $(v_i, v_j) \in \mathcal{E}$ . This concludes the proof. ■

**Remark 6.9** *Based on Lemma 6.8, it follows that  $\dim(\mathcal{N}(\mathbf{L})) \geq \dim(\mathcal{R})$ . Thus, the matrix weighted Laplacian  $\mathbf{L}$  has at least  $d$  zero eigenvalues. Let  $\{\lambda_i\}_{i=1,\dots,dn}$  be the eigenspectra of  $\mathbf{L}$ ; then we have*

$$0 = \lambda_1 = \dots = \lambda_d \leq \lambda_{d+1} \leq \dots \leq \lambda_{dn}.$$

**Lemma 6.10** *Under the consensus protocol (6.3), the average  $\bar{\mathbf{x}} = \frac{1}{n} \sum_{i=1}^n \mathbf{x}_i$  is invariant.*

*Proof:* The average state can be written as  $\bar{\mathbf{x}} = \frac{1}{n}(\mathbf{1}_n^\top \otimes \mathbf{I}_d)\mathbf{x}$ . Taking the derivative of  $\bar{\mathbf{x}}$  along the trajectory of (6.4) yields

$$\dot{\bar{\mathbf{x}}} = \frac{1}{n}(\mathbf{1}_n^\top \otimes \mathbf{I}_d)\dot{\mathbf{x}} = -\frac{1}{n}(\mathbf{1}_n^\top \otimes \mathbf{I}_d)\mathbf{L}\mathbf{x}. \quad (6.7)$$

Since  $\mathbf{L}$  is symmetric, if  $\mathbf{v} \in \mathcal{N}(\mathbf{L})$ , then  $\mathbf{v}^\top$  belongs to the right nullspace of  $\mathbf{L}$ . As a result,  $(\mathbf{1}_n^\top \otimes \mathbf{I}_d)\mathbf{L} = \mathbf{0}$  and it follows  $\dot{\bar{\mathbf{x}}} = \mathbf{0}$ , i.e. the system's average is invariant. ■

The following theorem characterizes the dynamical behavior of the consensus protocol (6.4).

**Theorem 6.11 (Stability)** *Assume that  $G$  is positive semi-connected. Then any trajectory of (6.4) asymptotically approaches the invariant set  $\mathcal{N}(\mathbf{L})$ .*

*Proof:* Consider the potential function  $V = \frac{1}{2}\|\mathbf{x}\|^2$ , which is positive definite, radially unbounded, and continuously differentiable. The derivative of  $V$  along the trajectory of (6.4) is given by  $\dot{V} = -\mathbf{x}^\top \mathbf{L}\mathbf{x} = -\sum_{(i,j) \in \mathcal{E}} (\mathbf{x}_i - \mathbf{x}_j)^\top \mathbf{A}_{ij}(\mathbf{x}_i - \mathbf{x}_j) \leq 0$ . It follows that  $\|\mathbf{x}\| \leq \|\mathbf{x}(0)\|$ , or i.e.,  $\mathbf{x}(t)$  is bounded. Further,  $\dot{V}$  is negative semidefinite and  $\dot{V} = 0$  if and only if  $\mathbf{x} \in \mathcal{N}(\mathbf{L})$ . Based on LaSalle's invariance principle, any trajectory of (6.4) asymptotically approaches the invariant set  $\mathcal{N}(\mathbf{L})$  as described in Lemma 6.8. ■

**Lemma 6.12** *If  $\mathcal{N}(\mathbf{L}) = \mathcal{R}$ , the system (6.4) has a unique equilibrium point  $\mathbf{x}^* = \mathbf{1}_n \otimes \bar{\mathbf{x}}$ .*

*Proof:* The fact that  $\mathbf{1}_n \otimes \bar{\mathbf{x}}$  is the unique equilibrium of (6.4) if  $\mathcal{N}(\mathbf{L}) = \mathcal{R}$  will be proved by contradiction. Let  $\{\mathbf{e}_i\}_{i=1,\dots,d}$  be a basis of  $\mathbb{R}^d$ , where  $\mathbf{e}_i = [0, \dots, 1, \dots, 0]^\top$  is a vector with all zero entries except for an 1 on the  $i$ th row. Suppose that there exists  $\mathbf{x}' \in \mathcal{R}$  such that  $\mathbf{x}' \neq \mathbf{x}^*$ . Since  $\mathbf{x}' \in \mathcal{R}$ , one writes

$$\mathbf{x}' = \sum_{i=1}^d \bar{x}'_i (\mathbf{1}_n \otimes \mathbf{e}_i) = \mathbf{1}_n \otimes \bar{\mathbf{x}}' = (\mathbf{1}_n \otimes \mathbf{I}_d)\bar{\mathbf{x}}',$$

where  $\bar{\mathbf{x}}' = [\bar{x}_1', \dots, \bar{x}_d']^\top$ . It follows from Lemma 6.10 that

$$\bar{\mathbf{x}} = \frac{1}{n}(\mathbf{1}_n^\top \otimes \mathbf{I}_d)\mathbf{x}' = \frac{1}{n}(\mathbf{1}_n^\top \otimes \mathbf{I}_d)(\mathbf{1}_n \otimes \mathbf{I}_d)\bar{\mathbf{x}}' = \frac{1}{n}(\mathbf{1}_n^\top \mathbf{1}_n \otimes \mathbf{I}_d)\bar{\mathbf{x}}' = \frac{1}{n}(n \otimes \mathbf{I}_d)\bar{\mathbf{x}}' = \bar{\mathbf{x}}'.$$

Thus,  $\mathbf{x}' = \mathbf{1}_n \otimes \bar{\mathbf{x}} = \mathbf{x}^*$ , which is a contradiction. This contradiction implies that  $\mathbf{x}^* = \mathbf{1}_n \otimes \bar{\mathbf{x}}$  is the unique equilibrium of (6.4).  $\blacksquare$

The following theorem gives a necessary and sufficient condition for (6.4) to globally achieve an average consensus.

**Theorem 6.13 (Average Consensus)** *The system (6.4) globally exponentially converges to the system's average  $\mathbf{x}^* = \mathbf{1}_n \otimes \bar{\mathbf{x}}$  if and only if  $\mathcal{N}(\mathbf{L}) = \mathcal{R}$ .*

*Proof:* (Necessity). This part will be proved by contradiction. Assume that (6.4) globally asymptotically converges to  $\mathbf{x}^* = \mathbf{1}_n \otimes \bar{\mathbf{x}}$  but  $\mathcal{N}(\mathbf{L}) \neq \mathcal{R}$ . From Lemma 6.8, there exists  $\mathbf{x}' \in \mathbb{R}^{dn}$  such that  $\mathbf{L}\mathbf{x}' = \mathbf{0}$  and  $\mathbf{x}' \notin \mathcal{R}$ . Thus,  $\mathbf{x} = \mathbf{x}'$  is also an equilibrium point of (6.4), and any trajectory with  $\mathbf{x}(0) = \mathbf{x}'$  stays at  $\mathbf{x}'$  for all  $t \geq 0$ . Thus,  $\mathbf{x}^*$  is not globally asymptotically stable, which contradicts the assumption.

(Sufficiency). Suppose that  $\mathcal{N}(\mathbf{L}) = \mathcal{R}$ . Following the proof of Theorem 6.11, any trajectory of (6.4) converges to  $\mathcal{N}(\mathbf{L}) = \mathcal{R}$ . It follows from Lemma 6.12 that  $\mathbf{x}^* = \mathbf{1}_n \otimes \bar{\mathbf{x}} \in \mathcal{N}(\mathbf{L})$  is the unique equilibrium point of (6.4).

Consider the potential function  $V = \frac{1}{2}\boldsymbol{\delta}^\top \boldsymbol{\delta}$ , where  $\boldsymbol{\delta} = \mathbf{x} - \mathbf{1}_n \otimes \bar{\mathbf{x}}$  is the disagreement vector. Then,  $V$  is positive definite, radially unbounded, and continuously differentiable. The derivative of  $V$  along the trajectory of (6.4) is

$$\dot{V} = \boldsymbol{\delta}^\top \dot{\boldsymbol{\delta}} = -\boldsymbol{\delta}^\top \mathbf{L}\mathbf{x} = -\boldsymbol{\delta}^\top \mathbf{L}\boldsymbol{\delta} \leq 0, \quad (6.8)$$

where in the third equality, one has used the fact that  $\mathbf{L}\boldsymbol{\delta} = \mathbf{L}\mathbf{x} - \mathbf{L}(\mathbf{1}_n \otimes \bar{\mathbf{x}}) = \mathbf{L}\mathbf{x} - \mathbf{L}(\mathbf{1}_n \otimes \mathbf{I}_d)\bar{\mathbf{x}} = \mathbf{L}\mathbf{x}$ . Moreover,  $\boldsymbol{\delta} \perp \mathcal{R}$  since  $(\mathbf{1}_n \otimes \mathbf{I}_d)^\top \boldsymbol{\delta} = (\mathbf{1}_n \otimes \mathbf{I}_d)^\top \mathbf{x} - (\mathbf{1}_n^\top \mathbf{1}_n \otimes \mathbf{I}_d)\bar{\mathbf{x}} = n\bar{\mathbf{x}} - n\bar{\mathbf{x}} = \mathbf{0}$ . Therefore,

we can write

$$\dot{V} = -\boldsymbol{\delta}^T \mathbf{L} \boldsymbol{\delta} \leq -\lambda_{d+1}(\mathbf{L}) \boldsymbol{\delta}^T \boldsymbol{\delta} \leq -\alpha V \leq 0, \quad (6.9)$$

where  $\alpha = 2\lambda_{d+1}(\mathbf{L}) > 0$ . Further,  $\dot{V} = 0$  if and only if  $\boldsymbol{\delta} = \mathbf{0}$ , or  $\mathbf{x} = \mathbf{x}^* = \mathbf{1}_n \otimes \bar{\mathbf{x}}$ . Therefore, the equilibrium  $\mathbf{x}^*$  is globally exponentially stable, i.e. (6.4) globally exponentially achieves an average consensus. ■

**Remark 6.14** Equation (6.9) shows that  $\lambda_{d+1}$ , the smallest positive eigenvalue of  $\mathbf{L}$ , determines the convergence rate of the matrix-weighted consensus protocol (6.4). Thus,  $\lambda_{d+1}$  is a performance index of the network, and this index is analogous to the algebraic connectivity of  $G$  in the usual consensus algorithm [90, 91].

In the usual consensus algorithm, the average consensus is asymptotically achieved if and only if the graph is connected and the weights are positive scalars [90, 108]. Thus, it is expected that (6.4) reaches an average consensus when all matrix weights are positive definite.

**Corollary 6.15** Under the consensus protocol (6.3), if  $A_{ij} > 0$  for all  $(v_i, v_j) \in \mathcal{E}$ , all agents globally exponentially achieve a consensus.

*Proof:* Since  $\mathbf{A}_k$ ,  $k = 1, \dots, m$ , are positive definite from the assumption, it follows that  $\mathcal{N}(\mathbf{L}) = \mathcal{N}(\mathbf{M}) = \mathcal{N}(\text{blkdiag}(\mathbf{A}_k^{1/2}) \bar{\mathbf{H}}) = \mathcal{N}(\bar{\mathbf{H}}) = \mathcal{R}$ . Thus, it follows from Theorem 6.13 that (6.4) globally exponentially achieves a consensus. ■

### 6.3 Algebraic graph theory of consensus and clustered consensus

In the previous section, Theorem 6.13 provides an algebraic condition for reaching a consensus. However, that condition requires finding the nullspace of  $\mathbf{L}$ . Corollary 6.15 gives a sufficient condition for achieving consensus. The condition is quite clear and straightforward. However, since the

condition is only sufficient, it might be conservative. In this section, we aim to find some conditions for consensus and clustered consensus related with the matrix-weighted graph  $G$ .

**Lemma 6.16** *If there exists a positive spanning tree in  $G$ , then an average consensus is globally exponentially achieved.*

*Proof:* Suppose  $G$  has a spanning tree  $\mathcal{T}$  having all edges with positive definite matrix weights. One can label the edges of  $G$  such that the  $n - 1$  edges in  $\mathcal{T}$  are  $e_1, e_2, \dots, e_{n-1}$  and the remaining  $m - n + 1$  edges in  $\mathcal{E}$  are  $e_n, e_{n+1}, \dots, e_m$ . The incidence matrix corresponding to this labeling can be written as

$$\mathbf{H} = \begin{bmatrix} \mathbf{H}_{\mathcal{E}(\mathcal{T})} \\ \mathbf{H}_{\mathcal{E} \setminus \mathcal{E}(\mathcal{T})} \end{bmatrix},$$

where  $\mathbf{H}_{\mathcal{E}(\mathcal{T})} \in \mathbb{R}^{(n-1) \times n}$  represents  $n - 1$  edges of  $\mathcal{T}$  and  $\mathbf{H}_{\mathcal{E} \setminus \mathcal{E}(\mathcal{T})} \in \mathbb{R}^{(m-n+1) \times n}$  represents the remaining edges in the graph. Note that the rows of  $\mathbf{H}_{\mathcal{E} \setminus \mathcal{E}(\mathcal{T})}$  are linearly dependent on the rows of  $\mathbf{H}_{\mathcal{E}(\mathcal{T})}$  [149]. Specifically, there exists a matrix  $\mathbf{T} \in \mathbb{R}^{(m-n+1) \times m}$  such that:

$$\mathbf{T}\mathbf{H}_{\mathcal{E}(\mathcal{T})} = \mathbf{H}_{\mathcal{E} \setminus \mathcal{E}(\mathcal{T})},$$

where  $\mathbf{T} = \mathbf{H}_{\mathcal{E} \setminus \mathcal{E}(\mathcal{T})}\mathbf{H}_{\mathcal{E}(\mathcal{T})}^\top(\mathbf{H}_{\mathcal{E}(\mathcal{T})}\mathbf{H}_{\mathcal{E}(\mathcal{T})}^\top)^{-1}$ . Thus, the incidence matrix can be expressed as

$$\mathbf{H} = \begin{bmatrix} \mathbf{H}_{\mathcal{E}(\mathcal{T})} \\ \mathbf{T}\mathbf{H}_{\mathcal{E}(\mathcal{T})} \end{bmatrix} = \begin{bmatrix} \mathbf{I}_{n-1} \\ \mathbf{T} \end{bmatrix} \mathbf{H}_{\mathcal{E}(\mathcal{T})}, \quad (6.10)$$

Any equilibrium point of (6.4) must satisfy

$$\dot{\mathbf{x}} = -\bar{\mathbf{H}}^\top \text{blkdiag}(\mathbf{A}_k) \bar{\mathbf{H}} \mathbf{x} = \mathbf{0}. \quad (6.11)$$

It follows that  $\mathbf{x}^\top \bar{\mathbf{H}}^\top \text{blkdiag}(\mathbf{A}_k) \bar{\mathbf{H}} \mathbf{x} = 0$ , or  $\|\text{blkdiag}(\mathbf{A}_k^{1/2}) \bar{\mathbf{H}} \mathbf{x}\|^2 = \|\mathbf{M}\mathbf{x}\|^2 = 0$ . Denoting  $\bar{\mathbf{T}} = \mathbf{T} \otimes \mathbf{I}_d$ , this equation is equivalent to

$$\mathbf{M}\mathbf{x} = \begin{bmatrix} \text{blkdiag}(\mathbf{A}_k^{1/2})_{k=1}^{n-1} \bar{\mathbf{H}}_{\mathcal{E}(\mathcal{T})} \mathbf{x} \\ \text{blkdiag}(\mathbf{A}_k^{1/2})_{k=n}^m \bar{\mathbf{T}} \bar{\mathbf{H}}_{\mathcal{E}(\mathcal{T})} \mathbf{x} \end{bmatrix} = \mathbf{0}. \quad (6.12)$$

Observe that  $\text{blkdiag}(\mathbf{A}_k^{1/2})\bar{\mathbf{H}}_{\mathcal{E}(\mathcal{T})}\mathbf{x} = \mathbf{0}$  is equivalent to  $\bar{\mathbf{H}}_{\mathcal{E}(\mathcal{T})}\mathbf{x} = \mathbf{0}$  since  $\mathbf{A}_k$ ,  $k = 1, \dots, n - 1$ , are positive definite (the corresponding edges are in the positive spanning tree). Further, since  $\mathbf{H}_{\mathcal{E}(\mathcal{T})}$  is the incidence matrix corresponding to a tree, we have  $\mathcal{N}(\mathbf{H}_{\mathcal{E}(\mathcal{T})}) = \mathcal{R}(\mathbf{1}_n)$ , which means  $\mathcal{N}(\bar{\mathbf{H}}_{\mathcal{E}(\mathcal{T})}) = \mathcal{R}(\mathbf{1}_n \otimes \mathbf{I}_d) = \mathcal{R}$ . It follows from Lemma 6.12 that the equilibrium is unique and is  $\mathbf{x}^* = \mathbf{1}_n \otimes \bar{\mathbf{x}}$ . Also, it is easy to check that  $\text{blkdiag}(\mathbf{A}_k^{1/2})_{k=n}^m \bar{\mathbf{T}} \bar{\mathbf{H}}_{\mathcal{E}(\mathcal{T})}\mathbf{x}^* = \mathbf{0}$ .

Finally, the stability of  $\mathbf{x} = \mathbf{x}^*$  follows from Theorem 6.13.  $\blacksquare$

**Lemma 6.17** *Suppose there exists a positive tree  $\mathcal{T} \subset G$  of  $l$  vertices. Under the consensus protocol 6.3,  $\mathbf{x}_i(t) \rightarrow \mathbf{x}_j(t)$ ,  $\forall i, j \in \mathcal{T}$ , as  $t \rightarrow \infty$ .*

*Proof:* Let the state vector be indexed as  $\mathbf{x} = [\mathbf{x}_{\mathcal{T}}^\top, \mathbf{x}_{\mathcal{V} \setminus \mathcal{V}(\mathcal{T})}^\top]^\top$ . The incidence matrix is written in the following form

$$\begin{array}{ccc} & \mathcal{V}(\mathcal{T}) & \mathcal{V} \setminus \mathcal{V}(\mathcal{T}) \\ \mathcal{E}(\mathcal{T}) & \left[ \begin{array}{cc} \mathbf{H}_1 & \mathbf{0} \\ \mathbf{H}_2 & \mathbf{0} \\ \mathbf{H}_3 & \mathbf{H}_4 \end{array} \right] & = \mathbf{H}, \\ \mathcal{E}(\mathcal{V}(\mathcal{T})) \setminus \mathcal{E}(\mathcal{T}) & & \end{array}$$

where  $[\mathbf{H}_1 \quad \mathbf{0}] \in \mathbb{R}^{(l-1) \times n}$  associates with the  $l$  edges belonging to the tree  $\mathcal{T}$ ,  $[\mathbf{H}_2 \quad \mathbf{0}]$  associates with the  $r - l + 1$  edges between vertices in  $\mathcal{V}(\mathcal{T})$  which do not belong to the tree, and  $[\mathbf{H}_3 \quad \mathbf{H}_4]$  associates with the remaining edges in  $\mathcal{E}$ . Similarly to the proof of Lemma 6.16,  $\mathbf{H}_2$  is linearly dependent on  $\mathbf{H}_1$  and this dependency is characterized by  $\mathbf{H}_2 = \mathbf{T}\mathbf{H}_1$ . Therefore, the equilibrium set of (6.4) must satisfy

$$\mathbf{M}\mathbf{x} = \left[ \begin{array}{c} \text{blkdiag}(\mathbf{A}_k^{1/2})_{k=1}^{l-1} \bar{\mathbf{H}}_1 \mathbf{x}_{\mathcal{T}} \\ \text{blkdiag}(\mathbf{A}_k^{1/2})_{k=l}^r \bar{\mathbf{T}} \bar{\mathbf{H}}_1 \mathbf{x}_{\mathcal{T}} \\ \text{blkdiag}(\mathbf{A}_k^{1/2})_{k=r+1}^m (\bar{\mathbf{H}}_3 \mathbf{x}_{\mathcal{T}} + \bar{\mathbf{H}}_4 \mathbf{x}_{\mathcal{V} \setminus \mathcal{V}(\mathcal{T})}) \end{array} \right] = \mathbf{0}. \quad (6.13)$$

Since  $\mathcal{T}$  is a positive tree,  $\text{blkdiag}(\mathbf{A}_k^{1/2})_{k=1}^{l-1}$  is positive definite. It follows  $\bar{\mathbf{H}}_1 \mathbf{x}_{\mathcal{T}} = \mathbf{0}$ . Further, since  $\mathbf{H}_1$  is the incidence matrix associated with a tree,  $\mathcal{N}(\bar{\mathbf{H}}_1) = \{\mathbf{1}_l \otimes \mathbf{I}_d\}$ . Hence, any equilibrium  $\mathbf{x}^*$  of (6.4) must have  $\mathbf{x}_{\mathcal{T}}^* \in \mathcal{N}(\bar{\mathbf{H}}_1)$ , i.e., all equilibrium states of  $l$  agents belonging to the positive tree  $\mathcal{T}$  are the same. Based on Theorem 6.11, the agents in  $\mathcal{T}$  asymptotically reach a consensus. ■

The following result provides a condition to determine whether or not two vertices belong to a same cluster.

**Theorem 6.18** *Given a positive tree  $\mathcal{T}$ , let the cluster  $\mathcal{C}(\mathcal{T})$  generated from  $\mathcal{T}$  be containing:*

- i. *all vertices in  $\mathcal{T}$ ,*
- ii. *any vertex  $v_i \notin \mathcal{T}$ , which defines the set*

$$\mathcal{S}_i = \{\mathcal{P}_k = \{v_1^k \dots v_{|\mathcal{P}_k|}^k\} | v_1^k = v_i, v_{|\mathcal{P}_k|}^k \in \mathcal{T}, \text{ and } \forall j = 1, \dots, |\mathcal{P}_k| - 1, v_j^k \notin \mathcal{T}\},$$

*satisfying the following conditions:*

- a. *for each path  $\mathcal{P}_k$ , denoting  $\mathcal{N}(\mathcal{P}_k) = \bigcup_{j=1}^{|\mathcal{P}_k|-1} \mathcal{N}(\mathbf{A}_{v_j^k v_{j+1}^k})$ , it holds*

$$\dim\left(\bigcap_{k=1}^{|\mathcal{S}_i|} \mathcal{N}(\mathcal{P}_k)\right) = 0 \quad (6.14)$$

- b. *each path  $\mathcal{P}_k \in \mathcal{S}_i$  has no loop, i.e.  $v_l \neq v_m, \forall v_l, v_m \in \mathcal{P}_k$*

*Then, under the consensus protocol (6.3), all agents in the cluster  $\mathcal{C}(\mathcal{T})$  have the same equilibrium state. Furthermore, in algorithmic perspective, the set  $\mathcal{S}_i$  is finite.*

*Proof:* First, all vertices in  $\mathcal{T}$  converge to a same value due to Lemma 6.17. Denote that the common value by  $\mathbf{x}_{\mathcal{T}}^*$ .

Next, consider a vertex  $v_i \notin \mathcal{T}$  satisfying the condition (ii). Now, we consider the condition (ii.a).

Let  $\mathbf{x}_i^*$  be the equilibrium state of agent  $i$ . Then, from the definition of  $\mathcal{N}(\mathcal{P}_k)$ , we can write

$$\mathbf{x}_i^* - \mathbf{x}_{\mathcal{T}}^* \in \mathcal{N}(\mathcal{P}_k), \forall \mathcal{P}_k \in \mathcal{S}_i. \quad (6.15)$$

It follows from (6.14) that the only solution for  $|\mathcal{S}_i|$  equations (6.15) is  $\mathbf{x}_i^* - \mathbf{x}_{\mathcal{T}}^* = \mathbf{0}$ , or  $\mathbf{x}_i^* = \mathbf{x}_{\mathcal{T}}^*$ .

Thus, the cluster  $\mathcal{C}(\mathcal{T})$  reaches a consensus. But, in the above condition (ii.a), there could be infinitely many paths from  $v_i$  to  $\mathcal{T}$  if there are loops. The condition (ii.b) ensures that the number of paths from  $v_i$  to  $\mathcal{T}$  is finite. To show this, suppose that  $\mathcal{P}_1$  and  $\mathcal{P}_2$  are two paths, and  $\mathcal{P}_2$  is obtained by adding loops to  $\mathcal{P}_1$ . Then,  $\mathcal{N}(\mathcal{P}_1) \subseteq \mathcal{N}(\mathcal{P}_2)$ . It follows  $\mathcal{N}(\mathcal{P}_1) \cap \mathcal{N}(\mathcal{P}_2) = \mathcal{N}(\mathcal{P}_1)$ ; thus it is not necessary to consider loops when checking the condition (6.14), which means that  $|\mathcal{S}_i|$  is finite.

Finally, consider a vertex  $i$  which does not satisfy both (i) and (ii). Let  $\mathcal{S}_i$  be the set of paths from  $v_i$  to  $\mathcal{T}$  with  $\dim(\bigcap_{k=1}^{|\mathcal{S}_i|} \mathcal{N}(\mathcal{P}_k)) \geq 1$ . Then clearly there exists a nontrivial solution, i.e.,  $\mathbf{x}_i^* - \mathbf{x}_{\mathcal{T}}^* \neq 0$ . ■

The following result follows immediately from Proposition 6.18.

**Corollary 6.19** *Consider a positive tree  $\mathcal{T}$  and a vertex  $v_i \notin \mathcal{T}$ . From  $v_i$  to  $v_j \in \mathcal{T}$ , if there exist at least two paths, which include positive semi-definite weighting matrices, such that Eq. (6.14) holds, then vertex  $v_i$  can be added into the cluster  $\mathcal{C}(\mathcal{T})$ .*

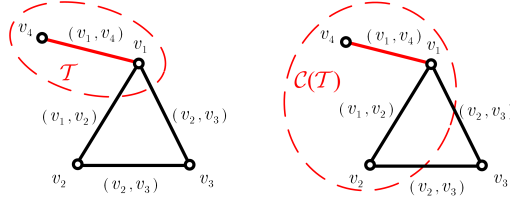


Figure 6.2. Illustration of the four-agent system in Example 6.1.

**Example 6.1** *To illustrate Proposition 6.18, consider a four-agent system in  $\mathbb{R}^3$  with the interaction graph as depicted in Figure 6.2. The matrix weights corresponding to the connections between the*

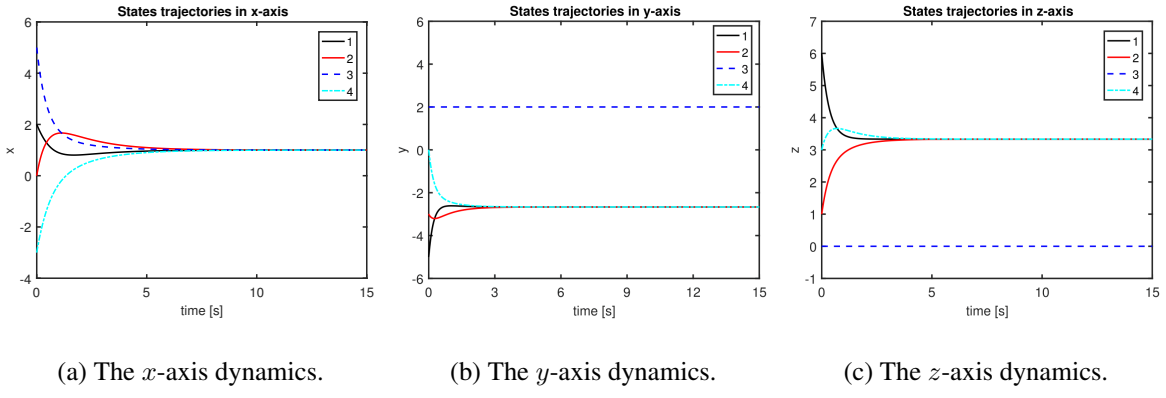


Figure 6.3. Example 1: The states' dynamics of four agents under the consensus protocol (6.3).

agents in the system are given by

$$\mathbf{A}_{12} = \begin{bmatrix} 0 & 0 & 0 \\ 0 & 1 & 0 \\ 0 & 0 & 1 \end{bmatrix}, \mathbf{A}_{13} = \begin{bmatrix} 1 & 0 & 0 \\ 0 & 0 & 0 \\ 0 & 0 & 0 \end{bmatrix}, \mathbf{A}_{23} = \begin{bmatrix} 1 & 0 & 0 \\ 0 & 0 & 0 \\ 0 & 0 & 1 \end{bmatrix} \text{ and } \mathbf{A}_{14} = \begin{bmatrix} 1 & 0 & 0 \\ 0 & 2 & 0 \\ 0 & 0 & 1 \end{bmatrix}.$$

It is easy to see that  $\mathbf{A}_{14}$  is positive definite while other matrix weights are positive semidefinite. As a result, there is a positive tree  $\mathcal{T}$  in the graph containing vertex  $v_1$  and vertex  $v_4$ . Moreover, we have  $\mathcal{N}(\mathbf{A}_{12}) = \text{span}\{[1, 0, 0]^T\}$ ,  $\mathcal{N}(\mathbf{A}_{13}) = \text{span}\{[0, 1, 0]^T, [0, 0, 1]^T\}$ , and  $\mathcal{N}(\mathbf{A}_{23}) = \text{span}\{[0, 1, 0]^T\}$ .

There are two paths (without loop) from vertex  $v_2$  to vertex  $v_1$  (also to the tree  $\mathcal{T}$ ):  $\mathcal{P}_1 = v_2v_1$ , and  $\mathcal{P}_2 = v_2v_3v_1$ . By definition, we have  $\mathcal{N}(\mathcal{P}_1) = \mathcal{N}(\mathbf{A}_{12}) = \text{span}\{[1, 0, 0]^T\}$ , and  $\mathcal{N}(\mathcal{P}_2) = \mathcal{N}(\mathbf{A}_{13}) \cup \mathcal{N}(\mathbf{A}_{23}) = \text{span}\{[0, 1, 0]^T, [0, 0, 1]^T\}$ . It follows  $\mathcal{N}(\mathcal{P}_1) \cap \mathcal{N}(\mathcal{P}_2) = \{\mathbf{0}\}$ , which further implies that agent 2 is in the same cluster  $\mathcal{C}(\mathcal{T})$  due to Theorem 6.18 (ii).

On the other hand, consider the vertex  $v_3$ . There are two paths from vertex 3 to the cluster  $\mathcal{C} = \{v_1, v_2, v_4\}$ :  $\mathcal{P}_3 = v_3v_1$  and  $\mathcal{P}_4 = v_3v_2$ . Since  $\mathcal{N}(\mathcal{P}_3) \cap \mathcal{N}(\mathcal{P}_4) = \mathcal{N}(\mathbf{A}_{23}) = \text{span}\{[0, 1, 0]^T\}$ , the vertex  $v_3$  does not belong to the cluster  $\mathcal{C}$ .

Trajectories of the states of three agents under consensus protocol (6.3) are depicted in Fig. 6.3.

Observe that  $x_1^* = x_2^* = x_4^* \neq x_3^*$ , as expected from the above discussion.

**Example 6.2** This example shows a counter-intuitive scenario that may happen under the matrix-weighted consensus. Consider a five-agent system in  $\mathbb{R}^2$  whose information flow is given by the matrix-weighted graph  $G$  as depicted in Fig. 6.4. The matrix weights are chosen as follows:

$$\mathbf{A}_{12} = \mathbf{A}_{24} = \begin{bmatrix} 1 & 0 \\ 0 & 0 \end{bmatrix}, \mathbf{A}_{13} = \mathbf{A}_{34} = \mathbf{A}_{35} = \begin{bmatrix} 0 & 0 \\ 0 & 1 \end{bmatrix}, \text{ and } \mathbf{A}_{25} = \begin{bmatrix} 1 & -1 \\ -1 & 1 \end{bmatrix}.$$

Observe that these matrices are all positive semidefinite and thus there is no positive tree in  $G$ . Let us use Proposition 6.18 to predict the behavior of this system under the matrix-weighted consensus protocol (6.3). We may easily calculate  $\mathcal{N}(\mathbf{A}_{12}) = \mathcal{N}(\mathbf{A}_{24}) = \text{span}\{[1, 0]^\top\}$ ,  $\mathcal{N}(\mathbf{A}_{13}) = \mathcal{N}(\mathbf{A}_{34}) = \mathcal{N}(\mathbf{A}_{35}) = \text{span}\{[0, 1]^\top\}$ , and  $\mathcal{N}(\mathbf{A}_{25}) = \text{span}\{[1, 1]^\top\}$ . Observe that there are four paths from  $v_4$  to  $v_1$  as follows:

- $\mathcal{P}_1 = v_4v_2v_1: \mathcal{N}(\mathcal{P}_1) = \mathcal{N}(\mathbf{A}_{24}) \cup \mathcal{N}(\mathbf{A}_{12}) = \text{span}\{[1, 0]^\top\}$ .
- $\mathcal{P}_2 = v_4v_3v_1: \mathcal{N}(\mathcal{P}_2) = \mathcal{N}(\mathbf{A}_{34}) \cup \mathcal{N}(\mathbf{A}_{13}) = \text{span}\{[0, 1]^\top\}$ .
- $\mathcal{P}_3 = v_4v_2v_5v_3v_1: \mathcal{N}(\mathcal{P}_3) = \mathcal{N}(\mathbf{A}_{24}) \cup \mathcal{N}(\mathbf{A}_{25}) \cup \mathcal{N}(\mathbf{A}_{12}) \cup \mathcal{N}(\mathbf{A}_{35}) = \mathbb{R}^2$ .
- $\mathcal{P}_4 = v_4v_3v_5v_3v_1: \mathcal{N}(\mathcal{P}_4) = \mathcal{N}(\mathbf{A}_{34}) \cup \mathcal{N}(\mathbf{A}_{35}) \cup \mathcal{N}(\mathbf{A}_{25}) \cup \mathcal{N}(\mathbf{A}_{12}) = \mathbb{R}^2$ .

Then, we find that  $\cap_{k=1}^4 \mathcal{P}_k = \text{span}\{[1, 0]^\top\} \cap \text{span}\{[0, 1]^\top\} = \emptyset$ , or i.e.,  $\dim(\cap_{k=1}^4 \mathcal{P}_k) = 0$ . According to Proposition 6.18, it is interesting that  $v_1$  and  $v_4$  are at a same cluster, call  $\mathcal{C}_1$ . A similar check shows that  $v_5$  does not belong to this cluster. There are thus four clusters in the graph:  $\mathcal{C}_1 = \{v_1, v_4\}$ ,  $\mathcal{C}_2 = \{v_2\}$ ,  $\mathcal{C}_3 = \{v_3\}$ , and  $\mathcal{C}_4 = \{v_5\}$ . This example is counter intuitive in the sense that, although agents 2 and 3 are neighbors of agent 1, they do not consent with agent 1. On the other hand, agent 4 consents with agent 1 while they are not neighbor. The trajectories of these agents are depicted in Fig. 6.5.

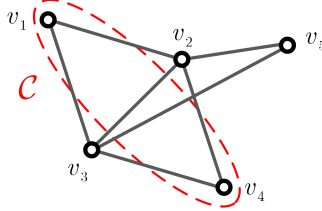


Figure 6.4. Illustration of the five-agent system in Example 6.2.

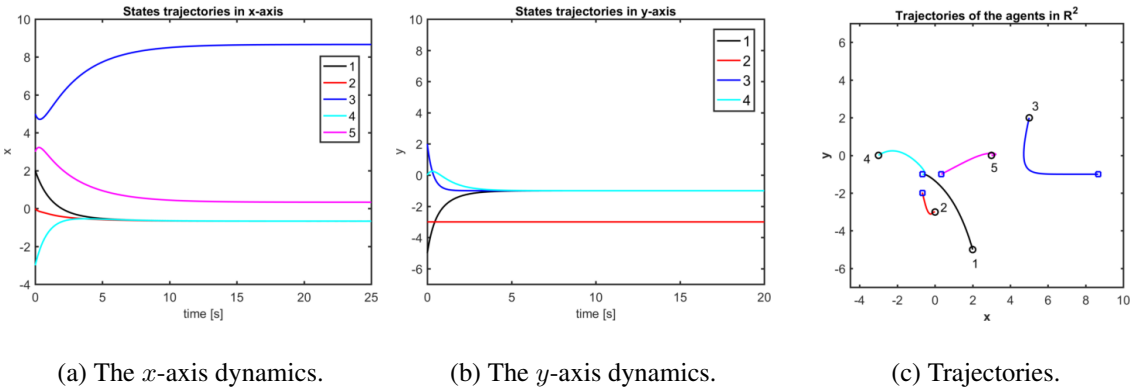


Figure 6.5. Example 2: The states' dynamics and trajectories of four agents under the consensus protocol (6.3).

Based on Theorem 6.18, one can further state the following corollaries.

**Corollary 6.20** Suppose a vertex  $v_i$  connects to a positive tree  $\mathcal{T} \subset G$  via the edge set  $\mathcal{S}_i = \{(v_i, v_j) | j \in \mathcal{N}_i, v_i \in \mathcal{V}(\mathcal{T})\}$ . If  $\sum_{(v_i, v_j) \in \mathcal{S}} \mathbf{A}_{ij}$  is positive definite, then under the consensus protocol (6.3), the equilibrium state of agent  $i$  is the same with the equilibrium state of all agents in  $\mathcal{T}$ .

*Proof:* From Lemma 6.17, we know that at equilibrium, all the states of all agents in the positive tree  $\mathcal{T}$  are the same. Let  $\mathbf{x}_{\mathcal{T}}^*$  denote this value. Also, let  $\mathbf{x}_i^*$  denote the equilibrium value of agent  $i$ . For each positive semidefinite edge  $(v_i, v_j) \in \mathcal{S}_i$  (see Fig. 6.6 for an illustration), from Lemma 6.8, we have

$$\mathbf{A}_{ij}(\mathbf{x}_i^* - \mathbf{x}_{\mathcal{T}}^*) = \mathbf{0}, \forall (v_i, v_j) \in \mathcal{S}_i.$$

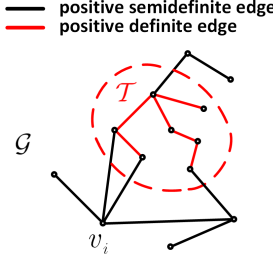


Figure 6.6. The vertex  $i$  connects to the positive tree  $\mathcal{T}$  through two semi-positive connections.

By adding the above equations, one can get

$$\left( \sum_{v_j \in \mathcal{S}_i} \mathbf{A}_{ij} \right) (\mathbf{x}_i^* - \mathbf{x}_{\mathcal{T}}^*) = \mathbf{0}. \quad (6.16)$$

Since  $\sum_{(v_i, v_j) \in \mathcal{S}_i} \mathbf{A}_{ij}$  is positive definite, i.e.  $\dim(\bigcap_{v_j \in \mathcal{S}_i} \mathcal{N}(\mathbf{A}_{ij})) = 0$ , equation (6.16) is satisfied if and only if  $\mathbf{x}_i^* = \mathbf{x}_{\mathcal{T}}^*$ .  $\blacksquare$

**Corollary 6.21** Suppose that there are two positive trees  $\mathcal{T}_1, \mathcal{T}_2$  in  $G$  which are connected via the edge set  $\mathcal{S} = \{(v_i, v_j) | v_i \in \mathcal{T}_1, v_j \in \mathcal{T}_2\}$ . If  $\sum_{(v_i, v_j) \in \mathcal{S}} \mathbf{A}_{ij}$  is positive definite, then under the consensus protocol (6.3), the equilibrium states of all agents in  $\mathcal{T}_1$  and  $\mathcal{T}_2$  are the same.

Figure 6.7 illustrates a scenario of Corollary 6.21. Two positive trees  $\mathcal{T}_1$  and  $\mathcal{T}_2$  are connected through three semi-positive connections. If the summation of three matrices associated with these connections is positive definite, the equilibrium states of agents in both trees are the same.

**Lemma 6.22 (Partitioning a graph into positive trees)** Given a graph  $G$ , consider a set of positive trees  $\{\mathcal{T}_1, \dots, \mathcal{T}_p\}$  ( $1 \leq p \leq n$ ), where

$$(i) \quad \mathcal{V}(\mathcal{T}_m) \cap \mathcal{V}(\mathcal{T}_l) = \emptyset, \quad \bigcup_{m=1}^p \mathcal{V}(\mathcal{T}_m) = \mathcal{V}(G),$$

(ii) For each  $\mathcal{T}_k$  ( $1 \leq k \leq p$ ),  $v_i, v_j \in \mathcal{V}(\mathcal{T}_k)$  if and only if there exists a positive path from  $v_i$  to  $v_j$ .

Then, the partition of  $G$  defined by  $\{\mathcal{V}(\mathcal{T}_1), \dots, \mathcal{V}(\mathcal{T}_p)\}$  is unique.

*Proof:* The following process gives a constructive way to find the partition:

At the first step, select a vertex  $v_1$ . The tree  $\mathcal{T}_1$  contains vertex  $v_1$  and all vertices that have a positive path to  $v_1$  is unique. Then, cross out all vertices in  $\mathcal{T}_1$ . The remaining vertices in  $\mathcal{V}(G) \setminus \mathcal{V}(\mathcal{T}_1)$  do not have a positive path to any vertices in  $\mathcal{V}(\mathcal{T}_1)$ . Note  $\mathcal{T}_1$  contains at least one vertex ( $v_1$ ). Thus,  $|\mathcal{V}(G) \setminus \mathcal{V}(\mathcal{T}_1)| < |\mathcal{V}(G)|$ .

Next, we choose the vertex in  $\mathcal{V}(G) \setminus \mathcal{V}(\mathcal{T}_1)$  with the smallest indexing. Similar to the first step, we find the positive tree  $\mathcal{T}_2$  associated with this vertex, and then cross out all vertices in  $\mathcal{T}_2$  from the current vertex set. The remaining vertices are  $\mathcal{V}(G) \setminus (\mathcal{V}(\mathcal{T}_1) \cup \mathcal{V}(\mathcal{T}_2))$ , which has less vertices than  $\mathcal{V}(G) \setminus \mathcal{V}(\mathcal{T}_1)$ .

We continue these processes, until there is no leftover vertex after crossing out all vertices from the last positive tree, say  $\mathcal{T}_p$ . At this point, we obtain a set of positive trees  $\{\mathcal{T}_1, \dots, \mathcal{T}_p\}$  ( $1 \leq p \leq n$ ). Obviously, this set satisfies both conditions (i) and (ii).

Because in each step, the vertex and the corresponding positive tree are unique, the partition  $\{\mathcal{V}(\mathcal{T}_1), \dots, \mathcal{V}(\mathcal{T}_p)\}$  is unique. ■

Let  $\mathcal{C}(\mathcal{T}_m)$  be the cluster generated from the positive tree  $\mathcal{T}_m$ . If there exists a vertex  $v_i \in \mathcal{C}(\mathcal{T}_m)$  satisfying the condition (ii) in Proposition 6.18 with a cluster  $\mathcal{C}(\mathcal{T}_l)$ , we can form a new cluster  $\mathcal{C}(\mathcal{T}_m) \cup \mathcal{C}(\mathcal{T}_l)$  by merging  $\mathcal{C}(\mathcal{T}_m)$  and  $\mathcal{C}(\mathcal{T}_l)$  together. By this way, we can extend the positive trees

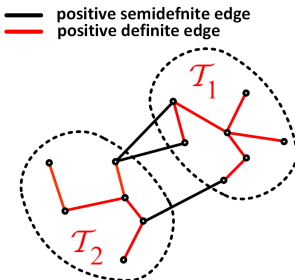


Figure 6.7. Two positive trees  $\mathcal{T}_1$  and  $\mathcal{T}_2$  are connected through three semi-positive connections.

in the graph. All vertices in the new cluster will reach a consensus under (6.3). To check whether two clusters  $\mathcal{C}(\mathcal{T}_m)$  and  $\mathcal{C}(\mathcal{T}_l)$  can be merged or not, it is sufficient to check condition (ii) in Proposition 6.18 for only one vertex  $v_i \in \mathcal{C}(\mathcal{T}_m)$  with regard to  $\mathcal{C}(\mathcal{T}_l)$ . This property comes from the fact that (6.14) is invariant for all vertices belonging to a same cluster.

Algorithm 1 proposes a solution for finding all clusters in the graph by iteratively checking condition (ii) in Proposition 6.18 and merging clusters together. The algorithm terminates after a finite number of steps and the output is a set of clusters  $\mathcal{C}_G = \{\mathcal{C}_1, \dots, \mathcal{C}_q\}$  ( $1 \leq q \leq p$ ) satisfying:

- $\mathcal{C}_m \cap \mathcal{C}_l = \emptyset$ ,  $\bigcup_{m=1}^q \mathcal{C}_m = \mathcal{V}(G)$ ,
- For  $1 \leq m \neq l \leq q$ ,  $\mathcal{C}_m$  and  $\mathcal{C}_l$  cannot be merged together, or i.e.  $\nexists v_i \in \mathcal{C}_m$  satisfying the condition (ii) in Proposition 6.18 with  $\mathcal{C}_l$ .

The main result of this section is stated in the following theorem.

**Theorem 6.23** *Under the consensus protocol (6.4), the average consensus is achieved if and only if  $G$  is spanned by a cluster.*

*Proof:* If  $G$  is spanned by a cluster, it follows from Proposition 6.18 that the equilibrium state of all agents in the graph are the same, i.e.,  $x^*$  is the unique equilibrium point of (6.4). Thus, the consensus is achieved globally exponentially based on Lemma 6.11. Meanwhile, if there is no cluster spanning  $G$ , it follows that the agents belonging to two different clusters of  $G$  may not agree. Thus, a consensus cannot be globally achieved. ■

**Remark 6.24** *Obviously, if the graph  $G$  has some disconnected components, under consensus protocol (6.3), the dynamics of each disconnected component do not influence the others. Suppose  $G$  is positive semiconnected and has  $p$  clusters after Algorithm 1 terminates. Define*

$$\mathcal{S}_{ij} \triangleq \{\mathcal{P}_k \mid \text{the starting (end) vertex of } \mathcal{P}_k \text{ is in } \mathcal{C}_i \text{ (resp., } \mathcal{C}_j)\},$$

the end states of each cluster satisfy:

$$\sum_{i=1}^q |C_i| \mathbf{x}_{\mathcal{C}_i}^* = n \bar{\mathbf{x}}, \quad (6.17)$$

$$\mathbf{x}_{\mathcal{C}_i}^* - \mathbf{x}_{\mathcal{C}_j}^* \in \bigcap_{k=1}^{|\mathcal{S}_{ij}|} \mathcal{N}(\mathcal{P}_k). \quad (6.18)$$

The solutions of equations (6.17)–(6.18) depend on matrix weights. Thus, we can design the matrix weights to obtain the desired number of clusters.

The following result follows from Theorems 6.13 and 6.23.

**Theorem 6.25** *Given a matrix-weighted graph  $G$ , there is a cluster spanning all vertices of  $G$  if and only if  $\mathcal{N}(\mathbf{L}) = \mathcal{R}$ .*

Before ending this section, we refer readers to Table 6.1, which gives a comparison between the usual consensus algorithm and the matrix-weighted consensus algorithm (6.3). Note that in Table 6.1, we find the computational cost as follow: Suppose an agent  $i$  has an average number of neighbor  $|\bar{\mathcal{N}}_i|$ . Each matrix multiplication  $\mathbf{A}_{ij} \mathbf{x}_i$  needs  $d^2$  multiplications and  $d(d-1)$  summations. Thus, in average, we need  $O(n \times d^2 \times |\bar{\mathcal{N}}_i|)$  calculations for each update.

## 6.4 Applications

### 6.4.1 Cluster consensus

This subsection presents an example of designing a clustered consensus network based on the matrix-weighted consensus algorithm. Consider a system of nine autonomous agents in the plane. We would like to gather the agents into three clusters and then rendezvous to the system's average. Assume that the agents can sense the relative position with regard to its neighbor and there is a common reference frame for all agents in the system. The state of each agent is represented by a

Table 6.1. Comparison between the scalar-weighted consensus and the matrix-weighted consensus.

Property	Scalar-weighted consensus	Matrix-weighted consensus
Information flow	Undirected connected scalar-weighted graph: $G = (\mathcal{V}, \mathcal{E}, \mathcal{A})$	Undirected semipositive connected matrix-weighted graph: $G = (\mathcal{V}, \mathcal{E}, \mathcal{A})$
Edge's weights	$a_{ij} > 0$ : $(v_i, v_j)$ exists. $a_{ij} = 0$ : $(v_i, v_j)$ does not exist.	$\mathbf{A}_{ij} > 0$ : $(v_i, v_j)$ is a positive definite edge. $\mathbf{A}_{ij} \geq 0$ : $(v_i, v_j)$ is a positive semidefinite edge. $\mathbf{A}_{ij} = 0$ : $(v_i, v_j)$ does not exist.
Graph Laplacian	$\mathbf{L} = \mathbf{H}^\top \text{diag}(a_k) \mathbf{H}$ $r(\mathbf{L}) \leq n - 1$	$\mathbf{L} = (\mathbf{H}^\top \otimes \mathbf{I}_d) \text{blkdiag}(\mathbf{A}_k)(\mathbf{H} \otimes \mathbf{I}_d)$ $r(\mathbf{L}) \leq d(n - 1)$
Consensus protocol	$\dot{x}_i = \sum_{v_j \in \mathcal{N}_i} (x_j - x_i)$ $\dot{\mathbf{x}} = -\mathbf{L}\mathbf{x}$	$\dot{\mathbf{x}}_i = \sum_{v_j \in \mathcal{N}_i} \mathbf{A}_{ij}(\mathbf{x}_j - \mathbf{x}_i)$ $\dot{\mathbf{x}} = -\mathbf{L}\mathbf{x}$
Consensus space	$\mathcal{R}(\mathbf{1}_n)$	$\mathcal{R}(\mathbf{1}_n \otimes \mathbf{I}_d)$
Conditions for reaching an average consensus	$\exists$ a tree spanning all vertices of $G$ . $\mathcal{N}(\mathbf{L}) = \mathcal{R}(\mathbf{1}_n)$ .	$\exists$ a cluster spanning all vertices in $G$ . $\mathcal{N}(\mathbf{L}) = \mathcal{R}(\mathbf{1}_n \otimes \mathbf{I}_d)$ .
Cluster consensus	Happens iff $G$ is not connected.	Happens iff $G$ is not connected or there does not exist a cluster spanning all vertices of $G$ .
Average computational cost	$O(n \times d \times  \bar{\mathcal{N}}_i )$	$O(n \times d^2 \times  \bar{\mathcal{N}}_i )$

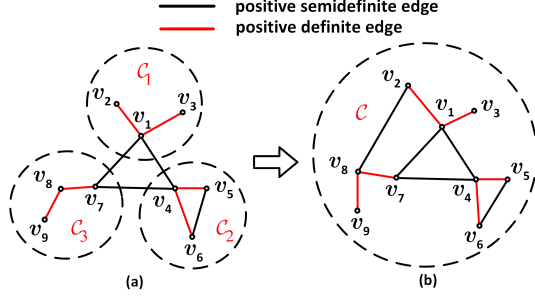


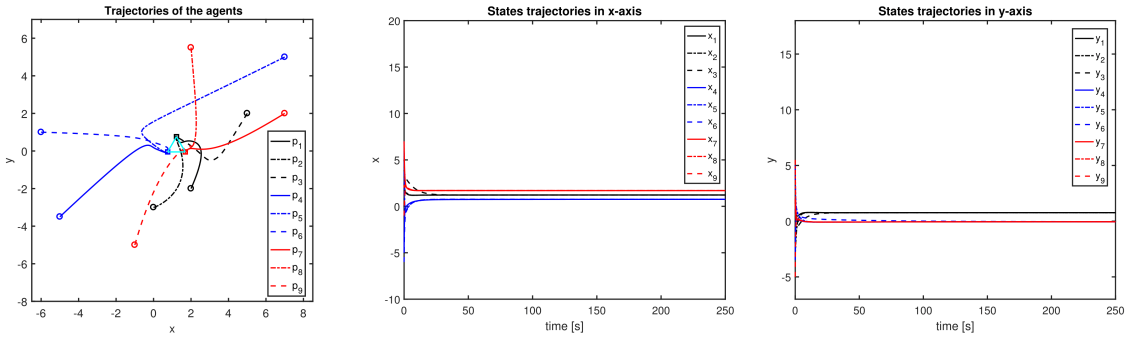
Figure 6.8. Two graphs used in simulations: graph (a) has three clusters, graph (b) has a spanning cluster.

vector  $\mathbf{p}_i = [x_i, y_i]^\top \in \mathbb{R}^2$ , and the consensus protocol is explicitly written as

$$\dot{\mathbf{p}}_i = \sum_{j \in \mathcal{N}_i} \mathbf{A}_{ij} (\mathbf{p}_j - \mathbf{p}_i), \quad \forall i = 1, \dots, 9.$$

In case 1, we want to gather the agents into three clusters. To this end, the matrix weights are chosen as follows:  $\mathbf{A}_{12} = \begin{bmatrix} 2 & 0 \\ 0 & 1 \end{bmatrix}$ ,  $\mathbf{A}_{13} = \begin{bmatrix} 2 & 3 \\ 3 & 5 \end{bmatrix}$ ,  $\mathbf{A}_{47} = \begin{bmatrix} 0 & 0 \\ 0 & 1 \end{bmatrix}$ ,  $\mathbf{A}_{14} = \begin{bmatrix} 0.75 & -0.433 \\ -0.433 & 0.25 \end{bmatrix}$ ,  $\mathbf{A}_{17} = \begin{bmatrix} 0.75 & 0.433 \\ 0.433 & 0.25 \end{bmatrix}$ ,  $\mathbf{A}_{45} = \begin{bmatrix} 1 & 0.5 \\ 0.5 & 1 \end{bmatrix}$ ,  $\mathbf{A}_{46} = \begin{bmatrix} 0.9518 & -0.2142 \\ -0.2142 & 0.0482 \end{bmatrix}$ ,  $\mathbf{A}_{56} = \begin{bmatrix} 1 & 0 \\ 0 & 0 \end{bmatrix}$ ,  $\mathbf{A}_{78} = \begin{bmatrix} 3 & 2 \\ 2 & 3 \end{bmatrix}$ , and  $\mathbf{A}_{89} = \begin{bmatrix} 2 & 0 \\ 0 & 2 \end{bmatrix}$ . Observe that  $(v_1, v_4)$ ,  $(v_1, v_7)$ ,  $(v_4, v_7)$ , and  $(v_5, v_6)$  are positive semi-definite edges while other edges are positive definite. Thus,  $G$  has three clusters:  $\mathcal{C}_1 = \{v_1, v_2, v_3\}$ ,  $\mathcal{C}_2 = \{v_4, v_5, v_6\}$ ,  $\mathcal{C}_3 = \{v_7, v_8, v_9\}$ . The equilibrium points of three clusters satisfy:  $\sum_{i=1}^3 |\mathcal{C}_i| \mathbf{p}_{\mathcal{C}_i}^* = \sum_{i=1}^9 \mathbf{p}_i(0)$ ,  $\mathbf{p}_{\mathcal{C}_1}^* - \mathbf{p}_{\mathcal{C}_2}^* \in \mathcal{N}(\mathbf{A}_{14})$ ,  $\mathbf{p}_{\mathcal{C}_1}^* - \mathbf{p}_{\mathcal{C}_3}^* \in \mathcal{N}(\mathbf{A}_{17})$ , and  $\mathbf{p}_{\mathcal{C}_1}^* - \mathbf{p}_{\mathcal{C}_3}^* \in \mathcal{N}(\mathbf{A}_{47})$ .

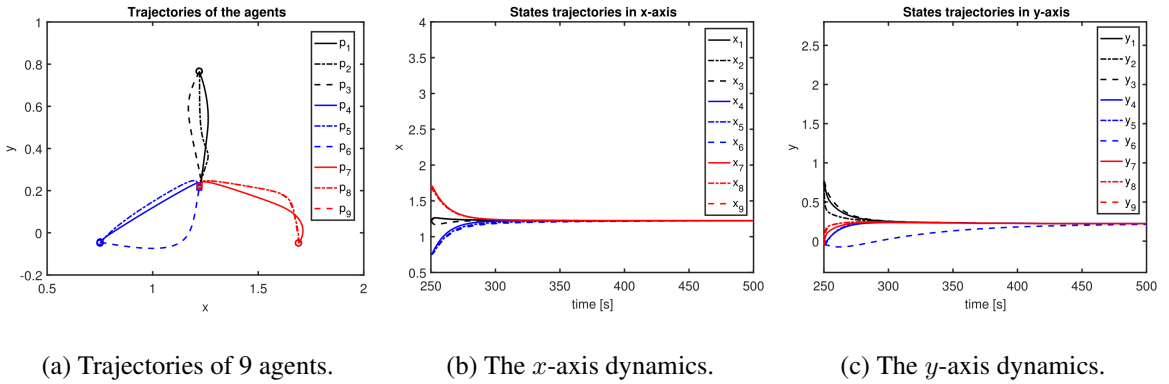
In case 2, we want all agents to rendezvous at a point. To this end, we change the graph a little by adding a positive semi-definite edge between vertices  $v_2$  and  $v_8$ . The corresponding matrix weight is given by  $\mathbf{A}_{28} = \begin{bmatrix} 0 & 0 \\ 0 & 1 \end{bmatrix}$ . This additional connection makes two clusters  $\mathcal{C}_1$  and  $\mathcal{C}_3$  satisfy Corollary 6.21 (i.e.,  $(\mathbf{A}_{17} + \mathbf{A}_{28})$  is positive definite); thus they can be merged into a cluster, called  $\mathcal{C}_{13}$ . It is



(a) Trajectories of 9 agents.

(b) The  $x$ -axis dynamics.(c) The  $y$ -axis dynamics.

Figure 6.9. Case 1: The nine-agent system in Fig. 6.8 under the consensus protocol (6.3).



(a) Trajectories of 9 agents.

(b) The  $x$ -axis dynamics.(c) The  $y$ -axis dynamics.

Figure 6.10. Case 2: Trajectories after the interaction graph switched to the graph in Fig. 6.8 (ii).

also due to Corollary 6.21 that the clusters  $\mathcal{C}_{13}$  and  $\mathcal{C}_2$  can be merged together (i.e.  $(A_{14} + A_{17})$  is positive definite). It follows that the graph has a spanning cluster  $\mathcal{C}$  in this case. Therefore, all agents will reach to an average consensus.

Simulation results in case 1 are shown in Fig. 6.9. The state trajectories in  $x$ - and  $y$ -axes are depicted in Figs. 6.9b and 6.9c, respectively. The corresponding positions of the agents are shown in Fig. 6.9a. It can be seen that all agents belong to a cluster converge to a same point in  $\mathbb{R}^2$ .

Simulation results in case 2 are shown in Fig. 6.10. Figure 6.10a depicts the nine agent trajectories after the interaction graph is switched to Fig. 6.8 (b). All agents asymptotically reach a common point in the plane.

#### 6.4.2 The bearing-constrained formation control problem

The bearing-based formation control problem in [59] can be considered as a special application of the matrix-weighted consensus problem. Here, the proposed formation control law for each agent is given by

$$\dot{\mathbf{p}}_i = - \sum_{j \in \mathcal{N}_i} \mathbf{P}_{\mathbf{g}_{ij}^*} (\mathbf{p}_i - \mathbf{p}_j), \quad (6.19)$$

where  $\mathbf{p}_i \in \mathbb{R}^d$  is the position of agent  $i$ . The control law (6.19) is exactly the consensus protocol (6.3) where the matrix weights are chosen to be the projection matrices  $\mathbf{P}_{\mathbf{g}_{ij}^*}$ . Here,  $\mathbf{g}_{ij}^*$  is a unit bearing vector which has been chosen to impose a constraint for the formation. Also, the projection matrix  $\mathbf{P}_{\mathbf{g}_{ij}^*} \triangleq \mathbf{I}_d - \mathbf{g}_{ij}^* \mathbf{g}_{ij}^{*\top}$  is symmetric, positive semidefinite. Moreover, the nullspace of  $\mathbf{P}_{\mathbf{g}_{ij}^*}$  is spanned by the bearing vector  $\mathbf{g}_{ij}^*$ , i.e.,  $\mathcal{N}(\mathbf{P}_{\mathbf{g}_{ij}^*}) = \mathcal{R}(\mathbf{g}_{ij}^*)$ . By specifying a set of desired bearing vectors  $\{\mathbf{g}_{ij}^*\}_{(i,j) \in \mathcal{E}}$  with regard to some desired formation  $\mathbf{p}^*$ , the nullspace of the *bearing Laplacian matrix*  $\mathbf{L}_b(\mathbf{p}^*) \in \mathbb{R}^{dn \times dn}$  can be designed. Note that the  $ij$ th block sub-matrix of  $\mathbf{L}_b$  is given by

$$\left\{ \begin{array}{ll} [\mathbf{L}_b]_{ij} = \mathbf{0}, & i \neq j, (v_i, v_j) \notin \mathcal{E}, \\ [\mathbf{L}_b]_{ij} = -\mathbf{P}_{\mathbf{g}_{ij}^*}, & i \neq j, (v_i, v_j) \in \mathcal{E}, \\ [\mathbf{L}_b]_{ii} = \sum_{j \in \mathcal{N}_i} \mathbf{P}_{\mathbf{g}_{ij}^*}, & i = 1, \dots, n. \end{array} \right.$$

Based on Theorem 6.11, the formation converges to the nullspace of  $\mathbf{L}_b$  which is  $\text{span}\{\mathcal{R}, \{\mathbf{p} = [\mathbf{p}_1^\top, \dots, \mathbf{p}_n^\top]^\top \in \mathbb{R}^{dn} | (\mathbf{p}_j - \mathbf{p}_i) = \alpha \mathbf{g}_{ij}^*, \alpha \in \mathbb{R}, \forall (v_i, v_j) \in \mathcal{E}\}\}$ . More detailed analysis and discussions on the bearing-constrained formation control can be found in [59, 72, 73].

---

**Algorithm 1** Finding clusters of a matrix-weighted graph  $G$ 

---

**Require:**  $G(\mathcal{V}, \mathcal{E}, \mathcal{A})$

```
1:  $i \leftarrow 0;$ 
2: Find the set of positive trees  $\{\mathcal{T}_1, \dots, \mathcal{T}_p\}$  in  $G$ ;
3:  $\mathcal{C}_G(0) \leftarrow \{\mathcal{C}_m = \{\mathcal{V}(\mathcal{T}_m)\}, m = 1, \dots, p\};$ 
4: repeat
5:    $\mathcal{C}_G(i + 1) \leftarrow \mathcal{C}_G(i);$ 
6:   check  $\leftarrow$  false;
7:   for all  $\mathcal{C}_m \in \mathcal{C}_G(i)$  do
8:     for all  $\mathcal{C}_l \in \mathcal{C}_G(i), l \neq m$  do
9:       if  $\exists v_i \in \mathcal{C}_l$  satisfies Theorem 6.18(ii) then
10:         $\mathcal{V}_{temp} \leftarrow \mathcal{V}(\mathcal{T}_m) \cup \mathcal{V}(\mathcal{T}_l);$ 
11:         $\mathcal{E}_{temp} \leftarrow \mathcal{E}(\mathcal{T}_m) \cup \mathcal{E}(\mathcal{T}_l) \cup \mathcal{S};$ 
12:         $\mathcal{C}_{temp} \leftarrow \mathcal{C}_m \cup \mathcal{C}_l;$ 
13:         $\mathcal{C}_G(i + 1) \leftarrow (\mathcal{C}_G(i + 1) \setminus \{\mathcal{C}_m, \mathcal{C}_l\}) \cup \{\mathcal{C}_{temp}\};$ 
14:        check  $\leftarrow$  true;
15:      break;
16:    end if
17:  end for
18:  if check == true then
19:    break;
20:  end if
21: end for
22:  $i \leftarrow i + 1;$ 
23: until  $\mathcal{C}_G(i) == \mathcal{C}_G(i - 1)$ 
```

---

# Chapter 7

## Further Results on Matrix-Weighted Consensus

### 7.1 Consensus with leader-following graphs

#### 7.1.1 Preliminaries and problem formulation

Consider a system consisting of  $n$  agents (followers) and a single leader. The dynamics of each agent is given by

$$\dot{\mathbf{x}}_i = \mathbf{u}_i, \quad \forall i = 1, \dots, n, \quad (7.1)$$

where  $\mathbf{x}_i \in \mathbb{R}^d$  and  $\mathbf{u}_i \in \mathbb{R}^d$  are agent  $i$ 's state vector and control input, respectively. The control input of each agent is influenced by its neighbors' states and the matrix weights, but is not influenced by any external input. The leader, labeled as  $i = 0$ , has its state  $\mathbf{x}_0 \in \mathbb{R}^d$  fixed, i.e.,

$$\dot{\mathbf{x}}_0 = \mathbf{0}. \quad (7.2)$$

The information flow between the  $n$  followers is described by a matrix-weighted graph  $\mathcal{G} = (\mathcal{V}, \mathcal{E}, \mathcal{A})$ . Here,  $\mathcal{V} = \{v_1, \dots, v_n\}$  is the set of vertices representing  $n$  followers,  $\mathcal{E} \subseteq \mathcal{V} \times \mathcal{V}$  is the set of edges in the graph,  $|\mathcal{E}| = m$ . An edge of  $\mathcal{G}$  between two vertices  $v_i$  and  $v_j$ ,  $v_i \neq v_j$ , denoted by  $(v_i, v_j)$ , indicates that two agents  $i$  and  $j$  exchange information in at least one state variable. The connection between  $i$  and  $j$  are characterized by a symmetric positive semidefinite matrix  $\mathbf{A}_{ij} \in \mathbb{R}^{d \times d}$ . For an undirected graph, if  $(v_i, v_j) \in \mathcal{E}$  then  $(v_j, v_i) \in \mathcal{E}$  and it is further assumed that  $\mathbf{A}_{ij} = \mathbf{A}_{ij}^\top = \mathbf{A}_{ji} \geq 0$  and  $\mathcal{A} = \{\mathbf{A}_{ji} | (v_i, v_j) \in \mathcal{E}\}$  is referred to as the matrix-weight set corresponding to the edge set  $\mathcal{E}$ . For a directed graph, an edge  $(v_i, v_j)$  is represented by an arrow from vertex  $v_j$  to vertex  $v_i$ , characterizing that agent  $i$  receives information from agent  $j$ . If there is an edge  $(v_i, v_j)$ ,

agent  $j$  is called a neighbor of  $i$ , and we have  $\mathbf{A}_{ij} = \mathbf{A}_{ij}^\top \geq 0$ ,  $\mathbf{A}_{ij} \in \mathcal{A}$ . Because the graph is directed,  $(v_i, v_j) \in \mathcal{E}$  does not imply  $(v_j, v_i) \in \mathcal{E}$ , and  $A_{ij}, A_{ji}$  are not necessarily equal. The set of neighbors of agent  $i$  is denoted by  $\mathcal{N}_i = \{j \in \{1, \dots, n\} | v_j \in \mathcal{V} \text{ and } (v_i, v_j) \in \mathcal{E}, v_j \neq v_i\}$ . A (directed) path  $\mathcal{P} = v_{i_1} \dots v_{i_k}$  is a sequence of directed edges  $(v_{i_j}, v_{i_{j+1}})$  in the graph. A graph is semipositively connected if there is a path between every pair of vertices. The semipositive connectedness arises because  $\mathbf{A}_{ij} \geq 0$ . A path  $\mathcal{P}$  forms a cycle if  $v_{i_1} \equiv v_{i_k}$ , and  $v_{i_j} \neq v_{i_1}, \forall, 1 < j < k$ . A directed acyclic graph is a directed graph that has no cycles [121].

The aim of this section is to study consensus problems with two types of leader-following graphs  $\bar{\mathcal{G}}$ . Each  $\bar{\mathcal{G}}$  has a single leader vertex and is defined as follows. Beginning with the graph  $\mathcal{G}$ , we add a vertex  $v_0$  (representing the leader), a set of directed edges  $\mathcal{E}_0$  from vertex  $v_0$  to some vertices  $v_i \in \mathcal{V}$ , and a corresponding set of matrix weights  $\mathcal{A}_0 = \{\mathbf{A}_{i0}, \forall i \in \{1, \dots, n\}\}$ . The matrix-weight  $\mathbf{A}_{i0}$  is positive semidefinite if agent  $i$  has access to the leader's state, i.e.  $(v_i, v_0) \in \mathcal{E}_0$ ; otherwise,  $\mathbf{A}_{i0} = \mathbf{0}$ . The graph  $\bar{\mathcal{G}} = \{\bar{\mathcal{V}}, \bar{\mathcal{E}}, \bar{\mathcal{A}}\}$  is directed, with  $\bar{\mathcal{V}} = \{v_0\} \cup \mathcal{V}$ ,  $\bar{\mathcal{E}} = \mathcal{E}_0 \cup \mathcal{E}$ , and  $\bar{\mathcal{A}} = \mathcal{A}_0 \cup \mathcal{A}$ . For the first problem, the follower graph  $G$  is undirected, and for the second problem, the follower graph  $G$  is directed. Specifically, the following system will be studied:

$$\dot{\mathbf{x}}_0 = \mathbf{0}, \quad (7.3a)$$

$$\dot{\mathbf{x}}_i = \sum_{j \in \mathcal{N}_i} \mathbf{A}_{ij}(\mathbf{x}_j - \mathbf{x}_i) + \mathbf{A}_{i0}(\mathbf{x}_0 - \mathbf{x}_i), \quad i = 1, \dots, n \quad (7.3b)$$

The leader-following system (7.3) is said to achieve leader-follower consensus if, for any initial state  $\mathbf{x}_i(0)$ ,  $i = 1, \dots, n$ , there holds  $\lim_{t \rightarrow \infty} \mathbf{x}_i(t) \rightarrow \mathbf{x}_0$ .

### 7.1.2 Analysis and discussion

We study conditions for reaching a matrix-weighted consensus under two leader-following graphs [150]. These conditions are then used to discuss related phenomena in social networks.

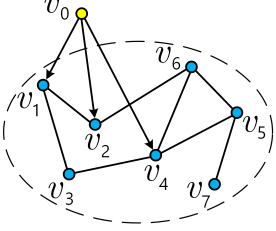


Figure 7.1. Leader-follower graph, with undirected follower graph.

### 7.1.2.1 Undirected follower interaction topology

The following assumptions are considered to study the system (7.3):

**Assumption 7.1** *The graph  $\mathcal{G}$  has a cluster containing all vertices in  $\mathcal{V}$ , or equivalently,  $\mathcal{N}(\mathbf{L}) = \mathcal{R} = \mathcal{R}(\mathbf{1}_n \otimes \mathbf{I}_d)$ .*

**Assumption 7.2**  $\sum_{i=1}^n \mathbf{A}_{i0}$  is positive definite.

Denote  $\mathbf{z}_i = \mathbf{x}_i - \mathbf{x}_0$ , for  $i = 1, \dots, n$ , and define  $\mathbf{z} \triangleq [\mathbf{z}_1^\top, \dots, \mathbf{z}_n^\top]^\top \in \mathbb{R}^{dn}$  as the stacked error vector. Equation (7.3b) can be rewritten as follows:

$$\dot{\mathbf{z}}_i = \sum_{j \in \mathcal{N}_i} \mathbf{A}_{ij} (\mathbf{z}_j - \mathbf{z}_i) - \mathbf{A}_{i0} \mathbf{z}_i, \quad i = 1, \dots, n. \quad (7.4)$$

In vector form, the dynamics (7.4) can be expressed as

$$\dot{\mathbf{z}} = -\mathbf{L}\mathbf{z} - \text{blkdiag}(\mathbf{A}_{i0})\mathbf{z} = -(\mathbf{L} + \text{blkdiag}(\mathbf{A}_{i0}))\mathbf{z}. \quad (7.5)$$

One can state the following lemmas.

**Lemma 7.1** *Under Assumption 7.1, the matrix  $\mathbf{M} = (\mathbf{L} + \text{blkdiag}(\mathbf{A}_{i0}))$  is positive definite if and only if  $\sum_{i=1}^n \mathbf{A}_{i0}$  is positive definite.*

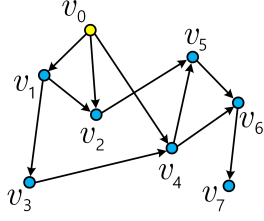


Figure 7.2. Leader-follower graph, with directed acyclic follower graph.

*Proof:* Under Assumption 7.1, the matrix-weighted Laplacian  $\mathbf{L}$  is positive semidefinite and  $\mathcal{N}(\mathbf{L}) = \mathcal{R}$  according to Theorem 6.25 in the previous chapter. Since  $\text{blkdiag}(\mathbf{A}_{i0})$  is positive semidefinite, it follows from Lemma 2.8 that

$$\mathcal{N}(\mathbf{M}) \subseteq \mathcal{N}(\mathbf{L}). \quad (7.6)$$

Let  $\{\mathbf{e}_k\}_{k=1,\dots,d}$  be the standard basis of  $\mathbb{R}^d$ , that is,  $\mathbf{e}_k \in \mathbb{R}^d$  is a vector whose  $k$ -th entry is equal to 1 and other entries are all zero. For any vector  $\mathbf{v} \in \mathcal{N}(\mathbf{L})$ , we can express  $\mathbf{v}$  as a linear combination as follow,

$$\mathbf{v} = \sum_{k=1}^d v_k (\mathbf{1}_n \otimes \mathbf{e}_k) = \mathbf{1}_n \otimes \left( \sum_{i=1}^d v_k \mathbf{e}_k \right), \quad (7.7)$$

where  $v_k \in \mathbb{R}$ ,  $k = 1, \dots, d$ , are scalars. For any  $\mathbf{v} \in \mathcal{N}(\mathbf{L})$ ,

$$\begin{aligned} \mathbf{v}^\top \mathbf{H} \mathbf{v} &= \mathbf{v}^\top (\mathbf{L} + \text{blkdiag}(\mathbf{A}_{i0})) \mathbf{v} \\ &= \mathbf{v}^\top \text{blkdiag}(\mathbf{A}_{i0}) \mathbf{v} \\ &= (\mathbf{1}_n^\top \otimes \left( \sum_{k=1}^d v_k \mathbf{e}_k^\top \right)) \text{blkdiag}(\mathbf{A}_{i0}) (\mathbf{1}_n \otimes \left( \sum_{k=1}^d v_k \mathbf{e}_k \right)) \\ &= \sum_{i=1}^n \left( \sum_{k=1}^d v_k \mathbf{e}_k^\top \right) \mathbf{A}_{i0} \left( \sum_{k=1}^d v_k \mathbf{e}_k \right) \\ &= \left( \sum_{k=1}^d v_k \mathbf{e}_k^\top \right) \left( \sum_{i=1}^n \mathbf{A}_{i0} \right) \left( \sum_{k=1}^d v_k \mathbf{e}_k \right). \end{aligned} \quad (7.8)$$

Suppose that  $\sum_{i=1}^n \mathbf{A}_{i0}$  is positive definite. Then it follows from (7.8) that  $\mathbf{v}^\top \mathbf{M} \mathbf{v} > 0, \forall \mathbf{v} \in \mathcal{N}(\mathbf{L})$ . Therefore, (7.6) implies that  $\mathcal{N}(\mathbf{M}) = \{\mathbf{0}\}$ , i.e.,  $\mathbf{M}$  is positive definite.

On the other hand, if  $\sum_{i=1}^n \mathbf{A}_{i0}$  is positive semidefinite but not positive definite, then we can always choose  $v_k, k = 1, \dots, d$ , such that  $\mathbf{v}' = \sum_{k=1}^d v_k \mathbf{e}_k^\top \neq \mathbf{0}$  is an eigenvector of  $\sum_{i=1}^n \mathbf{A}_{i0}$  corresponding to a zero eigenvalue. Also,  $\mathbf{v} = \mathbf{1}_d \otimes \mathbf{v}'$  is an eigenvector of  $\mathbf{M}$  corresponding to a zero eigenvalue. Thus,  $\mathbf{M}$  is positive semidefinite, but singular, in this case. ■

The main result of for the undirected follower topology problem is stated in the following theorem.

**Theorem 7.2** *Under Assumptions 7.1 and 7.2, the leader-following system (7.3) achieves leader-follower consensus, for all initial conditions  $\mathbf{x}_i \in \mathbb{R}^d, i = 1, \dots, n$ , exponentially fast.*

*Proof:* Under Assumptions 7.1 and 7.2, it follows from Lemma 7.1 that  $\mathbf{M} = \mathbf{L} + \text{blkdiag}(\mathbf{A}_{i0})$  is positive definite. Because (7.5) is a linear system ( $\dot{\mathbf{z}} = -\mathbf{H}\mathbf{z}$ ) and  $\mathbf{H}$  is positive definite, it follows that the origin is a globally exponentially stable equilibrium of (7.5). It follows from the definition of  $\mathbf{z}_i$  that leader-follower consensus is achieved as  $\mathbf{z}_i \rightarrow \mathbf{0}, \forall i = 1, \dots, n$ . ■

**Remark 7.3** *The convergence rate of (7.5) depends on the smallest eigenvalue of  $\mathbf{H}$ ,  $\lambda_1(\mathbf{H})$ , and the smallest nonzero eigenvalue of the matrix-weighted Laplacian  $\mathbf{L}$ ,  $\lambda_{d+1}(\mathbf{L})$ .*

Theorem 7.2 implies that clustering behavior happens when either the graph  $G$  does not have a spanning cluster or the communication from the leader to the follower agents in  $G$  is incomplete, i.e.,  $\sum_{i=1}^n \mathbf{A}_{i0}$  is singular.

### 7.1.2.2 Directed follower interaction topology

In this scenario, the following assumption on the system (7.3) is adopted:

**Assumption 7.3** The matrix  $\mathbf{M}_i = \sum_{j \in \mathcal{N}_i} \mathbf{A}_{ij}$  is positive definite for all  $i = 1, \dots, n$ .

Let  $\mathbf{z}_i = \mathbf{x}_i - \mathbf{x}_0$ ,  $i = 1, \dots, n$ , and  $\mathbf{z} = [\mathbf{z}_1^\top, \dots, \mathbf{z}_n^\top]^\top \in \mathbb{R}^{dn}$ . From Eq. (7.1), the  $\mathbf{z}$ -dynamics is written as follows:

$$\dot{\mathbf{z}} = -\mathbf{M}\mathbf{z}, \quad (7.9)$$

where  $\mathbf{M} = \mathbf{L} + \text{blkdiag}(\mathbf{A}_{i0})$  is the matrix given by

$$\mathbf{M} = \begin{bmatrix} \mathbf{A}_{10} & \mathbf{0} & \cdots & \mathbf{0} \\ -\mathbf{A}_{21} & \sum_{l=0}^1 \mathbf{A}_{2l} & \cdots & \mathbf{0} \\ \vdots & \vdots & \ddots & \vdots \\ -\mathbf{A}_{n1} & -\mathbf{A}_{n2} & \cdots & \sum_{l=0}^n \mathbf{A}_{nl} \end{bmatrix}.$$

The following Theorem on the system (7.9) can be proved.

**Theorem 7.4** Under Assumption 7.3, the leader-following system (7.3) achieves leader-follower consensus, for all initial conditions  $\mathbf{x}_i \in \mathbb{R}^d$ ,  $i \in \bar{\mathcal{V}}$ , exponentially fast.

*Proof:* Under Assumption 7.3, one has

$$\det(\lambda \mathbf{I}_{dn} - \mathbf{H}) = \prod_{i=1}^n \det(\lambda \mathbf{I}_d - \sum_{l=0}^n \mathbf{A}_{il}) = \prod_{i=1}^n \det(\lambda \mathbf{I}_d - \sum_{l \in \mathcal{N}_i} \mathbf{A}_{il}). \quad (7.10)$$

Since  $\mathbf{N}_i = \sum_{l \in \mathcal{N}_i} \mathbf{A}_{il}$ ,  $i = 1, \dots, n$  is positive definite, it follows from (7.10) that all eigenvalues of  $\mathbf{M}$  are strictly positive, or i.e.,  $-\mathbf{H}$  is Hurwitz stable. Thus, the origin  $\mathbf{z} = \mathbf{0}$  is a globally exponentially stable equilibrium of the system (7.9). The definition of  $\mathbf{z}_i$  then implies that leader-follower consensus is achieved. ■

The following question naturally arises from considering the result in Theorem 7.4: “What happens if, for one or more  $i$ ,  $\mathbf{N}_i$  is positive semidefinite and singular?”. The overall system will not achieve a consensus in this case. However, all follower agents can reach partial agreement on some states.

Since  $\mathbf{N}_i$  is symmetric, it is always diagonalizable. Let  $\mathbf{n}_k^i \in \mathbb{R}^d$ , be an eigenvector of  $\mathbf{N}_i$  corresponding to eigenvalue  $\xi_k$ , where  $k = 1, \dots, d$ . Then,  $\mathbf{v}_{d(i-1)+k} = \begin{bmatrix} \mathbf{0}_{d(i-1)}^\top & (\mathbf{n}_k^i)^\top & \mathbf{0}_{d(n-i)}^\top \end{bmatrix}^\top \in \mathbb{R}^{dn}$  is a right eigenvector of  $\mathbf{M}$  corresponding to the eigenvalue  $\lambda_{d(i-1)+k} = \xi_k$  (for  $i = 1, \dots, n$ , and  $k = 1, \dots, d$ ). Let  $\mathbf{r}_{d(i-1)+k}$  be the corresponding left eigenvector of  $\mathbf{M}$ . Since  $\{\mathbf{v}_l\}_{l=1,\dots,n}$  is a basis consisting of eigenvectors of  $\mathbf{M}$ , it follows  $\mathbf{M}$  is diagonalizable. From linear systems theory [151], solutions of (7.9) are given by

$$\mathbf{z}(t) = \sum_{i=1}^n \sum_{k=1}^d (\mathbf{v}_{d(i-1)+k}^\top \mathbf{z}(0)) \mathbf{r}_k e^{-\lambda_{d(i-1)+k} t} = \sum_{i=1}^n \sum_{k=1}^d ((\mathbf{n}_k^i)^\top \mathbf{z}_i(0)) \mathbf{r}_k e^{-\lambda_{d(i-1)+k} t}. \quad (7.11)$$

Thus, as  $t \rightarrow \infty$ , states corresponding to  $\lambda_{d(i-1)+k} = 0$  are invariant while other states converge to zero. The existence of some zero eigenvalues implies that a consensus is achieved if  $\mathbf{z}_i(0) \perp \mathcal{N}(\mathbf{N}_i)$ , for all  $i = 1, \dots, n$ , otherwise clustering phenomena happens.

Clustering has been observed as a consequence of different variations/differences in the consensus algorithm, but most existing results focus on algorithms concerning scalar variables. Negative weights were used to achieve bipartite consensus in [152], and to achieve cluster consensus in [153]. Bounded-confidence algorithms achieved clustering in [154], while individual stubbornness explained clustering phenomenon in [119]. To the author's knowledge, this chapter and the previous chapter are the first to obtain clustering behavior using matrix-weighted consensus algorithms.

### 7.1.2.3 Interpreting the results with application to social behaviors

In this section, further discussion on the two above problems is provided in the context of behavior of social networks. The leader-follower topologies studied are reflective of structured communities with a clear leader. The leader is responsible for deciding how the whole community reacts to the outside environment which might include outside information. Our first observation is that a decision or piece of information from the leader can disseminate to the community via several information

channels, e.g., documents, rules, or announcements, etc. Thus, matrix weights can describe the mixing of information in those information channels. Having matrix weights enables us to capture an individual's ability to place different weights on difference information sources. Allowing  $A_{ij}$  to vary between individuals allows for modeling of individual  $i$  allocating different trusts for different neighbor  $j$ .

The undirected follower topology models a general social network. The leader sends parts of information to a subset  $S$  of its followers ( $i \in S$  implies  $A_{i0}$  is positive semidefinite). In such a social structure, people can exchange information with friends, neighbors, and thus eventually the information from the leader passes to the whole network. The analysis suggests that the followers can reach a consensus to the leader's states if and only if (i) the network is spanned by a cluster (the community is well organized); and (ii)  $\sum_{i \in S} A_{i0}$  is positive definite (the aggregated information the leader sent is complete). Information disseminates as fast as the convergence rate of the undirected network.

The second topology is more reflective of a military society (hierarchy). Each follower  $i$  ( $i = 1, \dots, n$ ) has at least one immediate leader. In turn,  $i$  may be the leader of several other followers. Information can only pass in one direction, from leaders to followers. In this structure, the speed of information spreading to an agent depends on how close it is to the leader. For an agent to reach a consensus with its leader's state, it is required that the connection to its leader, characterized by  $N_i = \sum_{j \in \mathcal{N}_i} A_{ji}$ , be positive definite. Since communication is unidirectional, in general, this type of network has faster response and requires less communication cost. However, when an agent  $i$  does not have enough communication from its leader, or i.e.,  $N_i$  is only positive semidefinite, then  $i$  may not consent with its leader on some states. Consequently, agent  $i$ 's followers will also be affected by this misconnection. Thus, the hierarchical structure is less robust against failure/corruption inside the network.

## 7.2 Consensus with fixed and balanced matrix-weighted graphs

Given a system of  $n$  single integrator agents with matrix-weighted graph  $G = (\mathcal{V}, \mathcal{E}, \mathcal{A})$ , with the vertex set  $\mathcal{V} = \{v_1, \dots, v_n\}$ , the directed edge set  $\mathcal{E} = \{(v_i, v_j) \mid v_i, v_j \in \mathcal{V}, v_i \neq v_j\}$ , and the set of nonnegative matrix weights  $\mathcal{A} = \{\mathbf{A}_{ij} \geq 0 \mid v_i, v_j \in \mathcal{V}, v_i \neq v_j\}$ . Let  $\mathbf{L}(G) = [\mathbf{L}_{ij}]$  be a matrix-weighted Laplacian of dimension  $dn \times dn$  defined as follows:

$$\mathbf{L}_{ij} = \begin{cases} \sum_{j=1}^n \mathbf{A}_{ij}, & i = j, \\ -\mathbf{A}_{ij}, & i \neq j. \end{cases} \quad (7.12)$$

It is assumed that the graph  $G$  contains a directed spanning tree. Further, the matrix weights satisfy the following condition:

**Assumption 7.4 (Generalized balance condition)** *There exists a set of positive scalars  $p_1, \dots, p_n$  such that*

$$p_i \sum_{j=1}^n \mathbf{A}_{ij} = \sum_{j=1}^n p_j \mathbf{A}_{ji}, \quad (7.13)$$

or i.e., there exists a vector  $\mathbf{p} = [p_1, \dots, p_n]^\top$  with positive elements such that

$$(\mathbf{p}^\top \otimes \mathbf{I}_d) \mathbf{L} = \mathbf{0}_{d \times nd}. \quad (7.14)$$

Let  $\mathbf{x}_i \in \mathbb{R}^d$  denote the state vector of agent  $i$ . The  $n$ -agent system is said to achieve a consensus under the protocol (6.3) if and only if  $\mathbf{x}_i = \mathbf{x}_j, \forall i, j = 1, \dots, n$ . We have the following theorem:

**Theorem 7.5** *Suppose that  $G$  is strongly connected and the matrix weights satisfy Assumption 7.4 and there exists a positive spanning tree in  $G$ , the  $n$ -agent system (6.3) globally asymptotically reaches a consensus. Further,  $\mathbf{x}_i \rightarrow \mathbf{x}^* = (\sum_{i=1}^n p_i \mathbf{x}_i(0)) / \sum_{i=1}^n p_i$ , for all  $i = 1, \dots, n$ .*

Let  $\mathbf{P} \triangleq \text{diag}(p_i) \in \mathbb{R}^{n \times n}$ , the following lemma is essential to prove Theorem 7.5.

**Lemma 7.6** Under Assumption 7.4, the matrix

$$\mathbf{Q} = \bar{\mathbf{P}}\mathbf{L} + \mathbf{L}^\top\bar{\mathbf{P}}, \quad (7.15)$$

where  $\bar{\mathbf{P}} = \mathbf{P} \otimes \mathbf{I}_d$  is positive semidefinite.

*Proof:* There holds

$$\mathbf{x}^\top \bar{\mathbf{P}}\mathbf{L}\mathbf{x} = \sum_{i=1}^n p_i \mathbf{x}_i^\top \sum_{j=1}^n \mathbf{A}_{ij} (\mathbf{x}_j - \mathbf{x}_i) = \sum_{i,j=1}^n p_i \mathbf{x}_i^\top \mathbf{A}_{ij} (\mathbf{x}_i - \mathbf{x}_j). \quad (7.16)$$

From Assumption (7.13), one can write

$$\begin{aligned} \sum_{i=1}^n p_i \mathbf{x}_i^\top \sum_{j=1}^n \mathbf{A}_{ij} (\mathbf{x}_j - \mathbf{x}_i) &= \sum_{i=1}^n \mathbf{x}_i^\top (p_i \sum_{j=1}^n \mathbf{A}_{ij}) \mathbf{x}_i - \sum_{i,j=1}^n p_i \mathbf{x}_i^\top \mathbf{A}_{ij} \mathbf{x}_j \\ &= \sum_{i=1}^n \mathbf{x}_i^\top \left( \sum_{j=1}^n p_j \mathbf{A}_{ji} \right) \mathbf{x}_i - \sum_{i,j=1}^n p_i \mathbf{x}_i^\top \mathbf{A}_{ij} \mathbf{x}_j \\ &= \sum_{j=1}^n \mathbf{x}_j^\top \left( \sum_{i=1}^n p_i \mathbf{A}_{ij} \right) \mathbf{x}_j - \sum_{i,j=1}^n p_i \mathbf{x}_i^\top \mathbf{A}_{ij} \mathbf{x}_j \\ &= \sum_{i,j=1}^n p_i \mathbf{x}_j^\top \mathbf{A}_{ij} (\mathbf{x}_j - \mathbf{x}_i). \end{aligned} \quad (7.17)$$

Thus,

$$\begin{aligned} \mathbf{x}^\top \mathbf{Q} \mathbf{x} &= \mathbf{x}^\top \bar{\mathbf{P}}\mathbf{L}\mathbf{x} + \mathbf{x}^\top \mathbf{L}^\top \bar{\mathbf{P}}\mathbf{x} = 2\mathbf{x}^\top \bar{\mathbf{P}}\mathbf{L}\mathbf{x} \\ &= \sum_{i,j=1}^n p_i \mathbf{x}_i^\top \mathbf{A}_{ij} (\mathbf{x}_i - \mathbf{x}_j) + \sum_{i,j=1}^n p_i \mathbf{x}_j^\top \mathbf{A}_{ij} (\mathbf{x}_j - \mathbf{x}_i) \\ &= \sum_{i,j=1}^n p_i (\mathbf{x}_i - \mathbf{x}_j)^\top \mathbf{A}_{ij} (\mathbf{x}_i - \mathbf{x}_j). \end{aligned} \quad (7.18)$$

Since  $\mathbf{A}_{ij} \geq 0$ , equation (7.18) implies that  $\mathbf{Q}$  is positive semidefinite. Further  $\mathbf{x}^\top \mathbf{Q} \mathbf{x} = 0$  if and only if  $\mathbf{x}_j - \mathbf{x}_i \in \mathcal{N}(\mathbf{A}_{ij}), \forall (v_i, v_j) \in \mathcal{E}$ . ■

Due to properties of the matrix-weighted Laplacian, we have  $\mathbf{L}(\mathbf{1}_n \otimes \mathbf{I}_d) = \mathbf{0}_{dn \times d}$ , and  $\mathbf{L}^\top \bar{\mathbf{P}}(\mathbf{1}_n \otimes \mathbf{I}_d) = \mathbf{L}^\top (\mathbf{p} \otimes \mathbf{I}_d) = \mathbf{0}_{dn \times d}$ . Thus, the matrix  $\mathbf{Q}$  has  $d$  zero eigenvalues corresponding to a basis of  $\mathcal{R}$ . Further, since  $\mathbf{Q}$  is positive semidefinite, one can write  $\mathbf{Q} = \mathbf{C}^\top \mathbf{C}$  and rewrite (7.15) as follows:

$$\bar{\mathbf{P}}(-\mathbf{L}) + (-\mathbf{L})^\top \bar{\mathbf{P}} = -\mathbf{C}^\top \mathbf{C}. \quad (7.19)$$

The following corollary follows from (7.19):

**Corollary 7.7** *Under Assumption (7.13) and supposing that  $G$  contains a directed positive spanning tree, the unobservable space of the pair  $(\mathbf{C}, -\mathbf{L})$  is spanned by  $\mathcal{R}$ .*

*Proof:* Let  $G$  contain a directed positive spanning tree  $\mathcal{T}$ . Consider Eq. (7.18), for  $\mathbf{x}^\top \mathbf{Q} \mathbf{x} = 0$  one needs to have  $\mathbf{x}_j - \mathbf{x}_i \in \mathcal{N}(\mathbf{A}_{ij})$  for all  $(v_i, v_j)$  in  $\mathcal{T}$ . Since  $\mathbf{A}_{ij}$ s are positive definite, it follows that  $\mathbf{x}_j = \mathbf{x}_i$  for all  $v_i, v_j \in \mathcal{V}$ , or i.e.,  $\mathbf{x} \in \mathcal{R}$ . Note that  $\mathcal{N}(\mathbf{Q}) = \mathcal{N}(\mathbf{C})$ , it follows that when  $G$  contains a directed positive spanning tree, we have  $\mathcal{N}(\mathbf{C}) = \mathcal{R}$ . From linear system theory [151], the equation (7.19) shows that  $\mathcal{R}$  is the unobservable space of the pair  $(\mathbf{C}, -\mathbf{L})$ . ■

Following the proof in [155], one can now prove Theorem 7.5.

*Proof:* Consider the Lyapunov function  $V = \mathbf{x}^\top \bar{\mathbf{P}} \mathbf{x}$  which is positive definite and continuously differentiable everywhere. The derivative of  $V$  along a trajectory of (6.3) is

$$\dot{V} = 2\mathbf{x}^\top \bar{\mathbf{P}} \dot{\mathbf{x}} = -2\mathbf{x}^\top \bar{\mathbf{P}} \mathbf{L} \mathbf{x} = -\mathbf{x}^\top \mathbf{Q} \mathbf{x}. \quad (7.20)$$

It follows from Lemma 7.6 that  $\mathbf{Q} \geq 0$  and thus  $\dot{V} \leq 0$ . By LaSalle Invariant principle, the trajectories of (6.3) converge to the largest invariant set  $\{\mathbf{x} \in \mathbb{R}^{dn} | \dot{V} = 0\}$ . Since the graph has a positive spanning tree,  $\mathbf{Q}$  is positive semidefinite with nullspace  $\mathcal{R}$ . Thus,  $\mathbf{x} \rightarrow \mathcal{R}$  asymptotically. It follows that all agents globally asymptotically reaches a consensus, i.e.,  $\mathbf{x}_i \rightarrow \mathbf{x}^*, \forall i = 1, \dots, n$ . To determine the consensus vector, we observe that

$$(\mathbf{p}^\top \otimes \mathbf{I}_d) \dot{\mathbf{x}} = -(\mathbf{p}^\top \otimes \mathbf{I}_d) \mathbf{L} \mathbf{x} = \mathbf{0}, \quad (7.21)$$

which implies that the weighted vector sum  $(\mathbf{p}^\top \otimes \mathbf{I}_d) \mathbf{x} = \sum_{i=1}^n p_i \mathbf{x}_i$  is invariant under (6.3). Thus, the consensus value is given by  $\mathbf{x}^* = (\sum_{i=1}^n p_i \mathbf{x}_i(0)) / \sum_{i=1}^n p_i$ . ■

### 7.3 Consensus with switching matrix-weighted graphs

In this section, the consensus protocol with switching interaction graph is studied. Let the state of the system evolves according to the following dynamics

$$\dot{\mathbf{x}}(t) = -\mathbf{L}(G_\sigma)\mathbf{x}(t), \quad (7.22)$$

where  $\sigma$  is a piecewise constant switching signal taking value on a finite index set  $\mathcal{P}$ , and  $\Gamma = \{G_\sigma | \sigma \in \mathcal{P}\}$  is a parameterized set of graphs. Each graph  $G_\sigma \in \Gamma$  satisfies the assumptions of Theorem 7.5 (i.e., each graph is generalized balance and has a positive spanning tree). We assume that  $\sigma$  is asymptotically non-chattering [156], i.e., there exist positive constants  $\tau_D, N_0$  for which

$$N_\sigma(t, \tau) \leq N_0 + \frac{t - \tau}{\tau_D}, \quad t \geq \tau \geq 0, \quad (7.23)$$

where  $N_\sigma(t, \tau)$  denotes the number of discontinuities of  $\sigma$  in the open interval  $(\tau, t)$ .

Let  $\delta = [\delta_1^\top, \dots, \delta_n^\top]^\top = \mathbf{x} - \mathbf{1}_n \otimes \mathbf{x}^*$  be the disagreement vector, it follows from (7.22) that

$$\dot{\delta}(t) = -\mathbf{L}(G_\sigma)\delta(t). \quad (7.24)$$

Using the shorthand  $\mathbf{L}_\sigma = \mathbf{L}(G_\sigma)$ , as the set of graphs  $\Gamma$  has a finite number of elements, the set  $\{\mathbf{L}_\sigma | \sigma \in \mathcal{P}\}$  is a compact set of  $dn \times dn$  matrices. It follows from Lemma 7.6 and Corollary 7.7 that there exists a set  $\{\bar{\mathbf{P}}_\sigma | \sigma \in \mathcal{P}\}$  of symmetric positive definite  $dn \times dn$  matrices such that

$$\bar{\mathbf{P}}_\sigma(-\mathbf{L}_\sigma) + (-\mathbf{L}_\sigma)^\top \bar{\mathbf{P}}_\sigma = -\mathbf{C}_\sigma^\top \mathbf{C}_\sigma \leq 0, \quad p \in \mathcal{P}, \quad (7.25)$$

and

$$\delta^\top \bar{\mathbf{P}}_{\sigma_2} \delta \leq \delta^\top \bar{\mathbf{P}}_{\sigma_1} \delta, \quad (7.26)$$

at every point  $\mathbf{x}$  in the state space, at which  $\sigma$  can switch from  $\sigma_1$  to  $\sigma_2$ . The main result of this section is stated as follows.

**Theorem 7.8** Consider the system (7.31) with an asymptotically non-chattering switching signal  $\sigma$ .

Suppose that each graph  $G_\sigma \in \Gamma$  is generalized balance and has a directed spanning tree. Then, the origin is a uniformly globally asymptotically stable equilibrium of the system (7.24). Equivalently,  $\mathbf{x}$  will uniformly globally asymptotically converge to  $\mathbf{1}_n \otimes \mathbf{x}^*$ .

*Proof:* From Corollary 7.7, the unobservable space of each pair  $(C_\sigma, -L_\sigma)$  is  $\mathcal{R}$ . It follows that  $\mathcal{R}$  is  $-L_\sigma$ -invariant for all  $\sigma \in \mathcal{P}$  and contains the unobservable subspaces of all pairs  $(C_\sigma, -L_\sigma)$ . Further, observe that  $(p_\sigma^\top \otimes I_d)\dot{\delta} = \mathbf{0}$  which implies  $(p_\sigma^\top \otimes I_d)\delta$  is invariant. The intersection between  $\mathcal{R}$  and  $\mathcal{S}_d = \{\delta | (p_\sigma^\top \otimes I_d)\delta = (p_\sigma^\top \otimes I_d)\delta(0)\}$  is determined by solving the following equation:

$$(p_\sigma^\top \otimes I_d)(\mathbf{1}_n \otimes \delta^*) = (p_\sigma^\top \otimes I_d)\delta(0) \quad (7.27)$$

Equation (7.27) is equivalent to

$$\left( \sum_{i=1}^n p_{\sigma i} \right) \delta^* = \sum_{i=1}^n p_{\sigma i} \delta_i(0) = \sum_{i=1}^n p_{\sigma i} (\mathbf{x}_i - \mathbf{x}_i(0)) = \mathbf{0}, \quad (7.28)$$

where the last equality follows from the fact the the weighted vector sum  $\sum_{i=1}^n p_{\sigma i} \mathbf{x}_i$  is invariant. Since  $\sum_{i=1}^n p_{\sigma i} > 0$ , it follows from (7.28) that  $\delta^* = \mathbf{0}_d$ . Thus, the smallest subspace that is  $-L_\sigma$ -invariant for all  $\sigma \in \mathcal{P}$  and contains the unobservable subspaces of all pairs  $(C_\sigma, -L_\sigma)$  for the system (7.24) contains only the origin  $\delta = \mathbf{0}_{dn}$ .

Since the system (7.24) satisfies all conditions of [156, Theorem 4], any trajectory of (7.24) uniformly globally asymptotically converges to  $\delta = \mathbf{0}$ , or i.e., the  $n$  agents globally asymptotically reach a consensus under the switching consensus protocol (7.22). ■

#### 7.4 Consensus with time-delays

In this section, the matrix-weighted consensus protocol is studied when there are delays in the communication between neighbor agents. Communication delays are unavoidable when a large

amount of information are exchanged in a network. The LMI-based analysis in this section is inspired from [157].

Consider the consensus protocol with an undirected matrix-weighted graph  $G$  with time delays. For an edge  $(v_i, v_j) \in \mathcal{E}$ , we denote the time delay for information from  $j$  to  $i$  by  $\tau_{ij} > 0$ . Since the graph is undirected, it is assumed that  $\tau_{ij} = \tau_{ji}, \forall (v_i, v_j) \in \mathcal{E}$ .

The consensus protocol with communication time-delays can be written as follows:

$$\dot{\mathbf{x}}_i(t) = - \sum_{j \in \mathcal{N}_i} \mathbf{A}_{ij} (\mathbf{x}_i(t - \tau_{ij}) - \mathbf{x}_j(t - \tau_{ij})), \quad i = 1, \dots, n. \quad (7.29)$$

We can rewrite the dynamics (7.29) in the matrix form as follows:

$$\dot{\mathbf{x}}(t) = - \sum_{k=1}^r \mathbf{L}_k \mathbf{x}(t - \tau_k), \quad (7.30)$$

where  $r \leq |\mathcal{E}|$ ,  $\tau_k \in \{\tau_{ij} \mid i, j = 1, \dots, n\}$  for  $k = 1, \dots, r$ , and  $\mathbf{L}_k = [\mathbf{L}_{kij}] \in \mathbb{R}^{dn \times dn}$  is the matrix whose  $d \times d$  blocks are defined by

$$\mathbf{L}_{kij} = \begin{cases} -\mathbf{A}_{ij}, & j \neq i, \tau_k = \tau_{ij}, \\ \mathbf{0}_d, & j \neq i, \tau_k \neq \tau_{ij}, \\ -\sum_{j=1, j \neq i}^n \mathbf{L}_{kij}, & j = i. \end{cases}$$

It is observed that  $\mathbf{L}_k$  is a part of the Laplacian matrix corresponding to an update with time delay  $\tau_k$ , and  $\mathbf{L} = \sum_{k=1}^r \mathbf{L}_k$ . Since the graph is undirected,  $(\mathbf{1}_n^\top \otimes \mathbf{I}_d) \mathbf{L} = \mathbf{0}_{d \times nd}$  and  $(\mathbf{1}_n^\top \otimes \mathbf{I}_d) \mathbf{L}_k = \mathbf{0}_{d \times nd}$ , for  $k = 1, \dots, r$ . It follows that  $\mathbf{x}^* = \frac{1}{n} \sum_{i=1}^n \mathbf{x}_i(t)$  is time-invariant. Defining the disagreement vector  $\boldsymbol{\delta}$  as in the previous section, one can transform the equation (7.30) in the following form [158]:

$$\begin{aligned} \dot{\boldsymbol{\delta}}(t) &= - \sum_{k=1}^r \mathbf{L}_k \boldsymbol{\delta}(t - \tau_k) \\ &= -\mathbf{L} \boldsymbol{\delta}(t) + \sum_{k=1}^r \mathbf{L}_k (\boldsymbol{\delta}(t) - \boldsymbol{\delta}(t - \tau_k)) \\ &= -\mathbf{L} \boldsymbol{\delta}(t) + \sum_{k=1}^r \mathbf{L}_k \int_{t-\tau_k}^t \dot{\boldsymbol{\delta}}(s) ds. \end{aligned} \quad (7.31)$$

The stability of the system (7.31) is stated in the following theorem:

**Theorem 7.9** Consider the matrix-weighted consensus protocol with time delays (7.31). Suppose that  $\mathcal{N}(\mathbf{L}) = \mathcal{R}$ , and the time delays  $\tau_k$  are sufficient small such that the LMI (7.32) holds. Then, the origin is a globally asymptotically equilibrium of (7.31).

$$\mathbf{N} = \begin{bmatrix} -2\mathbf{E}^\top \mathbf{L} \mathbf{E} & \mathbf{E}^\top \mathbf{L}_1 \mathbf{E} & \dots & \mathbf{E}^\top \mathbf{L}_r \mathbf{E} \\ \mathbf{E}^\top \mathbf{L}_1 \mathbf{E} & -\tau_1^{-1} \mathbf{E}^\top \mathbf{E} & \dots & \mathbf{0}_{dn} \\ \vdots & \vdots & \ddots & \vdots \\ \mathbf{E}^\top \mathbf{L}_r \mathbf{E} & \mathbf{0}_{dn} & \dots & -\tau_r^{-1} \mathbf{E}^\top \mathbf{E} \end{bmatrix} + \tau \begin{bmatrix} -\mathbf{E}^\top \mathbf{L} \\ \mathbf{E}^\top \mathbf{L}_1 \\ \dots \\ \mathbf{E}^\top \mathbf{L}_r \end{bmatrix} \begin{bmatrix} -\mathbf{L} \mathbf{E} & \mathbf{L}_1 \mathbf{E} & \dots & \mathbf{L}_r \mathbf{E} \end{bmatrix} < 0 \quad (7.32)$$

*Proof:* Consider the Lyapunov–Razumikhin function  $V = V_1 + V_2$ , where  $V_1 = \dot{\boldsymbol{\delta}}(t)^\top \dot{\boldsymbol{\delta}}(t)$  and  $V_2 = \sum_{k=1}^r \int_0^{\tau_i} ds \int_{t-s}^t \dot{\boldsymbol{\delta}}(h)^\top \dot{\boldsymbol{\delta}}(h) dh$ . The derivatives of  $V_1$  and  $V_2$  along a trajectory of (7.31) are given by

$$\begin{aligned} \dot{V}_1 &= 2\dot{\boldsymbol{\delta}}(t)^\top \left( -\mathbf{L}\dot{\boldsymbol{\delta}}(t) + \sum_{k=1}^r \mathbf{L}_k \int_{t-\tau_k}^t \dot{\boldsymbol{\delta}}(s) ds \right) \\ &= -2\dot{\boldsymbol{\delta}}(t)^\top \mathbf{L}\dot{\boldsymbol{\delta}}(t) + 2\dot{\boldsymbol{\delta}}(t)^\top \sum_{k=1}^r \mathbf{L}_k \int_{t-\tau_k}^t \dot{\boldsymbol{\delta}}(s) ds, \end{aligned} \quad (7.33)$$

and

$$\dot{V}_2 = \tau \dot{\boldsymbol{\delta}}^\top(t) \dot{\boldsymbol{\delta}}(t) - \sum_{k=1}^r \int_{t-\tau_k}^t \dot{\boldsymbol{\delta}}^\top(s) \dot{\boldsymbol{\delta}}(s) ds \quad (7.34)$$

$$\leq \tau \dot{\boldsymbol{\delta}}^\top(t) \dot{\boldsymbol{\delta}}(t) - \sum_{k=1}^r \tau_k^{-1} \left( \int_{t-\tau_k}^t \dot{\boldsymbol{\delta}}(s) ds \right)^\top \left( \int_{t-\tau_k}^t \dot{\boldsymbol{\delta}}(s) ds \right) \quad (7.35)$$

where  $\tau = \sum_{i=1}^r \tau_i$ , and in (7.35) we have used the following inequality [159, Lemma 1]:

$$\int_{t-\tau_k}^t \dot{\boldsymbol{\delta}}^\top(s) \dot{\boldsymbol{\delta}}(s) ds \geq \tau_k^{-1} \left( \int_{t-\tau_k}^t \dot{\boldsymbol{\delta}}(s) ds \right)^\top \left( \int_{t-\tau_k}^t \dot{\boldsymbol{\delta}}(s) ds \right). \quad (7.36)$$

Defining  $\mathbf{y}(t) \triangleq [\dot{\boldsymbol{\delta}}^\top(t), \int_{t-\tau_1}^t \dot{\boldsymbol{\delta}}^\top(s) ds, \dots, \int_{t-\tau_r}^t \dot{\boldsymbol{\delta}}^\top(s) ds]^\top \in \mathbb{R}^{(r+1)nd}$ . From Eqs. (7.33), (7.35),

and (7.36), one gets

$$\dot{V}(t) \leq \mathbf{y}^\top(t) \mathbf{M} \mathbf{y}(t), \quad (7.37)$$

where

$$\mathbf{M} = \begin{bmatrix} -2\mathbf{L} & \mathbf{L}_1 & \dots & \mathbf{L}_r \\ \mathbf{L}_1 & -\tau_1^{-1}\mathbf{I}_{dn} & \dots & \mathbf{0}_{dn} \\ \vdots & \vdots & \ddots & \vdots \\ \mathbf{L}_r & \mathbf{0}_{dn} & \dots & -\tau_r^{-1}\mathbf{I}_{dn} \end{bmatrix} + \tau \begin{bmatrix} -\mathbf{L} \\ \mathbf{L}_1 \\ \vdots \\ \mathbf{L}_r \end{bmatrix} \begin{bmatrix} -\mathbf{L} \\ \mathbf{L}_1 \\ \vdots \\ \mathbf{L}_r \end{bmatrix}^T.$$

Since  $(\mathbf{1}_n^T \otimes \mathbf{I}_d)\boldsymbol{\delta} = (\mathbf{1}_n^T \otimes \mathbf{I}_d)\mathbf{x} - n\mathbf{x}^* = \mathbf{0}_d$ , one can define  $\boldsymbol{\delta} = \mathbf{E}\tilde{\boldsymbol{\delta}}$ , where  $\tilde{\boldsymbol{\delta}} = [\tilde{\boldsymbol{\delta}}_1^T, \dots, \tilde{\boldsymbol{\delta}}_{n-1}^T]^T$

and

$$\mathbf{E} = \begin{bmatrix} \mathbf{I}_{n-1} \\ \mathbf{1}_{n-1}^T \end{bmatrix} \otimes \mathbf{I}_d \in \mathbb{R}^{nd \times (n-1)d},$$

and rewrite (7.37) as follows:

$$\dot{V}(t) \leq \tilde{\mathbf{y}}^T(t) \bar{\mathbf{E}}^T \mathbf{M} \bar{\mathbf{E}} \tilde{\mathbf{y}}(t) = \tilde{\mathbf{y}}^T(t) \mathbf{N} \tilde{\mathbf{y}}(t), \quad (7.38)$$

where  $\tilde{\mathbf{y}}(t) = [\tilde{\boldsymbol{\delta}}^T(t), \int_{t-\tau_1}^t \dot{\tilde{\boldsymbol{\delta}}}^T(s)ds, \dots, \int_{t-\tau_r}^t \dot{\tilde{\boldsymbol{\delta}}}^T(s)ds]^T \in \mathbb{R}^{(r+1)(n-1)d}$ , and  $\bar{\mathbf{E}} = \mathbf{I}_{r+1} \otimes \mathbf{E} \in \mathbb{R}^{(r+1)nd \times (r+1)(n-1)d}$ . Since  $\mathbf{N} < 0$  due to the assumption, there exists  $\gamma > 0$  such that

$$\dot{V} \leq -\gamma \|\mathbf{y}(t)\|^2 \leq -\gamma \|\tilde{\boldsymbol{\delta}}(t)\|^2. \quad (7.39)$$

Further, since  $\|\boldsymbol{\delta}\|^2 = \|\tilde{\boldsymbol{\delta}}\|^2 + \|\boldsymbol{\delta}_n\|^2 = \|\tilde{\boldsymbol{\delta}}\|^2 + \|\sum_{i=1}^{n-1} \boldsymbol{\delta}_i\|^2 \leq \|\tilde{\boldsymbol{\delta}}\|^2 + (n-1)\sum_{i=1}^{n-1} \|\boldsymbol{\delta}_i\|^2 = \|\tilde{\boldsymbol{\delta}}\|^2 + (n-1)\|\tilde{\boldsymbol{\delta}}\|^2 = n\|\tilde{\boldsymbol{\delta}}\|^2$ , it follows that  $\dot{V} \leq -\gamma/n \|\boldsymbol{\delta}(t)\|^2$ , or the origin is an asymptotically stable equilibrium of (7.31) based on [158, Theorem 2.3]. ■

**Remark 7.10** Note that  $\mathcal{N}(\mathbf{L}) = \mathcal{R}$  implies that  $\mathbf{L}$  has eigenvalues  $0 = \lambda_1 = \dots = \lambda_d < \lambda_{d+1} \leq \dots \leq \lambda_{nd}$  [147]. For any  $\mathbf{z} \in \mathbb{R}^{(n-1)d}$ ,  $\mathbf{z} \neq \mathbf{0}_{(n-1)d}$ , we have  $(\mathbf{1}_n^T \otimes \mathbf{I}_d)(\mathbf{E}\mathbf{z}) = \mathbf{0}_{nd}$ . Thus,  $\mathbf{z}^T \mathbf{E}^T \mathbf{L} \mathbf{E} \mathbf{z} \geq \lambda_{d+1} \mathbf{z}^T \mathbf{E}^T \mathbf{E} \mathbf{z} > 0$ ; or the matrix  $\mathbf{E}^T \mathbf{L} \mathbf{E}$  is positive definite.

Consider the LMI (7.32). the matrix  $\mathbf{N}$  is a summation of two matrices: the first matrix is positive definite when  $\tau_k$ s are small, while the second matrices can be made small for small  $\tau_k$ s. This implies that the LMI (7.32) is always feasible if  $\tau_k$ s,  $k = 1, \dots, r$  are sufficiently small.

## **Part V**

# **Conclusions**

# Chapter 8

## Summary and Further Studies

This thesis studied three problems in distributed control of multi-agent systems, namely, bearing-based formation control, pointing consensus, and matrix-weighted consensus. The bearing based approaches have been used to design formation stabilization and pointing consensus strategies. Meanwhile, matrix-weighted consensus is a generalization of the bearing-constrained formation control and network localization problems [59, 73]. In the following sections, a summary and discussion on further research directions of each problem will be given.

### 8.1 Bearing-based formation control

In Part II, the bearing-only formation control problem has been studied with two types of graphs: leader-first follower and directed cycle. For LFF formations, the bearing-based Henneberg construction has been proposed. Then, three bearing-only control laws, including almost global stabilization, global stabilization or finite-time control laws, have been introduced and analyzed. Moreover, when the agents do not have access to a common orientation, bearing-based control with orientation alignment and global orientation estimation have been proposed. For directed cycle, a necessary and sufficient condition is derived for the feasibility of planar formations defined by a set of desired bearing vectors. Then, some results pertaining to the local asymptotic stability of the desired formation and instability of the undesired one for three- and  $n$ -agent formations are provided. Further, an extended analysis of the three agent case in  $\mathbb{R}^3$  was also presented.

For future works, bearing-based network localization is the dual problem of formation control

and thus may be further studied. Further analysis of bearing-based formation with moving leaders could be another research topic. Also, implementing the formation control strategy proposed in this thesis using only camera in quadcopter systems in outdoor environment is a challenging task. To this end, collision avoidance between agents should be considered. Preventing collision separately, using vision-based techniques, is required for the realization of bearing-only formation control laws. Another research direction could centered around maintaining bearing rigidity or constructing optimal frameworks in term of some bearing rigidity indices, which have been studied in distance rigidity [160–162]. Finally, it is hoped that the findings in this thesis will lead to further results on bearing-only formation control over more general directed graphs.

## 8.2 Pointing consensus

A decentralized solution to the pointing consensus problem in three-dimensional space was proposed in Part III. The solution was built up from solutions of three problems: bearing-only network localization, consensus, and bearing-only formation control. Two decentralized solutions to the Fermat-Weber location problem were also proposed to illustrate an application of our proposed solution. Although we only focused on three-dimensional space, the analysis can be easily extended to a higher dimensions without any difficulty.

For further studies, an immediate problem is studying the pointing consensus problem when all agents' local reference frames are not initially aligned. This setup may related to the bearing rigidity theories in  $SE(2)$  and  $SE(3)$  [54–56]. Moreover, if the desired target follows a time-varying trajectory or the agents are not stationary, the pointing consensus problem will become a cooperative target tracking problem, and the analysis will respectively become more complicated. Also, assume that all agents' local reference frame are not aligned, it could be interesting to consider the inverse problem of aligning the agents' local coordinates if their headings had initially pointed toward a same

point [163].

### 8.3 Matrix-weighted consensus

In Part IV, the matrix-weighted consensus algorithm has been studied. It was shown that the matrix-weighted consensus algorithm exhibits both common and unique characteristics comparing with the usual consensus algorithm. It is interesting that under the matrix-weighted consensus algorithm, connectedness of the undirected graph is not sufficient to guarantee the system to globally achieve a consensus. In fact, due to the existence of positive semidefinite connections, cluster consensus may easily happen in the system. It was proved that a global average consensus can be achieved if and only if the undirected matrix-weighted graph is spanned by only one cluster. An algorithm for finding all clusters in an undirected graph was also provided. For directed matrix weighted graphs, satisfying the generalized balanced condition and having a positive spanning tree are sufficient conditions to ensure a global average consensus. Matrix-weighted consensus with leader-following and switching interaction topologies, and with time delays have also been examined. Finally, we illustrated two possible applications of the matrix-weighted consensus protocol in cluster consensus and in bearing-based formation control problem.

Several problems on matrix-weighted consensus are still open for further studies. An immediate problem is finding a necessary and sufficient condition for achieving a consensus in directed networks. SVD can be useful in analysing this problem. Further, we can study consensus with different types of matrix weights, for examples, rotation matrices [118], complex numbers, quaternions, etc. Finally, it is meaningful to explore multilayer networks [164] in the framework of matrix-weighted consensus. In particular, the matrix-weighted consensus is useful in modeling and analysis of social networks [165, 166].

## Bibliography

1. K.-K. Oh, M.-C. Park, and H.-S. Ahn, “A survey of multi-agent formation control,” *Automatica*, vol. 53, pp. 424–440, 2015.
2. B. D. O. Anderson, C. Yu, B. Fidan, and J. M. Hendrickx, “Rigid graph control architectures for autonomous formations,” *Control Systems Magazine*, vol. 28, no. 6, pp. 48–63, 2008.
3. J. Aspnes, T. Eren, D. K. Goldenberg, A. S. Morse, W. Whiteley, Y. R. Yang, B. D. O. Anderson, and P. N. Belhumeur, “A theory of network localization,” *IEEE Transactions on Mobile Computing*, vol. 5, no. 12, pp. 1663–1678, 2006.
4. J. K. Hart and K. Martinez, “Environmental sensor networks: A revolution in the earth system science?” *Earth-Science Reviews*, vol. 78, no. 3-4, pp. 177–191, 2006.
5. J. W. Simpson-Porco, F. Dörfler, and F. Bullo, “Synchronization and power sharing for droop-controlled inverters in islanded microgrids,” *Automatica*, vol. 49, no. 9, pp. 2603–2611, 2013.
6. B.-Y. Kim, K.-K. Oh, K. L. Moore, and H.-S. Ahn, “Distributed coordination and control of multiple photovoltaic generators for power distribution in a microgrid,” *Automatica*, vol. 73, pp. 193–199, 2016.
7. F.-Y. Wang, “Agent-based control for networked traffic management systems,” *IEEE Intelligent Systems*, vol. 20, no. 5, pp. 92–96, 2005.
8. B.-Y. Kim and H.-S. Ahn, “Distributed coordination and control for a freeway traffic network using consensus algorithms,” *IEEE Systems Journal*, vol. 10, no. 1, pp. 162–168, 2016.
9. L. Krick, M. E. Broucke, and B. A. Francis, “Stabilisation of infinitesimally rigid formations of multi-robot networks,” *International Journal of Control*, vol. 82, no. 3, pp. 423–439, 2009.

10. K.-K. Oh and H.-S. Ahn, “Formation control of mobile agents based on inter-agent distance dynamics,” *Automatica*, vol. 47, pp. 2306–2312, 2011.
11. Y.-P. Tian and Q. Wang, “Global stabilization of rigid formations in the plane,” *Automatica*, vol. 49, pp. 1436–1441, 2013.
12. K. Sakurama, S. Azuma, and T. Sugie, “Distributed controllers for multi-agent coordination via gradient-flow approach,” *IEEE Transactions on Automatic Control*, vol. 60, no. 6, pp. 1471–1485, 2015.
13. H. G. de Marina, M. Cao, and B. Jayawardhana, “Controlling rigid formations of mobile agents under inconsistent measurements,” *IEEE Transactions on Robotics*, vol. 31, no. 1, pp. 31–39, 2015.
14. S. Mou, M.-A. Belabbas, A. S. Morse, Z. Sun, and B. D. O. Anderson, “Undirected rigid formations are problematic,” *IEEE Transactions on Automatic Control*, vol. 61, no. 10, pp. 2821–2836, 2016.
15. Z. Sun, S. Mou, B. D. O. Anderson, and M. Cao, “Exponential stability for formation control systems with generalized controllers: A unified approach,” *Systems & Control Letters*, vol. 93, no. 5, pp. 50–57, 2016.
16. J. M. Sullivan, “Evolution or Revolution?: The rise of UAVs,” *IEEE Technology and Society Magazine*, vol. 25, no. 3, pp. 43–49, 2006.
17. M. H. Trinh, G.-H. Ko, V. H. Pham, K.-K. Oh, and H.-S. Ahn, “Guidance using bearing-only measurements with three beacons in the plane,” *Control Engineering Practice*, vol. 51, pp. 81–91, 2016.

18. M. A. Lewis and K.-H. Tan, “High precision formation control of mobile robots using virtual structures,” *Autonomous robots*, vol. 4, no. 4, pp. 387–403, 1997.
19. B. J. Young, R. W. Beard, and J. M. Kelsey, “A control scheme for improving multi-vehicle formation maneuvers,” in *American Control Conference, 2001. Proceedings of the 2001*, vol. 2. IEEE, 2001, pp. 704–709.
20. J. A. Fax and R. M. Murray, “Information flow and cooperative control of vehicle formations,” *IEEE Transactions on Automatic Control*, vol. 49, no. 9, pp. 1465–1476, 2004.
21. G. Lafferriere, A. Williams, J. Caughman, and J. Veerman, “Decentralized control of vehicle formations,” *Systems & Control Letters*, vol. 54, pp. 899–910, 2005.
22. Z. Lin, L. Wang, Z. Han, and M. Fu, “Distributed formation control of multi-agent systems using complex laplacian,” *IEEE Transactions on Automatic Control*, vol. 59, no. 7, pp. 1765–1777, 2014.
23. K.-K. Oh and H.-S. Ahn, “Formation control and network localization via orientation alignment,” *IEEE Transactions on Automatic Control*, vol. 59, no. 2, pp. 540–545, 2014.
24. E. Montijano, E. Cristofalo, D. Zhou, M. Schwager, and C. Sagües, “Vision-based distributed formation control without an external positioning system,” *IEEE Transactions on Robotics*, vol. 32, no. 2, pp. 339–351, 2016.
25. B.-H. Lee and H.-S. Ahn, “Distributed formation control via global orientation estimation,” *Automatica*, vol. 73, pp. 125–129, 2016.
26. B.-H. Lee and H.-S. Ahn, “Formation control and network localization via distributed global orientation estimation in 3-D,” *arXiv preprint arXiv:1708.03591*, 2017.

27. T. Eren, W. Whiteley, A. S. Morse, P. N. Belhumeur, and B. D. O. Anderson, “Sensor and network topologies of formations with direction, bearing, and angle information between agents,” in *Proc. of the 42nd IEEE Conference on Decision and Control, Maui, HI, USA*, vol. 3. IEEE, 2003, pp. 3064–3069.
28. J. M. Hendrickx, B. D. O. Anderson, J.-C. Delvenne, and V. D. Blondel, “Directed graphs for the analysis of rigidity and persistence in autonomous agent systems,” *International Journal of Robust and Nonlinear Control*, vol. 17, pp. 960–981, 2007.
29. F. Dörfler and B. Francis, “Geometric analysis of the formation problem for autonomous robots,” *IEEE Transactions on Automatic Control*, vol. 55, no. 10, pp. 2379–2384, 2010.
30. K.-K. Oh and H.-S. Ahn, “Distance-based undirected formations of single-integrator and double-integrator modeled agents in N-dimensional space,” *International Journal of Robust and Nonlinear Control*, vol. 24, no. 12, pp. 1809–1820, 2014.
31. D. V. Dimarogonas and K. H. Johansson, “Further results on the stability of distance-based multi-robot formations,” in *American Control Conference, 2009. ACC’09*. IEEE, 2009, pp. 2972–2977.
32. M.-C. Park and H.-S. Ahn, “Stabilisation of directed cycle formations and application to two-wheeled mobile robots,” *IET Control Theory & Applications*, vol. 9, pp. 1338–1346, 2015.
33. V. H. Pham, M. H. Trinh, and H.-S. Ahn, “Formation control of rigid graphs with flex edges,” *International Journal of Robust and Nonlinear Control*, vol. 28, no. 6, pp. 2543–2559, 2018.
34. B. D. O. Anderson and C. Yu, “Range-only sensing for formation shape control and easy sensor network localization,” in *Control and Decision Conference (CCDC), 2011 Chinese*. IEEE, 2011, pp. 3310–3315.

35. M. Cao, C. Yu, and B. D. O. Anderson, “Formation control using range-only measurements,” *Automatica*, vol. 47, no. 4, pp. 776–781, 2011.
36. R. Suttner and Z. Sun, “Formation shape control based on distance measurements using Lie bracket approximations,” *arXiv preprint arXiv:1803.01606*, 2018.
37. M. Basiri, A. N. Bishop, and P. Jensfelt, “Distributed control of triangular formations with angle-only constraints,” *Systems & Control Letters*, vol. 59, no. 2, pp. 147–154, 2010.
38. A. N. Bishop and M. Basiri, “Bearing-only triangular formation control on the plane and the sphere,” in *Proc. of the 18th Mediterranean Conference on Control & Automation (MED), Morocco*, 2010, pp. 790–795.
39. A. N. Bishop, “Distributed bearing-only formation control with four agents and a weak control law,” in *Proc. of the 9th IEEE International Conference on Control & Automation, Santiago, Chile*, 2011, pp. 30–35.
40. S. Zhao, F. Lin, K. Peng, B. M. Chen, and T. H. Lee, “Distributed control of angle-constrained cyclic formations using bearing-only measurements,” *Systems & Control Letters*, vol. 63, pp. 12–24, 2014.
41. S. Zhao, F. Lin, P. K., B. M. Chen, and T. H. Lee, “Finite-time stabilisation of cyclic formations using bearing-only measurements,” *International Journal of Control*, vol. 87, no. 4, pp. 715–727, 2014.
42. I. Buckley and M. Egerstedt, “Infinitesimally shape-similar motions using relative angle measurements,” in *Proc. of the 2017 IEEE/RSJ International Conference on Intelligent Robots and Systems (IROS), Vancouver, BC, Canada*, 2017, pp. 1077–1082.

43. S.-H. Kwon, M. H. Trinh, K.-H. Oh, S. Zhao, and H.-S. Ahn, “Infinitesimal weak rigidity, formation control of three agents, and extension to 3-dimensional space,” *arXiv preprint arXiv:1803.09545*, 2018.
44. G. Jing, G. Zhang, H. W. J. Lee, and L. Wang, “Weak rigidity theory and its application to multi-agent formation stabilization,” *arXiv preprint arXiv:1804.02795*, 2018.
45. A. N. Bishop, I. Shames, and B. D. O. Anderson, “Stabilization of rigid formations with direction-only constraints,” in *Proc. of the 50th IEEE Conference on Decision and Control and European Control Conference, Orlando, Florida*, 2011, pp. 746–752.
46. T. Eren, “Formation shape control based on bearing rigidity,” *International Journal of Control*, vol. 85, no. 9, pp. 1361–1379, 2012.
47. E. Schoof, A. Chapman, and M. Mesbahi, “Bearing-compass formation control: A human-swarm interaction perspective,” in *Proc. of the 2014 American Control Conference, Portland, OR, USA*, 2014, pp. 3881–3886.
48. M. H. Trinh, K.-K. Oh, and H.-S. Ahn, “Angle-based control of directed acyclic formations with three-leaders,” in *Proc. of the 2014 IEEE International Conference on Mechatronics and Control (ICMC), China*, 2014, pp. 2268–2271.
49. S. Zhao and D. Zelazo, “Bearing rigidity and almost global bearing-only formation stabilization,” *IEEE Transactions on Automatic Control*, vol. 61, no. 5, pp. 1255–1268, 2016.
50. R. Tron, J. Thomas, G. Loianno, K. Daniilidis, and V. Kumar, “Bearing-only formation control with auxiliary distance measurements, leaders, and collision avoidance,” in *Proc. of the IEEE 55th Conference on Decision and Control (CDC), Las Vegas, NV, USA*, 2016, pp. 1806–1813.

51. M. H. Trinh, D. Mukherjee, D. Zelazo, and H.-S. Ahn, “Planar bearing-only cyclic pursuit for target capture,” in *Proc. of the 20th IFAC World Congress, Toulouse, France*, 2017, pp. 10 553–10 558.
52. M. H. Trinh, D. Mukherjee, D. Zelazo, and H.-S. Ahn, “Formations on directed cycles with bearing-only measurements,” *International Journal of Robust and Nonlinear Control*, vol. 28, no. 3, pp. 1074–1096, 2018.
53. A. Franchi and P. R. Giordano, “Decentralized control of parallel rigid formations with direction constraints and bearing measurements,” in *Proc. of the 51st IEEE Conference on Decision and Control, Maui, Hawaii, USA*, 2012, pp. 5310–5317.
54. D. Zelazo, P. R. Giordano, and A. Franchi, “Formation control using a SE(2) rigidity theory,” in *Proc. of the 54th IEEE Conference on Decision and Control (CDC), Osaka, Japan*, Dec. 2015, pp. 6121–6126.
55. F. Schiano, A. Franchi, D. Zelazo, and P. R. Giordano, “A rigidity-based decentralized bearing formation controller for groups of quadrotor UAVs,” in *Proc. of the 2016 IEEE/RSJ International Conference on Intelligent Robots and Systems (IROS 2016), Daejeon, South Korea*, 2016.
56. G. Michieletto, A. Cenedese, and A. Franchi, “Bearing rigidity theory in SE(3),” in *Proc. of the 55th IEEE Conference on Decision and Control (CDC), Las Vegas, NV, USA*, 2016.
57. M. H. Trinh, S. Zhao, Z. Sun, D. Zelazo, B. D. O. Anderson, and H.-S. Ahn, “Bearing based formation control of a group of agents with leader-first follower structure,” *Transactions on Automatic Control, in press*, pp. 1–16, 2019.
58. M. H. Trinh, B.-H. Lee, M. Ye, and H.-S. Ahn, “Bearing-based formation control and network

- localization via global orientation estimation,” in *Proc. of the IEEE Conference on Control Technology and Applications, Copenhagen, Denmark*, 2018.
59. S. Zhao and D. Zelazo, “Bearing-based formation stabilization with directed interaction topologies,” in *Proc. of the 54th IEEE Conference on Decision and Control, Osaka, Japan*, 2015, pp. 6115 – 6120.
  60. S. Zhao and D. Zelazo, “Bearing-based distributed control and estimation of multi-agent systems,” in *Proc. of the European Control Conference (ECC), Austria*, 2015, pp. 2202–2207.
  61. A. N. Bishop, M. Deghat, B. D. O. Anderson, and Y. Hong, “Distributed formation control with relaxed motion requirements,” *International Journal of Robust and Nonlinear Control*, vol. 25, no. 17, pp. 3210–3230, 2015.
  62. K. Fathian, D. I. Rachinskii, M. W. Spong, and N. R. Gans, “Globally asymptotically stable distributed control for distance and bearing based multi-agent formations,” in *Proc. of the American Control Conference (ACC), Boston, MA, USA*. IEEE, 2016, pp. 4642–4648.
  63. Z. Sun, M.-C. Park, B. D. O. Anderson, and H.-S. Ahn, “Distributed stabilization control of rigid formations with prescribed orientation,” *Automatica*, vol. 78, pp. 250–257, 2017.
  64. V. H. Pham, M. H. Trinh, and H.-S. Ahn, “A finite-time convergence of acyclic generically persistent formation in 3-d using relative position measurements,” in *Proc. of the 17th International Conference on Control, Automation and Systems (ICCAS), Jeju, South Korea*, 2017, pp. 230–235.
  65. M.-C. Park, H.-K. Kim, and H.-S. Ahn, “Rigidity of distance-based formations with additional subtended-angle constraints,” in *Proc. of the 17th International Conference on Control, Automation and Systems (ICCAS), Jeju, South Korea*, 2017, pp. 111–116.

66. S. G. Loizou and V. Kumar, “Biologically inspired bearing-only navigation and tracking,” in *Proc. of the 46th IEEE Conference on Decision and Control (CDC), New Orleans, LA, USA, 2007*, pp. 1386–1391.
67. M. H. Trinh, V. H. Pham, P. H. Hoang, J.-H. Son, and H.-S. Ahn, “A new bearing-only navigation law,” in *Proc. of the International Conference on Control, Automation and Systems (ICCAS)*, 2017, pp. 117–122.
68. M. Ye, B. D. O. Anderson, and C. Yu, “Multiagent self-localization using bearing only measurements,” in *Proc. of the 52nd IEEE Conference on Decision and Control, Florence, Italy, 2013*, pp. 2157–2162.
69. M. Deghat, I. Shames, B. D. O. Anderson, and C. Yu, “Localization and circumnavigation of a slowly moving target using bearing measurements,” *IEEE Transactions on Automatic Control*, vol. 59, no. 8, pp. 2182–2188, 2014.
70. W. Whiteley, *Some matroids from discrete applied geometry*, ser. Contemporary Mathematics, Vol. 137. AMS, 1996.
71. T. Eren, W. Whiteley, and P. N. Belhumeur, “Using angle of arrival (bearing) information in network localization,” in *Proc. of the 45th IEEE Conference on Decision and Control, San Diego, CA, USA, 2006*, pp. 4676–4681.
72. S. Zhao and D. Zelazo, “Translational and scaling formation maneuver control via a bearing-based approach,” *IEEE Transactions on Control of Network Systems*, vol. 4, no. 3, pp. 429–438, 2017.
73. S. Zhao and D. Zelazo, “Localizability and distributed protocols for bearing-based network localization in arbitrary dimensions,” *Automatica*, vol. 69, pp. 334–341, 2016.

74. R. Tron, L. Carlone, F. Dellaert, and K. Daniilidis, “Rigid components identification and rigidity control in bearing-only localization using the graph cycle basis,” in *Proc. of the American Control Conference, Chicago, IL, USA*, 2015, pp. 3911–3918.
75. B. D. O. Anderson, S. Dasgupta, and C. Yu, “Control of directed formations with a leader-first follower structure,” in *Proc. of the 46th IEEE Conference on Decision and Control, New Orleans, LA, USA*, 2007, pp. 2882–2887.
76. C. Yu, B. D. O. Anderson, S. Dasgupta, and B. Fidan, “Control of minimally persistent formations in the plane,” *SIAM Journal of Control and Optimization*, vol. 48, no. 1, pp. 206–233, 2009.
77. T. H. Summers, C. Yu, S. Dasgupta, and B. D. O. Anderson, “Control of minimally persistent leader-remote-follower and coleader formations in the plane,” *IEEE Transaction on Automatic Control*, vol. 56, pp. 2778–2792, 2011.
78. J. A. Marshall, M. E. Broucke, and B. A. Francis, “Formations of vehicles in cyclic pursuit,” *IEEE Transactions on Automatic Control*, vol. 49, no. 11, pp. 1963–1974, 2004.
79. D. Mukherjee and D. Ghose, “Generalization of deviated linear cyclic pursuit,” in *Proc. of the American Control Conference, Washington, DC, USA*, 2013, pp. 6163–6168.
80. D. Mukherjee and D. Ghose, “Deviated linear cyclic pursuit,” *Proc. of the Royal Society A*, vol. 471, no. 2184, p. 20150682, 2015.
81. K. Fathian, D. I. Rachinskii, T. H. Summers, and N. R. Gans, “Distributed control of cyclic formations with local relative position measurements,” in *Proc. of the 55th IEEE Conference on Decision and Control, Las Vegas, NV, USA*, 2016, pp. 49–56.

82. M. H. Trinh, K.-K. Oh, K. Jeong, and H.-S. Ahn, “Bearing-only control of leader first follower formations,” in *Proc. of the 14th IFAC Symposium on Large Scale Complex Systems: Theory and Applications, Riverside, CA, USA*, 2016, pp. 7–12.
83. D. Mukherjee, M. H. Trinh, D. Zelazo, and H.-S. Ahn, “Bearing-only cyclic pursuit in 2-d for capture of moving target,” in *57th Israel Annual Conference on Aerospace Science*, Israel, 2017.
84. K.-K. Oh and H.-S. Ahn, “Leader-follower type distance-based formation control of a group of autonomous agents,” *International Journal of Control, Automation and Systems*, vol. 15, pp. 1738–1745, 2017.
85. S. Mou, M. Cao, and A. S. Morse, “Target-point formation control,” *Automatica*, vol. 61, pp. 113–118, 2015.
86. S.-M. Kang and H.-S. Ahn, “Design and realization of distributed adaptive formation control law for multi-agent systems with moving leader,” *IEEE Transactions on Industrial Electronics*, vol. 63, no. 2, pp. 1268–1279, 2016.
87. D. Angeli, “An almost global notion of input to state stability,” *IEEE Transactions on Automatic Control*, vol. 6, no. 49, pp. 866–874, 2004.
88. D. Angeli and L. Praly, “Stability robustness in the presence of exponentially unstable isolated equilibria,” *IEEE Transactions on Automatic Control*, vol. 7, no. 56, pp. 1582–1592, 2011.
89. Z. Meng, B. D. O. Anderson, and S. Hirche, “Formation control with mismatched compasses,” *Automatica*, vol. 69, pp. 232–241, 2016.
90. R. Olfati-Saber, J. A. Fax, and R. M. Murray, “Consensus and cooperation in networked multi-agent systems,” *Proceedings of the IEEE*, vol. 95, no. 1, pp. 215–233, 2007.

91. M. Mesbahi and M. Egerstedt, *Graph Theoretic Methods in Multiagent Networks*. Princeton NJ: Princeton University Press, 2010.
92. T. Wongpiromsarn, K. You, and L. Xie, “A consensus approach to the assignment problem: Application to mobile sensor dispatch,” in *Proc. of the 8th IEEE International Conference on Control and Automation (ICCA)*, 2010, pp. 2024–2029.
93. B.-Y. Kim and H.-S. Ahn, “Consensus-based coordination and control for building automation systems,” *IEEE Transactions on Control Systems Technology*, vol. 23, no. 1, pp. 364–371, 2015.
94. A. Sarlette and R. Sepulchre, “Consensus optimization on manifolds,” *SIAM Journal of Control and Optimization*, vol. 48, no. 1, pp. 56–76, 2009.
95. W. Ren, “Distributed attitude alignment in spacecraft formation flying,” *International Journal of Adaptive Control and Signal Processing*, vol. 21, no. 2-3, pp. 95–113, 2007.
96. A. Moreira, P. Prats-Iraola, M. Younis, G. Krieger, I. Hajnsek, and K. P. Papathanassiou, “A tutorial on synthetic aperture radar,” *IEEE Geoscience and Remote Sensing Magazine*, vol. 1, no. 1, pp. 6–43, 2013.
97. G. Krieger, A. Moreira, H. Fiedler, I. Hajnsek, M. Werner, M. Younis, and M. Zink, “Tandem-x: A satellite formation for high-resolution sar interferometry,” *IEEE Transactions on Geoscience and Remote Sensing*, vol. 45, no. 11, pp. 3317–3341, 2007.
98. G. Krieger, H. Fiedler, and A. Moreira, “Earth observation with SAR satellite formations: new techniques and innovative products,” in *Proc. of the IAA Symposium on Small Satellites for Earth Observation*, 2009.

99. F. Zhang, P. Ramazi, and M. Cao, “Distributed concurrent targeting for linear arrays of point sources,” *Proc. of the 19th IFAC World Congress, Cape Town, South Africa*, vol. 47, no. 3, pp. 8323–8328, 2014.
100. M. H. Trinh, D. Zelazo, Q. V. Tran, and H.-S. Ahn, “Pointing consensus for rooted out-branching graphs,” in *Proc. of the American Control Conference, Milwaukee, WI*, 2018.
101. S. Zhao and D. Zelazo, “Bearing rigidity theory and its applications for control and estimation of network systems: Life beyond distance rigidity,” *IEEE Control Systems Magazine*, 2018.
102. F. Plastria, “The Weiszfeld algorithm: Proof, amendments, and extensions,” in *Foundations of Location Analysis, International Series Operational and Resources Management Science*, Springer, vol. 155, pp. 357–389, 2011.
103. H. Kuhn, “A note on Fermat’s problem,” *Mathematical Programming*, vol. 4, pp. 98–107, 1973.
104. J. Brimberg, “The Fermat–Weber location problem revisited,” *Mathematical Programming*, vol. 71, pp. 71–76, 1995.
105. L. Wang and F. Xiao, “Finite-time consensus problems for networks of dynamic agents,” *IEEE Transactions on Automatic Control*, vol. 55, no. 4, pp. 950–955, 2010.
106. E. Weiszfeld, “Sur le point pour lequel la somme des distances de  $n$  points données est minimum,” *Tôhoku Mathematics Journal*, vol. 43, pp. 355–386, 1937.
107. M. H. Trinh, B.-H. Lee, and H.-S. Ahn, “The Fermat-Weber location problem in single integrator dynamics using only local bearing angles,” *Automatica*, vol. 59, pp. 90–96, 2015.
108. R. Olfati-Saber and R. M. Murray, “Consensus problems in networks of agents with switching

- topology and time-delays,” *IEEE Transactions on Automatic Control*, vol. 49, no. 9, pp. 1520–1533, 2004.
109. W. Ren, R. W. Beard, and E. M. Atkins, “A survey of consensus problems in multi-agent coordination,” in *Proc. of the American Control Conference, Portland, OR, USA*, 2005, pp. 1859–1864.
110. W. Ren, “Multi-vehicle consensus with a time-varying reference state,” *Systems & Control Letters*, vol. 56, pp. 474–483, 2007.
111. J. Kim, J. Yang, H. Shim, J.-S. Kim, and J.-H. Seo, “Consensus of output-coupled linear multi-agent systems under fast switching network: Averaging approach,” *Automatica*, vol. 49, no. 1, pp. 267–272, 2013.
112. S. E. Tuna, “Conditions for synchronizability in arrays of coupled linear systems,” *IEEE Transactions on Automatic Control*, vol. 54, no. 10, pp. 2416–2420, 2009.
113. J. M. Hendrickx, “A lifting approach to models of opinion dynamics with antagonisms,” in *Proc. of the 53rd IEEE Conference on Decision and Control, Los Angeles, California, USA*, 2014, pp. 2118–2123.
114. W. Xia, M. Cao, and K. H. Johansson, “Structural balance and opinion separation in trust-mistrust social networks,” *IEEE Transactions on Control of Networked Systems*, vol. 3, no. 1, pp. 46–56, 2016.
115. P. Barooah and J. P. Hespanha, “Graph effective resistance and distributed control: Spectral properties and applications,” in *Proc. of the 45th IEEE conference on Decision and Control*. IEEE, 2006, pp. 3479–3485.

116. S. E. Tuna, “Synchronization under matrix-weighted Laplacian,” *Automatica*, vol. 73, pp. 76–81, 2016.
117. J. L. Ramirez, M. Pavone, E. Frazzoli, and D. W. Miller, “Distributed control of spacecraft formation via cyclic pursuit: Theory and experiments,” in *Prof. of American Control Conference (ACC), St. Louis, MO, USA*, 2009, pp. 4811–4817.
118. H.-S. Ahn, M. H. Trinh, and B.-H. Lee, “Consensus under misaligned orientations,” in *Proc. of the 17th International Conference on Control, Automation and Systems, Jeju, Korea*, 2017, pp. 283–288.
119. N. E. Friedkin, A. V. Proskurnikov, R. Tempo, and S. E. Parsegov, “Network science on belief system dynamics under logic constraints,” *Science*, vol. 354, no. 6310, pp. 321–326, 2016.
120. S. E. Parsegov, A. V. Proskurnikov, R. Tempo, and N. E. Friedkin, “Novel multidimensional models of opinion dynamics in social networks,” *IEEE Transactions on Automatic Control*, vol. 62, no. 5, pp. 2270–2285, 2017.
121. C. Godsil and G. Royle, *Algebraic graph theory*. Springer, 2001.
122. B. Bollobás, *Extremal graph theory*. Courier Corporation, 2004.
123. S. P. Bhat and D. S. Bernstein, “Finite-time stability of continuous autonomous systems,” *SIAM Journal of Control and Optimization*, vol. 38, no. 3, pp. 751–766, 1998.
124. G. Strang, *Linear Algebra and Its Applications*, 3rd ed. Brooks/Cole, 1988.
125. H. K. Khalil, *Nonlinear Systems*, 3rd ed. Prentice Hall, 2002.
126. W. Ren and R. W. Beard, “Consensus seeking in multiagent systems under dynamically changing topologies,” *IEEE Transactions on Automatic Control*, vol. 52, no. 11, pp. 1862–1868, 2007.

- ing interaction topologies,” *IEEE Transactions on Automatic Control*, vol. 50, no. 5, pp. 655–661, 2005.
127. G. Hardy, J. E. Littlewood, and G. Pólya, *Inequalities*, 2nd ed. Cambridge University Press: Cambridge Mathematical Library, 1952.
128. R. Horn and C. Johnson, *Matrix Analysis*. Cambridge University Press, 1990.
129. M. H. Trinh, D. Mukherjee, D. Zelazo, and H.-S. Ahn, “Finite-time bearing-only formation control,” in *Proc. of the 56th Conference on Decision and Control (CDC), Melbourne, Australia*, 2017, pp. 1578–1583.
130. S. Zhao, Z. Sun, D. Zelazo, M. H. Trinh, and H.-S. Ahn, “Laman graphs are generically bearing rigid in arbitrary dimensions,” in *Proc. of the 56th Conference on Decision and Control (CDC 2017), Melbourne, Australia*, 2017, pp. 3356–3361.
131. L. Mejias and I. F. M. P. Campoy, “Omnidirectional bearing-only see-and-avoid for small aerial robots,” in *Proc. of the 5th International Conference on Automation, Robotics and Applications, Wellington, New Zealand*, 2011, pp. 23–28.
132. T. Mori and S. Scherer, “First results in detecting and avoiding frontal obstacles from a monocular camera for micro unmanned aerial vehicles,” in *Proc. of the 2013 IEEE International Conference on Robotics and Automation (ICRA), Karlsruhe, Germany*, 2013, pp. 1750–1757.
133. M. H. Trinh, V. H. Pham, M.-C. Park, Z. Sun, B. D. O. Anderson, and H.-S. Ahn, “Comments on global stabilization of rigid formations in the plane [Automatica 49 (2013) 1436–1441],” *Automatica*, vol. 77, pp. 393–396, 2017.
134. D. Shevitz and B. Paden, “Lyapunov stability theory of nonsmooth systems,” *IEEE Transactions on Automatic Control*, vol. 39, no. 9, pp. 1910–1914, 1994.

135. J. Cortés, “Discontinuous dynamical systems - A tutorial on solutions, nonsmooth analysis, and stability,” *Control Systems Magazine, IEEE*, vol. 28, no. 3, pp. 36–73, 2008.
136. J. Cortés, “Finite-time convergent gradient flows with applications to network consensus,” *Automatica*, vol. 42, pp. 1993–2000, 2006.
137. M.-C. Park, Z. Sun, K.-K. Oh, B. D. O. Anderson, and H.-S. Ahn, “Finite-time convergence control for acyclic persistent formations,” in *Proc. of the IEEE International Symposium on Intelligent Control (ISIC), Juan Les Pins, France*, 2014, pp. 1608–1613.
138. Z. Sun, S. Mou, M. Deghat, B. D. O. Anderson, and A. S. Morse, “Finite time distance-based rigid formation stabilization and flocking,” in *Proc. of the 19th IFAC World Congress, Cape Town, South Africa*, 2014, pp. 9138–9189.
139. Y. Igarashi, T. Hatanaka, M. Fujita, and M. W. Spong, “Passivity-based attitude synchronization in  $\text{SE}(3)$ ,” *IEEE Transactions on Control Systems Technology*, vol. 17, no. 5, pp. 1119–1134, 2009.
140. K.-K. Oh and H.-S. Ahn, “Formation control of rigid bodies based on orientation alignment and position estimation,” in *Proc. of the 14th International Conference on Control, Automation and Systems (ICCAS 2014), Korea*, 2014, pp. 740–744.
141. J. Thunberg, W. Song, and X. Hu, “Distributed attitude synchronization control of multi-agent systems with directed topologies,” in *Proc. of the 10th World Congress on Intelligent Control and Automation, Beijing, China*, 2012, pp. 958–963.
142. J. Thunberg, W. Song, E. Montijano, Y. Hong, and X. Hu, “Distributed attitude synchronization control of multi-agent systems with switching topologies,” *Automatica*, vol. 50, no. 3, pp. 832–840, 2014.

143. B.-H. Lee and H.-S. Ahn, “Distributed estimation for the unknown orientation of the local reference frames in N-dimensional space,” in *Proc. of the 14th International Conference on Control, Automation, Robotics and Vision (ICARCV), Phuket, Thailand*, 2016.
144. M. H. Trinh, D. Zelazo, and H.-S. Ahn, “Pointing consensus and bearing-based solutions to the Fermat-Weber location problem,” *Transactions on Automatic Control, submitted*, 2018.
145. R. A. Freeman, P. Yang, and K. M. Lynch, “Stability and convergence properties of dynamic average consensus estimators,” in *Proc. of the 45th IEEE Conference on Decision and Control (CDC), San Diego, CA, USA*, 2006, pp. 338–343.
146. S. S. Kia, J. Cortés, and S. Martinez, “Singularly perturbed algorithms for dynamic average consensus,” in *Proc. of the European Control Conference (ECC), Zürich, Switzerland*, 2013, pp. 1758–1763.
147. M. H. Trinh and H.-S. Ahn, “Theory and applications of matrix-weighted consensus,” 2017, <https://arxiv.org/abs/1703.00129>.
148. M. H. Trinh, C. V. Nguyen, Y.-H. Lim, and H.-S. Ahn, “Matrix-weighted consensus and its applications,” *Automatica*, vol. 89, pp. 415–419, 2018.
149. D. Zelazo and M. Mesbahi, “Edge agreement: Graph-theoretic performance bounds and passivity analysis,” *IEEE Transactions on Automatic Control*, vol. 56, no. 3, pp. 554–555, 2011.
150. W. Ni and D. Cheng, “Leader-following consensus of multi-agent systems under fixed and switching topologies,” *Systems & Control Letters*, vol. 59, pp. 209–217, 2010.
151. P. Antsaklis and A. N. Michel, *Linear Systems*. Springer Science & Business Media, 2006.

152. C. Altafini, “Consensus problems on networks with antagonistic interactions,” *IEEE Transactions on Automatic Control*, vol. 58, no. 4, pp. 935–946, 2013.
153. J. Qin, C. Yu, and B. D. O. Anderson, “On leaderless and leader-following consensus for interacting clusters of second-order multi-agent systems,” *Automatica*, vol. 74, pp. 214–221, 2016.
154. R. Hegselmann and U. Krause, “Opinion dynamics and bounded confidence models, analysis, and simulation,” *Journal of Artificial Societies and Social Simulation*, vol. 5, no. 3, 2002.
155. H. Zhang, F. L. Lewis, and Z. Qu, “Lyapunov, adaptive, and optimal design techniques for cooperative systems on directed communication graphs,” *IEEE Transactions on Industrial Electronics*, vol. 59, no. 7, pp. 3026–3041, 2012.
156. J. P. Hespanha, “Extending LaSalle’s invariance principle to switched linear systems,” in *Proc. of the 40th IEEE Conference on Decision and Control, Orlando, FL, USA*, 2001, pp. 2496–2501.
157. Y. G. Sun, L. Wang, and G. Xie, “Average consensus in networks of dynamic agents with switching topologies and multiple time-varying delays,” *Systems & Control Letters*, vol. 57, no. 2, pp. 175–183, 2008.
158. V. B. Kolmanovskii and J.-P. Richard, “Stability of some linear systems with delays,” *IEEE Transactions on Automatic Control*, vol. 44, no. 5, pp. 984–989, 1999.
159. K. Gu, “An integral inequality in the stability problem of time-delay systems,” in *Proc. of the 39th IEEE Conference on Decision and Control, Sydney, NSW, Australia*, vol. 3, 2000, pp. 2805–2810.

160. G. Zhu and J. Hu, “Stiffness matrix and quantitative measure of formation rigidity,” in *Proc. of the 48th IEEE Conference on Decision and Control held jointly with the 28th Chinese Control Conference*, 2009, pp. 3057–3062.
161. D. Zelazo, A. Franchi, F. Allgöwer, H. H. Bülthoff, and P. R. Giordano, “Rigidity maintenance control for multi-robot systems,” in *Robotics: Science and Systems*, 2012, pp. 473–480.
162. M. H. Trinh, M.-C. Park, Z. Sun, B. D. O. Anderson, V. H. Pham, and H.-S. Ahn, “Further analysis on graph rigidity,” in *Proc. of the IEEE 55th Conference on Decision and Control (CDC), Las Vegas, NV, USA*, 2016, pp. 922–927.
163. Q. V. Tran, M. H. Trinh, and H.-S. Ahn, “Surrounding formation of star frameworks using bearing-only measurements,” in *Proc. of the European Control Conference (ECC), Limassol, Cyprus*, 2018.
164. S. Boccaletti, G. Bianconi, R. Criado, C. I. Del Genio, J. Gómez-Gardenes, M. Romance, I. Sendina-Nadal, Z. Wang, and M. Zanin, “The structure and dynamics of multilayer networks,” *Physics Reports*, vol. 544, no. 1, pp. 1–122, 2014.
165. M. H. Trinh, M. Ye, H.-S. Ahn, and B. D. O. Anderson, “Matrix-weighted consensus with leader-following topologies,” in *Proc. of the Asian Control Conference (ASCC), Gold Coast, Australia*, 2017, pp. 1795–1800.
166. M. Ye, M. H. Trinh, Y.-H. Lim, B. D. O. Anderson, and H.-S. Ahn, “Continuous-time opinion dynamics on multiple interdependent topics,” *Automatica, submitted*, 2018.

## Acknowledgements

First of all, I would like to express my deepest appreciation to my advisor, Prof. Hyo-Sung Ahn, for his patient guidance, encouragement and countless discussions. Prof. Ahn always listens to my immature ideas, encourages me to develop my ideas into publishable works, supports me to attend many conferences, and creates chances for me to meet and collaborate with different people. I am also thankful for his advice and help through the high and low points of my MS and then PhD time. This dissertation would not be possible without him.

It is my honor to have Prof. Euiseok Hwang, Prof. Jeong Ok Choi, Prof. Hyunsuk Kang, and Dr. Kwang-Kyo Oh as my committee members. Thank you so much for your time and effort taken to review and evaluate this dissertation.

I wish to thank Prof. Daniel Zelazo for inviting me to Technion and giving me the chance to study and discuss various topics on bearing rigidity. Six months in Israel is so important to the success of this thesis. Many thanks to Noam, Dwaipayan, Douglas and other people in Control Lab., for their assistance during my stay.

During my PhD, I have opportunities to discuss and learn from many researchers from other universities. I wish to thank Prof. Brian D. O. Anderson, Dr. Zhiyong Sun, Mengbin Ye (Australian National University, Australia), Prof. Daniel Zelazo, Dr. Dwaipayan Murkhejee (Technion, Israel), and Prof. Shiyu Zhao (University of Sheffield, UK) for their discussions and insightful comments on many topics. Many ideas generated from these discussions have been included in this thesis. I am honor to receive comments and learn from Prof. Brian D. O. Anderson. Despite of being a prominent scholar, he is always kind and friendly to a young graduate student like me.

I appreciate the former and current colleagues in Distributed Control and Autonomous Systems Laboratory (DCASL). I would like to thank Dr. Kwang-Kyo Oh for his guidance since I began

studying formation control. I appreciate Viet Hoang Pham, Dr. Myoung-Chul Park, Quoc Van Tran, Chuong Van Nguyen, Phuong Huu Hoang, Seong-Ho Kwan, Dr. Byung-Hun Lee and Prof. Young-Hun Lim for many discussions in lab's seminars and our collaborations. Thank you Gwi-Han Ko for your support on hardware experiments and helping me many times. Thank you Dr. Ji-Hwan Son, Dr. Seung-Ju Lee, Dr. Sung-Mo Kang, Dr. Hwan Hur, Dr. Byeong-Yeon Kim, Dr. Young-Cheol Choi, Dr. Sang-Chul Lee, Seok-Young Han, Jae-Gyeong Lee, Koog-Hwan Oh, Yoo-Bin Bae, Young-Hun John, Jin-Hee Son, Kyu-Hwan Kim, Han-Young Park, Hae-Jun Kim, Jae-Ryoung Byun, Hong-Jun Lee, Hong-Kyong Kim, Shin-Hyun Park, Chan-Yeong Jeong, and Mrs. Hyo-Jin Shim for creating a very supportive environment.

I acknowledge Korean government and Gwangju Institute of Science and Technology for the scholarship that supports my PhD study.

I would like to thank my Vietnamese friends at GIST and my roommate Faiyaz. Thank you for sharing with me a lot of memorable moments in Korea.

Finally and most importantly, I am grateful to my parents, my younger sister, and other family members, who have been always loving and supporting me unconditionally. This thesis is dedicated to them.